The Role of Ice Streams in the Demise of the British-Irish Ice Sheet

Niall Gandy

Submitted in accordance with the requirements for the

degree of

Doctor of Philosophy
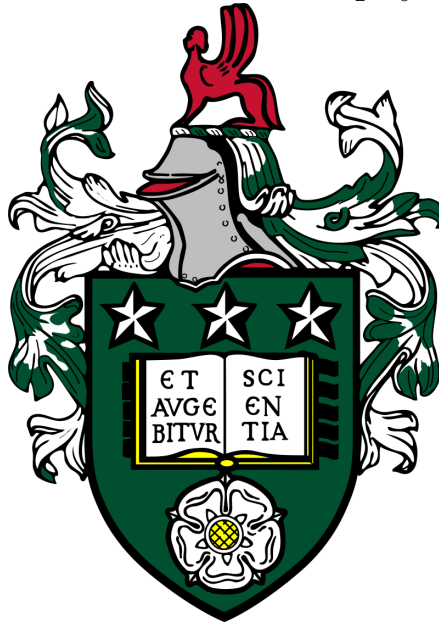
School of Earth and Environment

The University of Leeds

January 2020

Publication Statement

The candidate confirms that the work submitted is his own, except where work which has formed part of jointly authored publications has been included. The contribution of the candidate and the other authors to this work has been explicitly indicated below. The candidate confirms that appropriate credit has been given within the thesis where reference has been made to the work of others.

The work in Chapter 2 of the thesis has appeared in publication as follows: Marine ice sheet instability and ice shelf buttressing of the Minch Ice Stream, northwest Scotland. 2018. *The Cryosphere.* Niall Gandy, Lauren J. Gregoire, Jeremy C. Ely, Christopher D. Clark, David M. Hodgson, Victoria Lee, Tom Bradwell, and Ruza F. Ivanovic.

NG designed the study with LGJ and JCE. NG ran the simulations, performed the analysis, and wrote the paper with contributions from all authors. JCE produced the bed friction map used. VL developed the model code for frontal ablation. RFI provided the climate model data used. JCE, CDC, DMH, and TB contributed to the comparison to empirical data.

The work in Chapter 3 of the thesis has appeared in publication as follows: Exploring the ingredients required to successfully model the placement, generation, and evolution of ice streams in the British-Irish Ice Sheet. 2019. *Quaternary Science Reviews.* Niall Gandy, Lauren J. Gregoire, Jeremy C. Ely, Stephen L. Cornford, Christopher D. Clark, and David M. Hodgson.

NG designed the study with LJG and JCE. SLC and LJG developed the model code. NG ran the simulations, performed the analysis, and wrote the manuscript with contributions from all authors. JCE, CDC, and DMH contributed to the comparison to empirical data and interpretation of the results.

The work in Chapter 4 of the thesis is to be submitted to the *Journal of Geophysical Research*, with the authorship of Niall Gandy, Lauren J. Gregoire, Jeremy C. Ely, Stephen L. Cornford, Christopher D. Clark, and David M. Hodgson.

NG designed the study with LJG and JCE. NG ran the simulations, performed the analysis, and wrote the manuscript with guidance from LJG and contributions from all authors. SLC contributed to the design of the BISICLES model set-up. JCE, CDC, and DMH contributed to the comparisons to empirical data and interpretation of the results.

Acknowledgements

I would like to thank my primary supervisor, Dr. Lauren Gregoire, for stimulating discussions, for always providing the perfect balance of support and freedom, and for always encouraging my research. I have been very lucky to have such a supportive supervisor.

I would also like to thank both Dr. Jeremy Ely and Professor Chris Clark for first encouraging my interest in palaeo-glaciology, and for highlighting the advert for this PhD project 4 years ago. Thank you to Professor David Hodgson for always providing extremely valuable feedback, and always making me feel welcome in a large and friendly research group.

My manuscript co-authors also provided significant support. Thank you to Dr. Ruza Ivanovic for always asking stimulating and challenging questions, and to Dr. Stephen Cornford and Dr. Victoria Lee for their support with BISICLES, providing answers to streams of questions. Thank you to Dr. Tom Bradwell for helping to bridge the model-data divide.

Abstract

Accurate projection of the future evolution of the Greenland and Antarctic ice sheets is a key challenge of glaciology and climate science. Ice sheet flow is dominated by ice streams; narrow corridors of fast flow bounded laterally by slower flowing ice, discharging the majority of ice from an ice sheet. These ice streams are particularly vulnerable to retreat, and their behaviour evolves along with the ice sheet as a whole. These interactions contribute to uncertainty in projections of ice sheet evolution. In part, this uncertainty can be addressed by examining the palaeo record, providing information on ice stream behaviour over thousands of years.

This thesis presents a series of simulations of the British-Irish Ice Sheet using the latest generation BISICLES ice sheet model. Model simulations are used to determine the role of ice streams in the demise of the British-Irish Ice Sheet. First, BISICLES is used to examine the dynamical processes that control the retreat of a major ice stream of the British-Irish Ice Sheet, and this demonstrates vulnerability of the ice stream to Marine Ice Sheet Instability. Then a new basal sliding scheme is implemented coupled with thermo-mechanics, and this successfully models the placement and spacing of the majority of British-Irish Ice Sheet ice streams. Finally, simulations of the deglaciation style of the North Sea demonstrate the significant influence of the Norwegian Channel Ice Stream.

Through these simulations, in combination with novel model-data comparison techniques, the considerable role of ice streams in the demise of the British-Irish Ice Sheet is shown. Ice stream evolution and interaction with other factors driving

deglaciation needs to be adequately considered in the aim of projecting the future evolution of the Antarctic and Greenland ice sheets. Research such as presented here, modelling and reconstructing palaeo ice sheets, continues to advance this aim.

Contents

List of Figures

17

20

List of Tables

Abbreviations

AFDA Automated Flow Direction Analysis

APCA Automated Proximity and Conformity Analysis

ATAT Automated Timing Accordance Tool

BIIS British-Irish Ice Sheet

ELA Equillibrium Line Altitude

GIA Glacial Isostatic Adjustment

LGM Last Glacial Maximum

lLGM local Last Glacial Maximum

MISI Marine Ice Sheet Instability

MnIS Minch Ice Stream

MTBH Mid-trough Bedrock High

NROY Not Ruled Out Yet

OSL Optically Stimulated Luminescence

PDD Positive Degree Day

RSL Relative Sea Level

SIA Shallow Ice Approximation

SMB Surface Mass Balance

SST Sea Surface Temperature

TCN Terrestrial Cosmogenic Nuclide

Chapter 1

Introduction

As the climate continues to warm in the 21$^{\text{st}}$ century, there is an urgent need to understand the Antarctic and Greenland ice sheets' response to climate change. The polar ice sheets have a combined volume large enough to raise sea level by more than 65 meters, while some of the world's largest cities, critical infrastructure, agricultural regions, and natural habitats are less than 1 metre above sea level (Lenton et al., 2019). A challenge of projecting the future evolution of ice sheets is that polar ice sheets have been relatively stable for as long as observations have been possible, so the scale of expected change is far beyond what we see in the observational record. A key uncertainty is what role ice streams (fast flowing regions of an ice sheet) play during deglaciation.

However, over the past 2.5 million years ice sheets have varied in size considerably, with periods when ice has been more limited, and periods when ice has been much more extensive than the contemporary ice sheets (Lowe and Walker, 2014). Palaeo ice sheets also provide a record of past ice stream evolution. By investigating the behaviour of palaeo ice sheets we can better understand the mechanisms of future ice sheet change. In this thesis, I use a numerical model to investigate the role of ice streams in the demise of the British-Irish Ice Sheet (BIIS).

1.1 Context of this thesis

The Quaternary is the current geological period, which begun 2.5 million years ago. During the Quaternary, the climate oscillated between brief comparatively warm interglacial periods, such as the contemporary climate, and longer cold glacial periods, globally about 4-7 °C cooler than pre-industrial temperatures (Jouzel et al., 2007). The glacial periods allowed the extension of large ice sheets across the Northern Hemisphere, causing a ∼134 m lowering of sea level compared to today (Lambeck et al., 2014). These ice sheets had large impacts on the entire earth system, including global atmospheric and oceanic circulation (e.g. Hoskins and Karoly, 1981; Clark et al., 2001; Ivanovic et al., 2017; Löfverström and Lora, 2017; Gregoire et al., 2018).

The millennial scale oscillations of the Quaternary climate are caused by the interaction of three cycles of the earth's orbit around the sun (Figure 1.1); the cycles of eccentricity, obliquity, and precession (Milankovitch, 1941).

- Eccentricity is the shape of the earth's orbit, and has a periodicity of 100 ka. High eccentricity means the earth's orbit is more elliptical, while low eccentricity means a less elliptical orbit.

- Obliquity, or axial tilt, is the angle of the earth's rotational axis compared to its orbital plane, and has a periodicity of 41 ka. Greater obliquity increases the seasonality of the climate.

- Precession alters the direction of axial tilt when the earth is at perihelion (when the earth is closest to the sun due to its orbital eccentricity), and has a periodicity of 23 ka. Today the earth is at perihelion during the austral summer, partly the cause of more extreme summers in the southern hemisphere.

In combination, these cycles vary the amount and spatial distribution of solar radiative energy received through a year. This is the most fundamental input to
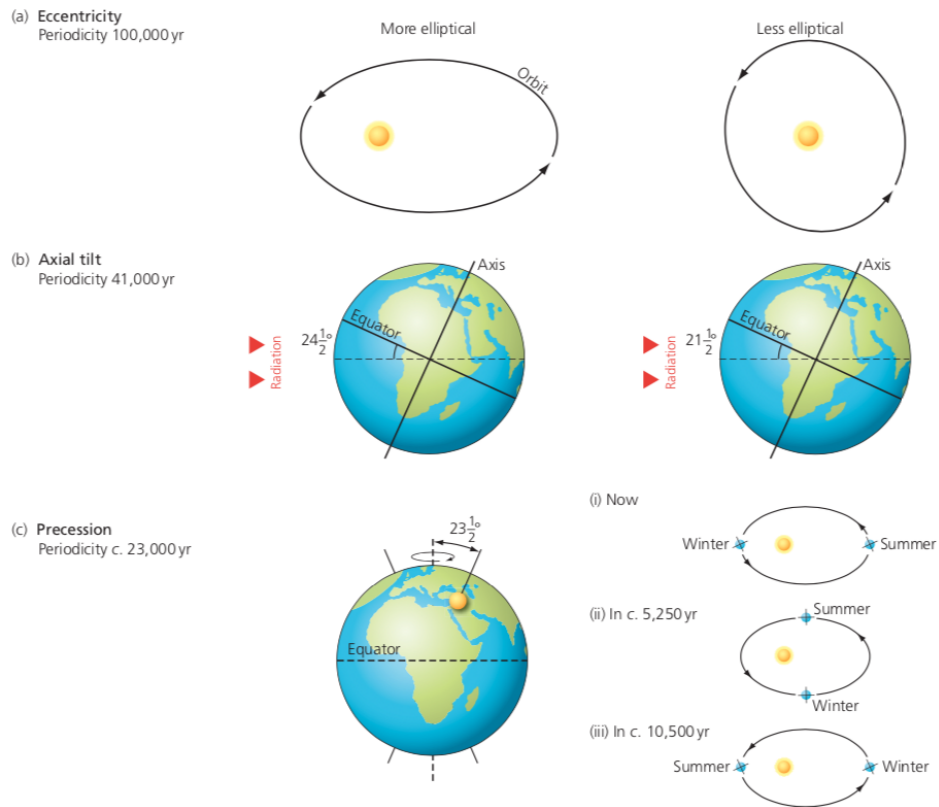
Figure 1.1: A summary of the three components of the Milankovitch orbital cycles; eccentricity, obliquity (or axial tilt), and precession. From Benn and Evans (2010).

the earth's climate system, and there are subsequent amplifying feedbacks within the atmosphere, ocean, and cryosphere. Once these amplifying feedbacks are considered, the temperature change is considerable enough to allow the growth of large ice sheets, covering most of North America and Europe (Figure 1.2), and lowering global sea levels by more than 100 m.
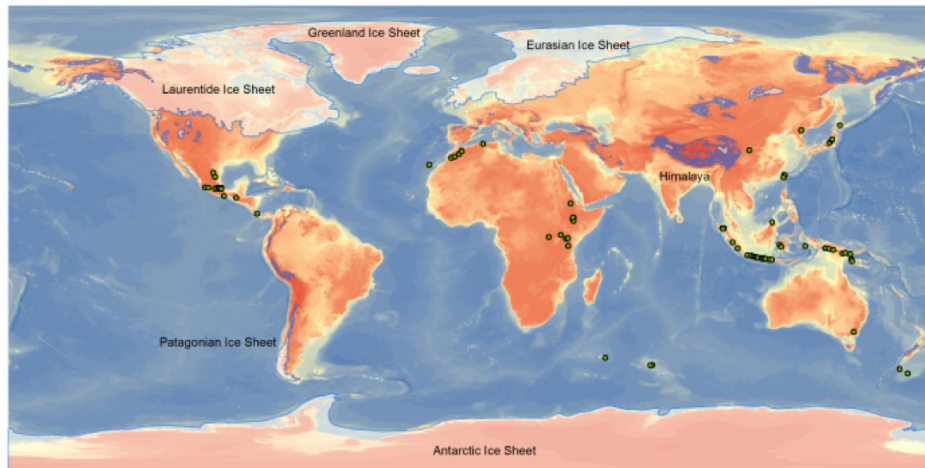
Figure 1.2: Ice sheet extent at the Last Glacial Maximum. Maximum extent is non-synchronous, $\sim$27-21 ka BP. From Ehlers et al. (2011).

1.2 Ice Sheets

Ice sheets are large ($>$50,000 km^2) bodies of ice that subsume the topography they sit on, and flow largely independently of undulations of the bed (Benn and Evans, 2010, p.6). In an idealised case, ice sheets accumulate mass in the accumulation zone through precipitation onto the ice sheet (Figure 1.3). Mass is lost in the ablation zone, at the margins of the ice sheet through both surface melting and calving into the ocean. Surface melting is often seasonal, and causes melted ice to runoff from the ice sheet.

Mass is transported from the accumulation zone to the ablation zone by ice flow. Ice flow is a combination of ice deformation under the force of gravity, and sliding between the ice sheet and its bed. An ice sheet in equilibrium will accumulate the same amount of mass as is lost through ablation and calving, and mass is transported between the accumulation and ablation zones through ice flow.

However, ice flow is heterogeneous across an ice sheet. The majority of ice flux is concentrated into ice streams, narrow corridors of fast ice flow (Rignot et al., 2011). Ice streams account for 90% of the discharge of the Antarctic Ice Sheet, despite only accounting for 13% of the ice sheet perimeter (Morgan et al., 1982). Ice streams are spatially and temporally variable, and can shutdown, reactivate,
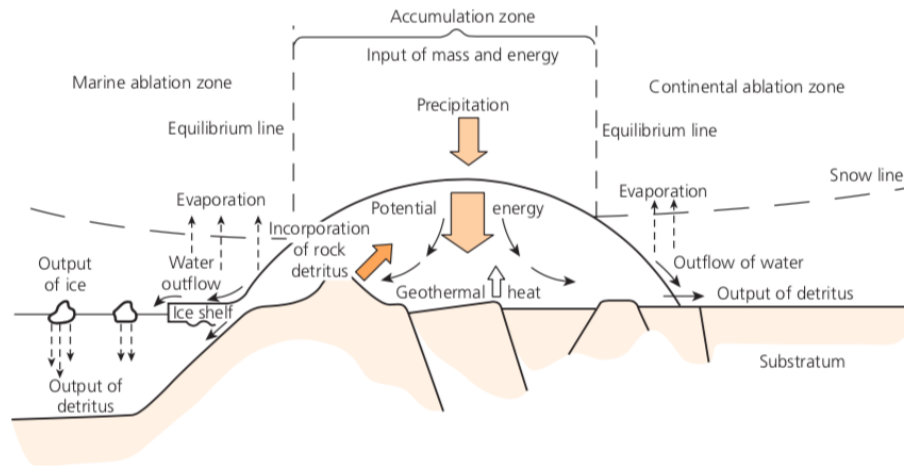
Figure 1.3: An idealised schematic of the key ice sheet processes of accumulation, ablation, and flow. From Brodzikowski and Loon (1991).

and migrate laterally (e.g. Conway et al., 2002; Joughin et al., 2005; Stokes et al., 2009; Ó Cofaigh et al., 2010). A motivation for studying ice stream processes is that large ice streams like the Pine Island Glacier and Thwaites Glacier are key points of vulnerability for the future evolution of the West Antarctic Ice Sheet (Shepherd et al., 2001; Jacobs et al., 2011; Tinto and Bell, 2011; Joughin et al., 2014). Given the importance of ice streams on ice sheet behaviour, it is impossible to understand long-term ice sheet evolution without considering long-term ice stream evolution (Winsborrow et al., 2010). A comprehensive map of ice streaming for contemporary ice sheets can be produced using satellite data (Rignot et al., 2011), and mapped for palaeo ice sheets using various reconstruction techniques (Margold et al., 2015) (Figure 1.4).
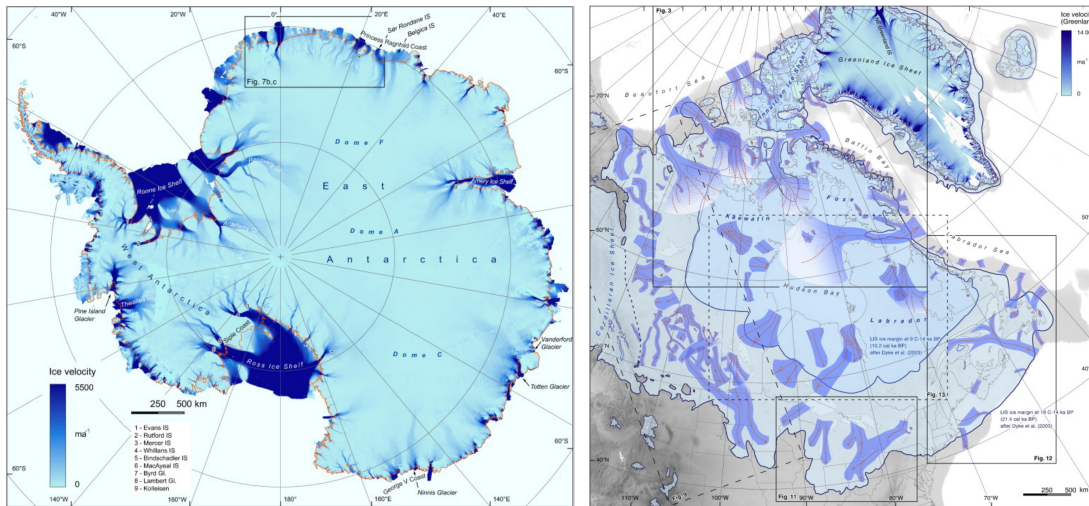
Figure 1.4: Observed ice velocities of the Antarctic Ice Sheet (left) and reconstructed ice streams of the North American Ice Sheet (right). Modified from Margold et al. (2015).

1.3   Reconstructing Ice Sheets

The extent, behaviour, and timing of past ice sheets can be reconstructed using a variety of empircal techniques. Perhaps the most fundamental method of reconstructing past ice sheets is through the identification and mapping of moraines. Moraines are ridges or mounds of material formed at the margin of a glacier or ice sheet, and thus after glacial recession they can be used to reconstruct the position of past margins. Landforms are also created in the subglacial environment of palaeo ice sheets, and are subsequently preserved following deglaciation. These landforms are key to reconstructing the behaviour of palaeo ice sheets, using the "glacial inversion" technique (Kieman and Borgström, 1996; Kleman et al., 2007). The mapping of subglacial landforms has been greatly accelerated by the advent of remote sensing techniques and Geographical Information Systems (GIS). Palaeo subglacial landforms form a "palimpsest" record – flow patterns are not formed synchronously, rather they are snapshots of various stages of an ice sheet's evolution (Boulton and Clark, 1990). By grouping areas of landforms together they form flowsets (Greenwood and Clark, 2008; Hughes et al., 2014), which can cross-cut each other.

Subglacial bedforms are commonly divided based on distinctions in scale and morphology (Ely et al., 2016). Flutes, drumlins, and Mega Scale Glacial Lineations (MSGL) all form aligned with palaeo ice flow. Flutes are small features, in the order of 1-10 m long, and 0.1-1 m wide (Gordon et al., 1992). Their small scale means they have poor preservation capability on palaeo ice sheet beds. Drumlins are larger features, typically 250-1000 m along-flow and 120-300 m across-flow, and MSGL are the largest and most elongate features, typically 1-9 km along flow and 100-200 m across flow (Spagnolo et al., 2014). Ribbed moraine (a subglacial feature, not in fact a glacial moraine) form transverse to flow direction, and are typically 300-1200 m across flow, and 150-300 m along flow (Hättestrand and Kleman, 1999). Ribbed moraine are indicative of slow or cold based ice flow, drumlins intermediate flow, and MSGL and highly elongate drumlins of fast flow and ice streaming (Ely et al., 2016).
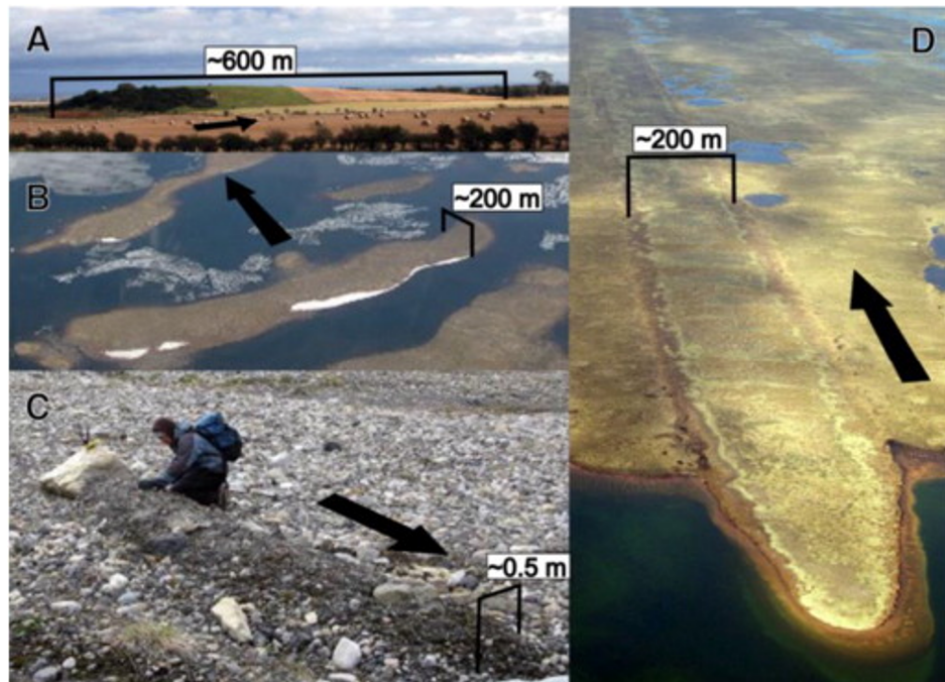
Figure 1.5: A variety of subglacial bedforms, with their orientation of ice flow indicated with black arrows. a) A drumlin, b) ribbed moraine, c) a flute, and d) a MSGL. From Ely et al. (2016).

Reconstructing the position of palaeo ice streams is particularly useful because ice streams are a key control on the dynamic behaviour of ice sheets (Hubbard

et al., 2009; Stokes et al., 2009; Stokes et al., 2016). Early mapping of palaeo ice stream location was based on the position of topographic troughs (e.g Dyke and Prest, 1987). This was later complemented with geologic evidence, such as erratic dispersal patterns (Dyke and Morris, 1988), convergent flowsets at a palaeo ice stream onset zones (Punkari, 1994), and the mapping of MSGL (Clark, 1993).

All the geological and geomorphological evidence used to reconstruct palaeo ice sheets is more valuable if it can be dated. Dating evidence for palaeo ice sheets usually comes from cosmogenic nuclide dating, luminescence dating, and radiocarbon dating;

- Cosmogenic dates are used extensively as a tool for ice sheet reconstruction (Bierman, 2007), and it can provide a constraint on both lateral and vertical ice sheet extent. Cosmogenic nuclides form in surface rocks because of bombardment by high-energy cosmic rays (Balco, 2011). This means the longer a rock is exposed, the greater the cosmogenic nuclide concentration at the surface. This is used to determine an age of exposure. Cosmogenic nuclides do not penetrate deep into a rock, so erosion of the surface (potentially during a glacial cycle) is adequate to reset the signal. An ideal sample for cosmogenic dating has no exposure to cosmic rays prior to glaciation, and no shielding from cosmic rays subsequent to glaciation. Therefore, geomorphological uncertainty can cause a large uncertainty in Cosmogenic nuclide dates.

- Optically Stimulated Luminescence (OSL) dating can date glacial landforms containing sand, such as sediments in glacial streams. When quartz-rich sediment is buried it is exposed to radiation from the surrounding sediment, accumulating a luminescence signal. When the sediment is exposed to sunlight any previous luminescence signal is removed. OSL ages constraining the Eurasian Ice Sheet demonstrate agreement with radiocarbon ages (Murray et al., 2007). Partial bleaching of the OSL signal is a chal-

lenge to producing reliable OSL dating constraints on ice sheet retreat. Incomplete bleaching causes ages to be older than expected.

- Radiocarbon dating can provide a date for organic material above or beneath glacial sediments, constraining the timing of a glacial advance or retreat. An isotope of carbon, ^{14}C, is absorbed by living organisms, and decays according to a known half-life following the death of the organism. Radiocarbon ages are subject to similar stratigraphic uncertainties as OSL and Cosmogentic dating, and the short half-life of ^{14}C means it cannot be used to date samples greater than $\sim$40,000 years old. Radiocarbon ages have been used extensively to constrain ice sheet margins, and have been combined into maps of large areas to reconstruct the timing of deglaciation of large ice sheets (Dyke, 2004; Hughes et al., 2011).

All methods for dating ice sheets have errors and limitations, and therefore it is useful to combine all three methods when reconstructing a palaeo ice sheet. For example, the DATED-1 project provides a database of 904 cosmogenic, 787 OSL, and 3756 radiocarbon dates to constrain the retreat of the Eurasian Ice Sheet (Hughes et al., 2011). Efforts have also been made to quality control dates in the literature (Small et al., 2017), which becomes particularly useful when reconstructing ice sheets with a large number of dates. Ultimately, dating palaeo glacial retreat provides evidence for rapid changes associated with ice sheet instabilities (e.g. Andrews et al., 1995; Davies et al., 2017; Bradwell et al., 2019b).

1.4 The British-Irish Ice Sheet

The British-Irish Ice Sheet was an ice sheet covering Ireland and northern Great Britain, last at maximum extent $\sim$27-23 ka BP (Clark et al., 2012). Reconstructions of the British-Irish Ice Sheet (BIIS) have existed for over a century, with Charles Lyell first becoming convinced that surficial deposits in Britain were of

glacial origin in the 1860s (Imbrie, 1979). Archibald Geikie produced a reconstruction of the extent of the BIIS in 1886 (Figure 1.6).

Figure 1.6: A reconstruction of the British-Irish Ice Sheet from 1886, a remarkably similar maximum extent to contemporary reconstructions (Clark et al., 2012), despite the sparsity of data. From Geikie (1886).

This historical reconstruction of the BIIS presents an ice sheet with extensive marine sectors. In the second half of the 20th century, the reconstructed extent of the BIIS became much smaller, with limited ice extent in south-west Ireland (McCabe, 1987), and no confluence between the BIIS and the Fennoscandian Ice Sheet in the North Sea (Balson and Jeffery, 1991; Bowen et al., 2002). With the advent of remote sensing techniques, the quantity of terrestrial geomorphological mapping greatly increased in the 1990s and 2000s (Clark et al., 2004; Smith et al., 2006), resulting in an ice sheet wide reconstruction of the BIIS from 30 to 15 ka BP (Clark et al., 2012). It was shown that ice was extensive across the British Isles, with significant offshore sectors and confluence with the Fennoscandian Ice Sheet (Figure 1.7). It was also shown that different sectors of the BIIS reached and receded from maximum extent at different times.

However, the Clark et al. (2012) reconstruction required assumptions of ice extent in large areas of the BIIS, particularly in marine sectors where geomor-
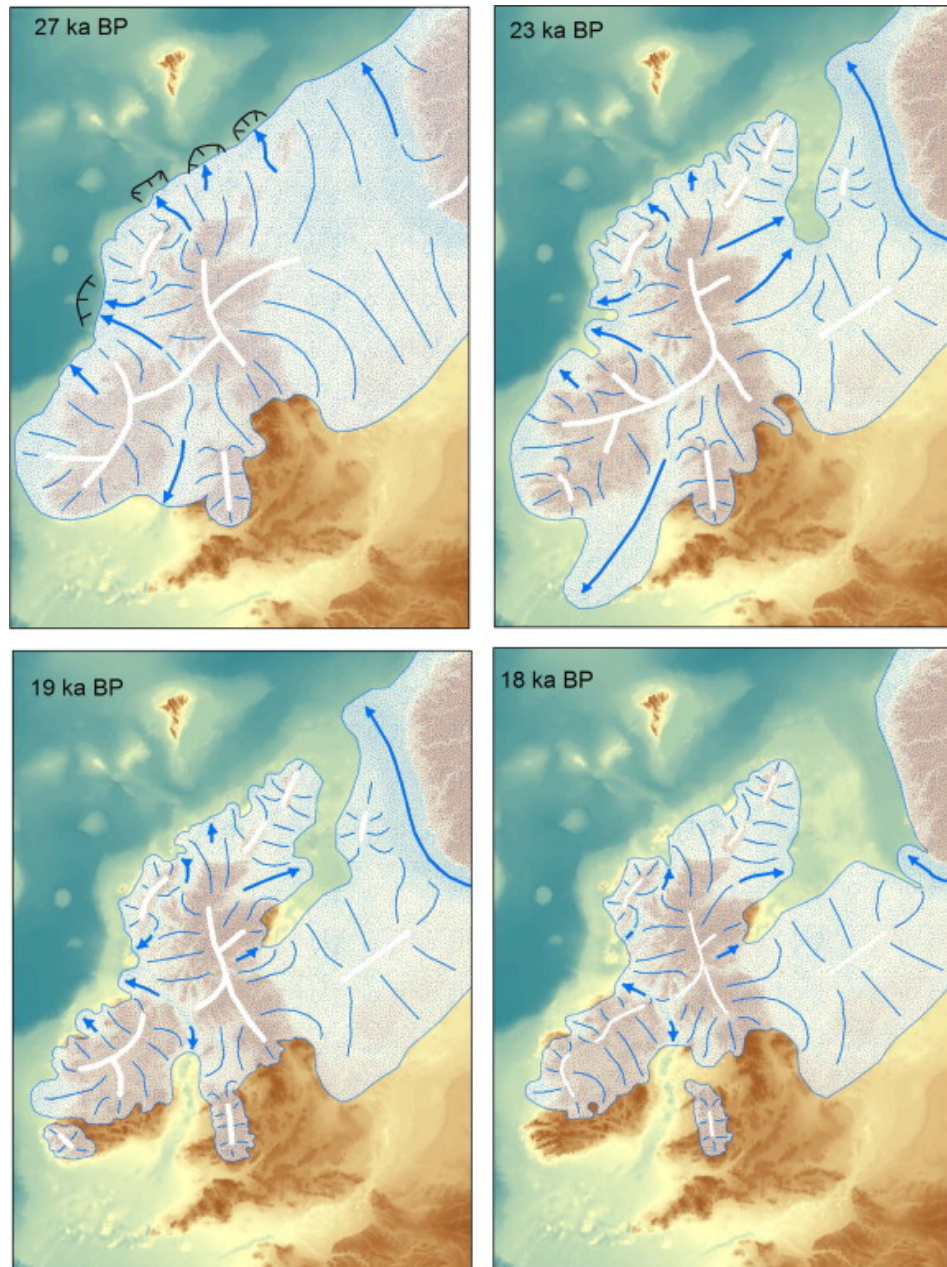
Figure 1.7: Reconstructed ice extent from Clark et al., 2012 at 27, 23, 19, and 18 ka BP. Empirical evidence is well constrained terrestrially, but relies on more inferred knowledge offshore. From Clark et al. (2012).

phological mapping and dating evidence was scarce. This is problematic because researching the deglaciation of the BIIS was partly motivated by potential analogues between the BIIS and contemporary marine ice sheets, but the marine sectors of the BIIS were the least well constrained, particularly in respect to dates and rates of retreat.

The BRITICE-CHRONO project, beginning in 2014, aimed to build on the prior reconstructions of the BIIS to become the best constrained ice sheet of the palaeo record. Two research cruises were used to collect shallow seismic reflection data and sediment cores orthogonal to the direction of retreat of the BIIS. The research cruises collected 18,000 km of shallow seismic data, 174 Terrestrial Cosmogenic Nuclide (TCN) dates, 146 OSL dates, and 333 radiocarbon dates. This large increase of empirical data led to ice sheet reconstructions of individual sectors of the BIIS (Callard et al., 2018; Chiverrell et al., 2018; Roberts et al., 2018; Wilson et al., 2018; Bradwell et al., 2019a,b; Ó Cofaigh et al., 2019; Scourse et al., 2019) and an overall ice sheet wide reconstruction (Clark et al., in prep).

Work from BRITICE-CHRONO has provided further evidence of an extensive BIIS. Evidence of ice reaching the Porcupine Bank (Lee Peters et al., 2015) and the continental shelf in the Celtic Sea (Praeg et al., 2015) show the ice sheet was more extensive than previously assumed (Clark et al., 2012). The project has also further demonstrated the non-synchronous behaviour of the BIIS, with early retreat in the northwest of the ice sheet (Callard et al., 2018; Bradwell et al., 2019b; Ó Cofaigh et al., 2019), before the southern margin of the ice sheet had reached maximum extent (Chiverrell et al., 2018). After over a century of reconstructions, the BIIS is now the best reconstructed ice sheet in the record. A small, dynamic, marine based ice sheet, rich in empirical data, it is a useful analogue to test ice sheet models also used to project the future of the Greenland and Antarctic Ice Sheets.

A key target outcome of BRITICE-CHRONO was the "engagement of modelling and evidence-based communities". As part of that target outcome, I attended a series BRITICE-CHRONO Ice Sheet Modelling Workshops, allowing engagement with the empirical community. This partnership also allowed access to geophysical data, mapping, and deglaciation ages collected as part of BRITICE-CHRONO, and to discuss evolving interpretations of the data. This engagement directly influenced model experimental design and subsequent interpretation.

1.5 Numerical Models of Ice Sheets

A numerical ice sheet model is a tool to explore the behaviour of a complex ice sheet system. Physical processes of ice sheets are observed, mathematically described, and then included as computer code. Numerical ice sheet models use a number of different approximations to simulate ice flow, generally from models with lots of assumptions (which are computationally cheap), to models with fewer assumptions (which can be computationally costly). Each type of ice sheet model has its benefits and appropriate use cases (Figure 1.8). The simplest (and computationally cheapest) 3D ice sheet models use a Shallow Ice Approximation (SIA) to calculate ice flow. SIA models do not include lateral drag with neighbouring valley walls or slower ice. It assumes that the basal shear stress of ice is balanced by the gravitational driving stress. SIA models are computationally cheap and therefore useful for particularly long palaeo ice sheet runs. However, a purely SIA ice sheet model cannot represent marine ice sheet dynamics, ice shelves, or ice streams (Hindmarsh, 2004).
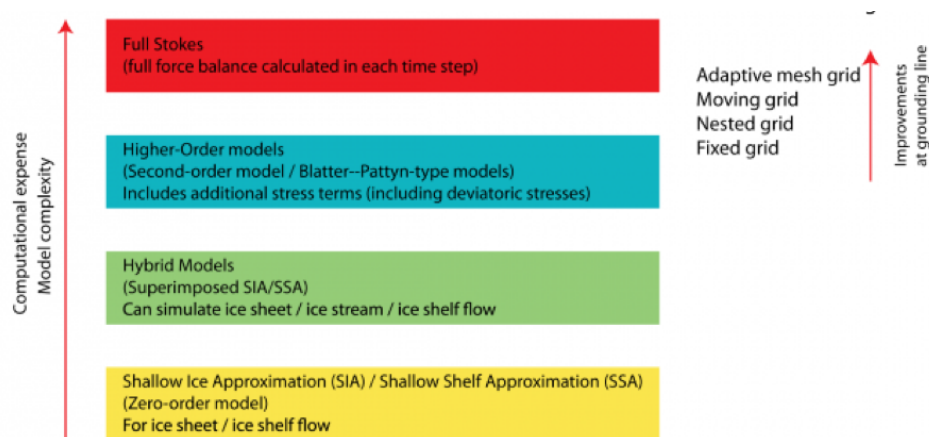
Figure 1.8: The "hierarchy of ice sheet models", from simple and computationally cheap at the bottom, to complex and computationally costly at the top. Modified from "An introduction to the hierarchy of ice sheet models", (Davies, 2015).

For ice shelves, where the basal shear stress can be assumed to be zero, a Shallow Shelf Approximation (SSA) can be used. However, an SSA model does not account for vertical variations in ice velocity, and therefore is not suitable for modelling the majority of an ice sheet. SIA and SSA models can be combined

into a Hybrid model. Hybrid models use the SIA approximation for the majority of the grounded ice sheet, SSA approximation from modelling ice shelves, and a combination in areas of ice streaming to account for basal sliding. Hybrid models are computationally efficient and have been used to simulate ice sheet evolution over long timescales, both for palaeo ice sheets (e.g. Seguinot et al., 2016, 2018; Niu et al., 2019) and future projections of contemporary ice sheets (Golledge et al., 2017; Aschwanden et al., 2019; Feldmann et al., 2019). PISM, a hybrid model, has demonstrated a good match to observations of ice stream position and velocity (Aschwanden et al., 2013). However, Hybrid models are unable to accurately simulate grounding line migration (Pattyn et al., 2012), a mechanism which is important to simulating the future of the West Antarctic Ice Sheet (Favier et al., 2014; Cornford et al., 2015).

The enhanced velocity of ice streams is facilitated by sliding between an ice sheet and its bed. Sliding where an ice sheet is frozen onto the bed is negligible (Fowler, 1986; Weber, 2000), but where a thin film of water exists sliding can become the dominant component of ice velocity. Runaway fast ice flow is stopped by non-local influences of sliding rates, including friction at the ice sheet bed, the form drag of the bed, and the influence of frozen beds. Sliding was expressed mathematically first by Weertman (1957), and then expressed with more realistic bed geometries by Nye (1969, 1970). Boulton (1982) describes the friction drag beneath ice sheets based on the Mohr-Coulomb equation, where basal drag is a function of the effective pressure and the fraction of the bed covered with debris, accounting for the deformation of a till layer between ice and bedrock. Numerous sliding laws have since been developed (e.g. Iverson et al., 2003; Tsai et al., 2015), and sliding laws are an essential component to accurately simulating ice sheet evolution.

A higher-order model incorporates effects not present in SIA, SSA, and hybrid models. These include longitudinal stresses, or "membrane stresses" (Hindmarsh, 2006). Higher-order models can accurately simulate grounding line migration

(Pattyn et al., 2012), but are computationally expensive, traditionally meaning that they were not suitable for simulations of large domains or long timescales. However, innovations in ice sheet model meshes have cut the computational requirements of higher-order models. For example, the BISICLES ice sheet model uses an adaptive mesh, where a series of nested grids can provide higher resolution at ice streams and the grounding line of an ice sheet (Figure 1.9). The configuration of these nested grids is recalculated as the ice sheet evolves, meaning that the high-resolution region can track the evolution of the grounding line. An unstructured mesh can also be used, as in the Úa ice sheet model (Gudmundsson, 2013), where the ice flow equations are solved on a mesh consisting of linear, quadratic, or cubic triangular elements. These innovations in ice sheet model meshes, along with increasing compute power, has allowed higher-order models to be used to simulate increasingly large domains and timescales (Seddik et al., 2012; Cornford et al., 2015; Lee et al., 2015).

Finally, Full Stokes models account for all 9 stress tensors of ice sheet flow, and therefore offers the best simulation of grounding line dynamics (Pattyn et al., 2012), although the benefits for modelling the ice sheet interior are minimal compared to lower-order models. Full stokes models are the most computationally expensive method of solving the ice flow equations, but savings can be made by just using the Full Stokes method near the ice sheet margin, while using a lower-order approximations for the majority of the ice sheet interior (Seroussi et al., 2012). However, Full Stokes models, or partial Full Stokes models, generally remain too computationally expensive to apply to large domains and timescales.
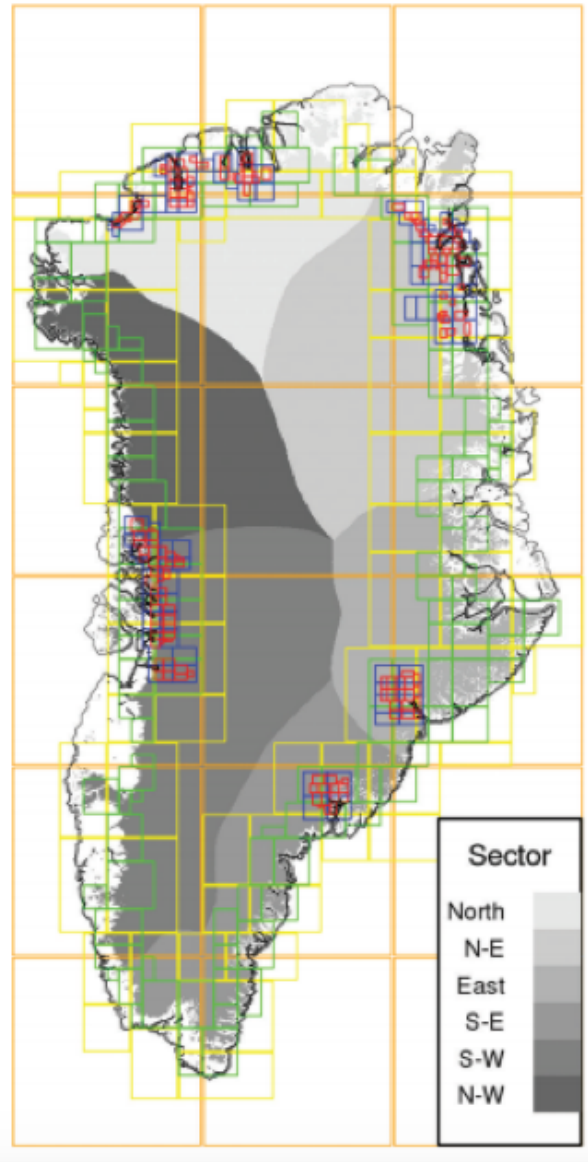
Figure 1.9: Adaptive mesh structure from a simulation of the Greenland Ice Sheet using BISICLES, with increasing resolution from 8 km (orange boxes), to 500 m (red boxes). From Lee et al. (2015)

1.6 Modelling the BIIS

A number of previous modelling experiments use the palaeo record of the BIIS. The BIIS is an ideal domain for model experiments because it is relatively small (about 1/3 the size of the West Antarctic Ice Sheet), has significant marine grounded sectors (Clark et al., 2012), is highly dynamic (e.g. Clark et al., 2012; Callard et al., 2018; Chiverrell et al., 2018; Bradwell et al., 2019b), and has a wealth of empirical data for extensive model-data comparison (Ely et al., 2019).

Geoffrey Boulton pioneered modelling the BIIS, whilst considering the growing knowledge of the ice sheet from geomorphological and geological surveys (Boulton et al., 1977). As well as aiming to replicate the deglaciation pattern inferred from the geomorphological evidence, these studies also helped to answer a number of ice dynamics questions. Boulton et al. (2003) highlighted the impact of topography in ice streaming dynamics, and the impact on overall ice sheet thickness. Boulton and Hagdorn (2006) used an ice sheet model driven by proxy climate data to suggest that the BIIS and the Fennoscandian Ice Sheet were confluent at the LGM, which has now been supported by geomorphological evidence from the North Sea (Sejrup et al., 1994; Graham et al., 2007).
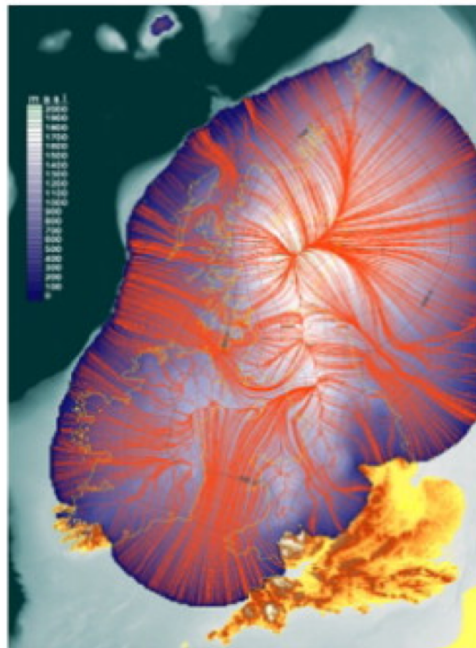
Figure 1.10: Snapshot of flowlines for the BIIS near maximum extent in a simulation of the full glacial cycle. Modified from Hubbard et al. (2009).

Hubbard et al. (2009) modelled the growth and retreat of the BIIS in the last glacial cycle, using a 3D thermo mechanical model, climatically forced using a Positive Degree Day (PDD) mass balance scheme (Figure 1.10). The results show a "twitching" ice sheet, that was rarely stationary. Simulations used the same model to simulate the advance of a Scottish ice cap during the Younger Dryas

(Hubbard, 1999), the Patagonian Ice Sheet (Hubbard et al., 2005), and the Welsh Ice Cap (Patton et al., 2013a,b).

A limitation of these experiments is that by using the Shallow Ice Approximation (SIA), incorporated with a sliding law, ice stream processes are poorly represented (Jackson and Kamb, 1997; Harrison et al., 1998). Indeed, the simulated pattern of ice stream behaviour has some differences to patterns observed in the contemporary record. This modelling approach also requires a grounding line parameterisation. In the Hubbard et al. (2009) simulations, confluence with the Fennoscandian Ice Sheet was also omitted, avoiding the need to model the entire Eurasian Ice Sheet, or prescribe a flux across the North Sea. More recently, however, Patton et al. (2016) and Patton et al. (2017) used the model to simulate the entire Eurasian Ice Sheet complex for the growth and retreat of the last glacial cycle. These simulations proved to be a good match to empirical data in the majority of sectors, but could not simulate the deglaciation of the North Sea if the maximum extent is allowed to advance as far as empirical evidence shows (Sejrup et al., 1994; King et al., 1998; Nygård et al., 2005). These simulations are subject to the same limitations of using the SIA.

Limitations of Previous Work
1. Empirical reconstructions of the BIIS assume marine influence from palaeo topography
2. Empirical reconstructions are unable to reconstruct ice shelves
3. Simulations of the BIIS lack the grounding line resolution to accurately simulate marine dynamics
4. Simulated ice streams of the BIIS are a poor match for the empirical evidence of ice stream location
5. The deglaciation dynamics of the North Sea have not been simulated in a way that is consistent with the majority of empirical data
6. The wide-ranging empirical data is rarely fully used to validate model simulations

Table 1.1: Limitations of previous empirical and modelling reconstructions of the BIIS.

Despite a wealth of simulations of the BIIS, there remain a number of challenges and opportunities to modelling the ice sheet. Prior simulations use a relatively coarse grounding line resolution and grounding line parameterisation (e.g. Hubbard et al., 2009; Patton et al., 2016, 2017) which has been shown to

be unable to accurately simulate grounding line migration (Pattyn et al., 2012). Higher order ice flow physics are also required to model ice streams of consistent width with varying resolution (Hindmarsh, 2009), but this is not used in previous simulations of the BIIS (e.g. Boulton and Hagdorn, 2006; Hubbard et al., 2009). Finally, the separation of the BIIS and the Fennoscandian Ice Sheets in the North Sea during the last deglaciation was only simulated in Patton et al. (2017) when the confluence of the two ice sheets was weak, whilst empirical evidence suggests a more extensive confluence (Hughes et al., 2016). Therefore, the deglaciation dynamics of the North Sea sector of the ice sheet has not yet been simulated in a manner that respects the majority of empirical evidence.

1.7 Research Aim

In the context described in the previous section, the aim of this thesis is;

To investigate the role of ice dynamics in the evolution of the British-Irish Ice Sheet.

Ice sheet model simulations, using the BISICLES ice sheet model, were used to address this aim. BISICLES is a marine ice sheet model, with L1L2 physics retained from the full Stokes equations (Cornford et al., 2013). BISICLES also has an adaptive mesh, allowing higher resolution at the grounding line, addressing point 3 (Table 1.1). To address limitations 1 and 2, I set out to demonstrate the marine influence on the BIIS numerically in a region where marine influence has been suggested from empirical evidence. New ice sheet model development to better simulate palaeo ice stream initiation and evolution addresses limitation 4, and this is used to simulate the deglaciation of the North Sea, addressing limitation 5. New model-data comparison tools are used to test new model results, addressing limitation 6.

1.8 Research Questions

To investigate the role of ice sheet dynamics, I have identified 3 research questions (Table 1.2). Each research chapter of this thesis (Chapters 2-4) address 2-3 research questions.

Research Questions (RQ)	Chapters
RQ1: What was the role of marine processes in the deglaciation of the British-Irish Ice Sheet?	2+4
RQ2: How can the position, spacing, and evolution of ice streams of the British-Irish Ice Sheet be accurately simulated?	2+3
RQ3: How can ice stream dynamics interact with other mechanisms driving deglaciation?	2+3+4

Table 1.2: A summary of the research questions addressed in this thesis. Further detail is provided in the subsequent sections.

1.8.1 RQ1: What was the role of marine processes in the deglaciation of the British-Irish Ice Sheet?

Potential similarities between the BIIS and the West Antarctic Ice Sheet are a key motivation for the extensive study of the deglaciation of the BIIS. A key similarity is the marine nature of both ice sheets; the majority of the BIIS was grounded below sea level at the last glacial maximum (Bradley et al., 2011; Clark et al., 2012). Many contemporary Antarctic ice streams are also marine based (Jenkins et al., 2010; Ross et al., 2012; Joughin et al., 2014), and are therefore vulnerable to Marine Ice Sheet Instability (MISI). Schoof (2007) demonstrated that no stable grounding line position is possible in areas of reversed bed slope. Consequently, an initial small retreat of the grounding line into a region of reversed bed slope can trigger a rapid and considerable grounding line migration (Schoof, 2007; Pattyn et al., 2012).

However, it has been shown that simulations of grounding line migration require not only consideration of bed topography, but also ice shelf buttressing, as the buttressing effect of an ice shelf can allow a stable grounding line on a retrograde bed slope (Gudmundsson, 2013). Ice shelves have a buttressing effect on the ice streams upstream of them, and the removal of large ice shelves in the

Antarctic peninsula has been linked with the subsequent acceleration and thinning of upstream glaciers (Scambos et al., 2004). This important mechanism is hard to empirically reconstruct for palaeo ice sheets as there is no clear geomorphic signature for the presence of an ice shelf. Therefore, modelling techniques are best to consider the effect of palaeo ice shelves.
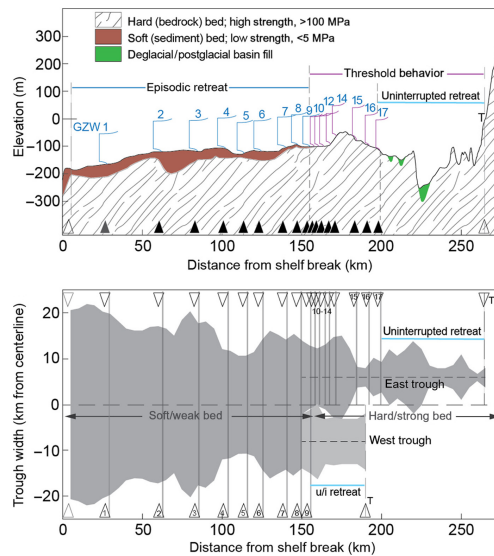
Figure 1.11: Empirical evidence of an instability during the retreat of the Minch Ice Stream, controlled by the depth (top panel) and width (bottom panel) of a topographic trough. From Bradwell et al. (2019b).

Contemporary ice streams have been shown to either be experiencing, or be vulnerable to, MISI (Favier et al., 2014; Joughin et al., 2014). MISI has also been empirically suggested for the Minch Ice Stream (Bradwell et al., 2019b), a large ice stream of the BIIS. This is inferred from an acceleration of retreat once the Minch Ice Stream enters a region of retrograde slope (Figure 1.11). However, unlike for the West Antarctic Ice Sheet, the potential for MISI of the BIIS has not been demonstrated numerically, and therefore the potential for MISI during deglaciation of the BIIS is uncertain.

1.8.2   RQ2: How can the position, spacing, and evolution of ice streams of the British-Irish Ice Sheet be accurately simulated?

Models of contemporary ice sheets can achieve a close fit to observed ice surface velocity using an optimisation technique to determine subglacial friction parameters (Morlighem et al., 2013). Spatially varying basal friction and ice softness parameters accounts for unknown bed and englacial properties. BISICLES simulations of contemporary Greenland (e.g. Lee et al., 2015) and Antarctica (e.g. Favier et al., 2014; Cornford et al., 2015) are a strong match for the empirical evidence, and do not allow the basal friction parameters to vary through time. However, centennial to millennial projections of future ice sheet change will require ice stream modelling that is capable of simulating ice stream evolution (Aschwanden et al., 2013; Aschwanden et al., 2019).

Whilst contemporary observations can produce detailed information on current ice sheets, they do not record the multi-decadal, centennial and millennial variability of the ice stream activity and position. Limited contemporary ice stream evolution has been observed, with the most studied example being the change in discharge of ice streams along the Siple Coast of West Antarctica (Retzlaff and Bentley, 1993; Conway et al., 2002). Therefore, the history of contemporary ice sheet observation is not yet long enough to observe the results of significant margin changes, ice temperature evolution, or basal friction evolution. The record from palaeo ice sheets offers an opportunity to test methods for modelling ice streams against an archive spanning millennia, rather than a contemporary snapshot of ice streaming.

Testing an ice sheet model against the palaeo record requires confidence in the empirical data. The BIIS arguably offers the most complete archive of data constraining the behaviour of an ice sheet and several ice streams over millennia. Using this wealth of empirical evidence, numerous ice stream locations have been

reconstructed both onshore and offshore with evidence from subglacial lineations (Hughes et al., 2014), trough mouth fans (Bradwell et al., 2008), and topographic troughs. The rich empirical record of the BIIS evolution offers the opportunity to test the skill of a model in simulating ice streams in places they have been empirically reconstructed.

The friction at the bed of an ice stream is likely to evolve due to a number of processes that operate at different timescales. Over long (millennial) timescales, glacial erosion and deposition can alter the force balance of the bed. Erosion may change the shape of basal obstacles, altering the form drag between the ice and the bed (Schoof, 2002). Sediment deposition may also mask smaller basal obstacles, and change regions where sediment deformation occurs (Bingham et al., 2017; Davies et al., 2018). The most rapid change to basal friction can occur due to subglacial hydrology, as differences in water routing, subglacial floods, and supra-glacial water inputs can all dramatically alter the volumes and spatial patterns of water at the bed over short (diurnal to decadal) timescales (Nye, 1976; Smith et al., 2007; Hewitt and Fowler, 2008). Model results suggest ice stream discharge of the Laurentide Ice Sheet was reduced in the late deglaciation (Stokes and Tarasov, 2010), but it is uncertain how ice stream discharge varied in the early deglaciation (Ullman et al., 2015; Stokes et al., 2016), and if this behaviour is consistent across different ice sheets.

1.8.3 RQ3: How can ice stream dynamics interact with other mechanisms driving deglaciation?

It is well established that ice streams interact with other mechanisms to drive deglaciation. For example, it has been shown that increased surface melting can route to the ice sheet bed, and cause a subsequent seasonal acceleration of an ice stream (Zwally et al., 2002). It has also been shown in idealised experiments that raising the Equilibrium Line Altitude (ELA) causes an acceleration of ice streams, increasing the rate of deglaciation (Robel and Tziperman, 2016). The surface

profile of a streaming ice sheet causes depressions in the ice surface where ice velocity is higher, meaning that ice streams are more vulnerable to surface melting than inter-stream regions of the ice sheet. Millennial scale climate variability, such as Heinrich events, suggest ice streams contribute to rapid ice sheet change (Calov et al., 2002; Alvarez-Solas et al., 2010; Ziemen et al., 2014). Further understanding interacting mechanisms of deglaciation is necessary to decrease the uncertainty of future ice sheet projections.

1.9   Research Approach

I address the research questions with a series of ice sheet modelling experiments. I use the BISICLES ice sheet model, a higher-order marine ice sheet model with L1L2 physics retained from the full-stokes equations. BISICLES is able to accurately simulate grounding line evolution of marine ice sheets (Cornford et al., 2016), necessary for simulating the dynamics of the marine portions of the BIIS. The higher-order physics means that BISICLES can be developed to simulate ice streams in a manner that is consistent with varying horizontal resolution (Hindmarsh, 2009).

I run BISICLES simulations on the High Performance Computing Facilities (HPC) at the University of Leeds. Simulations run on one node, consisting of either 16 cores (Chapter 2), or 24 cores (Chapter 3+4). I found that parallelisation beyond one node produced diminishing returns in decreased simulation time, though this result is specific HPC dependent. Simulation outputs are in HDF5 format, and I converted the output to NetCDF4 for further analysis.

To investigate RQ1, the potential for MISI of the Minch Ice Stream is investigated using the BISICLES ice sheet model. A series of diagnostic model experiments remove the influence of other factors, like ice sheet elevation feedbacks or sea level changes, to isolate the effect of MISI. The ice sheet is forced to retreat through a step-change warming in the atmosphere and ocean, and at 800 year intervals the atmosphere and ocean is re-cooled to test for hysteresis in

the retreat of the ice sheet. With the lapse rate feedback removed and no MISI, there should be no hysteresis in the retreat of the Minch Ice Stream. A hysteresis of retreat, coincident with the ice stream reaching a retrograde bed slope, would provide numerical evidence of MISI of a major ice stream of the BIIS.

The deglaciation experiment is re-run with ice shelves forcibly removed. Any differences in the retreat history with and without an ice shelf can be attributed to the buttressing effect of the ice shelf. The Minch Ice Stream is a useful domain to test the effect of ice shelf buttressing, because there are significant changes to the ice stream terminus through retreat, including significant changes in trough width and depth (Bradwell et al., 2019b).

The influence of MISI is also investigated in Chapter 4, simulating the Norwegian Channel Ice Stream. A 70 member ensemble of simulations of the North Sea deglaciation is run at 8 km horizontal resolution in the North Sea, but one ensemble member is re-run at a higher (1 km) horizontal resolution in order to simulate the grounding line dynamics and potential MISI of the Norwegian Channel Ice Stream.

To investigate RQ2, for empirically well constrained ice streams, a basal friction coefficient map is produced to act as a boundary condition for simulating ice streams of the BIIS. Regions of similar basal friction are classified based on observable surface morphological features and superficial geology maps. Basal friction coefficients are based on values from simulations of contemporary ice sheets (Favier et al., 2014; Cornford et al., 2015). However, this does not account for ice stream evolution, or ice streams that have not been mapped in the empirical record. To apply simulations to regions less well empirically constrained, the BISICLES ice sheet model was developed to simulate the spontaneous generation of ice streams, using a basal sliding law dependent on basal water pressure. This development is tested both with a symmetrical idealised ice sheet, as used in previous studies simulating ice stream generation (Payne and Dongelmans, 1997; Hindmarsh, 2009), and on the bed of the BIIS, demonstrating the ability to sim-

ulate ice stream initiation and evolution using BISICLES. This development is referred to as BISICLES_hydro.

I apply BISICLES_hydro to model an idealised version of the BIIS. The BIIS offers a realistic bed geometry to test BISICLES_hydro, along with the extensive empirical record of ice streaming to help test the skill of the model in simulating ice stream positions. These experiments idealise the climate forcing; the experiments are not intended to act as a reconstruction of the BIIS, rather the BIIS acts as a test-bed for BISICLES_hydro to simulate reasonable ice stream width, spacing and position over millennia.

I set up the model domain to cover the entire BIIS, and use an idealised climate forcing to run a 10,000 year advance phase, followed by a 10,000 year retreat phase. By simulating an idealised glacial cycle, evolution in ice stream position can be observed, and compared to the empirical record. I compare the simulated ice streams to empirically mapped ice streams both with qualitative comparisons, and a quantitative tool that compares modelled and mapped flowsets.

Recent advances in ice sheet modelling motivate new simulations of the North Sea deglaciation. In particular, the BISICLES ice sheet model's higher-order physics and adaptive mesh allows the accurate simulation of marine sectors of ice sheets (Cornford et al., 2013), such as the North Sea. The work addressing RQ2 also means that it is possible to simulate the initiation and evolution of ice streams. This means that two important controls on the North Sea deglaciation – marine dynamics and the influence of the NCIS – can now be simulated with increased skill in Chapter 4.

To investigate RQ3, I produce an ensemble of simulations of the deglaciation of the North Sea, using the state of the art BISICLES ice sheet model. I compare our simulated deglaciation to empirical evidence of ice margins, deglaciation timing, and ice sheet flow direction, and help determine the considerable influence of the NCIS on the deglaciation of the North Sea sector of the Eurasian Ice Sheet. Using simulations of the deglaciation of the North Sea, I investigate the mechanisms of

deglaciation of the Norwegian Channel Ice Stream. This is assisted with high-resolution (1 km) simulations of the ice stream during particularly rapid periods of grounding line retreat. These simulations allow for different mechanisms driving the deglaciation of the Norwegian Channel Ice Stream to be explored, along with the interaction between those mechanisms. RQ3 is also investigated with the results from simulations of the deglaciation of the Minch Ice Stream (Chapter 2), and the evolving position and behaviour of ice streams simulated for the entire BIIS (Chapter 3).

1.10   Thesis structure

The main body of this thesis is composed of journal manuscripts at different stages of publication, which each address different research questions of the thesis, although the research questions cross-cut the chapters. Chapter 2, *Marine ice sheet instability and ice shelf buttressing of the Minch Ice Stream, northwest Scotland*, primarily addresses RQ1. Through a series of idealised diagnostic ice sheet model experiments, Marine Ice Sheet Instability is numerically demonstrated in the late stages of retreat of the Minch Ice Stream, a mechanism which has been subsequently supported empirically (Bradwell et al., 2019b). The role of ice shelf buttressing during the later stages of retreat is also tested and discussed. The content of this chapter is from a manuscript published in *The Cryosphere* in 2018 (Gandy et al., 2018).

RQ2 is primarily addressed in Chapter 3, *Exploring the ingredients required to successfully model the placement, generation, and evolution of ice streams in the British-Irish Ice Sheet*. This chapter described a new basal sliding scheme implemented into BISICLES, coupled to an idealised basal hydrology model. Using this model development, the majority of empirically reconstructed ice streams of the BIIS are successfully simulated, with the spacing and location of ice streams matching the empirical record well. The simulated ice streams also prompted new empirical mapping of streamlined subglacial features. The content of this

chapter is from a manuscript published in *Quaternary Science Reviews* in 2019 (Gandy et al., 2019).

Chapter 4, *Saddle Collapse of the Eurasian Ice Sheet in the North Sea caused by combined ice flow, surface melt and marine ice sheet instabilities*, primarily addresses RQ3. This chapter uses the developments to BISICLES described in Chapter 3 to simulate the separation of the BIIS and the Fennoscandian Ice Sheet in the North Sea, using a large ensemble of simulations. The simulations show the separation is based on ice stream dynamics, surface melting, and marine ice sheet instabilities, all interacting. The content of this chapter is from a manuscript ready for submission to the *Journal of Geophysical Research* (Gandy et al., in prep).

References

Alvarez-Solas, J., S. Charbit, C. Ritz, D. Paillard, G. Ramstein, and C. Dumas (2010). "Links between ocean temperature and iceberg discharge during Heinrich events". In: *Nature Geoscience* 3.2, pp. 122–126. DOI: 10.1038/ngeo752.

Andrews, J., B. Maclean, M. Kerwin, W. Manley, A. Jennings, and F. Hall (1995). "Final stages in the collapse of the laurentide ice sheet, Hudson Strait, Canada, NWT: 14C AMS dates, seismics stratigraphy, and magnetic susceptibility logs". In: *Quaternary Science Reviews* 14.10, pp. 983–1004. DOI: 10.1016/0277-3791(95)00059-3.

Aschwanden, A., G. Aðalgeirsdóttir, and C. Khroulev (2013). "Hindcasting to measure ice sheet model sensitivity to initial states". In: *The Cryosphere* 7, pp. 1083–1093. DOI: 10.5194/tc-7-1083-2013.

Aschwanden, A., M. A. Fahnestock, M. Truffer, D. J. Brinkerhoff, R. Hock, C. Khroulev, R. Mottram, and S. A. Khan (2019). "Contribution of the Greenland Ice Sheet to sea level over the next millennium". In: *Science Advances* 5.6, eaav9396. DOI: 10.1126/sciadv.aav9396.

Balco, G. (2011). "Contributions and unrealized potential contributions of cosmogenic-nuclide exposure dating to glacier chronology, 1990–2010". In: *Quaternary Science Reviews* 30.1-2, pp. 3–27. DOI: 10.1016/J.QUASCIREV.2010.11.003.

Balson, P. S. and D. H. Jeffery (1991). *The glacial sequence of the southern North Sea.* A.A. Balkema, Rotterdam, pp. 245–253.

Benn, D. I. and D. J. A. Evans (2010). *Glaciers and glaciation.* Hodder Education.

Bierman, P. (2007). "Cosmogenic glacial dating, 20 years and counting". In: *Geology* 35.6, p. 575. DOI: `10.1130/focus062007.1`.

Bingham, R. G. et al. (2017). "Diverse landscapes beneath Pine Island Glacier influence ice flow". In: *Nature Communications* 8.1, p. 1618. DOI: `10.1038/s41467-017-01597-y`.

Boulton, G. S., A. S. Jones, K. M. Clayton, and M. J. Kenning (1977). "A British ice-sheet model and patterns of glacial erosion and deposition in Britain". In: *British Quaternary Studies: Recent Advances*, pp. 231–246.

Boulton, G. S. and C. D. Clark (1990). "A highly mobile Laurentide ice sheet revealed by satellite images of glacial lineations". In: *Nature* 346.6287, pp. 813–817. DOI: `10.1038/346813a0`.

Boulton, G. S. (1982). "Processes and Patterns of Glacial Erosion". In: *Glacial Geomorphology*. Springer Netherlands, pp. 41–87. DOI: `10.1007/978-94-011-6491-7_2`.

Boulton, G. S., M. Hagdorn, and N. R. Hulton (2003). "Streaming flow in an ice sheet through a glacial cycle". In: *Annals of Glaciology* 36, pp. 117–128. DOI: `10.3189/172756403781816293`.

Boulton, G. and M. Hagdorn (2006). "Glaciology of the British Isles Ice Sheet during the last glacial cycle: form, flow, streams and lobes". In: *Quaternary Science Reviews* 25.23-24, pp. 3359–3390. DOI: `10.1016/j.quascirev.2006.10.013`.

Bowen, D., F. Phillips, A. McCabe, P. Knutz, and G. Sykes (2002). "New data for the Last Glacial Maximum in Great Britain and Ireland". In: *Quaternary Science Reviews* 21.1-3, pp. 89–101. DOI: `10.1016/S0277-3791(01)00102-0`.

Bradley, S. L., G. A. Milne, I. Shennan, and R. Edwards (2011). "An improved glacial isostatic adjustment model for the British Isles". In: *Journal of Quaternary Science* 26.5, pp. 541–552. DOI: `10.1002/jqs.1481`.

Bradwell, T., D. Small, D. Fabel, C. D. Clark, R. C. Chiverrell, and M. H. Saher (2019a). "Pattern , style and timing of British-Irish Ice Sheet retreat : Shetland

and northern North Sea sector Pattern , style and timing of British – Irish Ice Sheet retreat : Shetland and northern North Sea sector". In: *Journal of Quaternary Science* November, jqs.3163. DOI: `10.1002/jqs.3163`.

Bradwell, T. et al. (2008). "The northern sector of the last British Ice Sheet: Maximum extent and demise". In: *Earth-Science Reviews* 88.3-4, pp. 207–226. DOI: `10.1016/j.earscirev.2008.01.008`.

Bradwell, T. et al. (2019b). "Ice-stream demise dynamically conditioned by trough shape and bed strength". In: *Science Advances* 5.4, eaau1380. DOI: `10.1126/sciadv.aau1380`.

Brodzikowski, K. and A. J. van Loon (1991). *Glacigenic sediments*. Elsevier, p. 674.

Callard, S. L. et al. (2018). "Extent and retreat history of the Barra Fan Ice Stream offshore western Scotland and northern Ireland during the last glaciation". In: *Quaternary Science Reviews* 201, pp. 280–302. DOI: `10.1016/J.QUASCIREV.2018.10.002`.

Calov, R., A. Ganopolski, V. Petoukhov, M. Claussen, and R. Greve (2002). "Large-scale instabilities of the Laurentide ice sheet simulated in a fully coupled climate-system model". In: *Geophysical Research Letters* 29.24, pp. 69–1–69–4. DOI: `10.1029/2002GL016078`.

Chiverrell, R. C. et al. (2018). "Ice margin oscillations during deglaciation of the northern Irish Sea Basin". In: *Journal of Quaternary Science* 33.7, pp. 739–762. DOI: `10.1002/jqs.3057`.

Clark, C. D. (1993). "Mega-scale glacial lineations and cross-cutting ice-flow landforms". In: *Earth Surface Processes and Landforms* 18.1, pp. 1–29. DOI: `10.1002/esp.3290180102`.

Clark, C. D., D. J. Evans, A. Khatwa, T. Bradwell, C. J. Jordan, S. H. Marsh, W. A. Mitchell, and M. D. Bateman (2004). *Map and GIS database of glacial landforms and features related to the last British Ice Sheet*. DOI: `10.1111/j.1502-3885.2004.tb01246.x`. arXiv: `arXiv:1011.1669v3`.

Clark, C. D., A. L. Hughes, S. L. Greenwood, C. Jordan, and H. P. Sejrup (2012). "Pattern and timing of retreat of the last British-Irish Ice Sheet". In: *Quaternary Science Reviews* 44, pp. 112–146. DOI: 10.1016/j.quascirev.2010.07.019.

Clark, P. U., S. J. Marshall, G. K. Clarke, S. W. Hostetler, J. M. Licciardi, and J. T. Teller (2001). "Freshwater forcing of abrupt climate change during the last glaciation". In: *Science* 293.5528, pp. 283–287. DOI: 10.1126/science.1062517.

Conway, H., G. Catania, C. F. Raymond, A. M. Gades, T. A. Scambos, and H. Engelhardt (2002). "Switch of flow direction in an Antarctic ice stream". In: *Nature* 419.6906, pp. 465–467. DOI: 10.1038/nature01081.

Cornford, S. L. et al. (2015). "Century-scale simulations of the response of the West Antarctic Ice Sheet to a warming climate". In: *Cryosphere* 9.4, pp. 1579–1600. DOI: 10.5194/tc-9-1579-2015.

Cornford, S. L., D. F. Martin, V. Lee, A. J. Payne, and E. G. Ng (2016). "Adaptive mesh refinement versus subgrid friction interpolation in simulations of Antarctic ice dynamics". In: *Annals of Glaciology* 57.73, pp. 1–9. DOI: 10.1017/aog.2016.13.

Cornford, S. L., D. F. Martin, D. T. Graves, D. F. Ranken, A. M. Le Brocq, R. M. Gladstone, A. J. Payne, E. G. Ng, and W. H. Lipscomb (2013). "Adaptive mesh, finite volume modeling of marine ice sheets". In: *Journal of Computational Physics* 232.1, pp. 529–549. DOI: 10.1016/j.jcp.2012.08.037.

Davies, B. J., M. J. Hambrey, N. F. Glasser, T. Holt, A. Rodés, J. L. Smellie, J. L. Carrivick, and S. P. Blockley (2017). "Ice-dammed lateral lake and epishelf lake insights into Holocene dynamics of Marguerite Trough Ice Stream and George VI Ice Shelf, Alexander Island, Antarctic Peninsula". In: *Quaternary Science Reviews* 177, pp. 189–219. DOI: 10.1016/J.QUASCIREV.2017.10.016.

Davies, D., R. G. Bingham, E. C. King, A. M. Smith, A. M. Brisbourne, M. Spagnolo, A. G. C. Graham, A. E. Hogg, and D. G. Vaughan (2018). "How

dynamic are ice-stream beds?" In: *The Cryosphere* 12.5, pp. 1615–1628. DOI: 10.5194/tc-12-1615-2018.

Dyke, A. S. (2004). "An outline of North American deglaciation with emphasis on central and northern Canada". In: *Developments in Quaternary Sciences* 2, pp. 373–424. DOI: 10.1016/S1571-0866(04)80209-4.

Dyke, A. S. and V. K. Prest (1987). "Late Wisconsinan and Holocene History of the Laurentide Ice Sheet". In: *Géographie physique et Quaternaire* 41.2, p. 237. DOI: 10.7202/032681ar.

Dyke, A. S. and T. F. Morris (1988). "DRUMLIN FIELDS, DISPERSAL TRAINS, and ICE STREAMS IN ARCTIC CANADA". In: *Canadian Geographer / Le Géographe canadien* 32.1, pp. 86–90. DOI: 10.1111/j.1541-0064.1988.tb00860.x.

Ehlers, J., J. Ehlers, P. Gibbard, and P. Hughes (2011). *Quaternary glaciations-extent and chronology: a closer look*. Elsevier.

Ely, J. C., C. D. Clark, M. Spagnolo, C. R. Stokes, S. L. Greenwood, A. L. Hughes, P. Dunlop, and D. Hess (2016). "Do subglacial bedforms comprise a size and shape continuum?" In: *Geomorphology* 257, pp. 108–119. DOI: 10.1016/J.GEOMORPH.2016.01.001.

Ely, J. C. et al. (2019). "Recent progress on combining geomorphological and geochronological data with ice sheet modelling, demonstrated using the last British–Irish Ice Sheet". In: *Journal of Quaternary Science*, pp. 1–15. DOI: 10.1002/jqs.3098.

Favier, L., G. Durand, S. L. Cornford, G. H. Gudmundsson, O. Gagliardini, F. Gillet-Chaulet, T. Zwinger, A. J. Payne, and A. M. Le Brocq (2014). "Retreat of Pine Island Glacier controlled by marine ice-sheet instability". In: *Nature Climate Change* 4.2, pp. 117–121. DOI: 10.1038/nclimate2094.

Feldmann, J., A. Levermann, and M. Mengel (2019). "Stabilizing the West Antarctic Ice Sheet by surface mass deposition". In: *Science advances* 5.7, eaaw4132. DOI: 10.1126/sciadv.aaw4132.

Fowler, A. C. (1986). "Sub-Temperate Basal Sliding". In: *Journal of Glaciology* 32.110, pp. 3–5. DOI: 10.3189/s0022143000006808.

Gandy, N., L. J. Gregoire, J. C. Ely, C. D. Clark, D. M. Hodgson, V. Lee, T. Bradwell, and R. F. Ivanovic (2018). "Marine Ice Sheet Instability and Ice Shelf Buttressing Influenced Deglaciation of the Minch Ice Stream, Northwest Scotland". In: *The Cryosphere* 12.July, pp. 1–24. DOI: 10.5194/tc-2018-116.

Gandy, N., L. J. Gregoire, J. C. Ely, S. L. Cornford, C. D. Clark, and D. M. Hodgson (2019). "Exploring the ingredients required to successfully model the placement, generation, and evolution of ice streams in the British-Irish Ice Sheet". In: *Quaternary Science Reviews* 223, p. 105915. DOI: 10.1016/J.QUASCIREV.2019.105915.

Golledge, N. R., R. H. Levy, R. M. McKay, and T. R. Naish (2017). "East Antarctic ice sheet most vulnerable to Weddell Sea warming". In: *Geophysical Research Letters* 44.5, pp. 2343–2351. DOI: 10.1002/2016GL072422.

Gordon, J. E., W. Brian Whalley, A. F. Gellatly, and D. M. Vere (1992). "The formation of glacial flutes: Assessment of models with evidence from Lyngsdalen, North Norway". In: *Quaternary Science Reviews* 11.7-8, pp. 709–731. DOI: 10.1016/0277-3791(92)90079-N.

Graham, A., L. Lonergan, and M. Stoker (2007). "Evidence for Late Pleistocene ice stream activity in the Witch Ground Basin, central North Sea, from 3D seismic reflection data". In: *Quaternary Science Reviews* 26.5-6, pp. 627–643. DOI: 10.1016/J.QUASCIREV.2006.11.004.

Greenwood, S. L. and C. D. Clark (2008). "Subglacial bedforms of the Irish Ice Sheet". In: *Journal of Maps* 4.1, pp. 332–357. DOI: 10.4113/jom.2008.1030.

Gregoire, L. J., R. F. Ivanovic, A. C. Maycock, P. J. Valdes, and S. Stevenson (2018). "Holocene lowering of the Laurentide ice sheet affects North Atlantic gyre circulation and climate". In: *Climate Dynamics* 51.9-10, pp. 3797–3813. DOI: 10.1007/s00382-018-4111-9.

Gudmundsson, G. H. (2013). "Ice-shelf buttressing and the stability of marine ice sheets". In: *The Cryosphere* 7, pp. 647–655. DOI: 10.5194/tc-7-647-2013.

Harrison, W. D., K. A. Echelmeyer, and C. F. Larsen (1998). "Measurement of temperature in a margin of Ice Stream B, Antarctica: implications for margin migration and lateral drag". In: *Journal of Glaciology* 44.148, pp. 615–624. DOI: 10.3189/S0022143000002112.

Hättestrand, C. and J. Kleman (1999). "Ribbed moraine formation". In: *Quaternary Science Reviews* 18.1, pp. 43–61. DOI: 10.1016/S0277-3791(97)00094-2.

Hewitt, I. J. and A. C. Fowler (2008). "Seasonal waves on glaciers". In: *Hydrological Processes* 22.19, pp. 3919–3930. DOI: 10.1002/hyp.7029.

Hindmarsh, R. C. A. (2004). "A numerical comparison of approximations to the Stokes equations used in ice sheet and glacier modeling". In: *Journal of Geophysical Research: Earth Surface* 109.F1. DOI: 10.1029/2003JF000065.

Hindmarsh, R. C. A. (2006). "The role of membrane-like stresses in determining the stability and sensitivity of the Antarctic ice sheets: back pressure and grounding line motion." In: *Philosophical transactions. Series A, Mathematical, physical, and engineering sciences* 364.1844, pp. 1733–67. DOI: 10.1098/rsta.2006.1797.

— (2009). "Consistent generation of ice-streams via thermo-viscous instabilities modulated by membrane stresses". In: *Geophysical Research Letters* 36.6, p. L06502. DOI: 10.1029/2008GL036877.

Hoskins, B. J. and D. J. Karoly (1981). "The steady linear response of a spherical atmosphere to thermal and orographic forcing." In: *Journal of the Atmospheric Sciences* 38.6, pp. 1179–1196. DOI: 10.1175/1520-0469(1981)038<1179:TSLROA>2.0.CO;2.

Hubbard, A. (1999). "High-resolution modeling of the advance of the Younger Dryas ice sheet and its climate in Scotland". In: *Quaternary Research* 52.1, pp. 27–43. DOI: 10.1006/qres.1999.2055.

Hubbard, A., T. Bradwell, N. Golledge, A. Hall, H. Patton, D. Sugden, R. Cooper, and M. Stoker (2009). "Dynamic cycles, ice streams and their impact on the extent, chronology and deglaciation of the British–Irish ice sheet". In: *Quaternary Science Reviews* 28.7-8, pp. 758–776. DOI: 10.1016/j.quascirev.2008.12.026.

Hubbard, A., A. S. Hein, M. R. Kaplan, N. R. J. Hulton, and N. Glasser (2005). "A modelling reconstruction of the last glacial maximum ice sheet and its deglaciation in the vicinity of the northern patagonian icefield, south america". In: *Geografiska Annaler: Series A, Physical Geography* 87.2, pp. 375–391. DOI: 10.1111/j.0435-3676.2005.00264.x.

Hughes, A. L., C. D. Clark, and C. J. Jordan (2014). "Flow-pattern evolution of the last British Ice Sheet". In: *Quaternary Science Reviews* 89, pp. 148–168. DOI: 10.1016/j.quascirev.2014.02.002.

Hughes, A. L., S. L. Greenwood, and C. D. Clark (2011). "Dating constraints on the last British-Irish Ice Sheet: a map and database". In: *Journal of Maps* 7.1, pp. 156–184. DOI: 10.4113/jom.2011.1145.

Hughes, A. L., R. Gyllencreutz, Ø. S. Lohne, J. Mangerud, and J. I. Svendsen (2016). "The last Eurasian ice sheets - a chronological database and time-slice reconstruction, DATED-1". In: *Boreas* 45.1. DOI: 10.1111/bor.12142.

Imbrie, J. (1979). *Ice ages: solving the mystery*. Harvard University Press.

Ivanovic, R. F., L. J. Gregoire, A. D. Wickert, P. J. Valdes, and A. Burke (2017). "Collapse of the North American ice saddle 14,500 years ago caused widespread cooling and reduced ocean overturning circulation". In: *Geophysical Research Letters* 44.1, pp. 383–392. DOI: 10.1002/2016GL071849.

Iverson, N. R., D. Cohen, T. S. Hooyer, U. H. Fischer, H. Jackson, P. L. Moore, G. Lappegard, and J. Kohler (2003). "Effects of basal debris on glacier flow". In: *Science* 301.5629, pp. 81–84. DOI: 10.1126/science.1083086.

Jackson, M. and B. Kamb (1997). "The marginal shear stress of Ice Stream B, West Antarctica". In: *Journal of Glaciology* 43.145, pp. 415–426. DOI: 10.3189/S0022143000035000.

Jacobs, S. S., A. Jenkins, C. F. Giulivi, and P. Dutrieux (2011). "Stronger ocean circulation and increased melting under Pine Island Glacier ice shelf". In: *Nature Geoscience* 4.8, pp. 519–523. DOI: 10.1038/ngeo1188.

Jenkins, A., P. Dutrieux, S. S. Jacobs, S. D. McPhail, J. R. Perrett, A. T. Webb, and D. White (2010). "Observations beneath Pine Island Glacier in West Antarctica and implications for its retreat". In: *Nature Geoscience* 3.7, pp. 468–472. DOI: 10.1038/ngeo890.

Joughin, I., B. E. Smith, and B. Medley (2014). "Marine ice sheet collapse potentially under way for the thwaites glacier basin, West Antarctica". In: *Science* 344.6185, pp. 735–738. DOI: 10.1126/science.1249055.

Joughin, I. et al. (2005). "Continued deceleration of Whillans ice stream West Antartica". In: *Geophysical Research Letters* 32.22, pp. 1–4. DOI: 10.1029/2005GL024319.

Jouzel, J., M. Stiévenard, S. Johnsen, A. Landais, V. Masson-Delmotte, A. Sveinbjornsdottir, F. Vimeux, U. von Grafenstein, and J. White (2007). "The GRIP deuterium-excess record". In: *Quaternary Science Reviews* 26.1-2, pp. 1–17. DOI: 10.1016/J.QUASCIREV.2006.07.015.

Kieman, J. and I. Borgström (1996). "Reconstruction of palaeo-ice sheets: The use of geomorphological data". In: *Earth Surface Processes and Landforms* 21.10, pp. 893–909. DOI: 10.1002/(SICI)1096-9837(199610)21:10<893::AID-ESP620>3.0.CO;2-U.

King, E. L., H. Haflidason, H. P. Sejrup, and R. Løvlie (1998). "Glacigenic debris flows on the North Sea Trough Mouth Fan during ice stream maxima". In: *Marine Geology* 152.1-3, pp. 217–246. DOI: 10.1016/S0025-3227(98)00072-3.

Kleman, J., C. Hättestrand, A. P. Stroeven, K. N. Jansson, H. De Angelis, and I. Borgström (2007). "Reconstruction of Palaeo-Ice Sheets - Inversion of their Glacial Geomorphological Record". In: *Glacier Science and Environmental Change*. Malden, MA, USA: Blackwell Publishing, pp. 192–198. DOI: 10 . 1002/9780470750636.ch38.

Lambeck, K., H. Rouby, A. Purcell, Y. Sun, and M. Sambridge (2014). "Sea level and global ice volumes from the Last Glacial Maximum to the Holocene". In: *Proceedings of the National Academy of Sciences of the United States of America* 111.43, pp. 15296–15303. DOI: 10.1073/pnas.1411762111.

Lee Peters, J., S. Benetti, P. Dunlop, and C. O. Cofaigh (2015). "Maximum extent and dynamic behaviour of the last BritisheIrish Ice Sheet west of Ireland". In: *Quaternary Science Reviews* 128, pp. 48–68. DOI: 10.1016/j.quascirev. 2015.09.015.

Lee, V., S. L. Cornford, and A. J. Payne (2015). "Initialization of an ice-sheet model for present-day Greenland". In: *Annals of Glaciology* 56.70, pp. 129–140. DOI: 10.3189/2015AoG70A121.

Lenton, T., J. Rockström, O. Gaffney, S. Rahmstorf, K. Richardson, W. Steffen, and H. J. Shellnhuber (2019). "Climate tipping points - too risky to bet against". In: *Nature* 575.7784, pp. 592–595. DOI: 10 . 1038 / d41586 – 019 – 03595–0.

Löfverström, M. and J. M. Lora (2017). "Abrupt regime shifts in the North Atlantic atmospheric circulation over the last deglaciation". In: *Geophysical Research Letters* 44.15, pp. 8047–8055. DOI: 10.1002/2017GL074274.

Lowe, J. and M. Walker (2014). *Reconstructing quaternary environments*. Taylor and Francis, pp. 1–538. DOI: 10.4324/9781315797496.

Margold, M., C. R. Stokes, and C. D. Clark (2015). "Ice streams in the Laurentide Ice Sheet: Identification, characteristics and comparison to modern ice sheets". In: *Earth-Science Reviews* 143, pp. 117–146. DOI: 10.1016/J.EARSCIREV. 2015.01.011.

McCabe, A. (1987). "Quaternary deposits and glacial stratigraphy in Ireland". In: *Quaternary Science Reviews* 6.3-4, pp. 259–299. DOI: 10.1016/0277-3791(87)90008-4.

Milankovitch, M. K. (1941). "Kanon der Erdbestrahlung und seine Anwendung auf das Eiszeitenproblem". In: *Royal Serbian Academy Special Publication* 133, pp. 1–633.

Morgan, V., T. Jacka, G. Akerman, and A. Clarke (1982). "Outlet Glacier and Mass-Budget Studies in Enderby, Kemp, and Mac. Robertson Lands, Antarctica". In: *Annals of Glaciology* 3, pp. 204–210. DOI: 10.3189/S0260305500002780.

Morlighem, M., H. Seroussi, E. Larour, and E. Rignot (2013). "Inversion of basal friction in Antarctica using exact and incomplete adjoints of a higher-order model". In: *J. Geophys. Res. Earth Surf* 118, pp. 1746–1753. DOI: 10.1002/jgrf.20125.

Murray, A., J. Svendsen, J. Mangerud, and V. Astakhov (2007). "Testing the accuracy of quartz OSL dating using a known-age Eemian site on the river Sula, northern Russia". In: *Quaternary Geochronology* 2.1-4, pp. 102–109. DOI: 10.1016/J.QUAGEO.2006.04.004.

Niu, L. U., G. Lohmann, S. Hinck, E. J. Gowan, and U. T. Krebs-Kanzow (2019). "The sensitivity of Northern Hemisphere ice sheets to atmospheric forcing during the last glacial cycle using PMIP3 models". In: *Journal of Glaciology* 65.252, pp. 645–661. DOI: 10.1017/jog.2019.42.

Nye, J. F. (1969). "Calculation on Sliding of Ice Over Wavy Surface using Newtonian Viscous Approximation". In: vol. 311. 1506, pp. 445–467. DOI: 10.1098/rspa.1969.0127.

— (1970). "Glacier Sliding Without Cavitation in a Linear Viscous Approximation". In: *Proceedings of the Royal Society of London. Series A, Mathematical and Physical Sciences.* Vol. 315. 1522. Royal Society, pp. 381–403. DOI: 10.1098/rspa.1970.0050.

Nye, J. F. (1976). "Water Flow in Glaciers: Jökulhlaups, Tunnels and Veins". In: *Journal of Glaciology* 17.76, pp. 181–207. DOI: 10.3189/S002214300001354X.

Nygård, A., H. P. Sejrup, H. Haflidason, and P. Bryn (2005). "The glacial North Sea Fan, southern Norwegian Margin: Architecture and evolution from the upper continental slope to the deep-sea basin". In: *Marine and Petroleum Geology* 22.1-2 SPEC. ISS. Pp. 71–84. DOI: 10.1016/j.marpetgeo.2004.12.001.

Ó Cofaigh, C., D. J. A. Evans, and I. R. Smith (2010). "Large-scale reorganization and sedimentation of terrestrial ice streams during late Wisconsinan Laurentide Ice Sheet deglaciation". In: *Geological Society of America Bulletin* 122.5-6, pp. 743–756. DOI: 10.1130/B26476.1.

Ó Cofaigh, C. et al. (2019). "Early deglaciation of the British-Irish Ice Sheet on the Atlantic shelf northwest of Ireland driven by glacioisostatic depression and high relative sea level". In: *Quaternary Science Reviews* 208, pp. 76–96. DOI: 10.1016/J.QUASCIREV.2018.12.022.

Patton, H., A. Hubbard, K. Andreassen, M. Winsborrow, and A. P. Stroeven (2016). "The build-up, configuration, and dynamical sensitivity of the Eurasian ice-sheet complex to Late Weichselian climatic and oceanic forcing". In: *Quaternary Science Reviews* 153, pp. 97–121. DOI: 10.1016/j.quascirev.2016.10.009.

Patton, H., A. Hubbard, N. F. Glasser, T. Bradwell, and N. R. Golledge (2013a). "The last Welsh Ice Cap: Part 1 - Modelling its evolution, sensitivity and associated climate". In: *Boreas* 42.3, pp. 471–490. DOI: 10.1111/j.1502-3885.2012.00300.x.

— (2013b). "The last Welsh Ice Cap: Part 2 - Dynamics of a topographically controlled icecap". In: *Boreas* 42.3, pp. 491–510. DOI: 10.1111/j.1502-3885.2012.00301.x.

Patton, H. et al. (2017). "Deglaciation of the Eurasian ice sheet complex". In: *Quaternary Science Reviews* 169, pp. 148–172. DOI: 10.1016/j.quascirev.2017.05.019.

Pattyn, F. et al. (2012). "Results of the Marine Ice Sheet Model Intercomparison Project, MISMIP". In: *The Cryosphere* 6, pp. 573–588. DOI: 10.5194/tc-6-573-2012.

Payne, A. J. and P. W. Dongelmans (1997). "Self-organization in the thermomechanical flow of ice sheets". In: *Journal of Geophysical Research: Solid Earth* 102.B6, pp. 12219–12233. DOI: 10.1029/97JB00513.

Praeg, D., S. McCarron, D. Dove, C. Ó Cofaigh, G. Scott, X. Monteys, L. Facchin, R. Romeo, and P. Coxon (2015). "Ice sheet extension to the Celtic Sea shelf edge at the Last Glacial Maximum". In: *Quaternary Science Reviews* 111, pp. 107–112. DOI: 10.1016/j.quascirev.2014.12.010.

Punkari, M. (1994). "Function of the ice streams in the Scandinavian ice sheet: analyses of glacial geological data from southwestern Finland". In: *Transactions of the Royal Society of Edinburgh: Earth Sciences* 85.4, pp. 283–302. DOI: 10.1017/S0263593300002054.

Retzlaff, R. and C. R. Bentley (1993). "Timing of stagnation of ice stream C, West Antarctica, from short- pulse radar studies of buried surface crevasses". In: *Journal of Glaciology* 39.133, pp. 553–561. DOI: 10.1017/S0022143000016440.

Rignot, E., J. Mouginot, and B. Scheuchl (2011). "Ice flow of the Antarctic ice sheet". In: *Science* 333.6048, pp. 1427–1430. DOI: 10.1126/science.1208336.

Robel, A. A. and E. Tziperman (2016). "The role of ice stream dynamics in deglaciation". In: *Journal of Geophysical Research: Earth Surface* 121.8, pp. 1540–1554. DOI: 10.1002/2016JF003937.

Roberts, D. H. et al. (2018). "Ice marginal dynamics of the last British-Irish Ice Sheet in the southern North Sea: Ice limits, timing and the influence of the Dogger Bank". In: *Quaternary Science Reviews* 198, pp. 181–207. DOI: 10.1016/J.QUASCIREV.2018.08.010.

Ross, N. et al. (2012). "Steep reverse bed slope at the grounding line of the Weddell Sea sector in West Antarctica". In: *Nature Geoscience* 5.6, pp. 393–396. DOI: 10.1038/ngeo1468.

Scambos, T. A., J. A. Bohlander, C. A. Shuman, and P. Skvarca (2004). "Glacier acceleration and thinning after ice shelf collapse in the Larsen B embayment, Antarctica". In: *Geophysical Research Letters* 31.18, p. L18402. DOI: 10.1029/2004GL020670.

Schoof, C. (2002). "Basal perturbations under ice streams: form drag and surface expression". In: *Journal of Glaciology* 48.162, pp. 407–416. DOI: 10.3189/172756502781831269.

— (2007). "Ice sheet grounding line dynamics: Steady states, stability, and hysteresis". In: *Journal of Geophysical Research* 112.F3, F03S28. DOI: 10.1029/2006JF000664.

Scourse, J. et al. (2019). "Advance and retreat of the marine-terminating Irish Sea Ice Stream into the Celtic Sea during the Last Glacial: Timing and maximum extent". In: *Marine Geology* 412, pp. 53–68. DOI: 10.1016/J.MARGEO.2019.03.003.

Seddik, H., R. Greve, T. Zwinger, F. Gillet-Chaulet, and O. Gagliardini (2012). "Simulations of the Greenland ice sheet 100 years into the future with the full Stokes model Elmer/Ice". In: *Journal of Glaciology* 58.209, pp. 427–440. DOI: 10.3189/2012JoG11J177.

Seguinot, J., G. Jouvet, M. Huss, M. Funk, S. Ivy-Ochs, and F. Preusser (2018). "Modelling last glacial cycle ice dynamics in the Alps". In: *The Cryosphere Discussions*, pp. 1–30. DOI: 10.5194/tc-2018-8.

Seguinot, J., I. Rogozhina, A. P. Stroeven, M. Margold, and J. Kleman (2016). "Numerical simulations of the Cordilleran ice sheet through the last glacial cycle". In: *The Cryosphere* 10.2, pp. 639–664. DOI: 10.5194/tc-10-639-2016.

Sejrup, H. P., H. Haflidason, I. Aarseth, E. King, C. F. Forsberg, D. Long, and K. Rokoengen (1994). "Late Weichselian glaciation history of the northern North Sea". In: *Boreas* 23.1, pp. 1–13. DOI: 10.1111/j.1502-3885.1994.tb00581.x.

Seroussi, H., H. Ben Dhia, M. Morlighem, E. Larour, E. Rignot, and D. Aubry (2012). "Coupling ice flow models of varying orders of complexity with the Tiling method". In: *Journal of Glaciology* 58.210, pp. 776–786. DOI: 10.3189/2012JoG11J195.

Shepherd, A., D. J. Wingham, J. A. Mansley, and H. F. Corr (2001). "Inland thinning of Pine Island Glacier, West Antarctica". In: *Science* 291.5505, pp. 862–864. DOI: 10.1126/science.291.5505.862.

Small, D. et al. (2017). "Devising quality assurance procedures for assessment of legacy geochronological data relating to deglaciation of the last British-Irish Ice Sheet". In: *Earth-Science Reviews* 164, pp. 232–250. DOI: 10.1016/J.EARSCIREV.2016.11.007.

Smith, A., T. Murray, K. Nicholls, K. Makinson, G. Aðalgeirsdóttir, A. Behar, and D. Vaughan (2007). "Rapid erosion, drumlin formation, and changing hydrology beneath an Antarctic ice stream". In: *Geology* 35.2, p. 127. DOI: 10.1130/G23036A.1.

Smith, M., J. Rose, and S. Booth (2006). "Geomorphological mapping of glacial landforms from remotely sensed data: An evaluation of the principal data sources and an assessment of their quality". In: *Geomorphology* 76.1-2, pp. 148–165. DOI: 10.1016/J.GEOMORPH.2005.11.001.

Spagnolo, M., C. D. Clark, J. C. Ely, C. R. Stokes, J. B. Anderson, K. Andreassen, A. G. C. Graham, and E. C. King (2014). "Size, shape and spatial arrangement of mega-scale glacial lineations from a large and diverse dataset". In: *Earth Surface Processes and Landforms* 39.11, n/a–n/a. DOI: 10.1002/esp.3532.

Stokes, C. R., M. Margold, C. D. Clark, and L. Tarasov (2016). "Ice stream activity scaled to ice sheet volume during Laurentide Ice Sheet deglaciation". In: *Nature* 530.7590, pp. 322–326. DOI: 10.1038/nature16947.

Stokes, C. R., C. D. Clark, and R. Storrar (2009). "Major changes in ice stream dynamics during deglaciation of the north-western margin of the Laurentide Ice Sheet". In: *Quaternary Science Reviews* 28.7-8, pp. 721–738. DOI: 10.1016/J.QUASCIREV.2008.07.019.

Stokes, C. R. and L. Tarasov (2010). "Ice streaming in the Laurentide Ice Sheet: A first comparison between data-calibrated numerical model output and geological evidence". In: *Geophysical Research Letters* 37.1. DOI: 10.1029/2009GL040990.

Tinto, K. J. and R. E. Bell (2011). "Progressive unpinning of Thwaites Glacier from newly identified offshore ridge: Constraints from aerogravity". In: *Geophysical Research Letters* 38.20. DOI: 10.1029/2011GL049026.

Tsai, V. C., A. L. Stewart, and A. F. Thompson (2015). "Marine ice-sheet profiles and stability under Coulomb basal conditions". In: *Journal of Glaciology* 61.226, pp. 205–215. DOI: 10.3189/2015JoG14J221.

Ullman, D. J., A. E. Carlson, F. S. Anslow, A. N. Legrande, and J. M. Licciardi (2015). "Laurentide ice-sheet instability during the last deglaciation". In: *Nature Geoscience* 8.7, pp. 534–537. DOI: 10.1038/ngeo2463.

Weber, J. E. (2000). "Non-temperate glacier flow over wavy sloping ground". In: *Journal of Glaciology* 46.154, pp. 453–458. DOI: 10.3189/172756500781833179.

Weertman, J. (1957). "On the Sliding of Glaciers". In: *Journal of Glaciology* 3.21, pp. 33–38. DOI: 10.3189/S0022143000024709.

Wilson, P., C. K. Ballantyne, S. Benetti, D. Small, D. Fabel, and C. D. Clark (2018). "Deglaciation chronology of the Donegal Ice Centre, north-west Ireland". In: *Journal of Quaternary Science* 34.1, jqs.3077. DOI: 10.1002/jqs.3077.

Winsborrow, M. C., C. D. Clark, and C. R. Stokes (2010). "What controls the location of ice streams?" In: *Earth-Science Reviews* 103.1-2, pp. 45–59. DOI: 10.1016/j.earscirev.2010.07.003.

Ziemen, F. A., C. B. Rodehacke, and U. Mikolajewicz (2014). "Coupled ice sheet–climate modeling under glacial and pre-industrial boundary conditions". In: *Climate of the Past* 10.5, pp. 1817–1836. DOI: 10.5194/cp-10-1817-2014.

Zwally, H. J., W. Abdalati, T. Herring, K. Larson, J. Saba, and K. Steffen (2002). "Surface melt-induced acceleration of Greenland ice-sheet flow". In: *Science* 297.5579, pp. 218–222. DOI: 10.1126/science.1072708.

Chapter 2

Marine ice sheet instability and ice shelf buttressing of the Minch Ice Stream, northwest Scotland

Abstract

Uncertainties in future sea level projections are dominated by our limited under-standing of the dynamical processes that control instabilities of marine ice sheets. The last deglaciation of the British–Irish Ice Sheet offers a valuable example to examine these processes. The Minch Ice Stream, which drained a large propor-tion of ice from the northwest sector of the British–Irish Ice Sheet during the last deglaciation, is constrained with abundant empirical data which can be used to inform, validate, and analyse numerical ice sheet simulations. We use BISICLES, a higher-order ice sheet model, to examine the dynamical processes that con-trolled the retreat of the Minch Ice Stream. We perform simplified experiments of the retreat of this ice stream under an idealised climate forcing to isolate the effect of marine ice sheet processes, simulating retreat from the continental shelf under constant "warm" surface mass balance and sub-ice-shelf melt. The model simulates a slowdown of retreat as the ice stream becomes laterally confined at

the mouth of the Minch strait between mainland Scotland and the Isle of Lewis, resulting in a marine setting similar to many large tidewater glaciers in Greenland and Antarctica. At this stage of the simulation, the presence of an ice shelf becomes a more important control on grounded ice volume, providing buttressing to upstream ice. Subsequently, the presence of a reverse slope inside the Minch strait produces an acceleration in retreat, leading to a "collapsed" state, even when the climate returns to the initial "cold" conditions. Our simulations demonstrate the importance of the Marine Ice Sheet Instability and ice shelf buttressing during the deglaciation of parts of the British–Irish Ice Sheet. We conclude that geological data could be applied to further constrain these processes in ice sheet models used for projecting the future of contemporary ice sheets.

2.1   Introduction

Attempts to model the future evolution of the West Antarctic Ice Sheet reveal large uncertainty in the extent of future mass loss (Feldmann and Levermann, 2015; Ritz et al., 2015). This is partly because many contemporary Antarctic ice streams are marine based (Jenkins et al., 2010; Ross et al., 2012) and are therefore vulnerable to Marine Ice Sheet Instability (MISI). Schoof (2007) demonstrated that no stable grounding line position is possible in areas of reversed bed slope. Consequently, any change in ice thickness at the grounding line can cause an irreversible grounding line migration with no change in external forcing. However, it has been shown that simulations of grounding line migration require not only consideration of bed topography, but also ice shelf buttressing (Gudmundsson, 2013), which can stabilise grounding lines on reverse sloping beds. The previous generation of ice sheet models do not accurately simulate the position of the grounding line due to the use of the shallow ice approximation (Veen, 2013), although significant improvements have been made using sub-grid parameterisation at the grounding line (Feldmann et al., 2014). Higher-order models have more success in accurately simulating the grounding line (Pattyn et al., 2012; Favier

et al., 2014), but are still sensitive to model resolution (Cornford et al., 2016) and the representation of basal sliding processes (Tsai et al., 2015; Nias et al., 2016; Gladstone et al., 2017).

It is essential for improved future predictions of ice sheet change to better understand the dynamics of marine ice sheets over millennial timescales. A numerical simulation of the palaeo Marguerite Bay Ice Stream, Antarctica, since the Last Glacial Maximum (LGM) shows that the episodic retreat was controlled by a combination of bed topography, ice stream width, and upstream response and that these controls are crucial to understanding centennial ice sheet evolution (Jamieson et al., 2012). A valuable case to examine these processes is the last deglaciation of the British–Irish Ice Sheet (BIIS), which had a number of marine-grounded sectors (Clark et al., 2012). While contemporary ice sheets offer a decadal-scale observational record, the palaeo record of the BIIS provides detailed proxy observations of ice sheet retreat over millennia. The behaviour of the BIIS has been studied for over a century, resulting in much information on flow patterns and margin positions against which ice sheet models can be compared (Clark et al., 2018). Information on the timing and pace of retreat has been considerably enhanced through the recent work of the BRITICE-CHRONO project, a multi-organisation consortium, which has collected data to better constrain the timing of retreat of the BIIS, particularly in marine sectors. The data-rich environment that the empirical record now holds makes it an attractive test bed for numerical ice sheet modelling experiments (e.g. Boulton et al., 2003; Boulton and Hagdorn, 2006; Hubbard et al., 2009; Patton et al., 2016, 2017). The modelling investigations of Boulton et al. (2003) and Hubbard et al. (2009) specifically highlighted the importance of ice stream dynamics in the evolution of the ice sheet. However, simulations of marine ice sheets, like the West Antarctic Ice Sheet or the BIIS, ideally require models that are able to simulate grounding line migration (Pattyn et al., 2012). The BISICLES ice sheet model was developed to efficiently and accurately model marine ice sheets (Cornford et al., 2013),

allowing for new simulations of the BIIS which explore marine influence on the ice sheet.

We investigate the marine influence on one very well-constrained ice stream of the BIIS, the Minch Ice Stream (MnIS), using the BISICLES ice sheet model. Here, we perform and analyse numerical modelling simulations to test two hypotheses of MnIS retreat: (1) that the ice stream experienced MISI and (2) that an ice shelf had an influential buttressing effect on the pace of retreat.

2.2 The Minch Ice Stream

The MnIS flowed northward from the northwest Scottish Highlands through the Minch strait (Figure 2.1). It reached its maximum extent, the edge of the continental shelf, at ∼27 ka BP (Bradwell et al., 2008), which we here refer to as the local Last Glacial Maximum (lLGM). The ice stream's flow was topographically constrained by the Outer Hebrides, and there is no geological evidence onshore or offshore that the ice stream migrated in position during the glacial cycle (Bradwell et al., 2007). Empirical (Bradwell et al., 2008; Clark et al., 2012) and numerical-model-based (Boulton and Hagdorn, 2006; Hubbard et al., 2009) studies show that this wide (∼50 km) ice stream drained a large proportion of ice that accumulated over the Scottish Highlands. The MnIS trough can be divided into the outer trough, which is predominantly smooth, with low-strength sediments, and the inner trough with an undulating bed and reduced early Quaternary sediment cover (Figure 2.1). The inner trough contains a Neoproterozoic bedrock high, here referred to as the Mid-trough Bedrock High (MTBH) (Figure 2.1). Either side of the MTBH, the Minch branches into east and west troughs (Figure 2.1).

There have been extensive onshore (e.g. Ballantyne and Stone, 2009; Bradwell, 2013) and offshore (e.g. Stoker and Bradwell, 2005; Bradwell et al., 2008; Bradwell and Stoker, 2015) studies of the MnIS catchment. Improved bathymetry data allow the identification of a reverse slope southward of the MTBH. This topography could facilitate MISI, potentially causing rapid retreat south of the
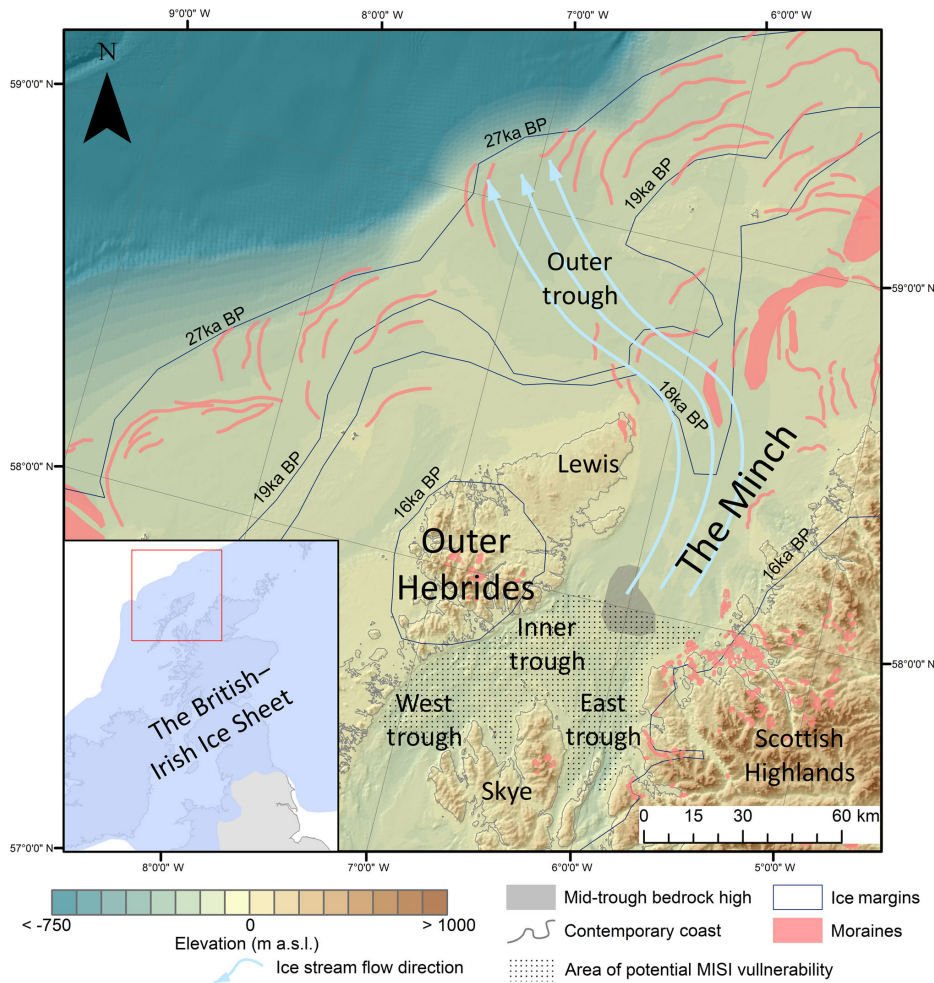
Figure 2.1: Location and geographical setting of the Minch Ice Stream. The inset shows the maximum extent of the British–Irish Ice Sheet from Clark et al. (2012). The red box indicates the Minch ice stream region shown in the larger map. Ice margins and dates are from Clark et al. (2012). Moraines are from the BRITICE glacial landform map, version 2 (Clark et al., 2018). The area of potential MISI vulnerability is inferred from the presence of marine retrograde slopes. Key locations mentioned in the text are labelled.

MTBH, and would explain the relative sparsity of the landform record between the MTBH and the terrestrial transition (Bradwell et al., 2008; Clark et al., 2018). Numerical modelling also allows for ice sheet processes that may be less evident in the empirical record, such as the influence of ice shelves to be tested. The detailed reconstructions of the MnIS provide an excellent opportunity to test whether ice sheet models reproduce behaviour recorded by the empirical data.

2.3   Methods

2.3.1   Model description and set-up

We perform numerical simulations with an idealised climate forcing to isolate the effect of marine ice sheet dynamics on the MnIS in order to determine whether the bathymetric set-up of the MnIS could have facilitated MISI. We use the BISICLES ice sheet model (Cornford et al., 2013) to simulate the MnIS. BISICLES is a higher-order ice sheet model with L1L2 physics retained from the full Stokes flow equations (Schoof and Hindmarsh, 2010) that was developed to efficiently and accurately model the dynamics of marine-grounded ice sheets. BISICLES uses adaptive mesh refinement to automatically increase resolution at high velocities and the grounding line, allowing ice stream dynamics and grounding line migration to be well represented, while having a lower resolution in the rest of the ice sheet ensures efficient model speed. Cornford et al. (2013) provides a full description of BISICLES. Although our focus for analysis is the MnIS, we set up the model domain to cover the majority of the BIIS at 4 km $\times$ 4 km resolution, excluding the central North Sea (Figure 2.2). Simulating a large portion of the BIIS prevents artefacts caused by domain boundary effects and allows for migration of ice catchments during deglaciation. For the set-up of the study, we set a 4 km $\times$ 4 km grid refined three times around the grounding line in the Minch sector to produce a maximum horizontal resolution of 500 m $\times$ 500 m. The simulations have 10 vertical levels. The friction law uses a linear (m=1) Weertman exponent in accordance with previous BISICLES experiments (Favier et al., 2014; Gong et al., 2017) that were used as the basis for bed friction coefficient map values. We use a calving model that simulates frontal ablation by advecting the calving front with a relative velocity equal to the modelled ice velocity at the front minus an ablation rate acting in a direction normal to the front. We prescribe a frontal ablation rate of 250 m yr^{-1} for all lLGM simulations and 350 m yr^{-1} for all simulations which prompt deglaciation. These frontal ablation values are

prescribed as it allows for ice shelf formation during retreat and a stable extent at the continental shelf edge (Figure 2.3) and causes only limited deglaciation if Surface Mass Balance (SMB) changes are not included (Figure 2.4a).
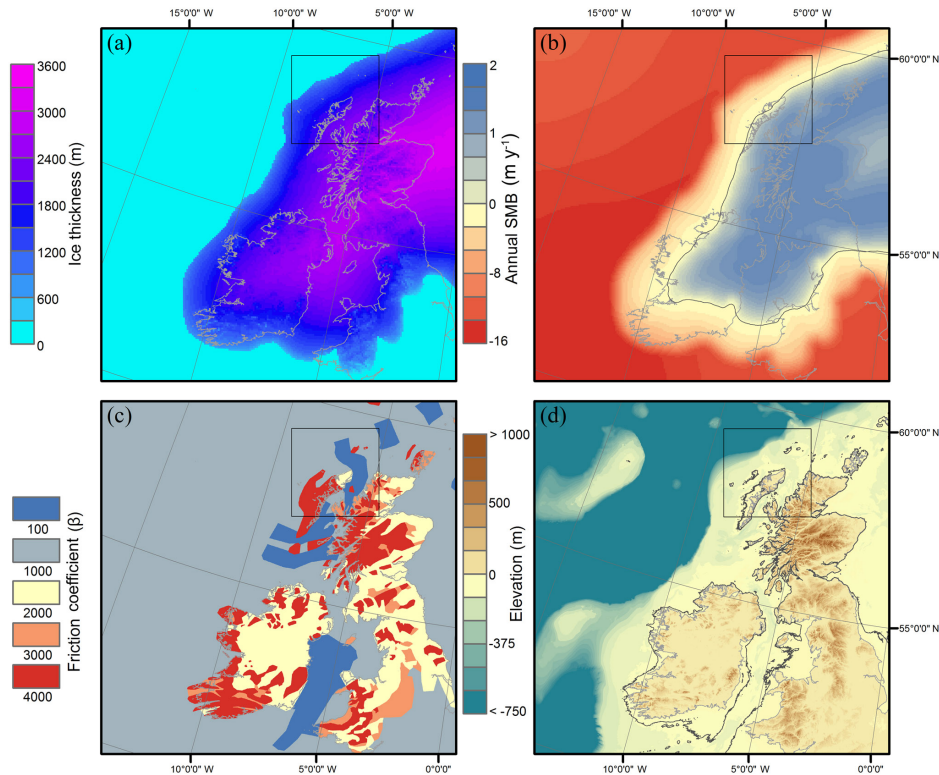
Figure 2.2: Initial conditions and boundary conditions for the equilibrium spin-up lLGM ice sheet simulation, showing the full domain of the simulations. The contemporary coast is shown as a thin grey line. (a) Initial ice thickness (m); (b) annual surface mass balance (m yr^{-1}), with the black contour line representing the equilibrium line (SMB =0 m w.e. yr^{-1}). (c) Bed friction coefficient (β); (d) isostatically adjusted bed topography (m) corresponding to 30 ka BP. The maps show the full ice sheet domain and the black boxes indicate the area of model grid refinement referred to as the Minch sector.

2.3.2 Initial conditions and spin-up

We set the initial conditions to the ice sheet state when the MnIS was at its maximum extent. To avoid the computational costs and uncertainties associated with simulating the full build-up of the ice sheet, we initialise ice thickness in the domain from a perfectly plastic ice sheet model (Gowan et al., 2016) fixed to the lLGM extent at the continental shelf break. The 27 ka BP margin of Clark et al. (2012) was used for the remainder of the BIIS. The 27 ka BP margins of

the perfectly plastic ice sheet model output match well with the reconstructed maximum extent of the MnIS (Bradwell et al., 2008).

To calculate SMB we use monthly mean surface air temperatures and monthly mean total precipitation from climate model simulations to drive a positive-degree day (PDD) mass balance model as in (Gregoire et al., 2015, 2016). We use the PDD model PyPDD (Seguinot, 2013), which accounts for the sub-annual evolution of snow cover, and meltwater refreezing. The PDD factors and refreezing ratio are summarised in Table 2.1. The PDD model is driven by mean temperature and precipitation data calculated from the final 50 years of the 26 ka BP bias-corrected equilibrium climate simulation described by Morris et al. (2018), run with the HadCM3 coupled atmosphere–ocean–vegetation general circulation model (Gordon et al., 2000; Pope et al., 2000; Valdes et al., 2017). This simulation is part of a series of "snapshot" equilibrium simulations covering the last deglaciation that are a refinement of those previously reported by Singarayer et al. (2011) with updated boundary conditions including ice mask, ice orography, bathymetry, and land–sea mask (Ivanovic et al., 2016). It belongs to the same set of simulations used by Swindles et al. (2018) and Morris et al. (2018) to recently derive the climate of the Holocene and since the LGM, respectively. We downscale surface air temperatures onto the pre-spin-up initial ice sheet surface using a lapse rate of 5.1 K km^{-1}, which has been identified as a suitable lapse rate for modelling the Eurasian Ice Sheet (Siegert and Dowdeswell, 2004).

Parameter	Value	Units
Weertman exponent	1	-
Ice temperature	268	K
Ice density	918	kg m^{-3}
PDD$_{ice}$ factor	0.008	m K^{-1} d^{-1}
PDD$_{snow}$ factor	0.003	m K^{-1} d^{-1}
Refreeze ratio	0.07	-
Snow-rain threshold	275.15	K
Lapse rate	5.1	K km^{-1}

Table 2.1: Key model variables and parameters.

To remove the effect of a SMB feedback, in which surface elevation change causes a positive feedback to SMB due to atmospheric lapse rate, the SMB is

decoupled from elevation feedback. In practice, this means that once surface air temperatures are downscaled onto the initial ice sheet surface elevation to create the SMB map for the domain, SMB does not evolve as the ice sheet surface elevation evolves; there is no lapse rate feedback. This removes the possibility for a SMB instability of retreat, allowing for any MISI during the ice sheet retreat to be isolated.

We prescribe a sub-ice-shelf melt rate using a linear relationship with Sea Surface Temperature (SST):

$$m = -10T \qquad (2.1)$$

where m is melt (metres of meltwater equivalent) and T is the temperature (K) above the freezing point of the ocean, assumed to be 274.95 K. This relationship between SST and sub-ice-shelf melt rate is based on measurements from Pine Island Glacier, Antarctica (Rignot and Jacobs, 2002). SST values are taken from the same climate simulation that is used to calculate SMB. However, initial SST temperatures are corrected by -2 °C as exploratory sensitivity tests show that the uncorrected SST does not allow for ice shelves to form at the lLGM. We correct the SST to permit for ice shelf formation, allowing the influence of the presence or removal of an ice shelf to be tested.

We assume that contemporary land properties were like the bed properties beneath the MnIS. The basal friction coefficient map was produced by grouping regions of similar bed friction, then prescribing values to those regions based on bed friction coefficient values from other studies. Regions of similar basal friction were classified into the following five groups based on observable surface morphological features in satellite imagery and DEMs and from the glacial map of Britain (Clark et al., 2018) as well as reference to superficial geology maps.

1. Palaeo ice streams are based upon the presence of mega-scale lineations, convergent flow patterns from subglacial bedforms, and previous reporting in the literature (Stokes and Clark, 1999; Margold et al., 2015). As the main

outlets for ice flow and fastest-flow regions, these regions were assigned the lowest basal friction coefficients (β): 100.

2. Marine sediments are defined based upon geological maps and the presence of characteristic marine bedforms. These are highly deformable and were therefore assigned a value of 1000, the second lowest basal friction coefficient (β).

3. Subglacial lineations or drumlins are identified on the glacial map and elevation models. Lineations are thought to represent reasonably fast ice flow and be the product of subglacial bed deformation (Ely et al., 2016). These were assigned an intermediate basal friction coefficient (β=2000).

4. Subglacial ribs or ribbed moraines are identified from previous mapping and elevation models. These are thought to be more characteristic of slower ice flow than that of subglacial lineations and were thus assigned a higher basal friction coefficient. β=3000 was prescribed here.

5. Exposed bedrock was assigned the highest basal friction coefficient. These high roughness areas were defined by their characteristic surface morphology and from geological maps and were prescribed the highest value bed friction coefficient (β=4000).

The values for bed friction coefficients used as input into BISICLES (Figure 2.2c) were based on studies of present-day ice streams using the same friction law Weertman exponent (m=1), which calculated coefficients by inverting observed surface velocities of Pine Island Glacier and Austfonna Basin 3 (Favier et al., 2014; Gong et al., 2017). This approach simulates an ice stream of a similar morphology as reconstructed using empirical data (Bradwell et al., 2007). Sensitivity tests reveal that the ice sheet volume is sensitive to changes in bed friction coefficient map (Figure 2.3a), but the extent of ice after a 6000-year spin-up remains comparable even with different magnitudes of basal friction as ice extent in our

experiments is primarily controlled by the continental shelf edge and surface mass balance (Figure 2.2b).
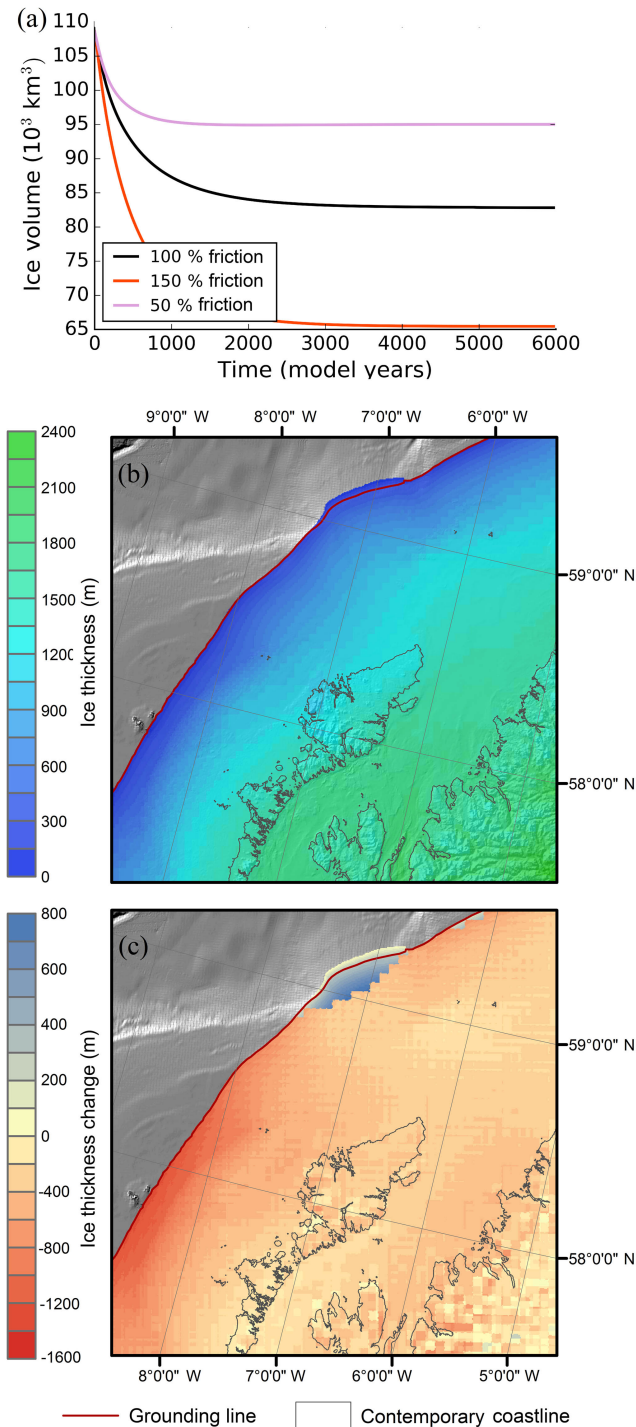
Figure 2.3: (a) Evolution of the ice sheet volume over the Minch sector during spin-up. (b) Simulated ice sheet thickness after 6000 model years of spin-up. (c) Ice thickness change between the start and end (year 6000) of the spin-up simulation (i.e. difference between Figs. 2a and 3b).

To recreate isostatically adjusted bed topography, we adjust modern topography using results from a Glacial Isostatic Adjustment (GIA) model (Figure 2.2d). GEBCO (Becker et al., 2009) provides modern offshore bathymetry, and SRTM (Farr et al., 2007) provides onshore topography. Isostatic adjustment uses results from the EUST3 GIA model (Bradley et al., 2011). EUST3 accounts for near-field and far-field isostatic adjustment due to ice loading. The Relative Sea Level (RSL) change from EUST3 at 30 ka BP is used to deform contemporary topography, maintaining a high-resolution ice sheet bed whilst also accounting for RSL change.

2.3.3 Experimental design

We designed our experiments to use an idealised representation of the external forcings of ice sheet retreat (surface mass balance and sub-shelf melt) in order to isolate the internal ice sheet mechanisms and instabilities of retreat. All experiments begin at a stable lLGM volume, with continental shelf edge glaciation and a small ice shelf (<4 km from shelf front to the grounding line) (Figure 2.3). Experiment set-up is summarised in Table 2.2. These experiments test the applicability of MISI to the MnIS. In reality, ice sheet evolution is a function of climate fluctuations, ice surface evolution, and sea level change as well as MISI. However, to isolate the effects of MISI, sea level is held constant throughout the experiments, there is no elevation–SMB feedback, and the climate change is a simple step change.

Name	Initial ice thickness	SMB	Sub shelf melt	Basal friction
SPINUP	Plastic thickness	26 ka BP	26.3 m yr^{-1}	Standard (Figure 2.4a)
RETREAT	SPINUP	26 ka BP + 1.5 K	47.1 m yr^{-1}	Standard
RETREAT_ATMOS	SPINUP	26 ka BP + 1.5 K	26.3 m yr^{-1}	Standard
RETREAT_OCN	SPINUP	26 ka BP	47.1 m yr^{-1}	Standard
READVANCE _xxxxyr	Retreat at model x year (800-year intervals)	26 ka BP	26.3 m yr^{-1}	Standard
RETREAT_NOSHELF	SPINUP	26 ka BP + 1.5 K	100 m yr^{-1}	Standard
READVANCE _COOLING	Stable READVANCE_8000yr	26 ka BP - 1.5 K	26.3 m yr^{-1}	Standard
SPINUP_MAXFRICT	Plastic thickness	26 ka BP	26.3 m yr^{-1}	Standard x 1.5
SPINUP_MINFRICT	Plastic thickness	26 ka BP	26.3 m yr^{-1}	Standard x 0.5

Table 2.2: Summary of experiment set-up and forcing. Plastic ice thickness is shown in Figure 2.2a, the SPINUP thickness in Figure 2.3b, and the difference between the plastic thickness and SPINUP thickness in Figure 2.3c. Surface mass balance at 26 ka BP is shown in Figure 2.2b.

Deglaciation

The end of the SPINUP simulation is used as the start point for the RETREAT experiment. In the simulation RETREAT, we use an idealised climate perturbation approach to trigger deglaciation, which consists of applying an instantaneous uniform warming of the surface air temperature by 1.5 K and SST by 2 K each month, without changing precipitation. The magnitude of these perturbations is based on changes between the 26 and 18 ka BP equilibrium climate simulations. The resulting SMB and sub-ice-shelf melt are then kept constant throughout the run. As for the SPINUP simulation, SMB is decoupled from an ice elevation–SMB feedback. Therefore, any change in the rate of ice sheet retreat is caused by internal ice sheet dynamics.

To test the relative role of ocean and atmospheric warming in driving the retreat, we ran RETREAT_ATMOS and RETREAT_OCN with only SMB or sub-ice-shelf melt rate perturbed, respectively. Both of these simulations only lead to partial deglaciation (Figure 2.4a), while the combination of both forcings (RETREAT) causes deglaciation to the northwest Scottish Highlands. We keep bed topography and sea level constant for the duration of the deglaciation simu-
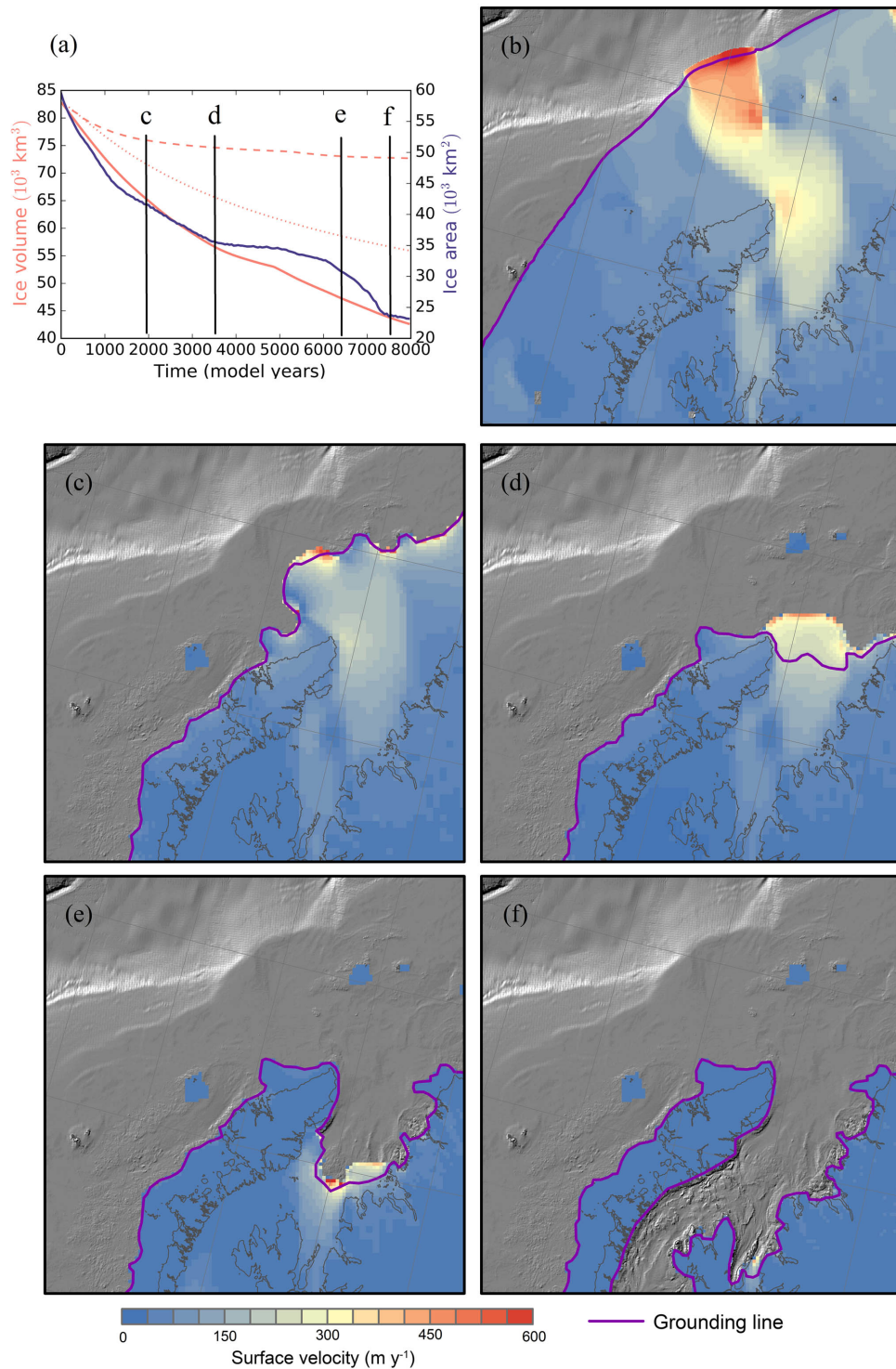
Figure 2.4: Evolution of the ice sheet in the Minch sector in the RETREAT simulation. The contemporary coast is shown as a thin grey line. (a) Time series of ice volume and area over the Minch sector. The dashed curve shows the volume response to RETREAT_OCN. The dotted curve shows the response to RETREAT_ATMOS. Ice surface velocity (b, c, d, e, f) at 0, 2000, 3500, 6300, and 7500 model years, respectively, with the grounding line shown in purple.

lations as an evolving sea level could interact with the process of MISI. Therefore, a constant sea level is necessary to understand the potential for MISI during the retreat of the MnIS. In reality, only a small RSL change (∼15 m sea level fall) would be expected because of the competing effects of BIIS expansion and global sea level fall (Bradley et al., 2011).

Reversibility of ice stream retreat

We test whether retreat is irreversible once it is initiated or whether ice volume and area recover to lLGM levels given a return to lLGM climate. In the experiment READVANCE, we test for the reversibility of ice stream retreat by reverting the climate perturbations during the deglaciation. A set of simulations was started from points at 800 years intervals through the RETREAT simulation with the boundary conditions returned to lLGM and run for 10,000 model years to allow the ice sheet to reach a new stable state (constant volume and extent). Here, ice sheet collapse is defined as an ice sheet not returning to its lLGM extent given lLGM boundary conditions following retreat.

Ice shelf influence

We tested whether an ice shelf is important in influencing the dynamics of the MnIS retreat by providing a buttressing force to reduce ice stream flux over the grounding line. To test this hypothesis, we ran a simulation (RETREAT_NOSHELF) in which the sub-ice-shelf melt rate was increased to 100 m yr^{-1} (52.9 m yr^{-1} higher than during the RETREAT simulation) in order to force the removal of the ice shelf during deglaciation. Note that, in this experiment, we kept the frontal ablation rates identical to RETREAT in order to isolate the effects of ice shelf buttressing, removing the influence of any increased ocean ice mass loss.

2.4 Results and discussion

2.4.1 Pattern of retreat

Imposing a constant SMB and sub-ice-shelf melt perturbation (simulation RE-TREAT) causes a retreat of the MnIS from the continental shelf edge to the highlands within 8000 model years (Figure 2.4). Although the SMB and sub-ice-shelf melt are constant through the simulation, with SMB decoupled from the change in surface elevation, the rate of volume and area change fluctuates through the simulation (Figure 2.4a), whilst an exponential decay in ice volume would be expected given a simple climate forcing (Nye, 1960, 1963; Johannesson et al., 1989; Harrison et al., 2003). The evolution of the ice stream during the RETREAT simulation can be divided into three stages; an initial retreat phase, a stagnation phase, and a late retreat phase. Volume loss is most rapid at the initial retreat phase (Figure 2.4b-d), reducing the domain's ice volume in the first 2000 model years by ∼25%. In the stagnation phase, between 2000 and 6300 model years of the simulation (Figure 2.4d-e), volume loss slows. Finally, during the late retreat phase volume loss slightly increases from 6300 model years onward (Figure 2.4e-f). The slower rate of volume loss in the stagnation phase occurs as the margin retreats beyond marine influence onto the Outer Hebrides for the majority of the domain. At this stage the ice stream is in a marine setting similar to many tidewater glaciers in Greenland and Antarctica (Joughin et al., 2008), and the re-acceleration of the late retreat phase only begins once the grounding line has retreated further south towards the inner trough of the Minch (Figure 2.4e).

The ice area loss produces a trend broadly similar to volume loss, although in the stagnation phase (3500 to 6300 model years) there is negligible area loss despite continuing volume loss (Figure 2.4a). This is associated with a near stagnation of the grounding line when the margin of the ice sheet has mostly retreated onshore and the marine-terminating ice stream becomes confined be-

tween the Scottish mainland and the Outer Hebrides (Figure 2.4d-e). During the stagnation phase ice loss occurs through thinning with limited change in margin position. As the thinning continues, the ice area begins to retreat more rapidly just after 6300 model years, which coincides with the start of a rapid margin retreat in the Minch (Figure 2.4e).

2.4.2 Role of ice shelf buttressing

Ice shelves provide a buttressing membrane stress to the ice streams flowing upstream of them (Hindmarsh, 2006). Ice stream acceleration in response to the sudden collapse of ice shelves has been observed in the contemporary Antarctic Peninsula (Scambos et al., 2004). The buttressing effect of ice shelves can also allow a stable grounding line position given a reverse sloping bed (Gudmundsson, 2013), meaning it is important to consider the impact of ice shelves when examining MISI. The ice shelf that forms during the simulations of the MnIS is initially unconstrained by topography or surrounding ice until the grounding line retreats during the stagnation phase of retreat at 6300 years (Figure 2.4e). It is therefore expected that removing the ice shelf from the simulations whilst triggering deglaciation will initially have a negligible impact on the retreat of the ice stream before having a greater impact once the ice shelf is constrained by surrounding grounded ice.

For the first 5000 model years the simulated grounded ice volumes diverge by less than 1 % in the simulations with RETREAT and without RETREAT_NOSHELF an ice shelf (Figure 2.5). After 5000 model years there is a notable divergence in the evolution of grounded ice volume of the two simulations, for which the simulation without an ice shelf has higher rates of mass loss compared to the simulation with ice shelves (Figure 2.5a). At the time of maximum volume difference between the simulations (7000 model years), the simulation RETREAT_NOSHELF has a grounded volume $\sim$2000 km^3 (10 %) smaller than the simulation RETREAT. However, the acceleration of mass loss during the late retreat phase occurs in
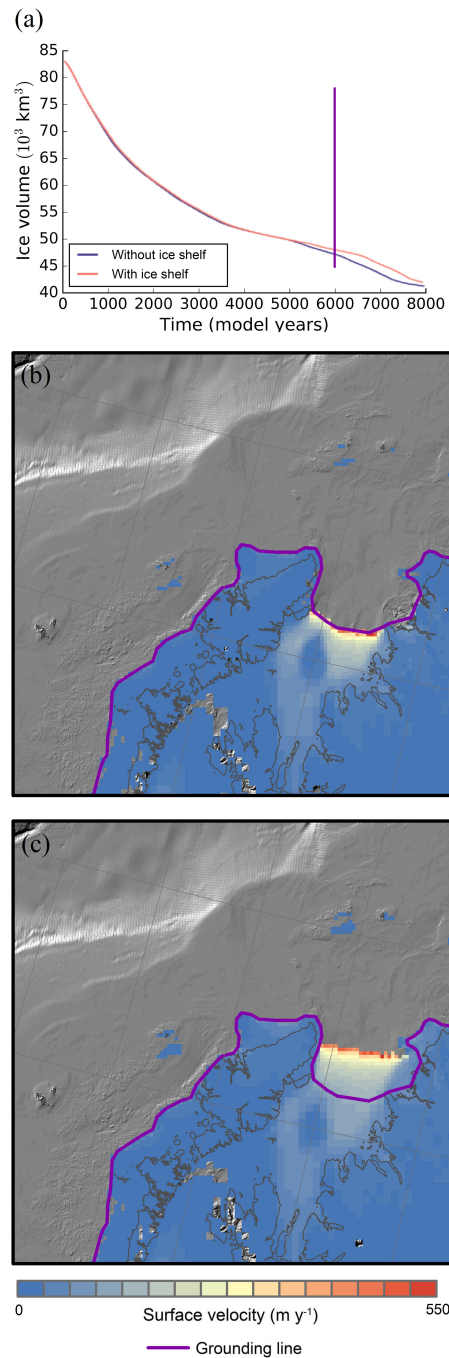
Figure 2.5: Effect of ice shelves. The contemporary coast is shown as a thin grey line. (a) Evolution of grounded ice sheet volume over the Minch sector in simulation RETREAT with ice shelves (red line) and RETREAT_NOSHELF in which ice shelves are forcibly removed (blue line). (b, c) Surface velocity and grounding line location (purple line) in RETREAT_NOSHELF (b) and RETREAT (c).

both simulations, suggesting the presence or removal of an ice shelf cannot prevent continued ice volume loss. Although the presence of an ice shelf affects the ice volume, it has almost no impact on the location of the grounding line and its chronology of retreat (e.g. Figure 2.5b-c), with the difference in the grounding

line location mostly within the finest resolution of the model (500 m). The removal of the ice shelf also means that the grounding line has no mechanism for stability on the reverse sloping bed retreat southward of the MTBH (Gudmundsson, 2013). These results suggest that the presence or absence of an ice shelf has only a limited influence on the spatial pattern and timing of MnIS retreat. A significant difference in ice volume is not reflected in grounding line position, showing that ice flux across the grounding line is important, not just the position of the grounding line. The significance of the ice shelf influence demonstrates that in order to be confident of the future evolution of our contemporary ice sheets, we need to be confident of the future evolution of ice shelves over centennial timescales.

The unconstrained nature of the Minch ice shelf at the start of the deglaciation makes the mechanics of ice shelf buttressing different from many areas of the contemporary West Antarctic Ice Sheet, where large ice shelves are buttressed laterally by surrounding ice or bedrock (Pritchard et al., 2012). In a number of prominent places in Antarctica, ice shelves are also pinned from underneath by bedrock rises (Matsuoka et al., 2015). This may suggest that the dynamics of the Minch ice shelf during the first stage of retreat are more analogous to East Antarctic ice shelves. The Minch ice shelf is not constrained laterally until the later stages of the deglaciation when the shelf is supported by surrounding ice (Figure 2.5), and the topographic setting is similar to examples of fjord-like confined glaciers in Greenland (Joughin et al., 2008). Whilst the MnIS and many Greenland ice streams can retreat beyond direct marine influence (Funder et al., 2011), this is not possible for Antarctic ice streams grounded in deeper troughs. Empirical evidence of the last Eurasian ice sheet has the western ice margin constrained by the continental shelf edge across the majority of the Atlantic margin (Hughes et al., 2016). This suggests that ice shelves at maximum ice extent across the Atlantic margin would be similar to the Minch ice shelf in the early stages of deglaciation, limited in size by the continental shelf break, and

unconstrained. It is likely, therefore, that ice shelves along this Atlantic margin were not influential in the retreat of the ice sheet until the grounding line retreated to areas laterally constrained by topography or surrounding ice.

2.4.3   Testing ice stream instability with readvance experiments

Given the bathymetric profile of the ice stream path (Figure 2.6), it would be expected that the MnIS would experience MISI ∼180 km along the A-B transect (Figure 2.6b). This is because of the reverse slope (downhill retreat) that the ice stream path would encounter in the later stages of the deglaciation after retreating beyond the MTBH. The experiment READVANCE returns the ice stream to the lLGM climate at 800-year intervals during the RETREAT experiment, in an attempt to recover the ice stream to lLGM extent.

For the first 5600 model years of the recovery experiment (READVANCE) ice volume returns to lLGM extent given a return to lLGM forcings. All simulations started from RETREAT at model years 800-5600 readvance to the lLGM extent. However, in simulations with a point of recovery (initial conditions) beyond 5600 model years, the ice stream does not recover to lLGM extent given lLGM boundary conditions (Figure 2.7); instead it evolves towards a reduced stable state with a volume ∼25 % smaller and an area ∼50 % smaller than the stable lLGM state (Figure 2.7a,b).

We identify two stable ice conditions in these READVANCE simulations given our initial lLGM forcings; a full shelf edge glaciation (Figure 2.7c) and a small Hebrides Ice Cap with glaciation in the Minch limited to the east trough (Figure 2.7d). The resulting stable extent of the ice stream is dependent on the evolution history of the ice stream; there is hysteresis in the MnIS evolution. Hysteresis of ice sheet evolution suggests an instability during the advance or retreat of an ice sheet (Schoof, 2007).
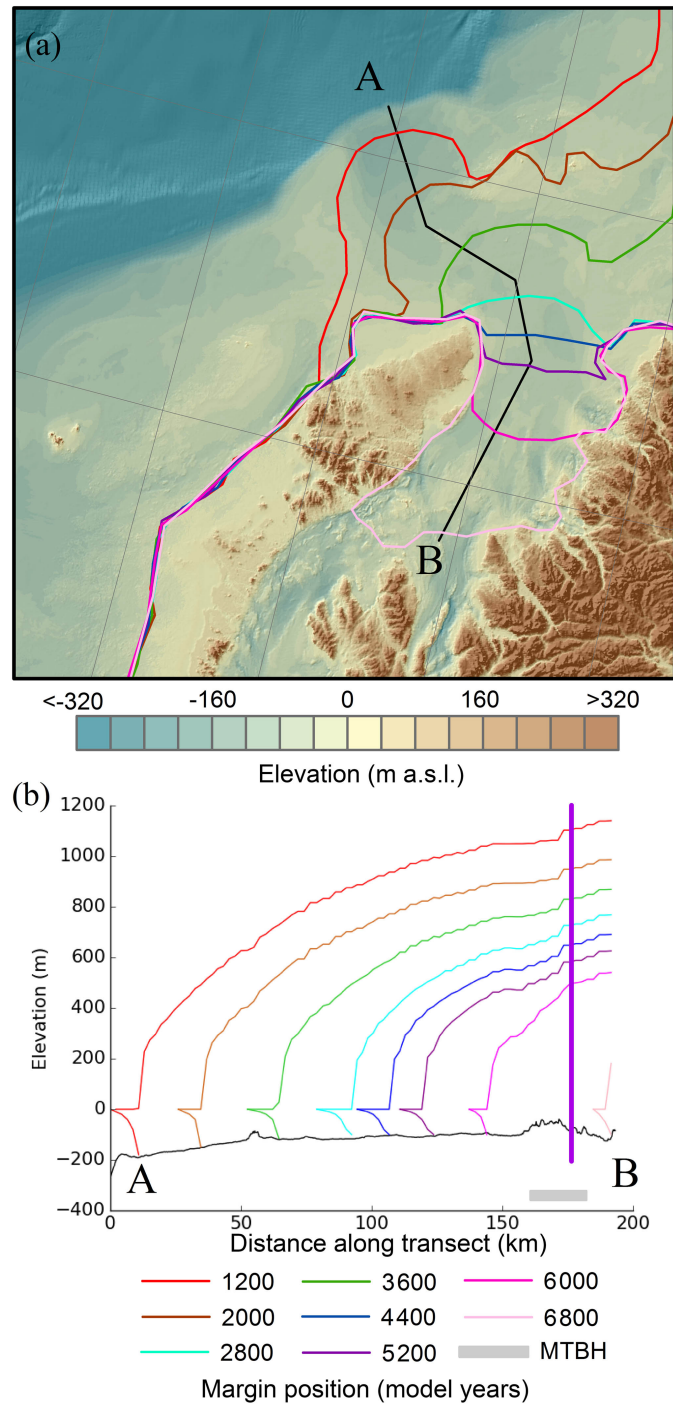
Figure 2.6: (a) The grounding line position of the ice sheet at 800-year intervals during the RETREAT simulation. (b) Transect through the ice stream showing the ice sheet elevation at the same intervals. The purple line marks the grounding line position in the stable "collapsed" ice sheet state from the READVANCE simulations (Figure 2.7d).

The zone of collapse is defined here as the point of divergence of recovery states; the position of the grounding line at which returning to lLGM forcing no longer allows recovery to initial lLGM extent and only allows recovery to the new
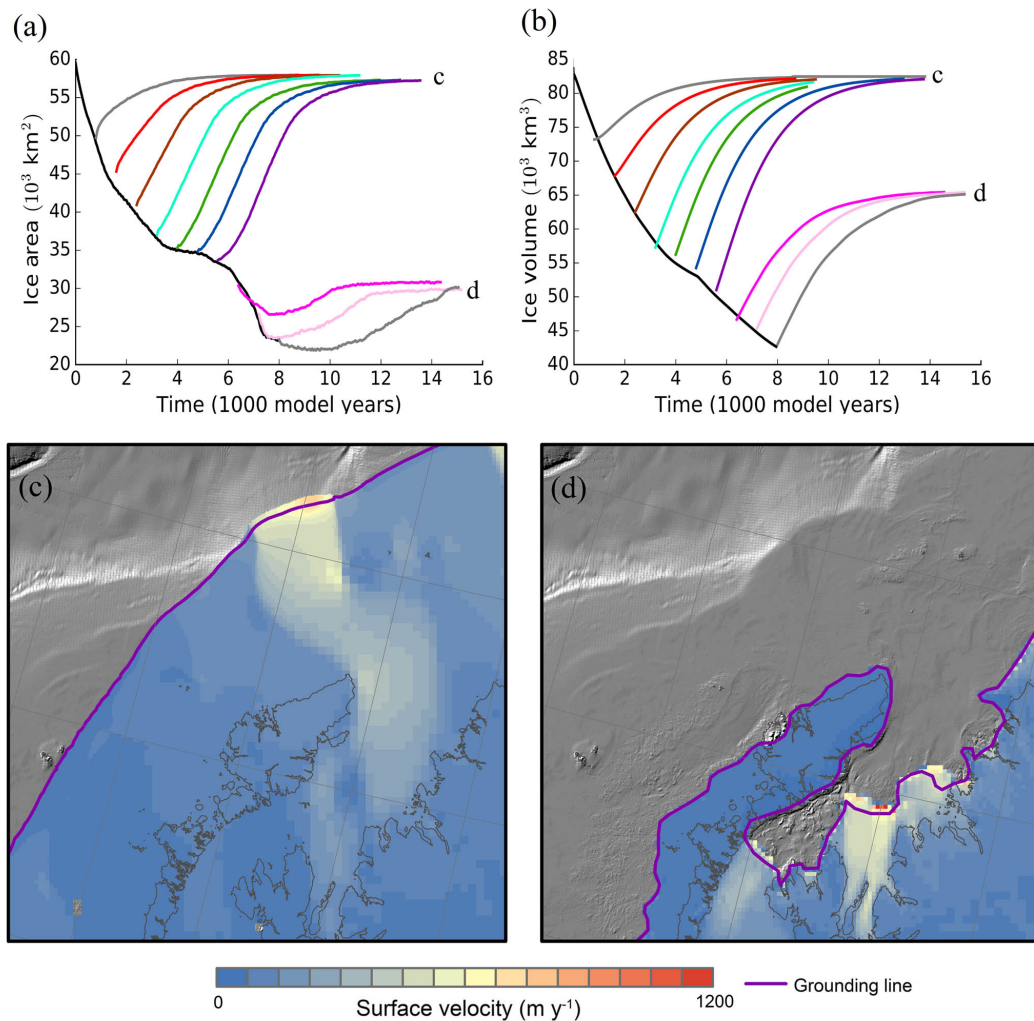
Figure 2.7: Results of the ensemble of READVANCE simulations testing insta-
bility in the Minch Ice Stream. The contemporary coast is shown as a thin grey
line. (a, b) Evolution of the ice sheet area (a) and volume (b) over the Minch
sector in the RETREAT (black) and READVANCE simulations (coloured lines).
Line colours correspond to those of (Figure 2.6), such that the initialisation of the
READVANCE simulations is 400 years later than the timing of the grounding
line positions shown in Figure 2.6. Labels "c" and "d" indicate the "maximum"
(c) and "collapsed" (d) stable states with corresponding panels showing the re-
spective surface ice sheet velocity (m yr^{-1}) and grounding line locations (purple
line).

stable condition of limited Minch glaciation (Figure 2.7d). The zone of collapse
occurs 5600–6400 model years into the retreat, ~180 km along the mapped AB
transect, as the margin retreats onto a retrograde bed slope (Figure 2.6). The
point of collapse is simulated to occur after the margin has retreated back from
the MTBH, suggesting that the MnIS transitions through a zone of instability at
this point, thus indicating that the observed hysteresis is caused by MISI.

As well as the influence of MISI, the morphology of the ice stream marine margin may also cause an instability during the retreat of the ice stream. For the majority of the retreat, the ice stream is buttressed to the east and west by surrounding ice (Figure 2.4). However, in the smaller stable state (Figure 2.7d), the ice stream is not buttressed on the western margin due to the bay forming in the west trough of the Minch. This removal of the lateral buttressing of the ice stream to the west may also contribute to the inability of the ice stream to recover the lLGM extent in this experiment.

The difference between the grounding line position at the zone of transition and at the collapse state, i.e. the magnitude of collapse, varied across the ice stream (Figure 2.8a). In the east trough the magnitude of collapse was limited, and a bathymetric transect shows only a limited reverse slope to facilitate MISI (Figure 2.8b). However, in the west trough the magnitude of collapse was more significant, and the bathymetric transects shows a more sustained reverse slope to facilitate MISI (Figure 2.8c).

With ice unable to advance beyond the MTBH in the recovery simulations, a mechanism is required to allow ice to first advance towards the shelf edge prior to the lLGM, but then be unable to advance after retreat from lLGM extent. Although this study started with an ice extent already at the lLGM extent, other studies such as Patton et al. (2016) successfully simulated the build-up of the entire Eurasian ice sheet, with ice overcoming the MTBH and reaching the shelf edge given an lLGM climate. The variability and uncertainty in the climate forcing could allow readvance back to the continental shelf edge. In particular, in our model, if the lLGM climate is uniformly cooled by 0.5 K across the entire domain ice readvances from a "collapsed" position to a lLGM position. It is reasonable that this small correction falls within the error of the climate simulations or variability in the climate during the build-up phase. Nonetheless, even with the cooled climate, recovery back to lLGM extent is considerably slower beyond 5600 model years. Despite cooling the climate to force a recovery to lLGM
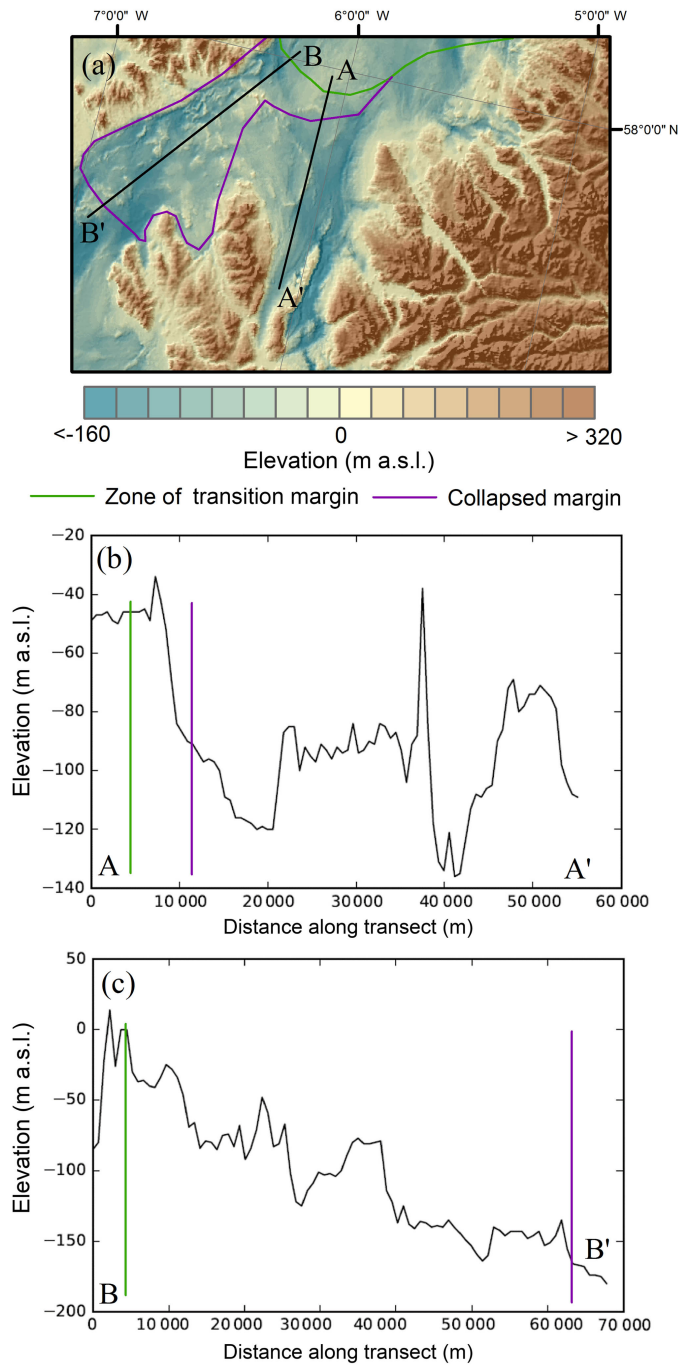
Figure 2.8: The difference in the effects of MISI between the east trough and the west trough. (a) The 6400-model-year RETREAT margin (green) and the stable "collapsed" extent margin (purple). (b) A-A' transect of bathymetry and collapse extent in the east trough. (c) B-B' transect of bathymetry and collapse extent in the west trough.

extent, a behavioural change in the ice stream readvance beyond 5600 model years remains.

Topographic changes over the course of the glacial cycle may also explain why the simulations did not readvance over the MTBH given lLGM conditions. These topographic changes would be present in two ways; changes in isostasy during the glacial cycle, and bed erosion and deposition. The simulations run on an ice sheet bed adjusted for isostasy at 30 ka BP, which exaggerates the reverse slope causing MISI. The original advance of the ice stream would likely be on a bed where the slope was reduced. Bed erosion could also increase the prominence of the hard bedrock topographic high after initial glaciation. According to the modelling of Patton et al. (2016), the MnIS is an area with high potential cumulative erosion at 37-19 ka BP. Both these mechanisms could exaggerate the reverse slope subsequent to glaciation, potentially allowing initial glacial advance, but not readvance from a retreated state. Therefore, this demonstrates the importance of understanding future topography evolution in understanding the long-term evolution of contemporary ice sheets.

2.4.4   Comparison to empirical reconstructions

To investigate the mechanism of marine influence on the MnIS, and simplify the experimental design, several assumptions were made which take the experiments away from "reality". In reality, the various controlling factors of ice sheet change would interact together to exaggerate or dampen the effect of MISI. For example, rebound of the ice sheet bed during deglaciation could dampen or eliminate the observed effect of MISI. Similarly, an elevation–SMB feedback could exaggerate any observed MISI as the ice sheet thins and retreats. Removing the experiments from a set-up akin to reality is justified to investigate the possibility of marine influence on the BIIS. The simulations test the applicability of MISI to such a bathymetric setting, but do not imply a relative importance of MISI. To consider relative importance, the simulations would also need to consider evolving sea level, elevation–SMB feedback, evolving climate, thermodynamics, and bed friction,

amongst others. This approach remains beyond the capability of current ice sheet models.

The resulting pattern of retreat from the RETREAT simulation has a number of similarities with previous retreat reconstructions (Bradwell et al., 2008; Clark et al., 2012; Hughes et al., 2016) despite the idealised nature of the climate forcing. For example, the margin appears to "hinge" on the northern point of the Isle of Lewis (Bradwell et al., 2007; Bradwell and Stoker, 2015). The margin also recesses into the Minch, with a small ice cap on the Outer Hebrides persisting during deglaciation. The idealised nature of the climate forcing means that pattern and relative rate of retreat can be compared to empirical reconstructions, but the absolute timing cannot. There are close similarities between the simulated retreat and reconstructed retreat in the later stages of the deglaciation. In the later stages of retreat the east trough contains a small ice stream whilst the west trough has fully deglaciated and formed a calving bay, evident in both the simulated (Figure 2.7d) and reconstructed retreats (Bradwell and Stoker, 2015). We take the key similarities of retreat pattern and margin morphology between the simulated retreat and reconstructed retreat as an indication that the main mechanisms that controlled the deglaciation of MnIS are mimicked in our simulations.

All simulations in this study use constant climate forcing, which does not account for the evolution of climate during the deglaciation of the BIIS. The fluctuations in volume and area change in the simulations are the signal of internal dynamical ice sheet processes, which do not include the feedback between SMB and elevation or any transient evolution of external forcing in climate and sea level.

The reconstructed retreat history of the MnIS is the result of both the ice sheet internal and external forcing signal. Therefore, the signals simulated in these experiments could be exaggerated or dampened by external forcing: the climate signal. This style of retreat is evident from the moraine record (Figure

2.1), which shows a series of back-stepping moraines across the continental shelf (Bradwell et al., 2008; Bradwell and Stoker, 2015; Clark et al., 2018). It is inferred that these moraines form during a period of relative stability of the margin. These large seabed moraines occur in several places across the shelf edge, but there is only one period during the RETREAT simulation when the margin is stable, when the margin passes the northernmost tip of the Isle of Lewis and enters the Minch (Figure 2.4a,d). The surface expressions of the large seabed moraines are present in the bed topography used in the simulations. However, the ice margin retreats over other areas with a greater surface expression than these morainic wedges with no stabilisation of the margin.

The area and volume loss acceleration during the late retreat phase, which we interpret as the beginning of MISI, in reality would also be influenced by the climate fluctuations. The magnitude of this area and volume loss would be exaggerated or dampened depending on the increasing or decreasing SMB of the ice sheet at any given period. Overall, the simulated volume and area change in these simulations is relatively smooth, whilst in reality climate fluctuations will have caused annual or even decadal dynamic margin fluctuations, more akin to the Hubbard et al. (2009) simulation of the ice sheet evolution which was driven by a transient climate.

Geomorphological studies of palaeo ice sheets are able to reconstruct the area of ice sheets. Reconstructing ice thickness, and therefore volume, requires the introduction of further uncertainties, like bed friction and SMB, and therefore it is sometimes assumed that area change can directly inform volume change of the ice sheet (Hughes et al., 2016). However, model simulations of palaeo ice sheets can consider both area and volume changes. In these simulations, although volume and area evolution showed a similar trend, the area evolution during RETREAT had more obvious pauses and accelerations in area loss than the pattern of volume loss. A change in ice stream velocity could also alter ice sheet volume without altering the ice sheet area, as shown by varying the bed friction in

the SPINUP experiment (Figure 2.3a). In this example, understanding the area change through geomorphic empirical evidence may overstate the magnitude of changes expected in volume loss.

An idealised climate warming perturbation was used to trigger deglaciation in the simulations (e.g. RETREAT) in order to isolate the internal mechanisms of retreat. However, the retreat is reconstructed to have begun before ∼27 ka BP, when the NGRIP δ18O record suggests a cooling rather than a warming climate over Greenland (Andersen et al., 2004). Whilst rapid deglaciation can be achieved in ice sheets with significant ice streaming due to ice stream acceleration (Robel and Tziperman, 2016), a climate trigger is required to increase the surface slopes at the ice sheet margin. Model results also suggest a generally cooling global climate at ∼27 ka BP (Singarayer and Valdes, 2010). The warming mechanism we used to trigger deglaciation in our simulations is not apparent in the climate record. The results of the RETREAT simulations also indicate that internal dynamical mechanisms alone would not have been sufficient to continue retreat until the triggering of MISI when the ice stream retreats past the MTBH. It seems that the MnIS was retreating in a cooling climate, but these simulations idealised climate forcing to isolate internal ice sheet instabilities and therefore do not reveal a mechanism that explains MnIS retreat in a cooling climate. There are two likely possibilities that could explain the MnIS retreating in a cooling climate (explained below): (i) internal mechanisms of the BIIS or (ii) a local SMB change of this sector of the ice sheet prior to ∼27 ka BP.

A local SMB change could be caused by atmospheric warming or a reduction in precipitation. Local warming of the northern British Isles, whilst the rest of the BIIS and other Northern Hemisphere ice sheets expanded, could be a mechanism to explain early MnIS retreat. The NGRIP ice core is more than the synoptic scale away from the Minch, and therefore could reasonably be local warming during global cooling. Given the uncertainty in palaeo climate modelling, particularly at high latitude due to sensitivity to ice sheet forcing (Singarayer and Valdes,

2010), it is a reasonable possibility that a local warming would not be included in the HadCM3 last glacial simulations used to force the ice sheet model. However, it seems unlikely that climate could be warming in the Minch whilst allowing rapid expansion for the remainder of the BIIS. Additionally, a local reduction in precipitation could be caused by a change in the position of the polar front, which would have been affected by the advance and retreat of the Northern Hemisphere ice sheets during the last glacial cycle (Oster et al., 2015). A migration in the polar front would likely affect the entire western margin of the BIIS, potentially causing the start of deglaciation to be asynchronous with the rest of the Northern Hemisphere (Scourse et al., 2009). However, as the forcing in these experiments remains idealised, this is only a speculative driver of early BIIS retreat.

Alternatively, internal mechanisms of the BIIS that were not simulated as part of this study could explain a retreating MnIS in a cooling climate. Two candidates for this mechanism are ice piracy from other catchments of the BIIS, or the initial advance of the MnIS being the result of a surge-type advance. The simulations presented here did not feature a lapse rate effect on SMB as the ice sheet surface lowered into a warmer climate. This process could help facilitate rapid retreat in a cooling climate, but could not be a trigger for retreat. During the retreat of the MnIS, ice was extending over Northern Ireland out to the shelf edge (Dunlop et al., 2010; Clark et al., 2012). It is theorised that a significant proportion of the ice feeding this advance came from the Hebrides ice stream, evidenced by large moraines northward of Donegal Bay. The source areas of the Hebrides ice stream will have significantly overlapped with the MnIS, and the advance of the Hebrides ice stream could have initiated ice piracy from the MnIS, causing retreat in a cooling climate. The initial advance of the MnIS could also have been caused by a surge-type advance, which subsequently retreated as the remainder of the ice sheet advanced. These experiments assumed an initial steady state at lLGM extent. Dating the advance of ice sheets is inherently more uncertain than retreat (Hughes et al., 2016). Although the significant trough mouth fan could

be taken as evidence for a relatively stable MnIS, it almost certainly formed over multiple glacial advance and retreat cycles (Bradwell and Stoker, 2015). These mechanisms are speculative and would require experiments with transient forcings to test. These internal instabilities would not have been represented in these simulations because a warming climate was used to trigger deglaciation, forcing the Hebrides ice stream to retreat rather than advance. Bed friction and topography also do not evolve during the simulation, meaning ice streams in the simulations cannot activate or shutdown due to sediment exhaustion, or bed hydrology changes. Bed hydrology evolution has been identified as a key control of ice streams, but this process remains challenging to incorporate into ice sheet models (Hewitt, 2013). These simulations therefore provide evidence for internal processes during the retreat of the MnIS, but the initial trigger for deglaciation of the MnIS in a cooling climate remains elusive.

2.5   Conclusions

We simulated the retreat of the MnIS from a position of maximum extent, using an idealised climate perturbation in order to identify the role of the internal dynamical mechanisms in ice sheet retreat. This simulation showed a retreat in three phases, an initial retreat (0–3500 model years), stagnation (3500–6300 model years), and a late retreat (after 6300 model years). The stagnation phase occurred as the ice stream retreated past the northernmost tip of the Isle of Lewis. This slowing of volume and area loss coincides with a significant proportion of the ice sheet margin retreating onto the Outer Hebrides, beyond marine influence. At this point in the simulation, the MnIS is in a marine setting similar to many retreating tidewater glaciers in Greenland and Antarctica. During this phase, a laterally constrained ice shelf provided buttressing to the ice stream. In the late retreat phase, the area and volume loss rate re-accelerated as the grounding line retreated on a reverse bed slope. We reversed the idealised climate perturbation regularly during this simulated deglaciation to test for instabilities of retreat.

After the re-acceleration of volume and area loss at 6300 model years, the ice sheet did not recover to lLGM volume and area given lLGM conditions. We suggest this result is evidence for a retreat of the MnIS caused by MISI.

We compared the simulated retreat to a simulation with the ice shelves removed, which was otherwise identical. The simulations show that ice shelves were not influential to the magnitude and pattern of retreat for the first 5000 model years of the simulated deglaciation, when the ice shelf was unconstrained. Once the margin had retreated into a trough geometry that constrained the ice shelf, the removal of the ice shelf caused higher ice stream velocities and a more rapid ice volume loss. We therefore find evidence for an influential ice shelf buttressing effect during MnIS deglaciation. Our simulations demonstrate the importance of MISI and ice shelf buttressing during retreat of the Minch ice stream. These processes currently represent the largest source of uncertainty in projecting the future evolution of the Antarctic ice sheet. We suggest that the detailed chronology of BIIS retreat currently being produced by the BRITICE-CHRONO project has the potential to constrain important processes controlling MISI in models used for future sea level projections.

Data Availability

We used a branch of the BISICLES ice sheet model, revision 3635 (https://anag-repo.lbl.gov/svn/BISICLES/public/branches/smb/, Lee, 2018). Output files and required input files to reproduce the described experiments can be found at https://doi.org/10/cvv7 (Gandy, 2018). Code for the PDD model used is available at https://doi.org/10.5281/zenodo.1476364 (Seguinot, 2018).

References

Andersen, K. K. et al. (2004). "High-resolution record of Northern Hemisphere climate extending into the last interglacial period". In: *Nature* 431.7005, pp. 147–151. DOI: 10.1038/nature02805.

Ballantyne, C. K. and J. O. Stone (2009). "Rock-slope failure at Baosbheinn, Wester Ross, NW Scotland: age and interpretation". In: *Scottish Journal of Geology* 45.2, pp. 177–181. DOI: 10.1144/0036-9276/01-388.

Becker, J. J. et al. (2009). "Global Bathymetry and Elevation Data at 30 Arc Seconds Resolution: SRTM30_PLUS". In: *Marine Geodesy* 32.4, pp. 355–371. DOI: 10.1080/01490410903297766.

Boulton, G. S., M. Hagdorn, and N. R. Hulton (2003). "Streaming flow in an ice sheet through a glacial cycle". In: *Annals of Glaciology* 36, pp. 117–128. DOI: 10.3189/172756403781816293.

Boulton, G. and M. Hagdorn (2006). "Glaciology of the British Isles Ice Sheet during the last glacial cycle: form, flow, streams and lobes". In: *Quaternary Science Reviews* 25.23-24, pp. 3359–3390. DOI: 10.1016/j.quascirev.2006.10.013.

Bradley, S. L., G. A. Milne, I. Shennan, and R. Edwards (2011). "An improved glacial isostatic adjustment model for the British Isles". In: *Journal of Quaternary Science* 26.5, pp. 541–552. DOI: 10.1002/jqs.1481.

Bradwell, T. (2013). "Identifying palaeo-ice-stream tributaries on hard beds: Mapping glacial bedforms and erosion zones in NW Scotland". In: *Geomorphology* 201, pp. 397–414. DOI: 10.1016/j.geomorph.2013.07.014.

Bradwell, T. and M. S. Stoker (2015). "Submarine sediment and landform record of a palaeo-ice stream within the British-Irish ice sheet". In: *Boreas* 44.2, pp. 255–276. DOI: 10.1111/bor.12111.

Bradwell, T., M. Stoker, and R. Larter (2007). "Geomorphological signature and flow dynamics of The Minch palaeo-ice stream, northwest Scotland". In: *Journal of Quaternary Science* 22.6, pp. 609–617. DOI: 10.1002/jqs.1080.

Bradwell, T. et al. (2008). "The northern sector of the last British Ice Sheet: Maximum extent and demise". In: *Earth-Science Reviews* 88.3-4, pp. 207–226. DOI: 10.1016/j.earscirev.2008.01.008.

Clark, C. D., A. L. Hughes, S. L. Greenwood, C. Jordan, and H. P. Sejrup (2012). "Pattern and timing of retreat of the last British-Irish Ice Sheet". In: *Quaternary Science Reviews* 44, pp. 112–146. DOI: 10.1016/j.quascirev.2010.07.019.

Clark, C. D. et al. (2018). "BRITICE Glacial Map, version 2: a map and GIS database of glacial landforms of the last British-Irish Ice Sheet". In: *Boreas* 47.1, 11–e8. DOI: 10.1111/bor.12273.

Cornford, S. L., D. F. Martin, V. Lee, A. J. Payne, and E. G. Ng (2016). "Adaptive mesh refinement versus subgrid friction interpolation in simulations of Antarctic ice dynamics". In: *Annals of Glaciology* 57.73, pp. 1–9. DOI: 10.1017/aog.2016.13.

Cornford, S. L., D. F. Martin, D. T. Graves, D. F. Ranken, A. M. Le Brocq, R. M. Gladstone, A. J. Payne, E. G. Ng, and W. H. Lipscomb (2013). "Adaptive mesh, finite volume modeling of marine ice sheets". In: *Journal of Computational Physics* 232.1, pp. 529–549. DOI: 10.1016/j.jcp.2012.08.037.

Dunlop, P., R. Shannon, M. McCabe, R. Quinn, and E. Doyle (2010). "Marine geophysical evidence for ice sheet extension and recession on the Malin Shelf: New evidence for the western limits of the British Irish Ice Sheet". In: *Marine Geology* 276.1-4, pp. 86–99. DOI: 10.1016/J.MARGEO.2010.07.010.

Farr, T. G. et al. (2007). "The Shuttle Radar Topography Mission". In: *Reviews of Geophysics* 45.2, RG2004. DOI: 10.1029/2005RG000183.

Favier, L., G. Durand, S. L. Cornford, G. H. Gudmundsson, O. Gagliardini, F. Gillet-Chaulet, T. Zwinger, A. J. Payne, and A. M. Le Brocq (2014). "Retreat of Pine Island Glacier controlled by marine ice-sheet instability". In: *Nature Climate Change* 4.2, pp. 117–121. DOI: 10.1038/nclimate2094.

Feldmann, J., T. Albrecht, C. Khroulev, F. Pattyn, and A. Levermann (2014). "Resolution-dependent performance of grounding line motion in a shallow model compared with a full-Stokes model according to the MISMIP3d inter-comparison". In: *Journal of Glaciology* 60.220, pp. 353–360. DOI: 10.3189/2014JoG13J093.

Feldmann, J. and A. Levermann (2015). "Collapse of the West Antarctic Ice Sheet after local destabilization of the Amundsen Basin". In: *Proceedings of the National Academy of Sciences* 112.46, pp. 14191–14196. DOI: 10.1073/pnas.1512482112.

Funder, S., K. K. Kjeldsen, K. H. Kjær, and C. Ó Cofaigh (2011). "The Greenland Ice Sheet During the Past 300,000 Years: A Review". In: *Developments in Quaternary Sciences* 15, pp. 699–713. DOI: 10.1016/B978-0-444-53447-7.00050-7.

Gladstone, R. M., R. C. Warner, B. K. Galton-Fenzi, O. Gagliardini, T. Zwinger, and R. Greve (2017). "Marine ice sheet model performance depends on basal sliding physics and sub-shelf melting". In: *The Cryosphere* 11.1, pp. 319–329. DOI: 10.5194/tc-11-319-2017.

Gong, Y., T. Zwinger, S. Cornford, R. Gladstone, M. Schäfer, and J. C. Moore (2017). "Importance of basal boundary conditions in transient simulations: Case study of a surging marine-terminating glacier on Austfonna, Svalbard". In: *Journal of Glaciology* 63.237, pp. 106–117. DOI: 10.1017/jog.2016.121.

Gordon, C., C. Cooper, C. A. Senior, H. Banks, J. M. Gregory, T. C. Johns, J. F. B. Mitchell, and R. A. Wood (2000). "The simulation of SST, sea ice

extents and ocean heat transports in a version of the Hadley Centre coupled model without flux adjustments". In: *Climate Dynamics* 16.2-3, pp. 147–168. DOI: 10.1007/s003820050010.

Gowan, E. J., P. Tregoning, A. Purcell, J. Lea, O. J. Fransner, R. Noormets, and J. A. Dowdeswell (2016). "ICESHEET 1.0: a program to produce paleo-ice sheet reconstructions with minimal assumptions". In: *Geosci. Model Dev* 9, pp. 1673–1682. DOI: 10.5194/gmd-9-1673-2016.

Gregoire, L. J., B. Otto-Bliesner, P. J. Valdes, and R. Ivanovic (2016). "Abrupt Bølling warming and ice saddle collapse contributions to the Meltwater Pulse 1a rapid sea level rise". In: *Geophysical Research Letters* 43.17, pp. 9130–9137. DOI: 10.1002/2016GL070356.

Gregoire, L. J., P. J. Valdes, and A. J. Payne (2015). "The relative contribution of orbital forcing and greenhouse gases to the North American deglaciation". In: *Geophysical Research Letters* 42.22, pp. 9970–9979. DOI: 10.1002/2015GL066005.

Gudmundsson, G. H. (2013). "Ice-shelf buttressing and the stability of marine ice sheets". In: *The Cryosphere* 7, pp. 647–655. DOI: 10.5194/tc-7-647-2013.

Harrison, W. D., C. F. Raymond, K. A. Echelmeyer, and R. M. Krimmel (2003). "A macroscopic approach to glacier dynamics". In: *Journal of Glaciology* 49.164, pp. 13–21. DOI: 10.3189/172756503781830917.

Hewitt, I. (2013). "Seasonal changes in ice sheet motion due to melt water lubrication". In: *Earth and Planetary Science Letters* 371-372, pp. 16–25. DOI: 10.1016/J.EPSL.2013.04.022.

Hindmarsh, R. C. A. (2006). "The role of membrane-like stresses in determining the stability and sensitivity of the Antarctic ice sheets: back pressure and grounding line motion." In: *Philosophical transactions. Series A, Mathematical, physical, and engineering sciences* 364.1844, pp. 1733–67. DOI: 10.1098/rsta.2006.1797.

Hubbard, A., T. Bradwell, N. Golledge, A. Hall, H. Patton, D. Sugden, R. Cooper, and M. Stoker (2009). "Dynamic cycles, ice streams and their impact on the extent, chronology and deglaciation of the British–Irish ice sheet". In: *Quaternary Science Reviews* 28.7-8, pp. 758–776. DOI: `10.1016/j.quascirev.2008.12.026`.

Hughes, A. L., R. Gyllencreutz, Ø. S. Lohne, J. Mangerud, and J. I. Svendsen (2016). "The last Eurasian ice sheets - a chronological database and time-slice reconstruction, DATED-1". In: *Boreas* 45.1. DOI: `10.1111/bor.12142`.

Ivanovic, R. F., L. J. Gregoire, M. Kageyama, D. M. Roche, P. J. Valdes, A. Burke, R. Drummond, W. R. Peltier, and L. Tarasov (2016). "Transient climate simulations of the deglaciation 21–9 thousand years before present (version 1) – PMIP4 Core experiment design and boundary conditions". In: *Geoscientific Model Development* 9.7, pp. 2563–2587. DOI: `10.5194/gmd-9-2563-2016`.

Jamieson, S. S. R., A. Vieli, S. J. Livingstone, C. Ó. Cofaigh, C. Stokes, C.-D. Hillenbrand, and J. A. Dowdeswell (2012). "Ice-stream stability on a reverse bed slope". In: *Nature Geoscience* 5.11, pp. 799–802. DOI: `10.1038/ngeo1600`.

Jenkins, A., P. Dutrieux, S. S. Jacobs, S. D. McPhail, J. R. Perrett, A. T. Webb, and D. White (2010). "Observations beneath Pine Island Glacier in West Antarctica and implications for its retreat". In: *Nature Geoscience* 3.7, pp. 468–472. DOI: `10.1038/ngeo890`.

Johannesson, T., C. F. Raymond, and E. D. Waddington (1989). "A simple method for determining the response time of glaciers". In: *Glacier Fluctuations and Climatic Change*, pp. 343–352. DOI: `10.1007/978-94-015-7823-3_22`.

Joughin, I., I. M. Howat, M. Fahnestock, B. Smith, W. Krabill, R. B. Alley, H. Stern, and M. Truffer (2008). "Continued evolution of Jakobshavn Isbrae following its rapid speedup". In: *Journal of Geophysical Research* 113.F4, F04006. DOI: `10.1029/2008JF001023`.

Margold, M., C. R. Stokes, and C. D. Clark (2015). "Ice streams in the Laurentide Ice Sheet: Identification, characteristics and comparison to modern ice sheets". In: *Earth-Science Reviews* 143, pp. 117–146. DOI: 10.1016/j.earscirev.2015.01.011.

Matsuoka, K. et al. (2015). "Antarctic ice rises and rumples: Their properties and significance for ice-sheet dynamics and evolution". In: *Earth Science Reviews* 150, pp. 724–745. DOI: 10.1016/j.earscirev.2015.09.004.

Morris, P. J., G. T. Swindles, P. J. Valdes, R. F. Ivanovic, L. J. Gregoire, M. W. Smith, L. Tarasov, A. M. Haywood, and K. L. Bacon (2018). "Global peatland initiation driven by regionally asynchronous warming." In: *Proceedings of the National Academy of Sciences of the United States of America* 115.19, pp. 4851–4856. DOI: 10.1073/pnas.1717838115.

Nias, I. J., S. L. Cornford, and A. J. Payne (2016). "Contrasting the Modelled sensitivity of the Amundsen Sea Embayment ice streams". In: *Journal of Glaciology* 62.233, pp. 552–562. DOI: 10.1017/jog.2016.40.

Nye, J. F. (1960). "The Response of Glaciers and Ice-Sheets to Seasonal and Climatic Changes". In: *Proceedings of the Royal Society A: Mathematical, Physical and Engineering Sciences* 256.1287, pp. 559–584. DOI: 10.1098/rspa.1960.0127.

— (1963). "On the Theory of the Advance and Retreat of Glaciers". In: *Geophysical Journal of the Royal Astronomical Society* 7.4, pp. 431–456. DOI: 10.1111/j.1365-246X.1963.tb07087.x.

Oster, J. L., D. E. Ibarra, M. J. Winnick, and K. Maher (2015). "Steering of westerly storms over western North America at the Last Glacial Maximum". In: *Nature Geoscience* 8.3, pp. 201–205. DOI: 10.1038/ngeo2365.

Patton, H., A. Hubbard, K. Andreassen, M. Winsborrow, and A. P. Stroeven (2016). "The build-up, configuration, and dynamical sensitivity of the Eurasian ice-sheet complex to Late Weichselian climatic and oceanic forcing". In: *Qua-*

ternary Science Reviews 153, pp. 97–121. DOI: `10.1016/j.quascirev.2016.10.009`.

Patton, H. et al. (2017). "Deglaciation of the Eurasian ice sheet complex". In: *Quaternary Science Reviews* 169, pp. 148–172. DOI: `10.1016/j.quascirev.2017.05.019`.

Pattyn, F. et al. (2012). "Results of the Marine Ice Sheet Model Intercomparison Project, MISMIP". In: *The Cryosphere* 6, pp. 573–588. DOI: `10.5194/tc-6-573-2012`.

Pope, V. D., M. L. Gallani, P. R. Rowntree, and R. A. Stratton (2000). "The impact of new physical parametrizations in the Hadley Centre climate model: HadAM3". In: *Climate Dynamics* 16.2-3, pp. 123–146. DOI: `10.1007/s003820050009`.

Pritchard, H. D., S. R. M. Ligtenberg, H. A. Fricker, D. G. Vaughan, M. R. van den Broeke, and L. Padman (2012). "Antarctic ice-sheet loss driven by basal melting of ice shelves". In: *Nature* 484.7395, pp. 502–505. DOI: `10.1038/nature10968`.

Rignot, E. and S. S. Jacobs (2002). "Rapid Bottom Melting Widespread near Antarctic Ice Sheet Grounding Lines". In: *Science* 296.5575, pp. 2020–2023. DOI: `10.1126/science.1070942`.

Ritz, C., T. L. Edwards, G. Durand, A. J. Payne, V. Peyaud, and R. C. A. Hindmarsh (2015). "Potential sea-level rise from Antarctic ice-sheet instability constrained by observations". In: *Nature* 528.7580, pp. 115–118. DOI: `10.1038/nature16147`. arXiv: `NIHMS150003`.

Robel, A. A. and E. Tziperman (2016). "The role of ice stream dynamics in deglaciation". In: *Journal of Geophysical Research: Earth Surface* 121.8, pp. 1540–1554. DOI: `10.1002/2016JF003937`.

Ross, N. et al. (2012). "Steep reverse bed slope at the grounding line of the Weddell Sea sector in West Antarctica". In: *Nature Geoscience* 5.6, pp. 393–396. DOI: `10.1038/ngeo1468`.

Scambos, T. A., J. A. Bohlander, C. A. Shuman, and P. Skvarca (2004). "Glacier acceleration and thinning after ice shelf collapse in the Larsen B embayment, Antarctica". In: *Geophysical Research Letters* 31.18, p. L18402. DOI: 10.1029/2004GL020670.

Schoof, C. (2007). "Ice sheet grounding line dynamics: Steady states, stability, and hysteresis". In: *Journal of Geophysical Research* 112.F3, F03S28. DOI: 10.1029/2006JF000664.

Schoof, C. and R. C. Hindmarsh (2010). "Thin-film flows with wall slip: An asymptotic analysis of higher order glacier flow models". In: *Quarterly Journal of Mechanics and Applied Mathematics* 63.1, pp. 73–114. DOI: 10.1093/qjmam/hbp025.

Scourse, J. D., A. I. Haapaniemi, E. Colmenero-Hidalgo, V. L. Peck, I. R. Hall, W. E. Austin, P. C. Knutz, and R. Zahn (2009). "Growth, dynamics and deglaciation of the last British–Irish ice sheet: the deep-sea ice-rafted detritus record". In: *Quaternary Science Reviews* 28.27-28, pp. 3066–3084. DOI: 10.1016/J.QUASCIREV.2009.08.009.

Seguinot, J. (2013). "Spatial and seasonal effects of temperature variability in a positive degree-day glacier surface mass-balance model". In: *Journal of Glaciology* 59.218, pp. 1202–1204. DOI: 10.3189/2013JoG13J081.

Siegert, M. J. and J. A. Dowdeswell (2004). "Numerical reconstructions of the Eurasian Ice Sheet and climate during the Late Weichselian". In: *Quaternary Science Reviews* 23.11-13, pp. 1273–1283. DOI: 10.1016/J.QUASCIREV.2003.12.010.

Singarayer, J. S., P. J. Valdes, P. Friedlingstein, S. Nelson, and D. J. Beerling (2011). "Late Holocene methane rise caused by orbitally controlled increase in tropical sources". In: *Nature* 470.7332, pp. 82–86. DOI: 10.1038/nature09739.

Singarayer, J. S. and P. J. Valdes (2010). "High-latitude climate sensitivity to ice-sheet forcing over the last 120 kyr". In: *Quaternary Science Reviews* 29.1-2, pp. 43–55. DOI: 10.1016/j.quascirev.2009.10.011.

Chapter 2

Stoker, M. S. and T. Bradwell (2005). "The Minch palaeo-ice stream, NW sector of the British–Irish Ice Sheet". In: *Journal of the Geological Society* 162.3, pp. 425–428. DOI: 10.1144/0016-764904-151.

Stokes, C. R. and C. D. Clark (1999). "Geomorphological criteria for identifying Pleistocene ice streams". In: *Annals of Glaciology* 28, pp. 67–74. DOI: 10.3189/172756499781821625.

Swindles, G. T. et al. (2018). "Ecosystem state shifts during long-term development of an Amazonian peatland". In: *Global Change Biology* 24.2, pp. 738–757. DOI: 10.1111/gcb.13950. arXiv: 0608246v3 [arXiv:physics].

Tsai, V. C., A. L. Stewart, and A. F. Thompson (2015). "Marine ice-sheet profiles and stability under Coulomb basal conditions". In: *Journal of Glaciology* 61.226, pp. 205–215. DOI: 10.3189/2015JoG14J221.

Valdes, P. J. et al. (2017). "The BRIDGE HadCM3 family of climate models: HadCM3@Bristol v1.0". In: *Geoscientific Model Development* 10.10, pp. 3715–3743. DOI: 10.5194/gmd-10-3715-2017.

Veen, C. van der (2013). *Fundamentals of glacier dynamics.* CRC Press, p. 399. DOI: 10.3189/2014JoG13J214.

Chapter 3

Exploring the ingredients required to successfully model the placement, generation, and evolution of ice streams in the British-Irish Ice Sheet

Abstract

Ice stream evolution is a major uncertainty in projections of the future of the Greenland and Antarctic Ice sheets. Accurate simulation of ice stream evolution requires an understanding of a number of "ingredients" that control the location and behaviour of ice stream flow. Here, we test the influence of geothermal heat flux, grid resolution, and bed hydrology on simulated ice streaming. The palaeo-record provides snapshots of ice stream evolution, with a particularly well constrained ice sheet being the British-Irish Ice Sheet (BIIS). We implement a new basal sliding scheme coupled with thermo-mechanics into the BISICLES ice sheet model, to simulate the evolution of the BIIS ice streams. We find that the

simulated location and spacing of ice streams matches well with the empirical reconstructions of ice stream flow in terms of position and direction when simple bed hydrology is included. We show that the new basal sliding scheme allows the accurate simulation for the majority of BIIS ice streams. The extensive empirical record of the BIIS has allowed the testing of model inputs, and has helped demonstrate the skill of the ice sheet model in simulating the evolution of the location, spacing, and migration of ice streams through millennia. Simulated ice streams also prompt new empirical mapping of features indicative of streaming in the North Channel region. Ice sheet model development has allowed accurate simulation of the palaeo record, and allows for improved modelling of future ice stream behaviour.

3.1 Introduction

Ice streams dominate discharge in our contemporary ice sheets, routing ice from the ice sheet interior to the margins (Bennett, 2003). Ice streams account for 90% of the discharge of the Antarctic Ice Sheet (Bamber et al., 2000), and a number of ice streams have been identified as key points of vulnerability for the future evolution of the Antarctic (e.g. Favier et al., 2014; Nias et al., 2016; Waibel, 2017) and Greenland (e.g. Joughin et al., 2008; Gillet-Chaulet et al., 2012; Hogg et al., 2016) ice sheets. Given the importance of ice stream dynamics on ice sheet evolution, understanding stream evolution is crucial to elucidating the future of the Antarctic and Greenland Ice Sheets.

Ice stream behaviour within advancing, stable, and retreating ice sheets remains unclear, and accurate simulation of these processes is a key challenge of glaciology (Hindmarsh, 2018, p. 625). Observations from contemporary ice sheets and reconstructions of palaeo ice sheets show that ice streams are spatially and temporally variable (Conway et al., 2002; Dowdeswell et al., 2006; Stokes et al., 2009; Ó Cofaigh et al., 2010a; Margold et al., 2015a), but the causes of this variability remain poorly understood (Siegert et al., 2004; Horgan and Anan-

dakrishnan, 2006; Peters et al., 2006). Simulations of contemporary ice sheets typically achieve a close fit to observed surface speeds using data assimilation techniques that tune ice sheet parameters such as effective drag (Gillet-Chaulet et al., 2012; Morlighem et al., 2013; Arthern et al., 2015; Gong et al., 2017). While this achieves a close match to observations over decadal timescales, it does not account for long-term changes to bed hydrology, meaning it is expected that such ice sheet simulations will diverge considerably from reality, even given a perfect climate forcing (Veen, 1999). And, when modelling regions without present-day ice cover, there are insufficient observations, rendering these data-hungry methods entirely useless. Studies of palaeo ice sheets use a variety of methods to represent basal friction, including relationships with basal elevation (Martin et al., 2011; Seguinot et al., 2016), sediment thickness (Peltier, 2004; Gregoire et al., 2012, 2015), or idealised bed classifications (Boulton and Hagdorn, 2006; Gandy et al., 2018). These representations use proxies of bed friction, and do not capture the evolution of basal hydrology over a glacial cycle.

Improved simulations of ice streams require a representation of the physical mechanisms of ice streaming. Ice streams achieve their enhanced velocity through basal processes, and typically occur over areas of low bed friction. The friction at the bed of an ice stream is likely to evolve due to a number of processes that operate at difference timescales. Over long (millennial) timescales, glacial erosion and deposition can alter the force balance of the bed. Erosion may change the shape of basal obstacles, altering the form drag between the ice and the bed (Schoof, 2002). Sediment deposition may also mask smaller basal obstacles, and change regions where sediment deformation occurs (Bingham et al., 2017; Davies et al., 2018).

The most rapid change to basal friction can occur due to subglacial hydrology, as differences in water routing, subglacial floods, and supra-glacial water inputs can all dramatically alter the volumes and spatial patterns of water at the bed over short (diurnal to decadal) timescales (Nye, 1976; Smith et al., 2007; Hewitt

and Fowler, 2008). Detailed kilometre-scale patterning of basal shear stress under ice streams, inferred through observations and inversions, has been deduced for the Antarctic and Greenland ice sheets (Sergienko et al., 2014), who used mathematical modelling to explain them by coupling water and ice flow. Corresponding geomorphological features in the palaeo-record have been observed (Stokes et al., 2016). The thermal regime of the ice, determined by basal friction, geothermal heat fluxes, and englacial ice temperatures, can also influence subglacial hydrology and sliding rates (Payne, 1995). Basal water pressure at the Whillans Ice Stream, West Antarctica, is close to the ice floatation pressure (Engelhardt and Kamb, 1997; Kamb, 2013), and increased surface melting has been linked to increased ice velocity of the Greenland ice sheet (Zwally et al., 2002), both suggesting that subglacial water availability and routing is a key control of ice streaming. Subglacial meltwater can promote ice streaming by saturating basal sediments, and thus encouraging sediment deformation and sliding across bedrock. However, the inaccessibility of basal environments is an obstacle to more robustly describing and understanding subglacial processes (Hewitt, 2011). The representation of ice streaming and subglacial hydrology has been a key area for development for numerical ice sheet models of varying complexity (Greve, 1997; Bougamont et al., 2011; Bueler and Pelt, 2015). Due to the uncertainty of basal processes simulations usually ignore some processes and idealise others. The palaeo record offers the chance to test whether ignoring and idealising some basal processes is appropriate.

Here, we aim to introduce an idealised representation of subglacial hydrology to simulate the ice stream and ice sheet evolution of the British-Irish Ice Sheet (BIIS). To meet this aim, we address the following objectives: 1) we describe new development of the BISICLES ice sheet model; 2) we employ the BIIS palaeo archive of ice stream locations to test the skill of the ice sheet model in simulating ice stream advance and retreat over the millennial timescale; 3) we discuss the ingredients required to accurately model ice streams of the BIIS.

3.1.1   Background

Ice stream modelling

Accurately simulating ice streams within an ice sheet model is a key concern because of the large influence of ice streams on ice sheet behaviour and stability. Grounded ice streams with marine margins have been identified as points of vulnerability in the future evolution of ice sheets, in particular the West Antarctic Ice Sheet, because ice streams on a retrograde bed slope are prone to Marine Ice Sheet Instability (MISI) (Schoof, 2007). Theoretical investigations of MISI have almost exclusively assumed an ice sheet sliding on bedrock with a viscous power-law relationship between velocity and stress (Hindmarsh and Meur, 2001; Schoof, 2007; Gladstone et al., 2018). However, there is some evidence that a Coulomb friction approach may be applicable close to the grounding line (Iverson et al., 1998; Schoof, 2006). Recent work has shown that a combined Coulomb and viscous power-law approach changes ice sheet profiles, and causes the stable grounding line position to be in shallower water than a plastic power-law only approach (Tsai et al., 2015).

Models of contemporary ice sheets have achieved a close fit to the observed ice surface velocities (Morlighem et al., 2013), using an optimisation technique to determine subglacial friction parameters to match surface velocities. In effect, a spatially varying basal friction parameter obtained accounts for unknown bed and englacial properties. Simulations of contemporary Greenland (e.g. Lee et al., 2015) and Antarctica (e.g. Favier et al., 2014; Cornford et al., 2015) are a strong match for the empirical evidence, and may well be a suitable starting point for decadal to centennial future projections, but typically do not allow the basal friction parameters to vary through time. Therefore, centennial to millennial future projections will require ice stream modelling that is capable of ice stream evolution (Aschwanden et al., 2013). Currently, ice sheet models have success modelling ice streams through a theory of thermomechanical instability, where fast ice flow is allowed once the ice has reached the basal pressure melting

point (Hindmarsh, 2018). This spontaneous generation of ice streams has been modelled given a flat bed (Payne and Dongelmans, 1997), with regularly spaced ice streams forming due to thermomechanical instabilities of ice sheet flow. Hindmarsh (2009) showed the importance of simulating both horizontal longitudinal and lateral stresses – membrane stresses - when modelling ice stream generation. Idealised experiments that incorporate a representation of subglacial hydrology demonstrate that ice stream formation can be a response to basal water flow rather than ice sheet thermomechanics (Kyrke-Smith et al., 2013).

Applying ice stream modelling to contemporary and palaeo ice sheets is challenging owing to the complexity and scale of real ice sheet beds. The simulation of evolving ice streams has been undertaken in a number of palaeo (e.g. Hubbard et al., 2009; Jamieson et al., 2012; Patton et al., 2016; Gandy et al., 2018; Seguinot et al., 2018) and contemporary (Aschwanden et al., 2013; Aschwanden et al., 2019) studies. Despite progress in simulating ice streams, the skill of models to generate ice streams that evolve over the millennial time-scale has not been adequately tested against the empirical palaeo record.

Palaeo ice streams

Whilst contemporary observations can produce detailed information on current ice sheets, they do not record the multi-decadal, centennial and millennial variability of the ice stream activity and position. Limited contemporary ice stream evolution has been observed, with the most studied example being the change in discharge of ice streams along the Siple Coast of West Antarctica (Retzlaff and Bentley, 1993; Conway et al., 2002). Therefore, the history of contemporary ice sheet observation is not yet long enough to observe the results of significant margin changes, ice temperature evolution, or basal friction evolution. The record from palaeo ice sheets offers an opportunity to test methods for modelling ice streams against an archive spanning millennia, rather than a contemporary snapshot of ice streaming. The imprint of palaeo ice streams can be determined from

a set of well-established diagnostic geomorphological and sedimentological signatures (Stokes and Clark, 1999; Clark and Stokes, 2001; Margold et al., 2015b), such as MSGL (Clark, 1993), Trough Mouth Fans (Vorren and Laberg, 1997), and subglacial bedform convergence (Everest et al., 2005). Increased mapping of palaeo-ice stream tracks (Hughes et al., 2014; Margold et al., 2015b) offers a record of ice stream and ice sheet evolution over millennia. Efforts to both relatively and absolutely date flowsets of palaeo ice sheets have been extensive (Greenwood and Clark, 2009; Margold et al., 2015b; Hughes et al., 2016; Small et al., 2017; Margold et al., 2018), resulting in a wealth of palaeo ice sheet mapping.

Whilst the palaeo-record offers a test-bed for ice stream modelling, the modelling of palaeo-ice stream location and evolution can also inform empirical reconstruction efforts. The landform record is increasingly well documented, but will always be an incomplete record of ice sheet behaviour. A model that has sufficient skill to simulate empirically well constrained ice streams may highlight potential locations of unmapped ice streams. In this manner, the model benefits from the extensive testing opportunity provided by the palaeo record, and in turn models can also help target work to extend the empirical record. This creates a symbiotic relationship between numerical modelling and empirical reconstructions.

The British-Irish Sheet

Testing an ice sheet model against the palaeo record requires confidence in the empirical data. The British-Irish Ice Sheet (BIIS) arguably offers the most complete archive of data constraining the behaviour of an ice sheet and several ice streams over millennia. Mapping of glacial features has greatly expanded since the advent of remote sensing techniques (Clark et al., 2004; Smith et al., 2006), complementing significant chronology work (Hughes et al., 2011). Recently, a wealth of offshore data collection has considerably expanded the palaeo archive of the BIIS (e.g. Bradwell et al., 2008b; Ó Cofaigh et al., 2016; Dove et al., 2017).

Empirical work spanning decades has cumulatively led to an extensive palaeo archive for the BIIS (Clark et al., 2018).

Using this wealth of empirical evidence, numerous ice stream locations have been reconstructed both onshore and offshore with evidence from subglacial lineations (Hughes et al., 2014), trough mouth fans (Bradwell et al., 2008b), and topographic troughs. Reconstruction of large ice streams offshore are numbered on Figure 3.1 and Table 3.1, and include the Rona [01] (Bradwell et al., 2008b), the Foula [02] (Bradwell et al., 2008b), the Minch [03] (Stoker and Bradwell, 2005), the Barra Fan [05] (Finlayson et al., 2014), the Irish Sea [10] (Chiverrell et al., 2013), the Celtic Sea [11] (Scourse et al., 2009), the North Sea Lobe [15] (Dove et al., 2017), the Firth of Forth [16] (Hughes et al., 2014), and the Moray Firth [17] (Merritt et al., 1995) (Figure 3.1, Table 3.2). Smaller ice streams are also reconstructed onshore, including the Tweed (Everest et al., 2005), and the Tyne Gap (Livingstone et al., 2015).

Whilst the record of ice streaming of the BIIS is extensive, it is almost certainly incomplete. The production and preservation of evidence for ice streaming is spatially inconsistent. There is limited evidence of ice streaming on the Irish west coast; despite streaming occurring around the majority of marine margins of contemporary ice sheets. Evidence from the North Sea is also unclear. There, the relatively flat bathymetry should allow ice streams locations not predetermined by topography, allow mobile positioning, and therefore a less clear empirical record. Evidence for similar ice-stream systems has been found in the Canadian Shield (Ó Cofaigh et al., 2010b). Holocene erosion and sedimentation during marine transgression in both the North Sea basin and offshore western Ireland is likely another considerable obstacle to mapping landforms of the last glacial cycle.

Numerical simulations of the BIIS have highlighted the importance of ice streaming to the growth and retreat of the ice sheet (Boulton et al., 2003; Hubbard et al., 2009; Patton et al., 2017). In particular, Hubbard et al. (2009) simulated an ice sheet exhibiting cyclical "binge-purge" behaviour that was controlled by
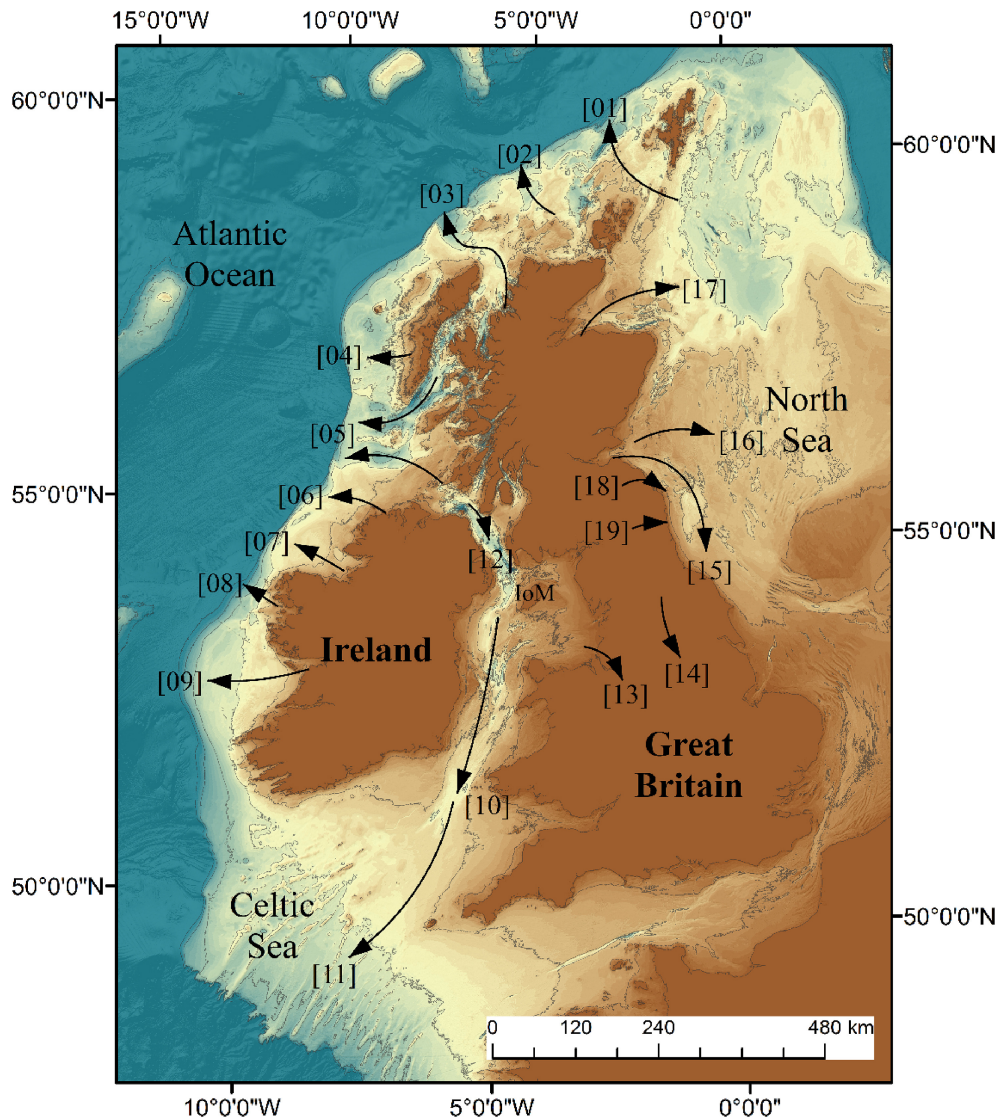
Figure 3.1: The location of BIIS palaeo ice streams. IoM = Isle of Man. Grey contours show contemporary bathymetry from -240 m in 40 m intervals.

the dynamics of spatially and temporally variable ice streams. Nevertheless, the rich empirical record of the BIIS offers an underused archive to test developments in ice sheet models. Whilst reconstruction-based modelling (Hubbard et al., 2009; Patton et al., 2016, 2017) has proved informative in understanding long-term ice sheet evolution, an idealised approach (Boulton et al., 2003; Gandy et al., 2018), is more suited to an investigation of the processes of ice sheet change.

Reference	Start point	Length (yr)	SMB	Geothermal Heat Flux	Standard Parameter Variation
SPIN-UP	N/A	20,000	Masked (Figure 3.2b)	60 mW m^{-2}	N/A
ADVANCE	SPIN-UP end	10,000	0.3 m/y (>500 m as.l), or 0.0 m/y	60 mW m^{-2}	N/A
RETREAT	ADVANCE end	10,000	Masked on AD-VANCE extents	60 mW m^{-2}	N/A
ADVANCE_GEOTHERMAL	SPIN-UP end	10,000	0.3 m/y (>500 m as.l), or 0.0 m/y	Variable (Figure 3.3c)	N/A
RETREAT_GEOTHERMAL	ADVANCE end	10,000	Masked on ADVANCE_GEOTHERMAL extents	Variable (Figure 3.3c)	N/A
MAX_FRICT	ADVANCE 3000 years	1,000	0.3 m/y (>500 m as.l), or 0.0 m/y	60 mW m^{-2}	Weertman friction coefficient (C) = 6,000
MIN_FRICT	ADVANCE 3000 years	1,000	0.3 m/y (>500 m as.l), or 0.0 m/y	60 mW m^{-2}	Weertman friction coefficient (C) = 1,500
MAX_TILL	ADVANCE 3000 years	1,000	0.3 m/y (>500 m as.l), or 0.0 m/y	60 mW m^{-2}	Maximum till water depth (W_0) = 4 m
MIN_TILL	ADVANCE 3000 years	1,000	0.3 m/y (>500 m as.l), or 0.0 m/y	60 mW m^{-2}	Maximum till water depth (W_0) = 1 m
MAX_COULOMB	ADVANCE 3000 years	1,000	0.3 m/y (¿>500 m as.l), or 0.0 m/y	60 mW m^{-2}	Coulomb friction coefficient (f) = 0.75
MIN_COULOMB	ADVANCE 3000 years	1,000	0.3 m/y (>500 m as.l), or 0.0 m/y	60 mW m^{-2}	Coulomb friction coefficient (f) = 0.25
MAX_GEOTHERMAL	ADVANCE 3000 years	1,000	0.3 m/y (>500 m as.l), or 0.0 m/y	120 mW m^{-2}	N/A
MIN_GEOTHERMAL	ADVANCE 3000 years	1,000	0.3 m/y (>500 m as.l), or 0.0 m/y	30 mW m^{-2}	N/A

Table 3.1: Summary of experiment set-ups. The results of sensitivity experiments (experiments with the prefix "MAX" or "MIN") are presented in Figure A.3.

#	Name	Empirical evidence	Simulated?	Group	Key references
01	Foula Ice Stream	TMF, bathymetric trough	Advance + Retreat	A	(Bradwell et al., 2008b, 2019)
02	Rona Ice Stream	TMF, bathymetric trough	Advance + Retreat	A	Bradwell et al. (2008b)
03	Minch Ice Stream	TMF, bathymetric trough, GZWs	Advance + Retreat	A	(Bradwell et al., 2008b; Bradwell and Stoker, 2015; Bradwell et al., 2019)
04	St Kilda Ice Stream	Figure 3.12	Advance + Retreat	B	N/A
05	Barra Fan Ice Stream	TMF, bathymetric trough, bed forms	Advance + Retreat	A	Finlayson et al. (2014)
06	Sheephaven Ice Stream	None	Advance + Retreat	B	N/A
07	Donegal Bay Ice Stream	None	Advance + Retreat	B	N/A
08	Clew Bay Ice Stream	None	Advance + Retreat	B	N/A
09	Galway Bay Ice Stream	None	Maximum extent	B	N/A
10	Irish Sea Ice Stream	Bathymetric trough	Retreat	A	Chiverrell et al. (2013)
11	Celtic Sea Ice Stream	Margin evidence, reconstructions	None	C	Scourse et al. (2009)
12	North Channel Ice Stream	Figure 3.11	Advance + Retreat	A	N/A
13	Cheshire Lobe	Lobate margin	Retreat	A	Clark et al. (2012)
14	York Vale Ice Stream	Lobate margin	Retreat	A	Bateman et al. (2015)
15	North Sea Lobe	MSGL, margin evidence	Retreat	A	(Bateman et al., 2015; Dove et al., 2017)
16	Forth Ice Stream	MSGL	Retreat	A	Hughes et al. (2014)
17	Moray Ice Stream	Bathymetric trough	Retreat	A	Merritt et al. (1995)
18	Tweed Ice Stream	Drumlin convergence	None	C	Everest et al. (2005)
19	Tyne Gap Ice Stream	Drumlin convergence	None	C	Livingstone et al. (2015)

Table 3.2: Ice streams of the BIIS, split into groups according to the availability of simulation and empirical evidence. The location of each ice stream is shown in Figure 3.1 and Figure 3.8.

3.2   Methods

We use the BISICLES marine ice sheet model, to which we have added a simple scheme that allows for sliding where basal water is present. BISICLES has previously been successfully applied to simulations of contemporary ice sheets, accurately simulating ice streams using a statistical inversion technique (Favier et al., 2014; Cornford et al., 2015; Lee et al., 2015; Nias et al., 2016; Gong et al., 2017). Here, we refer to this new version of the model as BISICLES_hydro, which is described below. BISICLES is a vertically integrated ice sheet model with L1L2 physics retained from the full Stokes flow equations (Schoof and Hindmarsh, 2010), including an approximation of membrane stress. These membrane stresses are necessary for producing ice streams of accurate width independent of resolution (Hindmarsh, 2009).

The key addition to BISICLES in this paper is the use of a sliding law which is sensitive to the presence of till water. The sliding law divides the ice sheet into Weertman- and Coulomb-friction regions (Tsai et al., 2015), accommodating both laws by setting the basal shear stress as the minimum of the two stresses, i.e.

$$|\boldsymbol{\tau}_b| = min[C(|\boldsymbol{u}_b|)^{\frac{1}{m}}, f(\sigma_0 - p_w)] \qquad (3.1)$$

C is a friction coefficient here a constant equal to 3000 Pa m$^{-1/3}$a$^{1/3}$, based on medium values from other experiments using BISICLES (Favier et al., 2014; Gong et al., 2017; Gandy et al., 2018), adjusted for the flow law exponent. The basal velocity is $\boldsymbol{u}_b$, and m is related to Glen's flow law exponent, n (Glen, 1955; Weertman, 1957). The Coulomb friction coefficient f is $\sim$0.5 (Tsai et al., 2015), and values between 0.33 and 0.5 have been measured for glacial tills in the laboratory (Iverson et al., 1998). We chose as 0.5 as in other studies (Nias et al., 2018), and based on sensitivity with lower and higher values (Fig. S2). The ice pressure is σ_0, and p_w is the water pressure. In practice, this means that

most of the grounded ice-sheet base experiences Weertman power-law sliding, while a small area near the grounding line will experience Coulomb sliding. The sliding law for τ_b is followed when ice is grounded, and τ_b is 0 once ice is floating. Nias et al. (2018) tested the influence of this sliding law using BISICLES, and found simulations with the Coulomb sliding law experience greater grounding line retreat than simulations with a Weertman sliding law. Ice thermodynamics is considered using an enthalpy transport scheme according to Aschwanden et al. (2012), where an energy density,

$$E = H_c + Lw \tag{3.2}$$

is conserved rather than temperature T alone; H_c is the specific heat capacity, w is water fraction and L is the specific latent heat of fusion. Basal hydrology is approximated according to Van Pelt and Oerlemans (2012), considering balance of water just in a vertical column, ignoring horizontal transport. Note, though, that moisture can be transported horizontally within temperate ice. At the base of the ice, frictional heating occurs due to basal sliding. When basal ice is at the pressure-melting point, excess energy is used to melt the ice. The evolution of thickness of the till-stored water layer, W, evolves through a simple equation,

$$\frac{\partial w}{\partial t} = \frac{m}{p_w} - D \tag{3.3}$$

where m is the basal melt rate, ρ_w is the density of fresh water, and D is the vertical till-stored water drainage rate, set at 0.005 m/a. The till-stored water drain rate controls the overall water balance and saturation of the till layer, and therefore the magnitude of ice streaming. This value is based on sensitivity experiments (Section S2). Till-stored water does not diffuse horizontally, or have any horizontal drainage, with all of these details approximated by D. Basal water pressure, p_{bw}, is given by,

$$p_{bw} = \alpha \rho g H \left(\frac{min(W, W_0)}{W_0} \right) \qquad (3.4)$$

Here, W_0 is the maximum allowed value of W, set at 2 m, beyond which the till is saturated. A uniform 2 m maximum till-water layer thickness was set, consistent with (Van Pelt and Oerlemans, 2012) and with sensitivity experiments (Fig. S2), allowing simulated ice stream width that best matched empirical data. α is a factor defining the maximum ratio of pore-water pressure (p_w) to overburden pressure, which is achieved in the case of till saturation. We use $\alpha = 0.99$, in accordance with observations that $\alpha \sim 1$ (Luthi et al., 2002). g is the acceleration due to gravity (9.81 m s^{-2}). When using the Coulomb portion of the sliding law basal shear stress is a function of the basal water pressure, whilst basal water pressure is a function of the amount of basal water present influenced by basal temperature. These adaptations allow for ice stream formation, in a similar way that hydrology has previously been approximated in PISM (Van Pelt and Oerlemans, 2012), with the addition of the combined Weertman-Coulomb sliding law.

3.3 Application to the BIIS

We apply the BISICLES_hydro to model an idealised version of the BIIS. The BIIS offers a realistic bed geometry to test BISICLES_hydro, along with the extensive empirical record of ice streaming to help test the skill of the model in simulating ice stream positions. These experiments idealise the climate forcing; the experiments are not intended to act as a reconstruction of the BIIS, rather the BIIS acts as a test-bed for BISICLES_hydro to simulate reasonable ice stream width, spacing and position over millennia.

3.3.1 Model-setup

We set up the model domain to cover the entire BIIS (Figure 3.2). The easternmost domain edge runs through the North Sea, placed so that as simulated ice reaches the domain edge its normal velocity is set to zero and thus an ice divide forms. This is to represent the effect of confluence between the BIIS and Fennoscandian Ice Sheet in the North Sea during the last glacial cycle (Sejrup et al., 2016; Roberts et al., 2018). This is only an approximation of the effect of confluence, and therefore streaming features close to the eastern margin may be susceptible to domain-edge artefacts. We use an 8 km × 8 km horizontal grid, with one level of refinement at the ice sheet margin, producing a 4 km × 4 km horizontal grid. The simulations have 10 vertical levels. The Weertman portion of the sliding law uses a non-linear ($m = 3$) exponent. We use a crevasse calving model, which models the penetration of basal and surface crevasses (Nick et al., 2010).
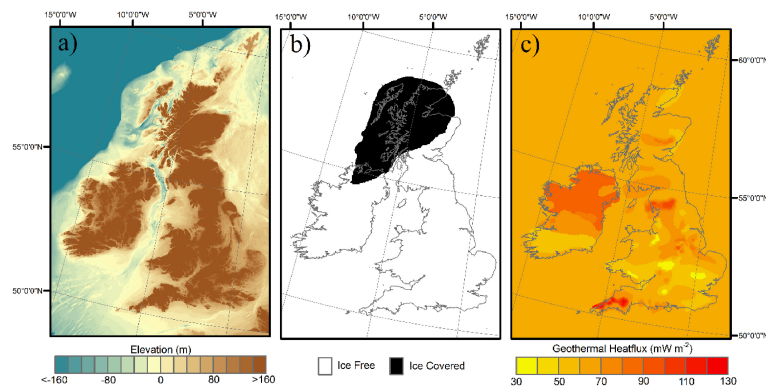
Figure 3.2: Boundary conditions for the experiments, showing the full domain of the simulations. (a) Bed topography, (b) Ice mask for the ice dome produced in the spin-up simulation, and (c) Geothermal heat flux used in experiments "Geothermal".

To recreate isostatically adjusted bed topography, we adjust modern topography using reconstructions from a Glacio-Isostatic Adjustment (GIA) model (Bradley et al., 2011) (Figure 3.2a). GEBCO (Becker et al., 2009) provides modern offshore bathymetry, and SRTM (Farr et al., 2007) provides onshore topography. The Relative Sea Level (RSL) change from at 30ka BP is used to deform

contemporary topography, maintaining a high-resolution ice sheet bed whilst also accounting for RSL change. RSL is constant through all experiments; the bed does not evolve after the initial RSL correction.

Calculation of the surface heat flux uses an idealised elevation-constant surface temperature of 268 K in all experiments. In the majority of experiments, geothermal heat flux is uniformly set at 60 mW m^{-2} across the domain. In experiment GEOTHERMAL, onshore geothermal heat flux is set to contemporary geothermal heat flux measurements (Busby, 2010; Farrell et al., 2014), which is assumed an appropriate proxy for geothermal heat flux during the last glacial cycle. Owing to the absence of sufficient measurements, offshore geothermal heat flux is set at 60 mW m^{-2}.

The simulations aim to grow and shrink an ice sheet in an idealised cycle, rather than provide a reconstruction of the BIIS. Although a more idealised surface mass balance forcing can be used, the scheme must force a simulated ice sheet that resembles the actual evolution of the BIIS well enough so as not to impede comparisons of modelled and empirically reconstructed ice streams, as ice stream position is influenced by ice sheet geometry. The simulations are split into three subsequent experiments with varying surface mass balance forcing (Table 3.1). First, the ice sheet is grown for 20,000 years from no ice using an ice mask (Figure 3.2b). A surface mass balance of 0.3 m/y is applied in the ice mask, and a mass balance of -5.0 m/y applied outside the ice mask. A 2-phase spin-up is used, with the hydrology adaptations discussed in section 2, introduced at model year 10,000 to preserve computer time during the original build-up of the ice dome. From the end of the SPIN-UP experiment, an idealised climate is used to advance and retreat the ice sheet. During the ADVANCE phase, the surface mass balance is defined as;

$$m = \begin{cases} 0.3, & h>0 \\ 0.0, & h \leq 500 \\ -2.0, & h = 0.0 \end{cases} \tag{3.5}$$

where m is the annual surface mass balance (m/y), and h is the surface elevation of ice. This forcing allows an advance that reaches a maximum extent after 10,000 years which is comparable to empirical reconstructions (Clark et al., 2012). Every 25 years through the ADVANCE experiment, a mask is created based on the modelled output (Figure 3.3). The mask sets values of 0.3 where the ice sheet elevation is > 500 m, 0.0 where the ice sheet elevation is ≤ 500 m, and -2.0 where the no ice is present. Then the retreat is forced using the masked SMB maps in reverse order, i.e. the mask produced using the 9,000 model year extent forces the 11,000 SMB, the 8,000 year mask forces the 12,000 SMB etc. (Figure 3.3). The 500 m ELA provides a balance between too slow and too rapid retreat of the ice sheet in the retreat phase. The surface mass balance forcing is updated every 25 model years. This forcing method creates a near-symmetric pattern of advance and retreat.
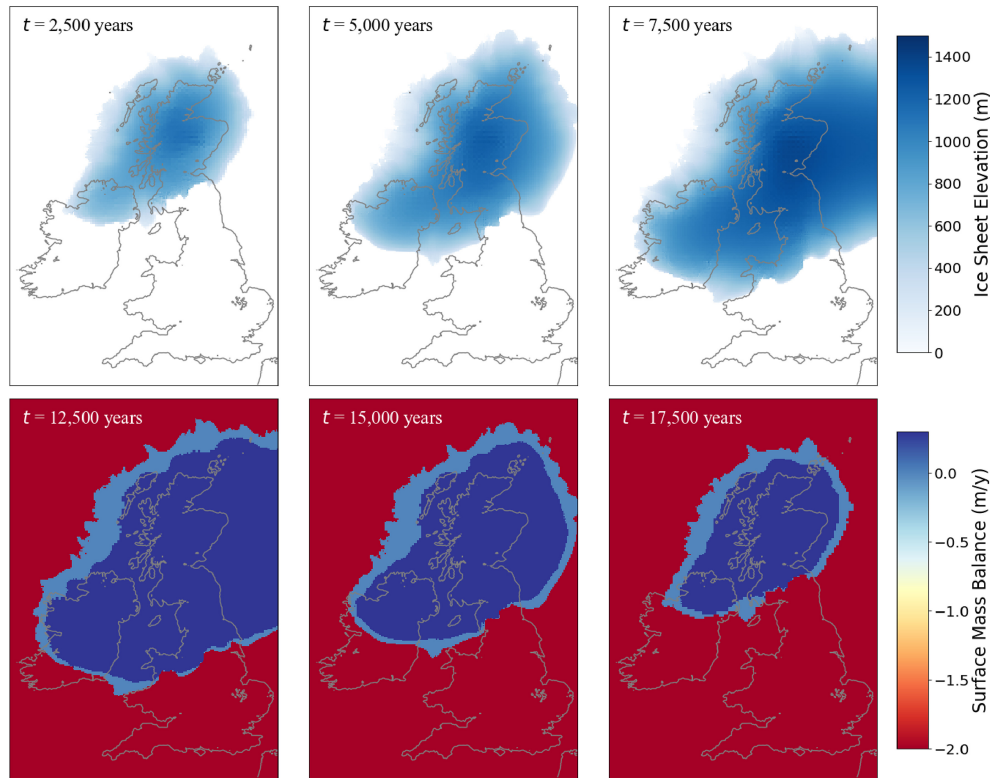
Figure 3.3: Illustration of the surface mass balance calculation for the RETREAT experiment. The top row shows simulated ice sheet elevation during the ADVANCE experiment, and the bottom row the resulting surface mass balance masks produced.

3.3.2   Model-data comparison

We compare modelled and empirically reconstructed ice streams, considering ice stream position, spacing, flow direction, and evolution. To allow for consistent identification of ice streams in the simulations we define an ice stream as a region with surface velocity exceeding 500 m/y 8 km from the margin. Qualitative comparisons between modelled and empirical ice streams were made based on position and spacing, and flow directions. This was completed for topographically well-focussed ice streams since these are the locations where the flow direction can be empirically reconstructed with most certainty. The empirically reconstructed palaeo flow direction is determined as the mean orientation of the topographic trough centreline. Together, these were used to create a map of empirically reconstructed flow directions for known ice streams of the BIIS.

We use the tool developed by Li et al. (2007), Automated Flow Direction Analysis (AFDA), to compare empirical and model derived flow directions. AFDA calculates the mean residual angle and variance of offset between modelled and empirically derived ice-flow directions. A threshold of $<10°$ mean resultant vector and <0.03 mean resultant variance was used to assess model-data agreement, derived from values previously used in the literature (Napieralski et al., 2007; Ely et al., 2019).

3.4 Model results

The skill of the simulations to produce ice streams of a reasonable width, position, and flow direction is highly dependent on the "ingredients" included in the simulations. A simulation with no basal hydrology coupling does not simulate ice streaming (Figure 3.4e). Simulations using BISICLES_hydro achieve ice stream generation in manner that is a good match to empirical data, and demonstrates good consistency in the simulated ice stream position, spacing and width across a range of horizontal resolutions (Figure 3.4a–d). Consistent ice stream width means that ice catchments are also consistent across varying horizontal resolutions, allowing margin evolution to not vary considerably between resolutions (Figure 3.4a–d.). The minimal resolution dependency could be explained by either the inclusion of membrane stresses (Hindmarsh, 2009), or topographical constraints on both ice stream position and width. With increasing resolution there is convergence of simulated velocity (Figure 3.4f). At 4 km resolution and beyond the pattern of ice streaming is qualitatively and quantitatively similar(Table A.2).
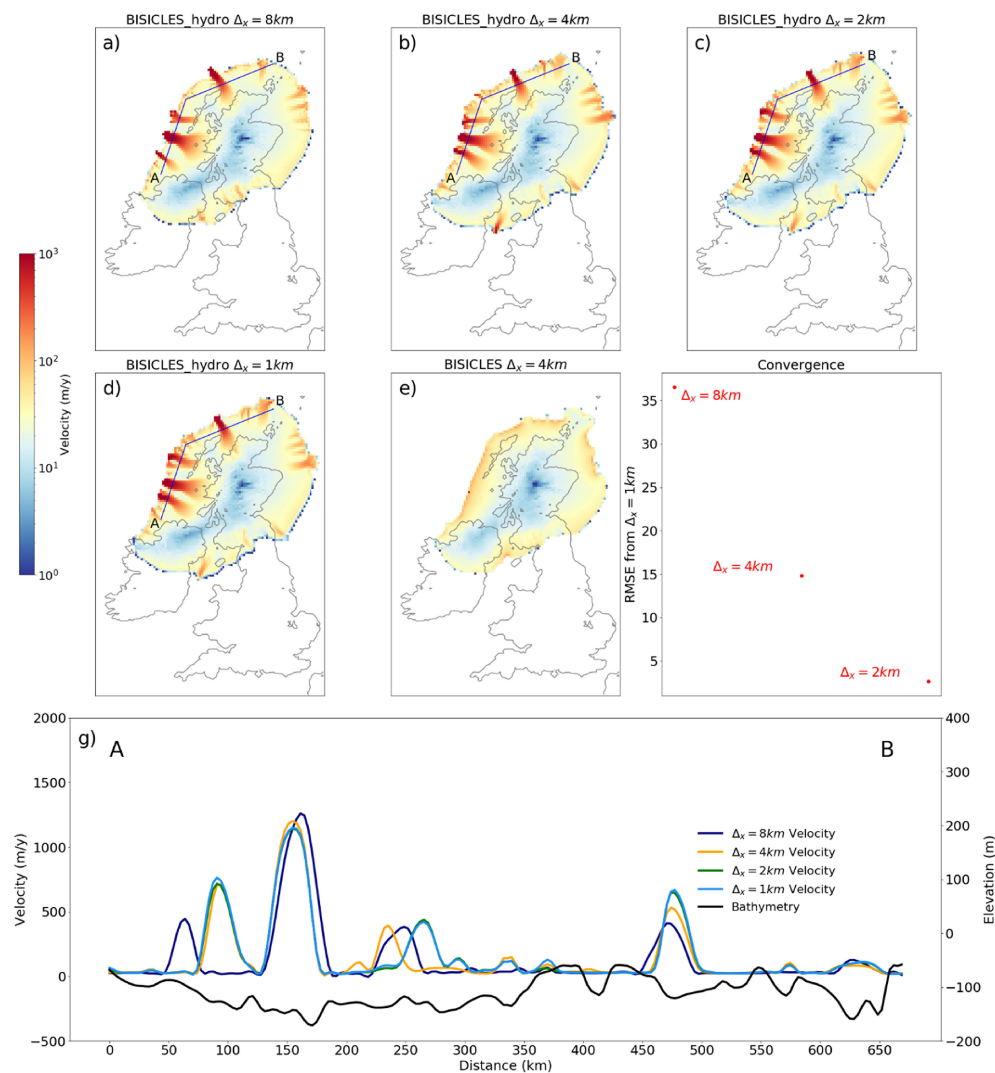
Figure 3.4: Variations in ice stream occurrence, position, and width. All ice surface velocity maps are at 4,000 model years into the ADVANCE experiment. a) BISICLES_hydro at 8 km horizontal resolution. b-d) BISICLES_hydro at 1, 2, and 3 levels of mesh refinement respectively. e) Without the hydrological approximation. f) RMSE of the BISICLES_hydro simulated velocities at 0, 1, and 2 levels of refinement from 3 levels of refinement. g) Ice surface velocity and bathymetry for the transect shown in panels a–d.

3.4.1 ADVANCE and RETREAT

At the end of the SPIN-UP experiment, there are four major ice streams draining the ice sheet (Figure 3.5a). As the ice sheet advances during the ADVANCE experiment, the position of some ice streams migrate, and the number of ice streams increases (Figure 3.5a–e). Some ice streams remain spatially and temporally consistent, concurrent with the position of ice streams marked in Figure 3.1, the Minch Ice Stream [3], the Barra Fan Ice Stream [5], the Rona Ice Stream

[2], and a Donegal Bay Ice Stream [7]. The Foula Ice Stream [1] is consistently present from 2,500 model years onwards, but changes flow direction by ∼45° as the margin position changes.
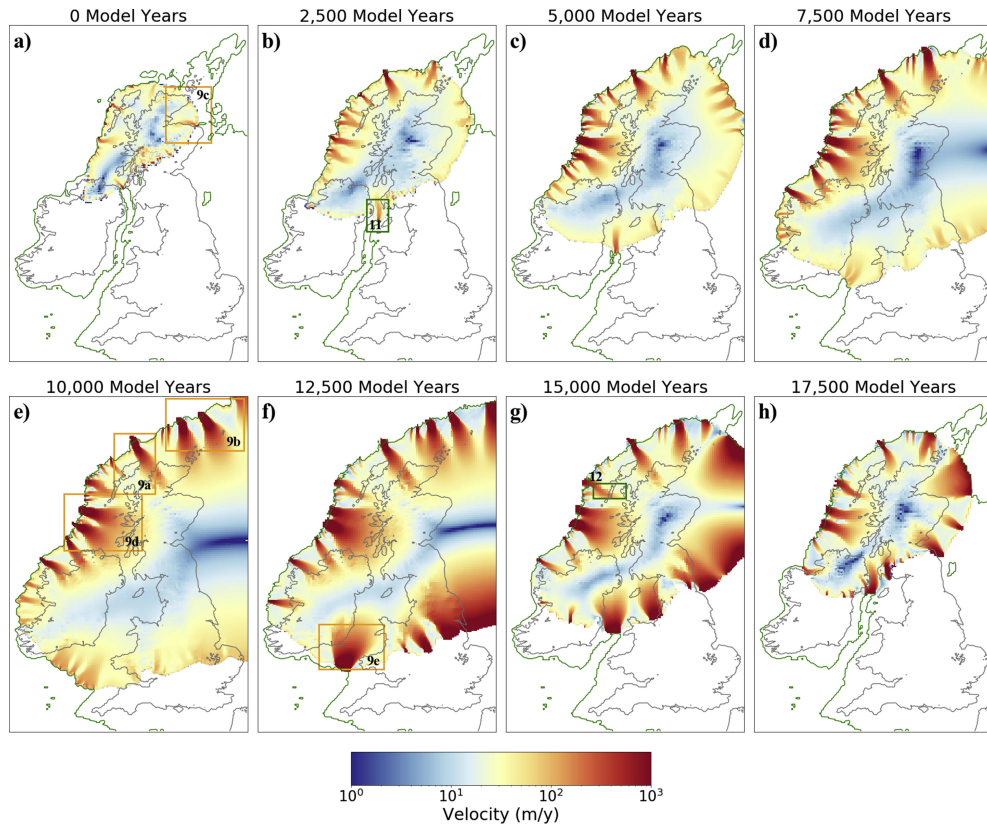
Figure 3.5: Ice velocity at 2,500 model year intervals during the ADVANCE (a–e) and RETREAT (f–h) experiments. Orange boxes highlight ice streams with significant empirical evidence (Figure 3.9). Green boxes highlight ice streams with empirical evidence presented in this research (Figure 3.11, Figure 3.12). The green contour shows the 0 m bed elevation, and the ice sheet grounding line.

At the maximum extent of the ice sheet, at 10,000 model years (Figure 3.5e), the number of ice streams around the ice sheet margin has increased during the ADVANCE phase. Ten ice streams have formed on the western-board of the ice sheet, which has a marine margin at the Atlantic Ocean. The areal extent here is controlled by the extent of the continental shelf, as ice cannot extend beyond the shelf break. A similar effect has been modelled on the southern margin of the Laurentide Ice Sheet, where advance into deeper lakes initiates increased calving (Cutler et al., 2001). Ice streams are less prominent along the southern margin, and migrate laterally during the ADVANCE phase.

During the RETREAT experiment (model years 10,000–20,000) all the non-transitory ice streams of advance remain consistent spatially and temporally. Streaming along the southern margin increases, and a large ice stream forms in the Irish Sea (Figure 3.5f). Smaller ice streams form onshore, concurrent with the Vale of Cheshire and York, although these stop streaming by 15,000 model years (Figure 3.5g and h). At 12,500 model years, two large ice streams drain the ice sheet on the eastern domain edge in the North Sea. These large features are an artefact of the ice sheet being separated from the domain edge following confluence during the ADVANCE experiments, and therefore are not comparable with the empirical record. Once the ice sheet is separated from the eastern domain edge (∼15,000 model years), ice streams in the North Sea area have a comparable size and spacing to other ice streams simulated around the margin.

During the ice sheet advance, steeper margin and shallow interior surface slopes occur along the southern margin (Figure 3.6), as is expected on an advancing margin. In the retreat phase the SMB imposes melting at the southern margin of the ice sheet. This lowering steepens the ice surface at the ice stream onset zone, accelerating ice streaming and resulting in a shallower surface profile downstream of the onset zone. This means that during the advance phase there is only extensive streaming along the northern margin, whilst streaming also occurs along the southern margin during the retreat phase (Figure 3.6). The feedback between SMB and ice stream behaviour has been demonstrated numerically (Robel and Tziperman, 2016), and this effect has been shown to promote rapid deglaciation. Experiments of the evolution of the BIIS with a realistic climate forcing also produce ice streams with high temporal variability (Hubbard et al., 2009).
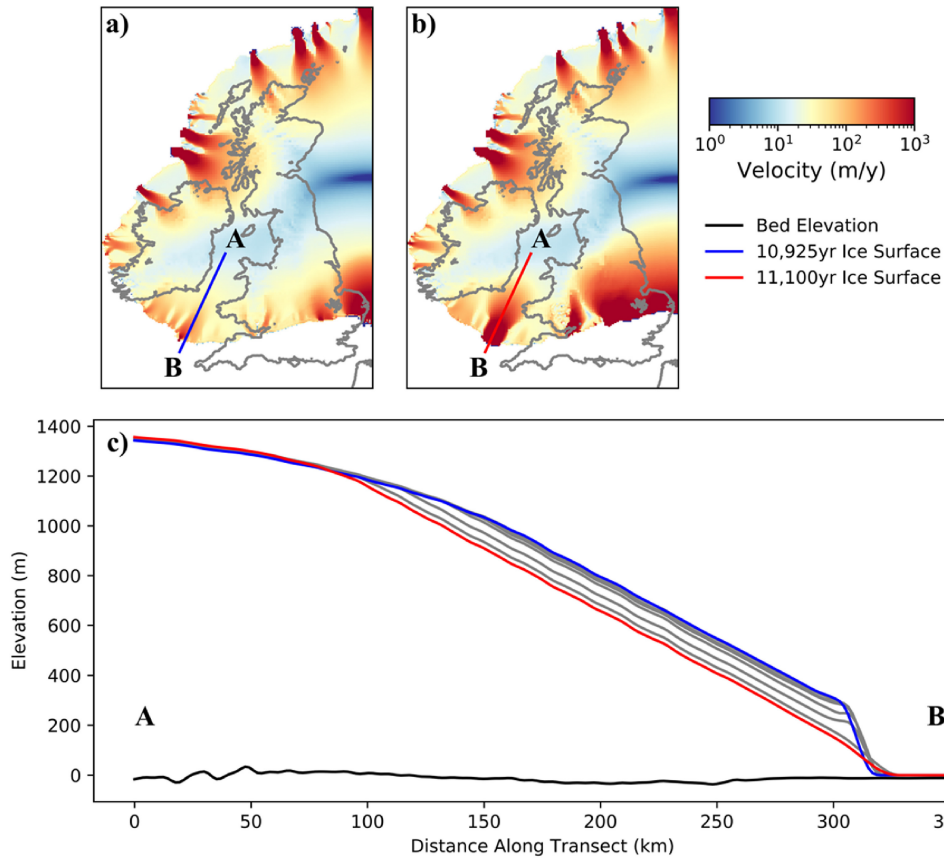
Figure 3.6: Transect of the ice surface at a period before and after the onset of significant ice streaming in the Celtic Sea (10,925 and 11,100 model years respectively). Grey curves show the ice surface at 25 year intervals between the two snapshots.

3.4.2 Variable geothermal heat flux

Introducing a spatially variable geothermal heat flux produces limited changes to the pattern of ice streaming simulated for most of the ice sheet. The width and spacing of the ice streams is almost identical (Figure 3.7). The dominant ice streams identified from the ADVANCE and RETREAT experiments (i.e. coincident with the Minch Ice Stream, and the Barra Fan Ice Streams) remain constant in the variable geothermal heat flux experiments. The region of highest geothermal heat flux in the domain, in South-west England, is not covered by ice, both in these simulations and according to empirical reconstructions (Clark et al., 2012), so has no impact on the ice stream dynamics simulated. Other comparative "hot spots" also produce a minimal effect, despite being ice covered. The higher geothermal heat flux over the North of Ireland does not cause signifi-

cant change in the margin position as the ice sheet advances over Ireland (Figure 3.7b,f).
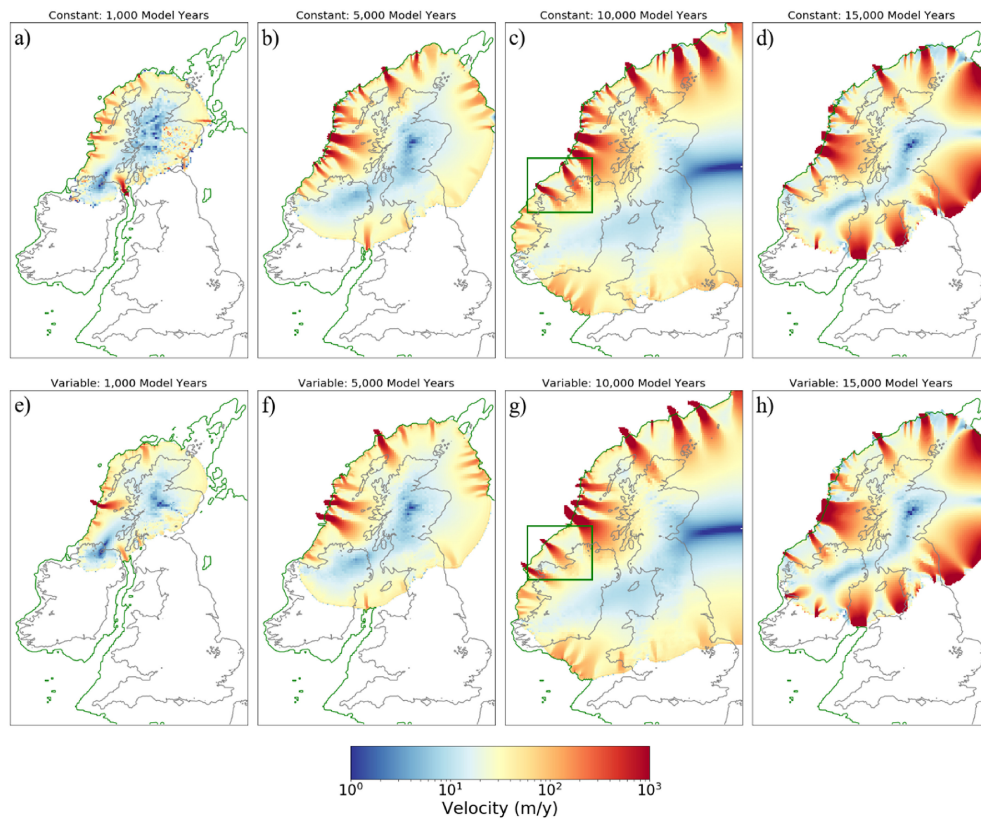
Figure 3.7: Ice velocity at 5,000 year intervals for the ADVANCE and RETREAT experiments with a spatially uniform geothermal heat flux (a–d), and a spatially varied geothermal heat flux (e–h). The green box in panel c and g highlight the key region of difference between the experiments.

The primary change in the ice stream configuration is on the west coast of Ireland, where the geothermal heat flux is comparatively high (Figure 3.2c). In the spatially constant geothermal heat flux experiment an ice stream is simulated coincident with Donegal Bay (Figure 3.1[7]), with a second ice stream to the north in the Sheephaven ice stream region (location indicated in Figure 3.1[6]). In the spatially variable geothermal heat flux experiment, an ice stream is still simulated in Donegal Bay, but to the south in Clew Bay rather than the north (Figure 3.1[8]). In this region of the ice sheet, there are no significant bathymetric troughs, suggesting that variable geothermal heat flux becomes a comparatively more significant control on ice stream form and location in western Ireland than the rest of the BIIS. This demonstrates that geothermal heat flux can be an

Chapter 3

important control on ice stream location, but only in regions where other more significant controls, like topographic troughs, are not present. Including a spatially variable geothermal heat flux is not a necessary ingredient for modelling the majority of ice streams of the BIIS when using the physics in BISICLES_hydro, but is more influential on the western Irish coast.

3.5 Model-data comparison

We compare simulated and empirically-based ice streams using both qualitative comparisons of position and spacing and a quantitative tool. Ice streams of the BIIS are split into three categories; ice streams that are simulated by the model and have empirical evidence (group A), ice streams that are simulated by the model but have no empirical evidence yet published (group B), ice streams that are not simulated but have been reconstructed empirically (group C). The majority of ice streams simulated here (11/19) are supported by empirical evidence (Table 3.2).

3.5.1 Group A

Group A are the eleven BIIS ice streams simulated here and supported by the empirical record (Table 3.2, Figure 3.8). Four of the most consistent ice streams in the simulations coincide with the locations of the four ice streams with the strongest empirical evidence. Each of the ice streams (the Barra Fan Ice Streams, the Minch Ice Stream, the Rona Ice Stream, and the Foula Ice Stream) are associated with a clear bathymetric trough (Figure 3.9), and terminate at major Trough Mouth Fans (Bradwell et al., 2008b). These are thick accumulations of sediment fed across an ice stream marine margin (Vorren and Laberg, 1997). The bathymetric troughs and associated Trough Mouth Fans are strong empirical evidence of sustained ice streaming, which the model here shows significant skill in simulating.
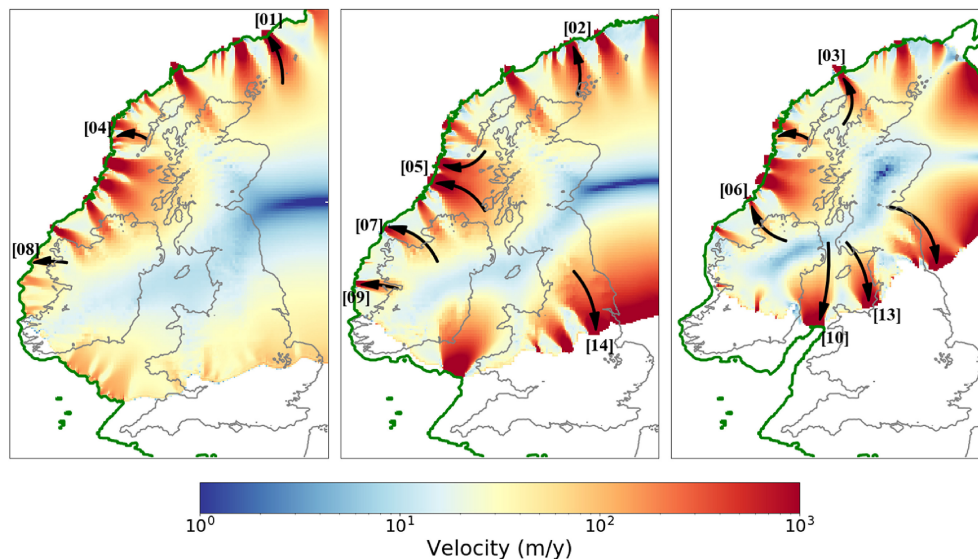
Figure 3.8: Ice velocity at 10,000, 12,500, and 15,000 model years. Locations of key ice streams empirically reconstructed in the literature are highlighted with black arrows, with ice streams numbered as in Figure 3.1 and Table 3.2. The wide ice streams in the North Sea are caused by a domain-edge effect.

A number of ice streams in Group A form in bathymetric troughs, and therefore colocation between the reconstructed and simulated ice streams was likely. However, some of the Group A ice streams form in relatively minor bathymetric troughs, like the North Sea Lobe, the Forth Ice Stream, and the Moray Ice Stream. In these examples, the simulations show significant skill in simulating empirically reconstructed ice streams with subtle bathymetric confinement. Although bathymetry does not directly control the position of these ice streams, neighbouring trough controlled ice streams can influence their position. This means that the skill of the model in simulating ice streams in significant bathymetric troughs allows the model to show skill in simulating ice streams away from bathymetric troughs.

The empirically well-constrained ice streams in bathymetric troughs allow a quantitative comparison between simulated ice streams and empirically reconstructed ice stream paths using AFDA (Li et al., 2007; Napieralski et al., 2007; Ely et al., 2019). The Automated Flow Direction Analysis (AFDA) tool calculates the mean residual vector and variance between simulated and reconstructed ice flow. Figure 3.10 shows the resulting mean residual vector and variance of
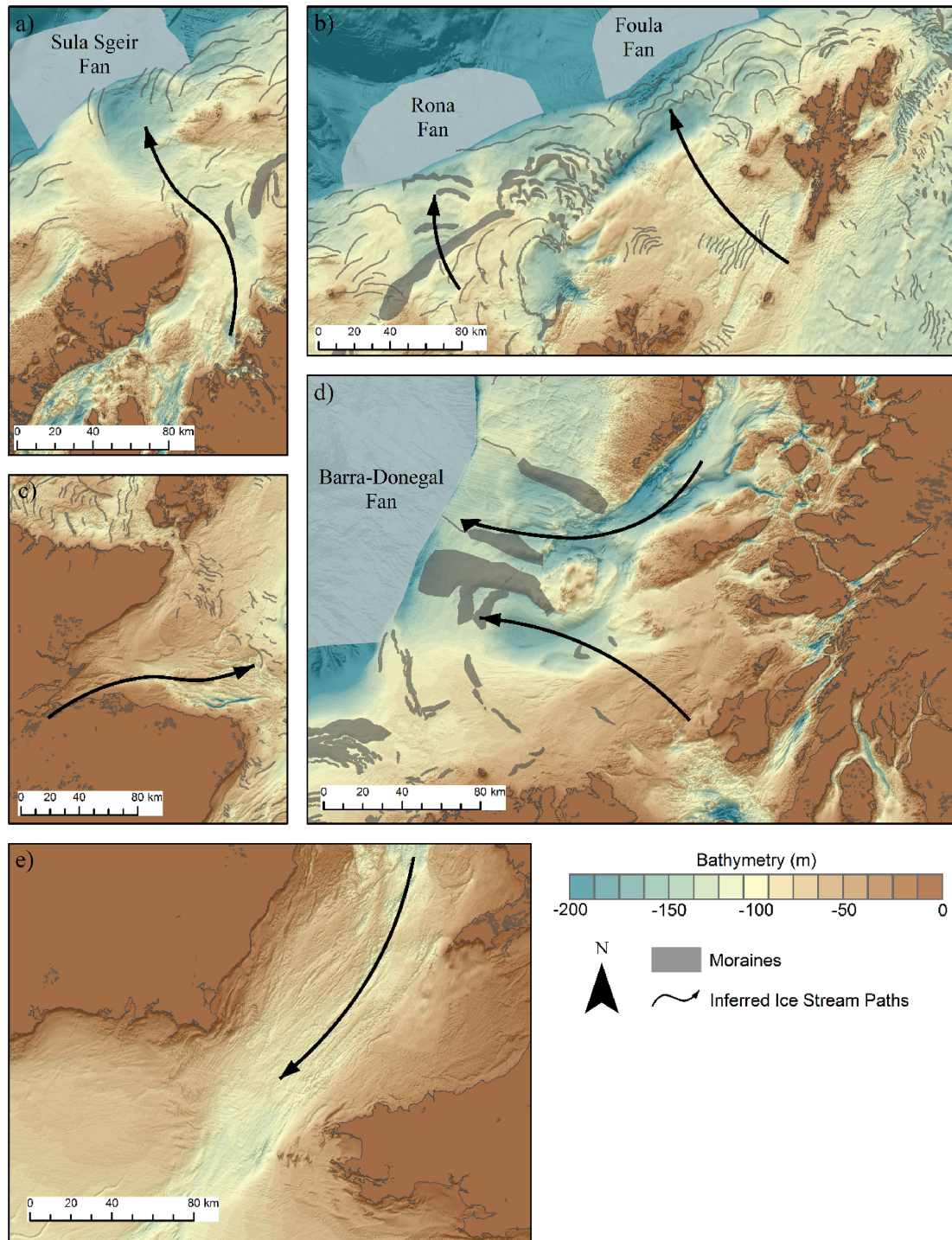
Figure 3.9: Bathymetry and geomorphological landforms of five empirically well constrained ice streams, a) The Minch Ice Stream, b) The Foula and Rona Ice Streams, c) The Moray Firth Ice Stream, d) The Barra Fan Ice Streams, and e) the Irish Sea Ice Stream.

the flow direction for the duration of each ice stream's simulation. The Rona Ice Stream (Figure 3.10b) is the strongest match between simulated and empirical evidence, with an average mean residual vector of 5°, and only brief excursions

above the data-model match criteria. The Minch and the Barra Fan Ice Streams also perform reasonably well during periods of the ADVANCE and RETREAT experiments.
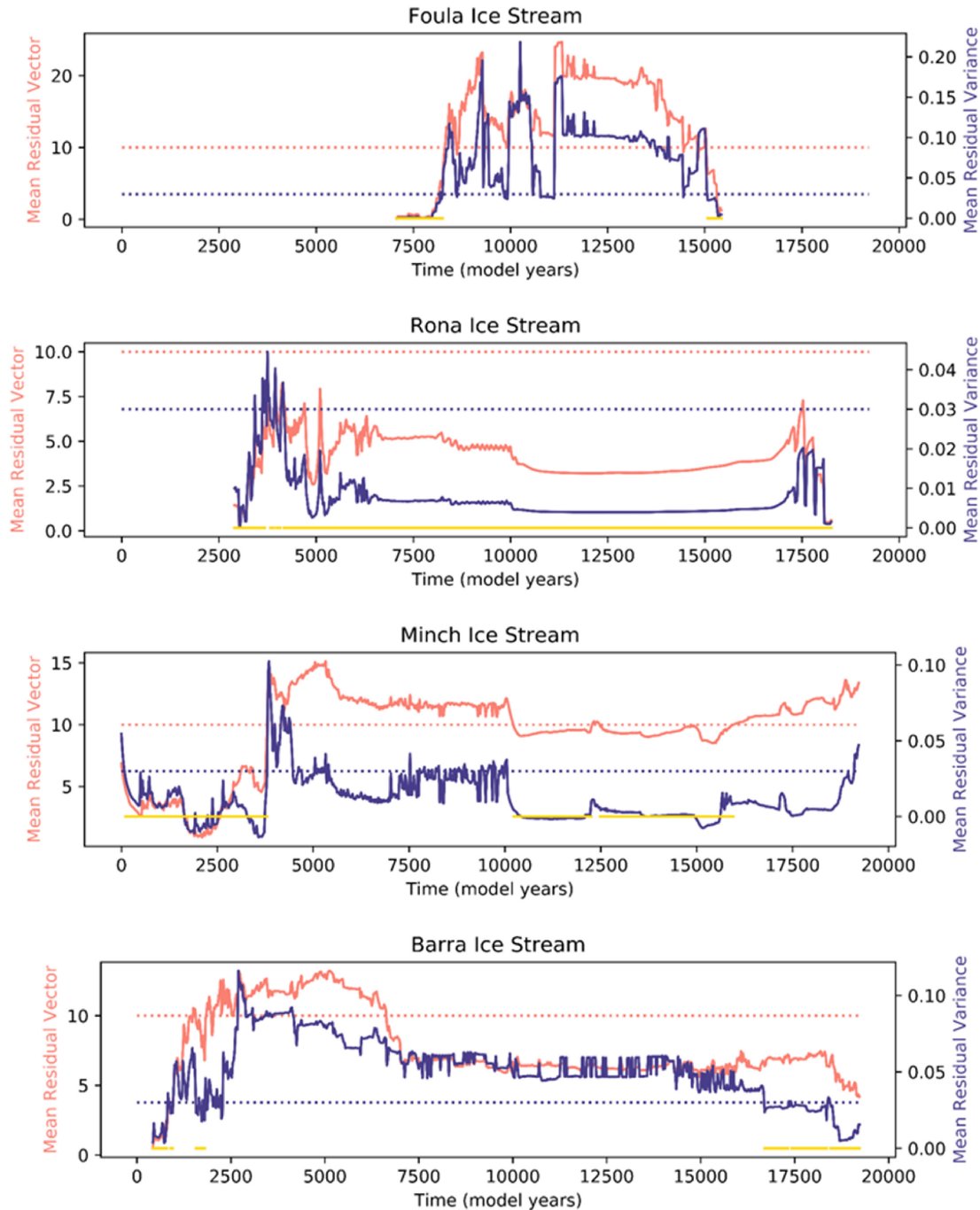
Figure 3.10: Mean residual vector and mean residual variance between modelled and empirically reconstructed flow for four simulated ice streams. Dashed lines show the threshold mean residual vector and mean residual variance used to identify model-data agreement. The yellow highlight shows times of model-data agreement.

The Foula ice stream is the shortest-lived ice stream, streaming from 8,500 to 15,000 model years (Figure 3.5e and f), and matches empirical flow directions at the start and end of the ice stream's existence, but there is no model-data match during the majority of the ice stream's occupancy. There is significant flow direction change of the Foula ice stream during the simulation, as the shape of the margin changes during confluence with the eastern domain edge.

The results from AFDA confirm the qualitative conclusion that for many ice streams there is often a strong match between model and empirical data. The empirically best-constrained ice streams of the ice sheet form in significant bathymetric troughs (Figure 3.9), which the model demonstrates significant skill in simulating. Whilst there may be a weaker model match for ice streams that are less bathymetrically controlled, like the North Sea and western Irish margin, the empirical reconstruction of flow direction is also less well constrained in these regions. The AFDA scores are sensitive to variations in the empirical reconstruction, so poorly constrained ice streams are not suitable for meaningful comparison.

A number of simulated ice streams are more prominent during the retreat phase than the advance phase. These ice streams include the Moray Firth Ice Stream, the North Sea Lobe, and the Irish Sea Ice Stream. The retreat forcing increases the propensity of the ice sheet to stream along the southern margin (Robel and Tziperman, 2016). The simulated ice streams of the retreat phase generally form in positions with strong empirical evidence, like the North Sea Lobe (Dove et al., 2017). Ice streams that are simulated only during the retreat of the ice sheet form in less significant bathymetric troughs than the Minch, Barra Fan, Foula, and Rona Ice Streams. It seems, therefore, that these have a lower propensity to stream, until triggered by the ice sheet retreat.

3.5.2 Group B

Simulated ice streams without published empirical evidence form the second largest group of ice streams of the BIIS; group B (Table 3.2). Empirical evidence for ice streaming is inconsistently preserved by subsequent erosion and deposition. Because of this, the empirical record is, and will always be, incomplete. Given the apparent skill of the model (Group A), that ice streams may be simulated which are currently unmapped, is not a basis for discounting the model results.

The presence of simulated ice streams with no published empirical evidence stimulated us to conduct a re-examination of the empirical record in these areas. This is most prominent for the Irish west coast, where a number of ice streams are simulated, but without empirical evidence for streaming reported. Here, high rates of sedimentation during the Holocene may be obscuring bathymetric troughs and subglacial lineations. In the future, seismic reflection data may reveal these features.

In other areas, improved bathymetric data coverage allows new mapping to reveal evidence of ice streaming in regions simulated here. A North Channel Ice Stream, flowing in the Irish Sea west of the Isle of Man, is simulated in the advance and retreat of the ice sheet (Figure 3.5). Recent bathymetric multibeam data, from the UK Hydrographic Office with point data gridded into an 8 m horizontal grid, allows major subglacial lineations in this region to be mapped (Figure 3.11). Two hill-shades were created for the gridded bathymetric data, illuminating from 045° to 315° to avoid azimuth biasing (Smith and Clark, 2005). Hill-shaded bathymetry is overlain with translucent bathymetry to aid with geomorphological feature mapping. The mapped subglacial lineations are elongate (typically 2–6 km long and 100s of m wide), indicative of high ice velocities (Clark, 1993; Stokes and Clark, 1999; Spagnolo et al., 2014; Ely et al., 2016). This example demonstrates how model results can motivate and steer empirical work, here leading to the

identification of a North Channel palaeo-ice stream that has not been previously documented.
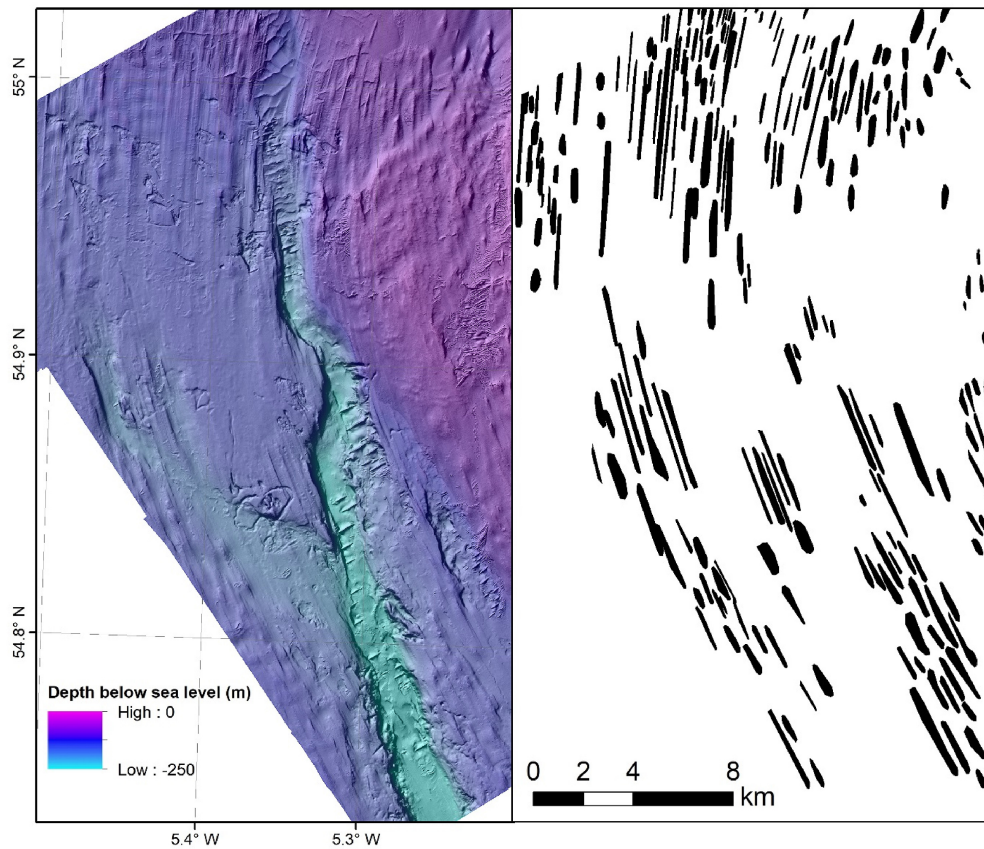
Figure 3.11: Subglacial landform mapping of the North Channel Ice Stream. a) Seafloor bathymetry, and b) Resulting map of elongate subglacial bedforms.

A St Kilda ice stream (flowing just south of the Scottish archipelago St Kilda) is also consistently simulated throughout the glacial cycle. Here, the bathymetric data does not provide evidence for subglacial lineations, but there is some circumstantial evidence for ice streaming (Figure 3.12). A small bathymetric trough is evident, encouraging ice flow between South Uist and Barra. The region is predominantly exposed bedrock, potentially caused by the extensive ice stream erosion (e.g. Bradwell et al., 2008a; Newton et al., 2018). Whilst the evidence for the North Channel Ice Stream is direct, the empirical evidence for a St Kilda Ice Stream remains circumstantial. However, the model results could encourage more targeted empirical data collection to investigate the evidence for a palaeo-ice stream.
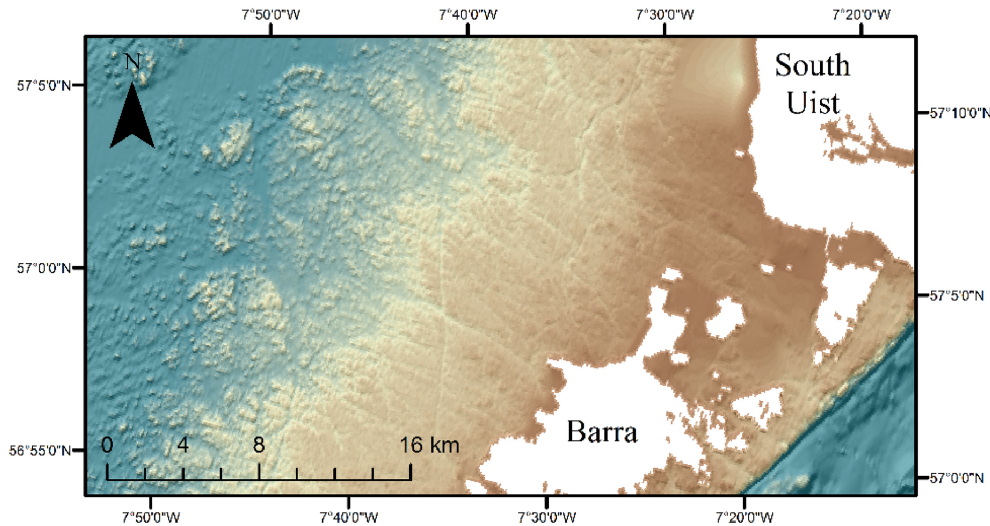
Figure 3.12: Bathymetry of the path of the simulated St Kilda ice stream. Bathymetry data source: UKHO and GEBCO.

Overall, whilst the majority of ice streams simulated have strong evidence in the empirical record, there are a handful of ice streams simulated with no empirical evidence. This offers an opportunity for targeted empirical data collection and analysis to find evidence for or against ice streams simulated in these experiments, which is supported by increasing quality of bathymetric products (Becker et al., 2009; Calewaert et al., 2016), and greater collection of shallow reflection seismic data (O'Brien et al., 2016; Stewart, 2016).

3.5.3 Group C

A small number of BIIS ice streams have empirical evidence but are not simulated here (Group C). This includes the Tweed Ice Stream (Figure 3.1[18]), evidenced by extensive mapping of streamlined subglacial bedforms (Everest et al., 2005). The flow of the Tweed Ice Stream is dependent on margin positions in a complex region of the ice sheet (Livingstone et al., 2015). The simulations here are not intended to be a margin reconstruction of the BIIS, and do not include the complex margin history expected in this region.

The Celtic Sea Ice Stream is the ice stream of the BIIS with the greatest width that is not consistently present in the simulations. The southern margin of

the simulated ice sheet in the Celtic Sea never reaches as far south as empirical reconstructions (Scourse et al., 2009). The limited model extent compared to empirical data in this region may be due to a lack of persistent ice streaming during the advance phase, the lack of a simulated large surge event, or because the idealised SMB forcing in this case is sufficiently different than reality in this sector. Whilst the empirical evidence is able to constrain the extent of the Celtic Sea Ice Stream (Scourse et al., 2009; Praeg et al., 2015), the flow geometry is difficult to reconstruct owing to a lack of subglacial bedforms. The differences in the empirical evidence between the Celtic Sea Ice Stream and other ice streams of the BIIS, along with the low model skill compared to high skill for other ice streams, suggests that the Celtic Sea Ice Stream was mechanistically different to the other ice streams of the BIIS.

3.6 Discussion

3.6.1 Required ingredients for modelling ice streams

Here we discuss which model ingredients are crucial to successfully model ice streams, which are desirable, and which can be deemed as not important. The most important model ingredient in these experiments is the representation of idealised subglacial hydrology, in these experiments as a till-water layer coupled with the Coulomb portion of the sliding law, as without this the ice sheet model does not spontaneously generate ice streams (Figure 3.4e). An adequate horizontal resolution is also an important model ingredient, the Minch Ice Stream modelled down to 4-1 km resolution (Figure 3.4d) achieves an improved AFDA score than when it is simulated at 8 km resolution (Table A.2). However, lower-order models experience more significant resolution dependency (Hindmarsh, 2009), and if an experiment was also considering grounding line dynamics using a model of sufficient physical complexity, like BISICLES, resolution could also be considered a crucial model ingredient.

Depending on the context of the experiments, additional model ingredients are required. The representation of SMB has an influence on ice stream behaviour, evident by the increased streaming along the BIIS southern margin when SMB became negative (Figure 3.6), and previous experiments (Robel and Tziperman, 2016). An accurate SMB also has a number of secondary effects. For example, ice streams of central northern England were likely not simulated here because they are dependent on complex margin and ice dome changes that cannot be simulated with an idealised SMB scheme. A spatially variable geothermal heat flux was also determined to be non-crucial for the BIIS but might be important for simulating ice streams of other ice sheets, like the Northeast Greenland Ice Stream (Rysgaard et al., 2018). Previous simulations of ice streams of the BIIS also used a spatially uniform geothermal heat flux (Hubbard et al., 2009).

Finally, some model ingredients were either ignored or highly idealised in this study and are not important in this experimental context. For example, a good match to empirical data was achieved despite a spatially uniform Weertman coefficient, Coulomb friction angle, maximum till-water depth, and till-water drain rate. Varying these parameters does change the pattern of ice streaming (Figure A.3), but representing these factors as spatially variable is not a necessary model ingredient in this case. However, a more realistic representation of the subglacial environment, including factors such as variable bed geology, and/or improved process understanding may prove to be a more influential model ingredient for other ice sheets, and could help improve the simulation of the Celtic Sea Ice Stream.

The horizontal transport of meltwater is a process that remains unrepresented in the model. The supraglacial, englacial, and subglacial transport has been observed to redistribute water on short timescales (Andrews et al., 2014), and has been identified as a key control on ice sheet velocity (Zwally et al., 2002; Hewitt, 2013). Meltwater transport also evolves annually (Chandler et al., 2013), and is expected to be a mechanism to cause ice stream evolution. Although the

experiments here achieve a close fit to empirical data without a representation of horizontal meltwater transport, future model development should include this mechanism and test for its influence in a variety of ice sheet contexts.

3.6.2   Ice stream controls

Winsborrow et al. (2010) reviewed the literature on palaeo and contemporary ice streams, and compiled seven factors that control ice stream location. They are, in the order of importance that Winsborrow et al. (2010) proposes, topographic troughs, marine margins, soft beds, abundant meltwater, smooth beds, high geothermal heat flux, and topographic steps. Whilst ice streams will spontaneously form due to thermo-mechanical coupling of ice flow (Payne and Dongelmans, 1997), these seven factors controls the relative position of ice streams. Of the seven factors, only soft beds are not represented in these simulations as bed friction coefficient is idealised to be uniform across the domain.

For the BIIS, the influence of topographic troughs and steps are considered together, as the features co-exist at the ice sheet bed. Supporting the Winsborrow et al. (2010) hierarchy of controls, these simulations suggest that bed topography is the primary control of ice stream location for the BIIS. The primary large, and spatially and temporally consistent ice streams in the simulations, are all located in bathymetric troughs; the Minch Ice Stream, the Barra Fan Ice Streams, the Rona Ice Stream, and the Foula Ice Stream (Figure 3.9). However, not all simulated ice streams form in well-defined topographic troughs, like the North Sea Lobe, Forth Ice Stream, and the ice streams of the Irish west coast. Ice streams without well-defined topographic control are more likely to be sensitive to weaker controls on ice stream location, demonstrated by the change in ice stream location in Northwest Ireland when considering a varying geothermal heat flux (Figure 3.7). Ice streams outside a topographic trough also exhibit greater resolution dependency (Figure 3.4g). An idealised experiment of a square ice sheet on a flat bed (Figure A.2) also shows greater resolution dependency than

on a real bed (Figure 3.4), suggesting that these ice streams may also be more sensitive to resolution.

The position of topographically controlled ice streams has an indirect control on ice streams with weaker topographic control. It has been shown here (Fig. S1), and in previous research (Payne and Dongelmans, 1997; Hindmarsh, 2009) that even on a flat bed regularly spaced ice streams will form around the margin of an ice sheet. Therefore, whilst topographic troughs will determine the location of some of the ice streams of the BIIS, other ice streams would be expected to form between these ice streams even on flat beds. Ice sheet models on flat beds predict regular spacing of ice streams; but on a real bed with topographic variation, some ice streams would be anchored in topographic troughs and the predominant spacing control then fixes the position of other non-topographic ice streams.

The simulations also support the expected strong influence of marine margins, with the most spatially and temporally consistent ice streams occurring along the western board of the ice sheet, with a marine margin in the Atlantic Ocean. Many simulated ice streams with a marine margin are also in bathymetric troughs, although the ice streams of the western Ireland coast have a marine margin without large troughs. Calving at the margin of the ice sheet lowers the surface profile, allowing the capture of more ice from the catchment, and thus increased ice streaming. Ice streams that advance and retreat onshore, for example through central and southern England (Figure 3.1d and e), do not stream constantly, unlike the majority of ice streams with a marine margin. Therefore, there is evidence from these simulations that a marine margin is a strong control of behaviour of BIIS ice streams, but not necessarily ice stream location.

The saturation of the till-water layer is a control on the water pressure, which is in turn a variable in the Coulomb portion of the sliding law. The saturation of the till-water layer is influenced by the geothermal heat flux, maximum till-water layer thickness, and the till-water drain factor. Whilst there is a strong

relation between the location of modelled ice streams and regions of a saturated till-water layer (Figure 3.13), the till-water layer saturation is not the sole control on ice stream position. On the southern and eastern margin there are a number of regions of saturation, whilst ice streaming does not occur. However, no ice streams are apparent in regions with low till-water layer saturation. The increased velocity of an ice stream increases frictional heating, and therefore increases the saturation of the till water layer. The relationship between the saturation of the till-water layer and ice velocity means evidence of cold-based ice (Bierman et al., 2015; MacGregor et al., 2016) can be a strong constraint on model results.
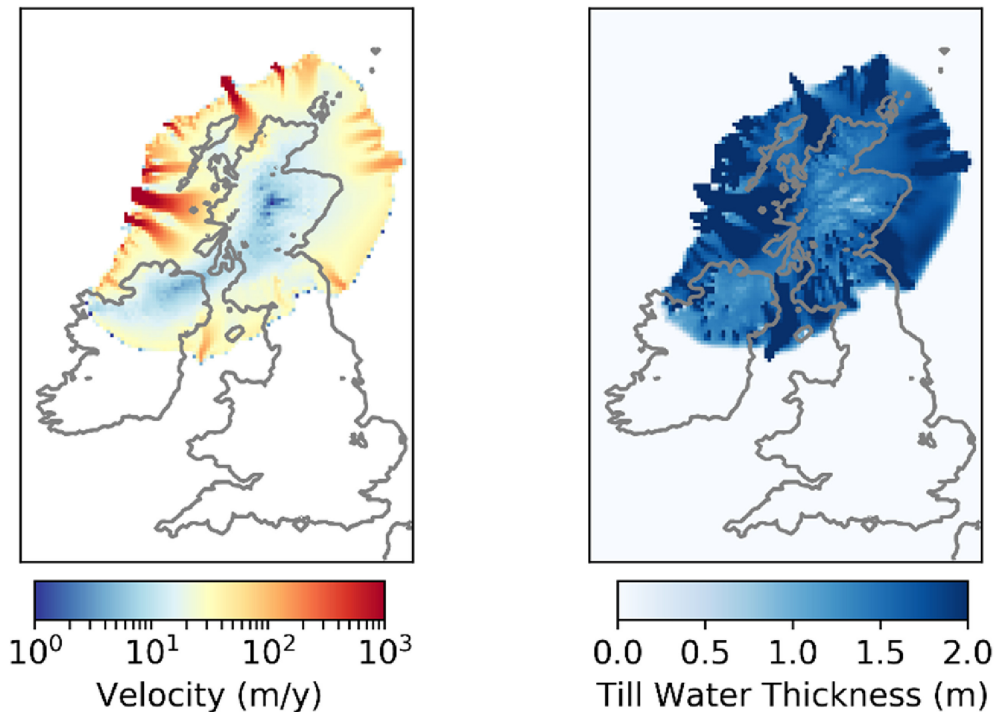
Figure 3.13: a) Ice Velocity at t = 4,000 years. b) Till water thickness at t = 4,000 years.

The relatively limited influence of the geothermal heat flux is highlighted by the experiments ADVANCE_GEOTHERMAL and RETREAT_GEOTHERMAL, suggesting that the spatial distribution of geothermal heat flux is only a weak control on the formation and location of ice streams. The most significant difference to ice streaming made by a spatially variable geothermal heat flux is in western Ireland, where the influence of bathymetric troughs is weak. The relatively small influence of geothermal heat flux has been supported by Winsborrow

et al. (2010). However, it is important to note that there is only a limited range of geothermal heat flux values across the domain. Geothermal heat flux could be an important control of ice stream formation and location in domains with weaker other controls on ice stream location and a wider range of geothermal heat flux values. For example, it has been suggested that the location and unusual geometry of the Northeast Greenland Ice Stream may be influenced by a geothermal heat flux hot spot at the ice sheet bed (Rysgaard et al., 2018).

3.6.3   Model evaluation

The comparison between the simulated and empirically reconstructed ice streams can be used to evaluate the skill of the ice sheet model at producing ice streams in reasonable locations. The qualitative and quantitative similarities between the simulated ice streams and the ice streams recorded in the empirical data suggests that the model has significant skill. The simulations consistently produce ice streams in areas of strong empirical evidence. Therefore it would be reasonable to apply this to other palaeo ice sheets where the empirical record is less complete. If the model can consistently simulate expected ice stream and ice sheet evolution over millennia for a diverse range of palaeo ice sheets, the model would be expected to have sufficient skill to project medium- and long-term evolution of the Greenland and Antarctic Ice Sheets.

However, some mechanisms are not represented in the model, which could be influential to ice stream formation and location, including water drainage from the ice surface to the bed (Das et al., 2008; Krawczynski et al., 2009), and ice stream freeze on and shutdown (Christoffersen and Tulaczyk, 2003). These simulations include no representation of spatially variable maximum till-water layer thickness, deformability, or porosity. We consider these geological controls on ice stream formation and location as second order factors given the similarities between simulated ice streams and empirical ice streams show here, but this will not necessarily be the case for all ice streams in all ice sheets. For example, the

poor representation of the Celtic Sea Ice Stream in these simulations may be the result of the lack of representation of key geological parameters that may help produce large surging lobes. For example, the lack of horizontal meltwater transport in the simulations still allows good model-data fit for the majority of ice streams, but may be a more important process for the Celtic Sea Ice Stream. A thermomechanical induced surge would also be highly sensitive to model set-up and subsequent evolution, and would be a challenge to reproduce in simulations. Overall, the method described of modelling palaeo-ice streams demonstrates significant skill in producing expected ice streams, especially given the lack of spatial variability in geological parameters in our experiments.

3.6.4 Model-data symbiosis

It is important that palaeo-ice sheet reconstructions use the wealth of information available from both the empirical record and numerical modelling experiments (Andrews, 1982), but in reality this has proved difficult to implement. Comparison between simulated and empirical data is generally limited, with the exception of the comparison between ice sheets and RSL using GIA modelling (Kuchar et al., 2012; Patton et al., 2017). Despite this, tools to aid the comparison of model and empirical data have been developed (Li et al., 2007; Napieralski et al., 2007; Ely et al., 2019). As simulated and empirical data becomes more extensive, the foundations are in place for a symbiotic relationship between simulated and empirical data, where models benefit, and benefit from, empirical data, resulting in improved palaeo reconstructions, and future ice sheet projections.

Here, the empirical palaeo archive has proved to be a good test of the skill of an ice sheet model's ability to produce ice streams. Empirical data permit qualitative and quantitative assessment of ice sheet model skill at simulating ice streams of reasonable position and spacing. Simulations with a more advanced forcing, primarily a less idealised climate forcing, can benefit from a more extensive suite of model-data comparison tools than the single tool used here. For example,

Ely et al. (2019) describe a suite of three tools to compare simulated palaeo ice streams with empirical evidence, which compare margin position, flow direction, and advance and retreat timing.

Simulated data can also complement empirical data collection and analysis by indicating the potential locations of palaeo ice streams. An intriguing candidate, highlighted here, is the St Kilda ice stream (Figure 3.12), which is simulated consistently throughout the advance and retreat of the ice sheet but empirical evidence for this ice stream remains circumstantial. The simulations also point to the potential for west coast of Ireland ice streams, with potential empirical evidence subsequently covered in significant Holocene deposits. This means that surficial evidence for these potential ice streams may not exist, but could be mapped through extensive seismic reflection data (Graham et al., 2007; Emery et al., 2019; Knutz et al., 2019), which would be important for the dynamics of a significant marine portion of the BIIS.

Modelling results can also assist reconstructions of ice sheet behaviour in regions where there is limited empirical data. For example, despite extensive empirical efforts, the deglaciation dynamics of the North Sea remain uncertain (Roberts et al., 2007; Sejrup et al., 2016; Dove et al., 2017). An ice sheet model with sufficient skill to model evolving ice stream dynamics could help test the feasibility of empirical reconstructions. This process of an ice sheet model being used to identify physically plausible glaciation patterns could also be applied to other empirically uncertain regions of the ice sheet, like the Porcupine Bank (Lee et al., 2015), or the Celtic Sea Ice Stream (Scourse et al., 2009).

3.6.5 Contemporary ice stream modelling

The evolution of ice streams is a considerable uncertainty in projections of Greenland and Antarctic response to climate change (Vaughan and Arthern, 2007), and thus is a considerable uncertainty in projecting long-term global sea level rise (Bamber and Aspinall, 2013). The method of inverting ice stream parameters

from surface velocities, which is common in studies projecting future ice sheet evolution (Morlighem et al., 2013), is not suitable for medium-to long-term projections because it does not properly account for the evolution of bed hydrology as the ice sheet evolves (Aschwanden et al., 2013). A statistical inversion of the surface velocity of an ice sheet will produce a close match to the observed ice sheet in the short-term. However, over centennial timescales the observed and modelled ice sheets would diverge because of the evolving nature of ice streams, even given a perfect climate forcing.

Therefore, to project the medium-to long-term evolution of the Greenland and Antarctic Ice Sheets, an ice sheet model is required that simulates ice stream location, spacing, and evolution accurately without inverting ice stream parameters from contemporary ice sheet surface velocity. BISICLES_hydro simulated ice streams without requiring inversion, and accurately simulates ice stream position, spacing, and evolution as suggested by empirical data from the palaeo record. Future work could validate ice velocities simulated with this scheme against measured contemporary ice velocities of the Greenland and Antarctic Ice Sheet. It would also be useful to test the model on sectors of palaeo ice sheets with a less dominant topographic control on ice stream locations, like the southern margin of the Laurentide and Fennoscandian ice sheets, and to experiment with a more realistic transient climate and ocean forcing. These sectors would also provide a stronger test of the model's ability to simulate terrestrial ice streams, which are infrequent for the BIIS. Assuming sufficient skill, this model would have the potential to be used to project the medium-to long-term evolution of the Greenland and Antarctic Ice Sheets.

Further development could also be made in the representation of englacial and subglacial meltwater transport. Although the model achieves a good match to empirical evidence without these representations, there is empirical evidence that meltwater transport is an important control on ice velocity evolution (Zwally et al., 2002). Meltwater transport may prove to be more important in other ice

sheet contexts, and may improve the representation of the Celtic Sea Ice Stream. Meltwater transport is an important process that remains either not included or highly idealised in ice sheet models.

This work demonstrates that the palaeo record is an ideal test for new ice sheet models that simulate ice stream evolution without the need for statistical inversion. Simulations of palaeo ice sheets have already been compared to RSL records through GIA modelling (Simpson et al., 2009; Kuchar et al., 2012; Auriac et al., 2016), and flowsets (Patton et al., 2016). In addition, we suggest that new ice sheet models developed with the aim of projecting the evolution of the Greenland and Antarctic Ice Sheets over the centennial and millennial timescale should be tested against empirical data of ice stream flow direction from well-constrained sectors of the palaeo record to test for sufficient model skill.

3.7 Conclusions

We developed the BISICLES ice sheet model to simulate the spontaneous generation and evolution of ice streams during the advance and retreat of ice sheets. We model basal sliding by using a Coulomb law dependent on basal water pressure, with a simple scheme for local calculating the local balance of water in a till layer. This development allows for the simulation of ice streams that evolve along with the ice sheet. We tested the skill of an ice sheet model's ability to simulate ice streams using the palaeo-record of the BIIS. The palaeo record offers the opportunity to test the skill of the model at simulating ice stream location, spacing, and evolution across a multi-millennial glacial cycle. Despite several assumptions, namely a uniform bed friction coefficient, a highly idealised surface mass balance forcing, and uniform maximum till-water layer thickness, the simulated ice streams strongly match empirically reconstructed ice streams of the BIIS. Results of our simulations suggest that the major controls on ice streaming of the BIIS are topographic troughs and marine margins. We found a spatially

variable geothermal heat flux to have only a minor local impact of the pattern of ice streaming, where topographic features are less pronounced.

The simulated ice streams of the BIIS demonstrates the high model skill of ice stream placement and evolution over millennial timescales. With application of this model to more diverse palaeo and modern settings, it could be determined if the model has sufficient skill to model the future evolution of the Antarctic and Greenland ice sheets over the medium- and long-term. Using a model that adequately accounts for ice stream evolution is crucial to future projections of ice sheet change. Ice sheet simulations working in tandem with empirical data therefore can help progress our simulations of future ice sheet evolution towards greater accuracy.

Data Availability

We used a branch of the BISICLES ice sheet model, revision 3776 (https://anag-repo.lbl.gov/svn/BISICLES/public/branches/slc_dev_2018). Output files and required input files to reproduce the described experiments can be found at https://data.mendeley.com/datasets/w5tn37pkym/1 (Gandy, 2019).

References

Andrews, J. T. (1982). "On the reconstruction of pleistocene ice sheets: A review". In: *Quaternary Science Reviews* 1.1, pp. 1–30. DOI: 10.1016/0277-3791(82)90017-8.

Andrews, L. C., G. A. Catania, M. J. Hoffman, J. D. Gulley, M. P. Lüthi, C. Ryser, R. L. Hawley, and T. A. Neumann (2014). "Direct observations of evolving subglacial drainage beneath the Greenland Ice Sheet". In: *Nature* 514. DOI: 10.1038/nature13796.

Arthern, R. J., R. C. A. Hindmarsh, and C. R. Williams (2015). "Flow speed within the Antarctic ice sheet and its controls inferred from satellite observations". In: *Journal of Geophysical Research: Earth Surface* 120.7, pp. 1171–1188. DOI: 10.1002/2014JF003239.

Aschwanden, A., G. Aðalgeirsdóttir, and C. Khroulev (2013). "Hindcasting to measure ice sheet model sensitivity to initial states". In: *The Cryosphere* 7, pp. 1083–1093. DOI: 10.5194/tc-7-1083-2013.

Aschwanden, A., E. Bueler, C. Khroulev, and H. Blatter (2012). "An enthalpy formulation for glaciers and ice sheets". In: *Journal of Glaciology* 58.209. DOI: 10.3189/2012JoG11J088.

Aschwanden, A., M. A. Fahnestock, M. Truffer, D. J. Brinkerhoff, R. Hock, C. Khroulev, R. Mottram, and S. A. Khan (2019). "Contribution of the Greenland Ice Sheet to sea level over the next millennium". In: *Science Advances* 5.6, eaav9396. DOI: 10.1126/sciadv.aav9396.

Auriac, A., P. Whitehouse, M. Bentley, H. Patton, J. Lloyd, and A. Hubbard (2016). "Glacial isostatic adjustment associated with the Barents Sea ice sheet: A modelling inter-comparison". In: *Quaternary Science Reviews* 147, pp. 122–135. DOI: 10.1016/J.QUASCIREV.2016.02.011.

Bamber, J. L. and W. P. Aspinall (2013). "An expert judgement assessment of future sea level rise from the ice sheets". In: *Nature Climate Change* 3.4, pp. 424–427. DOI: 10.1038/nclimate1778.

Bamber, J. L., D. G. Vaughan, and I. Joughin (2000). "Widespread complex flow in the interior of the antarctic ice sheet". In: *Science* 287.5456, pp. 1248–1250. DOI: 10.1126/science.287.5456.1248.

Bateman, M. et al. (2015). "Last glacial dynamics of the Vale of York and North Sea lobes of the British and Irish Ice Sheet". In: *Proceedings of the Geologists' Association* 126.6, pp. 712–730. DOI: 10.1016/J.PGEOLA.2015.09.005.

Becker, J. J. et al. (2009). "Global Bathymetry and Elevation Data at 30 Arc Seconds Resolution: SRTM30_PLUS". In: *Marine Geodesy* 32.4, pp. 355–371. DOI: 10.1080/01490410903297766.

Bennett, M. R. (2003). "Ice streams as the arteries of an ice sheet: their mechanics, stability and significance". In: *Earth-Science Reviews* 61.3-4, pp. 309–339. DOI: 10.1016/S0012-8252(02)00130-7.

Bierman, P. R., P. T. Davis, L. B. Corbett, N. A. Lifton, and R. C. Finkel (2015). "Cold-based Laurentide ice covered New England's highest summits during the Last Glacial Maximum". In: *Geology* 43.12, G37225.1. DOI: 10.1130/G37225.1.

Bingham, R. G. et al. (2017). "Diverse landscapes beneath Pine Island Glacier influence ice flow". In: *Nature Communications* 8.1, p. 1618. DOI: 10.1038/s41467-017-01597-y.

Bougamont, M., S. Price, P. Christoffersen, and A. J. Payne (2011). "Dynamic patterns of ice stream flow in a 3-D higher-order ice sheet model with plastic

bed and simplified hydrology". In: *Journal of Geophysical Research* 116.F4, F04018. DOI: 10.1029/2011JF002025.

Boulton, G. S., M. Hagdorn, and N. R. Hulton (2003). "Streaming flow in an ice sheet through a glacial cycle". In: *Annals of Glaciology* 36, pp. 117–128. DOI: 10.3189/172756403781816293.

Boulton, G. and M. Hagdorn (2006). "Glaciology of the British Isles Ice Sheet during the last glacial cycle: form, flow, streams and lobes". In: *Quaternary Science Reviews* 25.23-24, pp. 3359–3390. DOI: 10.1016/j.quascirev.2006.10.013.

Bradley, S. L., G. A. Milne, I. Shennan, and R. Edwards (2011). "An improved glacial isostatic adjustment model for the British Isles". In: *Journal of Quaternary Science* 26.5, pp. 541–552. DOI: 10.1002/jqs.1481.

Bradwell, T. and M. S. Stoker (2015). "Submarine sediment and landform record of a palaeo-ice stream within the British-Irish ice sheet". In: *Boreas* 44.2, pp. 255–276. DOI: 10.1111/bor.12111.

Bradwell, T., M. Stoker, and M. Krabbendam (2008a). "Megagrooves and streamlined bedrock in NW Scotland: The role of ice streams in landscape evolution". In: *Geomorphology* 97.1-2, pp. 135–156. DOI: 10.1016/J.GEOMORPH.2007.02.040.

Bradwell, T. et al. (2008b). "The northern sector of the last British Ice Sheet: Maximum extent and demise". In: *Earth-Science Reviews* 88.3-4, pp. 207–226. DOI: 10.1016/j.earscirev.2008.01.008.

Bradwell, T. et al. (2019). "Ice-stream demise dynamically conditioned by trough shape and bed strength". In: *Science Advances* 5.4, eaau1380. DOI: 10.1126/sciadv.aau1380.

Bueler, E. and W. van Pelt (2015). "Mass-conserving subglacial hydrology in the Parallel Ice Sheet Model version 0.6". In: *Geoscientific Model Development* 8.6, pp. 1613–1635. DOI: 10.5194/gmd-8-1613-2015.

Busby, J. (2010). *Geothermal Prospects in the United Kingdom.* Tech. rep., pp. 25–29.

Calewaert, J.-B., P. Weaver, V. Gunn, P. Gorringe, and A. Novellino (2016). "The European Marine Data and Observation Network (EMODnet): Your Gateway to European Marine and Coastal Data". In: Springer, Cham, pp. 31–46. DOI: `10.1007/978-3-319-32107-3_4`.

Chandler, D. M. et al. (2013). "Evolution of the subglacial drainage system beneath the Greenland Ice Sheet revealed by tracers". In: *Nature Geoscience* 6, p. 24. DOI: `10.1038/NGEO1737`.

Chiverrell, R. C. et al. (2013). "Bayesian modelling the retreat of the Irish Sea Ice Stream". In: *Journal of Quaternary Science* 28.2, pp. 200–209. DOI: `10.1002/jqs.2616`.

Christoffersen, P. and S. Tulaczyk (2003). "Signature of palaeo-ice-stream stagnation: Till consolidation induced by basal freeze-on". In: *Boreas* 32.1, pp. 114–129. DOI: `10.1111/j.1502-3885.2003.tb01433.x`.

Clark, C. D. (1993). "Mega-scale glacial lineations and cross-cutting ice-flow landforms". In: *Earth Surface Processes and Landforms* 18.1, pp. 1–29. DOI: `10.1002/esp.3290180102`.

Clark, C. D., D. J. Evans, A. Khatwa, T. Bradwell, C. J. Jordan, S. H. Marsh, W. A. Mitchell, and M. D. Bateman (2004). *Map and GIS database of glacial landforms and features related to the last British Ice Sheet.* DOI: `10.1111/j.1502-3885.2004.tb01246.x`. arXiv: `arXiv:1011.1669v3`.

Clark, C. D., A. L. Hughes, S. L. Greenwood, C. Jordan, and H. P. Sejrup (2012). "Pattern and timing of retreat of the last British-Irish Ice Sheet". In: *Quaternary Science Reviews* 44, pp. 112–146. DOI: `10.1016/j.quascirev.2010.07.019`.

Clark, C. D. and C. R. Stokes (2001). "Extent and basal characteristics of the M'Clintock Channel Ice Stream". In: *Quaternary International* 86.1, pp. 81–101. DOI: `10.1016/S1040-6182(01)00052-0`.

Clark, C. D. et al. (2018). "BRITICE Glacial Map, version 2: a map and GIS database of glacial landforms of the last British-Irish Ice Sheet". In: *Boreas* 47.1, 11–e8. DOI: 10.1111/bor.12273.

Conway, H., G. Catania, C. F. Raymond, A. M. Gades, T. A. Scambos, and H. Engelhardt (2002). "Switch of flow direction in an Antarctic ice stream". In: *Nature* 419.6906, pp. 465–467. DOI: 10.1038/nature01081.

Cornford, S. L. et al. (2015). "Century-scale simulations of the response of the West Antarctic Ice Sheet to a warming climate". In: *Cryosphere* 9.4, pp. 1579–1600. DOI: 10.5194/tc-9-1579-2015.

Cutler, P. M., D. M. Mickelson, P. M. Colgan, D. R. MacAyeal, and B. R. Parizek (2001). "Influence of the Great Lakes on the dynamics of the southern Laurentide ice sheet: Numerical experiments". In: *Geology* 29.11, p. 1039. DOI: 10.1130/0091-7613(2001)029<1039:IOTGLO>2.0.CO;2.

Das, S. B., I. Joughin, M. D. Behn, I. M. Howat, M. A. King, D. Lizarralde, and M. P. Bhatia (2008). "Fracture Propagation to the Base of the Greenland Ice Sheet During Supraglacial Lake Drainage". In: *Science* 320.5877, pp. 778–781. DOI: 10.1126/SCIENCE.1153360.

Davies, D., R. G. Bingham, E. C. King, A. M. Smith, A. M. Brisbourne, M. Spagnolo, A. G. C. Graham, A. E. Hogg, and D. G. Vaughan (2018). "How dynamic are ice-stream beds?" In: *The Cryosphere* 12.5, pp. 1615–1628. DOI: 10.5194/tc-12-1615-2018.

Dove, D., D. J. Evans, J. R. Lee, D. H. Roberts, D. R. Tappin, C. L. Mellett, D. Long, and S. L. Callard (2017). "Phased occupation and retreat of the last British–Irish Ice Sheet in the southern North Sea; geomorphic and seismostratigraphic evidence of a dynamic ice lobe". In: *Quaternary Science Reviews* 163, pp. 114–134. DOI: 10.1016/j.quascirev.2017.03.006.

Dowdeswell, J. A., D. Ottesen, and L. Rise (2006). "Flow switching and large-scale deposition by ice streams draining former ice sheets". In: *Geology* 34.4, p. 313. DOI: 10.1130/G22253.1.

Ely, J. C., C. D. Clark, M. Spagnolo, C. R. Stokes, S. L. Greenwood, A. L. Hughes, P. Dunlop, and D. Hess (2016). "Do subglacial bedforms comprise a size and shape continuum?" In: *Geomorphology* 257, pp. 108–119. DOI: 10.1016/J.GEOMORPH.2016.01.001.

Ely, J. C. et al. (2019). "Recent progress on combining geomorphological and geochronological data with ice sheet modelling, demonstrated using the last British–Irish Ice Sheet". In: *Journal of Quaternary Science*, pp. 1–15. DOI: 10.1002/jqs.3098.

Emery, A. R., D. M. Hodgson, N. L. Barlow, J. L. Carrivick, C. J. Cotterill, and E. Phillips (2019). "Left High and Dry: Deglaciation of Dogger Bank, North Sea, Recorded in Proglacial Lake Evolution". In: *Frontiers in Earth Science* 7, p. 234. DOI: 10.3389/feart.2019.00234.

Engelhardt, H. and B. Kamb (1997). "Basal hydraulic system of a West Antarctic ice stream: constraints from borehole observations". In: *Journal of Glaciology* 43.144, pp. 207–230. DOI: 10.3189/S0022143000003166.

Everest, J., T. Bradwell, and N. Golledge (2005). "Subglacial landforms of the tweed palaeo-ice stream". In: *Scottish Geographical Journal* 121.2, pp. 163–173. DOI: 10.1080/00369220518737229.

Farr, T. G. et al. (2007). "The Shuttle Radar Topography Mission". In: *Reviews of Geophysics* 45.2, RG2004. DOI: 10.1029/2005RG000183.

Farrell, T., A. Jones, M. Muller, M. Feely, A. Brock, M. Long, and T. Waters (2014). "IRETHERM: The geothermal energy potential of Irish radiothermal granites". In: *EGU General Assembly 2014, held 27 April - 2 May, 2014 in Vienna, Austria, id.6749* 16.

Favier, L., G. Durand, S. L. Cornford, G. H. Gudmundsson, O. Gagliardini, F. Gillet-Chaulet, T. Zwinger, A. J. Payne, and A. M. Le Brocq (2014). "Retreat of Pine Island Glacier controlled by marine ice-sheet instability". In: *Nature Climate Change* 4.2, pp. 117–121. DOI: 10.1038/nclimate2094.

Finlayson, A., D. Fabel, T. Bradwell, and D. Sugden (2014). "Growth and decay of a marine terminating sector of the last BritisheIrish Ice Sheet: a geomorphological reconstruction". In: *Quaternary Science Reviews* 83, pp. 28–45. DOI: 10.1016/j.quascirev.2013.10.009.

Gandy, N., L. J. Gregoire, J. C. Ely, C. D. Clark, D. M. Hodgson, V. Lee, T. Bradwell, and R. F. Ivanovic (2018). "Marine Ice Sheet Instability and Ice Shelf Buttressing Influenced Deglaciation of the Minch Ice Stream, Northwest Scotland". In: *The Cryosphere* 12.July, pp. 1–24. DOI: 10.5194/tc-2018-116.

Gillet-Chaulet, F., O. Gagliardini, H. Seddik, M. Nodet, G. Durand, C. Ritz, T. Zwinger, R. Greve, and D. G. Vaughan (2012). "Greenland ice sheet contribution to sea-level rise from a new-generation ice-sheet model". In: *Cryosphere* 6.6, pp. 1561–1576. DOI: 10.5194/tc-6-1561-2012.

Gladstone, R. M., Y. Xia, and J. Moore (2018). "Neutral equilibrium and forcing feedbacks in marine ice sheet modelling". In: *The Cryosphere* 12.11, pp. 3605–3615. DOI: 10.5194/tc-12-3605-2018.

Glen, J. W. (1955). "The creep of polycrystalline ice". In: *Proceedings of the Royal Society of London. Series A. Mathematical and Physical Sciences* 228.1175, pp. 519–538. DOI: 10.1098/rspa.1955.0066.

Gong, Y., T. Zwinger, S. Cornford, R. Gladstone, M. Schäfer, and J. C. Moore (2017). "Importance of basal boundary conditions in transient simulations: Case study of a surging marine-terminating glacier on Austfonna, Svalbard". In: *Journal of Glaciology* 63.237, pp. 106–117. DOI: 10.1017/jog.2016.121.

Graham, A., L. Lonergan, and M. Stoker (2007). "Evidence for Late Pleistocene ice stream activity in the Witch Ground Basin, central North Sea, from 3D seismic reflection data". In: *Quaternary Science Reviews* 26.5-6, pp. 627–643. DOI: 10.1016/J.QUASCIREV.2006.11.004.

Greenwood, S. L. and C. D. Clark (2009). "Reconstructing the last Irish Ice Sheet 2: a geomorphologically-driven model of ice sheet growth, retreat and

dynamics". In: *Quaternary Science Reviews* 28.27-28, pp. 3101–3123. DOI: 10.1016/j.quascirev.2009.09.014.

Gregoire, L. J., A. J. Payne, and P. J. Valdes (2012). "Deglacial rapid sea level rises caused by ice-sheet saddle collapses". In: *Nature* 487.7406, pp. 219–222. DOI: 10.1038/nature11257.

Gregoire, L. J., P. J. Valdes, and A. J. Payne (2015). "The relative contribution of orbital forcing and greenhouse gases to the North American deglaciation". In: *Geophysical Research Letters* 42.22, pp. 9970–9979. DOI: 10.1002/2015GL066005.

Greve, R. (1997). "Application of a polythermal three-dimensional ice sheet model to the Greenland Ice Sheet: Response to steady-state and transient climate scenarios". In: *Journal of Climate* 10.5, pp. 901–918. DOI: 10.1175/1520-0442(1997)010<0901:AOAPTD>2.0.CO;2.

Hewitt, I. J. and A. C. Fowler (2008). "Seasonal waves on glaciers". In: *Hydrological Processes* 22.19, pp. 3919–3930. DOI: 10.1002/hyp.7029.

Hewitt, I. (2013). "Seasonal changes in ice sheet motion due to melt water lubrication". In: *Earth and Planetary Science Letters* 371-372, pp. 16–25. DOI: 10.1016/J.EPSL.2013.04.022.

Hewitt, I. J. (2011). "Modelling distributed and channelized subglacial drainage: the spacing of channels". In: *Journal of Glaciology* 57.202, pp. 302–314. DOI: 10.3189/002214311796405951.

Hindmarsh, R. (2018). "Ice Sheet and Glacier Modelling". In: *Past Glacial Environments*, pp. 607–663. DOI: 10.1016/B978-0-08-100524-8.00019-1.

Hindmarsh, R. C. (2009). "Consistent generation of ice-streams via thermo-viscous instabilities modulated by membrane stresses". In: *Geophysical Research Letters* 36.6, p. L06502. DOI: 10.1029/2008GL036877.

Hindmarsh, R. C. and E. L. Meur (2001). "Dynamical processes involved in the retreat of marine ice sheets". In: *Journal of Glaciology* 47.157, pp. 271–282. DOI: 10.3189/172756501781832269.

Hogg, A. E., A. Shepherd, N. Gourmelen, and M. Engdahl (2016). "Grounding line migration from 1992 to 2011 on Petermann Glacier, North-West Greenland". In: *Journal of Glaciology* 62.236, pp. 1104–1114. DOI: 10.1017/jog.2016.83.

Horgan, H. J. and S. Anandakrishnan (2006). "Static grounding lines and dynamic ice streams: Evidence from the Siple Coast, West Antarctica". In: *Geophysical Research Letters* 33.18, n/a–n/a. DOI: 10.1029/2006GL027091.

Hubbard, A., T. Bradwell, N. Golledge, A. Hall, H. Patton, D. Sugden, R. Cooper, and M. Stoker (2009). "Dynamic cycles, ice streams and their impact on the extent, chronology and deglaciation of the British–Irish ice sheet". In: *Quaternary Science Reviews* 28.7-8, pp. 758–776. DOI: 10.1016/j.quascirev.2008.12.026.

Hughes, A. L., C. D. Clark, and C. J. Jordan (2014). "Flow-pattern evolution of the last British Ice Sheet". In: *Quaternary Science Reviews* 89, pp. 148–168. DOI: 10.1016/j.quascirev.2014.02.002.

Hughes, A. L., S. L. Greenwood, and C. D. Clark (2011). "Dating constraints on the last British-Irish Ice Sheet: a map and database". In: *Journal of Maps* 7.1, pp. 156–184. DOI: 10.4113/jom.2011.1145.

Hughes, A. L., R. Gyllencreutz, Ø. S. Lohne, J. Mangerud, and J. I. Svendsen (2016). "The last Eurasian ice sheets - a chronological database and time-slice reconstruction, DATED-1". In: *Boreas* 45.1. DOI: 10.1111/bor.12142.

Iverson, N. R., T. S. Hooyer, and R. W. Baker (1998). "Ring-shear studies of till deformation: Coulomb-plastic behavior and distributed strain in glacier beds". In: *Journal of Glaciology* 44.148, pp. 634–642. DOI: 10.3189/S0022143000002136.

Jamieson, S. S. R., A. Vieli, S. J. Livingstone, C. Ó. Cofaigh, C. Stokes, C.-D. Hillenbrand, and J. A. Dowdeswell (2012). "Ice-stream stability on a reverse bed slope". In: *Nature Geoscience* 5.11, pp. 799–802. DOI: 10.1038/ngeo1600.

Joughin, I., I. M. Howat, M. Fahnestock, B. Smith, W. Krabill, R. B. Alley, H. Stern, and M. Truffer (2008). "Continued evolution of Jakobshavn Is-

brae following its rapid speedup". In: *Journal of Geophysical Research* 113.F4, F04006. DOI: 10.1029/2008JF001023.

Kamb, B. (2013). "Basal Zone of the West Antarctic Ice Streams and its Role in Lubrication of Their Rapid Motion". In: American Geophysical Union (AGU), pp. 157–199. DOI: 10.1029/AR077p0157.

Knutz, P. C., A. M. W. Newton, J. R. Hopper, M. Huuse, U. Gregersen, E. Sheldon, and K. Dybkjær (2019). "Eleven phases of Greenland Ice Sheet shelf-edge advance over the past 2.7 million years". In: *Nature Geoscience* 12.5, pp. 361–368. DOI: 10.1038/s41561-019-0340-8.

Krawczynski, M. J., M. D. Behn, S. B. Das, and I. Joughin (2009). "Constraints on the lake volume required for hydro-fracture through ice sheets". In: *Geophysical Research Letters* 36.10, p. L10501. DOI: 10.1029/2008GL036765.

Kuchar, J., G. Milne, A. Hubbard, H. Patton, S. Bradley, I. Shennan, and R. Edwards (2012). "Evaluation of a numerical model of the British-Irish ice sheet using relative sea-level data: implications for the interpretation of trimline observations". In: *Journal of Quaternary Science* 27.6, pp. 597–605. DOI: 10.1002/jqs.2552.

Kyrke-Smith, T. M., R. F. Katz, and A. C. Fowler (2013). "Subglacial hydrology and the formation of ice streams". In: *Proceedings of the Royal Society A: Mathematical, Physical and Engineering Sciences* 470.2161, pp. 20130494–20130494. DOI: 10.1098/rspa.2013.0494.

Lee, V., S. L. Cornford, and A. J. Payne (2015). "Initialization of an ice-sheet model for present-day Greenland". In: *Annals of Glaciology* 56.70, pp. 129–140. DOI: 10.3189/2015AoG70A121.

Li, Y., J. Napieralski, J. Harbor, and A. Hubbard (2007). "Identifying patterns of correspondence between modeled flow directions and field evidence: An automated flow direction analysis". In: *Computers & Geosciences* 33.2, pp. 141–150. DOI: 10.1016/J.CAGEO.2006.06.016.

Livingstone, S. J., D. H. Roberts, B. J. Davies, D. J. A. Evans, C. Ó Cofaigh, and D. M. Gheorghiu (2015). "Late Devensian deglaciation of the Tyne Gap Palaeo-Ice Stream, northern England". In: *Journal of Quaternary Science* 30.8, pp. 790–804. DOI: 10.1002/jqs.2813.

Luthi, M., M. Funk, A. Iken, S. Gogineni, and M. Truffer (2002). "Mechanisms of fast flow in Jakobshavns Isbræ, Greenland, Part III: measurements of ice deformation, temperature and cross-borehole conductivity in boreholes to the bedrock". In: *Journal of Glaciology* 48.162, pp. 369–385. DOI: 10.3189/172756502781831322.

MacGregor, J. A. et al. (2016). "A synthesis of the basal thermal state of the Greenland Ice Sheet". In: *Journal of Geophysical Research: Earth Surface* 121.7, pp. 1328–1350. DOI: 10.1002/2015JF003803.

Margold, M., C. R. Stokes, and C. D. Clark (2015a). "Ice streams in the Laurentide Ice Sheet: Identification, characteristics and comparison to modern ice sheets". In: *Earth-Science Reviews* 143, pp. 117–146. DOI: 10.1016/j.earscirev.2015.01.011.

— (2015b). "Ice streams in the Laurentide Ice Sheet: Identification, characteristics and comparison to modern ice sheets". In: *Earth-Science Reviews* 143, pp. 117–146. DOI: 10.1016/J.EARSCIREV.2015.01.011.

— (2018). "Reconciling records of ice streaming and ice margin retreat to produce a palaeogeographic reconstruction of the deglaciation of the Laurentide Ice Sheet". In: *Quaternary Science Reviews* 189, pp. 1–30. DOI: 10.1016/J.QUASCIREV.2018.03.013.

Martin, M. A., R. Winkelmann, M. Haseloff, T. Albrecht, E. Bueler, C. Khroulev, and A. Levermann (2011). "The Potsdam Parallel Ice Sheet Model (PISM-PIK) – Part 2: Dynamic equilibrium simulation of the Antarctic ice sheet". In: *The Cryosphere* 5.3, pp. 727–740. DOI: 10.5194/tc-5-727-2011.

Merritt, J. W., C. A. Auton, and C. R. Firth (1995). "Ice-proximal glaciomarine sedimentation and sea-level change in the inverness area, Scotland: A review of

the deglaciation of a major ice stream of the British Late Devensian ice sheet". In: *Quaternary Science Reviews* 14.3, pp. 289–329. DOI: 10.1016/0277-3791(95)00008-D.

Morlighem, M., H. Seroussi, E. Larour, and E. Rignot (2013). "Inversion of basal friction in Antarctica using exact and incomplete adjoints of a higher-order model". In: *J. Geophys. Res. Earth Surf* 118, pp. 1746–1753. DOI: 10.1002/jgrf.20125.

Napieralski, J., A. Hubbard, Y. Li, J. Harbor, A. P. Stroeven, J. Kleman, G. Alm, and K. N. Jansson (2007). "Towards a GIS assessment of numerical ice-sheet model performance using geomorphological data". In: *Journal of Glaciology* 53.180, pp. 71–83. DOI: 10.3189/172756507781833884.

Newton, M., D. J. Evans, D. H. Roberts, and C. R. Stokes (2018). "Bedrock mega-grooves in glaciated terrain: A review". In: *Earth-Science Reviews* 185, pp. 57–79. DOI: 10.1016/j.earscirev.2018.03.007.

Nias, I. J., S. L. Cornford, and A. J. Payne (2018). "New Mass-Conserving Bedrock Topography for Pine Island Glacier Impacts Simulated Decadal Rates of Mass Loss". In: *Geophysical Research Letters* 45.7, pp. 3173–3181. DOI: 10.1002/2017GL076493.

Nias, I. J., S. L. Cornford, and A. J. Payne (2016). "Contrasting the Modelled sensitivity of the Amundsen Sea Embayment ice streams". In: *Journal of Glaciology* 62.233, pp. 552–562. DOI: 10.1017/jog.2016.40.

Nick, F. M., C. J. Van Der Veen, A. Vieli, and D. I. Benn (2010). "A physically based calving model applied to marine outlet glaciers and implications for the glacier dynamics". In: *Journal of Glaciology* 56.199, pp. 781–794. DOI: 10.3189/002214310794457344.

Nye, J. F. (1976). "Water Flow in Glaciers: Jökulhlaups, Tunnels and Veins". In: *Journal of Glaciology* 17.76, pp. 181–207. DOI: 10.3189/S002214300001354X.

Ó Cofaigh, C. O., D. J. A. Evans, and I. R. Smith (2010a). "Large-scale reorganization and sedimentation of terrestrial ice streams during late Wisconsinan

Laurentide Ice Sheet deglaciation". In: *Geological Society of America Bulletin* 122.5-6, pp. 743–756. DOI: 10.1130/B26476.1.

Ó Cofaigh, C., S. Benetti, P. Dunlop, and X. Monteys (2016). "Arcuate moraines on the continental shelf NW of Ireland". In: *Geological Society, London, Memoirs* 46.1, pp. 253–254. DOI: 10.1144/M46.39.

Ó Cofaigh, C., D. J. A. Evans, and I. R. Smith (2010b). "Large-scale reorganization and sedimentation of terrestrial ice streams during late Wisconsinan Laurentide Ice Sheet deglaciation". In: *Geological Society of America Bulletin* 122.5-6, pp. 743–756. DOI: 10.1130/B26476.1.

O'Brien, P. E. et al. (2016). "Submarine glacial landforms on the cold East Antarctic margin". In: *Geological Society, London, Memoirs* 46.1, pp. 501–508. DOI: 10.1144/M46.172.

Patton, H., A. Hubbard, K. Andreassen, M. Winsborrow, and A. P. Stroeven (2016). "The build-up, configuration, and dynamical sensitivity of the Eurasian ice-sheet complex to Late Weichselian climatic and oceanic forcing". In: *Quaternary Science Reviews* 153, pp. 97–121. DOI: 10.1016/j.quascirev.2016.10.009.

Patton, H. et al. (2017). "Deglaciation of the Eurasian ice sheet complex". In: *Quaternary Science Reviews* 169, pp. 148–172. DOI: 10.1016/j.quascirev.2017.05.019.

Payne, A. J. (1995). "Limit cycles in the basal thermal regime of ice sheets". In: *Journal of Geophysical Research: Solid Earth* 100.B3, pp. 4249–4263. DOI: 10.1029/94JB02778.

Payne, A. J. and P. W. Dongelmans (1997). "Self-organization in the thermomechanical flow of ice sheets". In: *Journal of Geophysical Research: Solid Earth* 102.B6, pp. 12219–12233. DOI: 10.1029/97JB00513.

Peltier, W. (2004). "Global Glacial Isostasy and the Surface of the Ice-age Earth: The ICE-5G (VM2) Model and GRACE". In: *Annual Review of Earth and*

Planetary Sciences 32.1, pp. 111–149. DOI: `10.1146/annurev.earth.32.082503.144359`.

Peters, L. E., S. Anandakrishnan, R. B. Alley, J. P. Winberry, D. E. Voigt, A. M. Smith, and D. L. Morse (2006). "Subglacial sediments as a control on the onset and location of two Siple Coast ice streams, West Antarctica". In: *Journal of Geophysical Research* 111.B1, B01302. DOI: `10.1029/2005JB003766`.

Praeg, D., S. McCarron, D. Dove, C. Ó Cofaigh, G. Scott, X. Monteys, L. Facchin, R. Romeo, and P. Coxon (2015). "Ice sheet extension to the Celtic Sea shelf edge at the Last Glacial Maximum". In: *Quaternary Science Reviews* 111, pp. 107–112. DOI: `10.1016/j.quascirev.2014.12.010`.

Retzlaff, R. and C. R. Bentley (1993). "Timing of stagnation of ice stream C, West Antarctica, from short- pulse radar studies of buried surface crevasses". In: *Journal of Glaciology* 39.133, pp. 553–561. DOI: `10.1017/S0022143000016440`.

Robel, A. A. and E. Tziperman (2016). "The role of ice stream dynamics in deglaciation". In: *Journal of Geophysical Research: Earth Surface* 121.8, pp. 1540–1554. DOI: `10.1002/2016JF003937`.

Roberts, D. H., R. V. Dackombe, and G. S. P. Thomas (2007). "Palaeo-ice streaming in the central sector of the British-Irish Ice Sheet during the Last Glacial Maximum: evidence from the northern Irish Sea Basin". In: *Boreas* 36.2, pp. 115–129. DOI: `10.1111/j.1502-3885.2007.tb01186.x`.

Roberts, D. H. et al. (2018). "Ice marginal dynamics of the last British-Irish Ice Sheet in the southern North Sea: Ice limits, timing and the influence of the Dogger Bank". In: *Quaternary Science Reviews* 198, pp. 181–207. DOI: `10.1016/J.QUASCIREV.2018.08.010`.

Rysgaard, S., J. Bendtsen, J. Mortensen, and M. K. Sejr (2018). "High geothermal heat flux in close proximity to the Northeast Greenland Ice Stream". In: *Scientific Reports* 8.1, p. 1344. DOI: `10.1038/s41598-018-19244-x`.

Schoof, C. (2002). "Basal perturbations under ice streams: form drag and surface expression". In: *Journal of Glaciology* 48.162, pp. 407–416. DOI: 10.3189/172756502781831269.

— (2006). "Variational methods for glacier flow over plastic till". In: *Journal of Fluid Mechanics* 555, pp. 299–320. DOI: 10.1017/S0022112006009104.

— (2007). "Ice sheet grounding line dynamics: Steady states, stability, and hysteresis". In: *Journal of Geophysical Research* 112.F3, F03S28. DOI: 10.1029/2006JF000664.

Schoof, C. and R. C. Hindmarsh (2010). "Thin-film flows with wall slip: An asymptotic analysis of higher order glacier flow models". In: *Quarterly Journal of Mechanics and Applied Mathematics* 63.1, pp. 73–114. DOI: 10.1093/qjmam/hbp025.

Scourse, J. D., A. I. Haapaniemi, E. Colmenero-Hidalgo, V. L. Peck, I. R. Hall, W. E. Austin, P. C. Knutz, and R. Zahn (2009). "Growth, dynamics and deglaciation of the last British–Irish ice sheet: the deep-sea ice-rafted detritus record". In: *Quaternary Science Reviews* 28.27-28, pp. 3066–3084. DOI: 10.1016/J.QUASCIREV.2009.08.009.

Seguinot, J., G. Jouvet, M. Huss, M. Funk, S. Ivy-Ochs, and F. Preusser (2018). "Modelling last glacial cycle ice dynamics in the Alps". In: *The Cryosphere Discussions*, pp. 1–30. DOI: 10.5194/tc-2018-8.

Seguinot, J., I. Rogozhina, A. P. Stroeven, M. Margold, and J. Kleman (2016). "Numerical simulations of the Cordilleran ice sheet through the last glacial cycle". In: *The Cryosphere* 10.2, pp. 639–664. DOI: 10.5194/tc-10-639-2016.

Sejrup, H. P., C. D. Clark, and B. O. Hjelstuen (2016). "Rapid ice sheet retreat triggered by ice stream debuttressing: Evidence from the North Sea". In: *Geology* 44.5, pp. 355–358. DOI: 10.1130/G37652.1.

Sergienko, O. V., T. T. Creyts, and R. C. A. Hindmarsh (2014). "Similarity of organized patterns in driving and basal stresses of Antarctic and Greenland

ice sheets beneath extensive areas of basal sliding". In: *Geophysical Research Letters* 41.11, pp. 3925–3932. DOI: 10.1002/2014GL059976.

Siegert, M. J., J. Taylor, A. J. Payne, and B. Hubbard (2004). "Macro-scale bed roughness of the siple coast ice streams in West Antarctica". In: *Earth Surface Processes and Landforms* 29.13, pp. 1591–1596. DOI: 10.1002/esp.1100.

Simpson, M. J., G. A. Milne, P. Huybrechts, and A. J. Long (2009). "Calibrating a glaciological model of the Greenland ice sheet from the Last Glacial Maximum to present-day using field observations of relative sea level and ice extent". In: *Quaternary Science Reviews* 28.17-18, pp. 1631–1657. DOI: 10.1016/J. QUASCIREV.2009.03.004.

Small, D., S. Benetti, D. Dove, C. K. Ballantyne, D. Fabel, C. D. Clark, D. M. Gheorghiu, J. Newall, and S. Xu (2017). "Cosmogenic exposure age constraints on deglaciation and flow behaviour of a marine-based ice stream in western Scotland, 21–16 ka". In: *Quaternary Science Reviews* 167, pp. 30–46. DOI: 10.1016/j.quascirev.2017.04.021.

Smith, A., T. Murray, K. Nicholls, K. Makinson, G. Aðalgeirsdóttir, A. Behar, and D. Vaughan (2007). "Rapid erosion, drumlin formation, and changing hydrology beneath an Antarctic ice stream". In: *Geology* 35.2, p. 127. DOI: 10.1130/G23036A.1.

Smith, M., J. Rose, and S. Booth (2006). "Geomorphological mapping of glacial landforms from remotely sensed data: An evaluation of the principal data sources and an assessment of their quality". In: *Geomorphology* 76.1-2, pp. 148–165. DOI: 10.1016/J.GEOMORPH.2005.11.001.

Smith, M. J. and C. D. Clark (2005). "Methods for the visualization of digital elevation models for landform mapping". In: *Earth Surface Processes and Landforms* 30.7, pp. 885–900. DOI: 10.1002/esp.1210.

Spagnolo, M., C. D. Clark, J. C. Ely, C. R. Stokes, J. B. Anderson, K. Andreassen, A. G. C. Graham, and E. C. King (2014). "Size, shape and spatial arrangement

of mega-scale glacial lineations from a large and diverse dataset". In: *Earth Surface Processes and Landforms* 39.11, n/a–n/a. DOI: 10.1002/esp.3532.

Stewart, M. A. (2016). "Assemblage of buried and seabed tunnel valleys in the central North Sea: from morphology to ice-sheet dynamics". In: *Geological Society, London, Memoirs* 46.1, pp. 317–320. DOI: 10.1144/M46.140.

Stoker, M. S. and T. Bradwell (2005). "The Minch palaeo-ice stream, NW sector of the British–Irish Ice Sheet". In: *Journal of the Geological Society* 162.3, pp. 425–428. DOI: 10.1144/0016-764904-151.

Stokes, C. R. and C. D. Clark (1999). "Geomorphological criteria for identifying Pleistocene ice streams". In: *Annals of Glaciology* 28, pp. 67–74. DOI: 10.3189/172756499781821625.

Stokes, C. R., C. D. Clark, and R. Storrar (2009). "Major changes in ice stream dynamics during deglaciation of the north-western margin of the Laurentide Ice Sheet". In: *Quaternary Science Reviews* 28.7-8, pp. 721–738. DOI: 10.1016/J.QUASCIREV.2008.07.019.

Stokes, C. R., M. Margold, and T. T. Creyts (2016). "Ribbed bedforms on palaeo-ice stream beds resemble regular patterns of basal shear stress ('traction ribs') inferred from modern ice streams". In: *Journal of Glaciology* 62.234, pp. 696–713. DOI: 10.1017/jog.2016.63.

Tsai, V. C., A. L. Stewart, and A. F. Thompson (2015). "Marine ice-sheet profiles and stability under Coulomb basal conditions". In: *Journal of Glaciology* 61.226, pp. 205–215. DOI: 10.3189/2015JoG14J221.

Van Pelt, W. J. and J. Oerlemans (2012). "Numerical simulations of cyclic behaviour in the Parallel Ice Sheet Model (PISM)". In: *Journal of Glaciology* 58.208, pp. 347–360. DOI: 10.3189/2012JoG11J217.

Vaughan, D. G. and R. Arthern (2007). "CLIMATE CHANGE: Why Is It Hard to Predict the Future of Ice Sheets?" In: *Science* 315.5818, pp. 1503–1504. DOI: 10.1126/science.1141111.

Veen, C. J. van der (1999). "Evaluating the performance of cryospheric models". In: *Polar Geography* 23.2, pp. 83–96. DOI: 10.1080/10889379909377667.

Vorren, T. O. and J. S. Laberg (1997). "Trough mouth fans — palaeoclimate and ice-sheet monitors". In: *Quaternary Science Reviews* 16.8, pp. 865–881. DOI: 10.1016/S0277-3791(97)00003-6.

Waibel, M. S. (2017). "A Numerical Model Investigation of the Role of the Glacier Bed in Regulating Grounding Line Retreat of Thwaites Glacier, West Antarctica". PhD thesis.

Weertman, J. (1957). "On the Sliding of Glaciers". In: *Journal of Glaciology* 3.21, pp. 33–38. DOI: 10.3189/S0022143000024709.

Winsborrow, M. C., C. D. Clark, and C. R. Stokes (2010). "What controls the location of ice streams?" In: *Earth-Science Reviews* 103.1-2, pp. 45–59. DOI: 10.1016/j.earscirev.2010.07.003.

Zwally, H. J., W. Abdalati, T. Herring, K. Larson, J. Saba, and K. Steffen (2002). "Surface melt-induced acceleration of Greenland ice-sheet flow". In: *Science* 297.5579, pp. 218–222. DOI: 10.1126/science.1072708.

Chapter 4

Saddle collapse of the Eurasian Ice Sheet in the North Sea caused by combined ice flow, surface melt, and marine ice sheet instabilities

Abstract

The North Sea sector of the Eurasian ice sheet formed the confluence between the British-Irish Ice Sheet and the Fennoscandian Ice Sheet. The expected complex glacial history, and relevance to the deglaciation of two palaeo ice sheets, has motivated significant reconstruction work. Despite this growing empirical evidence, the pattern of deglaciation of the North Sea sector of the Eurasian ice sheet remains unresolved, and previous numerical simulations of the deglaciation of the North Sea have struggled to capture the confluence and separation of the British-Irish and Fennoscandian Ice Sheets. We ran an ensemble of 70 experiments simulating the deglaciation of the North Sea between 23-18 ka BP using

the BISICLES ice sheet model. We used a suite of novel quantitative model-data comparison tools to identify plausible simulations of deglaciation that match empirical data for ice flow, margin position, and retreat ages, allowing comparisons to large amounts of empirical data. In ensemble members that best match the empirical data, the North Sea deglaciates through the collapse of the marine-based Norwegian Channel Ice Stream, unzipping the confluence between the British-Irish Ice Sheet and the Fennoscandian Ice Sheet. Thinning of the Norwegian Channel Ice Stream causes surface temperature feedbacks, rapid grounding line retreat, and ice stream acceleration, further driving separation of the British-Irish and the Fennoscandian Ice Sheets through the saddle collapse mechanism. These simulations are the first of the North Sea deglaciation that respect the majority of empirical evidence, and therefore provide considerable insights into the deglaciation style of the North Sea sector.

4.1   Introduction

At the Last Glacial Maximum (LGM) the North Sea sector of the Eurasian Ice Sheet was at the confluence of two ice sheets, the British-Irish Ice Sheet (BIIS) to the west, and the Fennoscandian Ice Sheet to the east. Broadly, the North Sea sector was a shallow marine basin, topographically dominated by the Norwegian Channel, a deep ($\sim$200-600 m) trough on the western Norwegian coast (Figure 4.1). The North Sea sector is an important part of the palaeo ice sheet record for a number of reasons, with marine, lacustrine, and terrestrial margins. The northern marine margin may have been vulnerable to the same marine processes that are in effect in contemporary West Antarctica (Shepherd et al., 2001; Favier et al., 2014; Joughin et al., 2014). These marine processes allow instabilities of retreat, which represent the largest source of uncertainty for future sea level projections, so understanding the deglaciation of marine ice sheet sectors is a key challenge of glaciology. Ice sheet evolution over the North Sea basin is also important in understanding the Relative Sea Level (RSL) change of the basin

since the last deglaciation (Bradley et al., 2011), and the history of glaciation is a key cause of the complicated stratigraphy that needs to be understood to plan the deep foundations required for wind turbine developments in the North Sea (Emery et al., 2019). All considered, the requirement to better understand the deglaciation of the North Sea sector of the Eurasian Ice Sheet has motivated significant prior empirical and modelling work (e.g. Boulton and Hagdorn, 2006; Dove et al., 2017; Patton et al., 2017; Roberts et al., 2018).
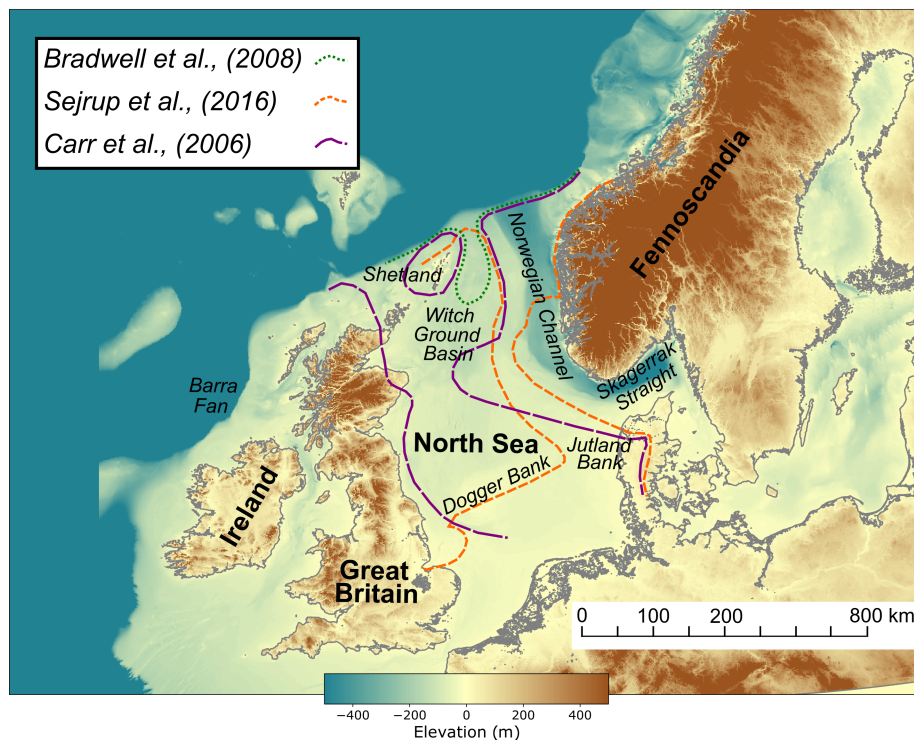
Figure 4.1: The bathymetry of the North Sea. Locations mentioned in the text are marked. Approximate margins at the initiation ice sheet separation from Bradwell et al. (2008), Carr et al. (2006), and Sejrup et al. (2016) are shown.

Despite this importance, the deglaciation dynamics of the North Sea sector remain poorly understood (Phillips et al., 2017). Indeed, Hughes et al. (2016) suggests that the North Sea, along with the eastern Barents-Kara Sea, are the "most ambiguous sectors" of the Eurasian Ice Sheet. The marine nature of the catchment makes empirical work challenging, and studies of the controls of retreat are limited (e.g. Cotterill et al., 2017; Dove et al., 2017; Phillips et al., 2018; Roberts et al., 2018; Emery et al., 2019). Based on the limited marine evidence,

20th century reconstructions of the BIIS and Fennoscandian Ice Sheet did not suggest ice sheet confluence in the North Sea (Boulton et al., 1985). However, more extensive offshore work in the 1990s and 2000s revealed glacial sediments in shallow marine cores, and extended seismic surveys across the North Sea (Sejrup et al., 1994; Graham et al., 2007), suggesting confluence between the two ice sheets. Improved bathymetric data also helped to map ice sheet flow and margin features in the North Sea (Bradwell et al., 2008; Sejrup et al., 2016).

Extensive confluence between the BIIS and Fennoscandian Ice Sheet is now accepted (Sejrup et al., 1994; Graham et al., 2007), but the mechanism and timing of the subsequent separation of the ice sheets is unclear. For example, using evidence from high resolution geomorphological mapping Sejrup et al. (2016) suggested the deglaciation of the North Sea was triggered by the retreat of the large Norwegian Channel Ice Stream (NCIS), leading to the debuttressing of adjacent ice, and an "unzipping" of the BIIS and Fennoscandian Ice Sheet originating from the Norwegian Channel. However, other studies (Carr et al., 2006; Bradwell et al., 2008) suggest the initial separation of the two ice sheets occurred to the west of the Norwegian Channel, initially retreating back into the deeper bathymetry of the Witch Ground Basin, forming a calving bay (Figure 4.1). The NCIS remained fully advanced to the continental shelf edge while areas of the North Sea deglaciated. This is unusual because it is expected that the NCIS will have been more vulnerable to retreat from marine and climate forcing than the neighbouring inter-ice stream margin.

A reconstruction of deglaciation based on the DATED-1 database followed the reconstructed Bradwell et al. (2008) calving bay, suggesting the initial ice sheet separation was to the west of the Norwegian Channel (Hughes et al., 2016). In this reconstruction, a large embayment in the north of the North Sea sector developed, while confluence between the BIIS and Fennoscandian Ice Sheets remained in the south of the North Sea, and the NCIS remained extended to the trough mouth. However, the sparsity of dates in the North Sea means that these reconstructions

are tentative (Hughes et al., 2016). For example, there is conflicting evidence of the timing of retreat of the NCIS (Sejrup et al., 1994; King et al., 1998; Svendsen et al., 2015) Additionally, the formation of a large embayment in the north of the North Sea while the NCIS remained extended and active is enigmatic, and potentially glaciologically implausible (Clark et al., 2012; Hughes et al., 2016), as there is no contemporary analogue for an ice stream laterally unbounded along one flank. Ultimately, although empirical constraints on the deglaciation of the North Sea have improved, considerable uncertainty remains both in the point of initial separation of the BIIS and Fennoscandian Ice Sheets (Bradwell et al., 2008; Sejrup et al., 2016), and subsequent evolution of ice retreat in the southern North Sea (Dove et al., 2017; Roberts et al., 2018).

Numerical modelling has not resolved the uncertain deglaciation dynamics of the North Sea either. Boulton and Hagdorn (2006) simulated the confluence of the BIIS and the Fennoscandian Ice Sheet, and found that due to a diminished ablation area after initial confluence the ice sheet thickness increases rapidly to form an ice divide running east-west across the North Sea. This has implications for ice flow, meaning it is unlikely the NCIS flowed the ∼700 km length of the Norwegian Channel concurrently. This numerical modelling work helped address some uncertainties regarding the confluence of the BIIS and Fennoscandian Ice Sheets, but does not simulate the subsequent deglaciation of the North Sea sector. These shallow ice approximation simulations did not account for key processes of ice streaming (Hindmarsh, 2009) or grounding line migration (Schoof, 2007), likely to have been important to the deglaciation of the North Sea.

More recently, an ensemble of simulations investigated the advance (Patton et al., 2016) and retreat (Patton et al., 2017) of the Eurasian Ice Sheet. This simulation has the BIIS and Fennoscandian Ice Sheets splitting in the North Sea shortly after 22.4 ka BP, followed by a broadly radial retreat of the BIIS in the North Sea. The simulation of the entire ice sheet is a good match for empirical data in many sectors, but there is a mismatch in the North Sea sector. For

example, the simulated NCIS was ∼400 km short of the continental shelf edge at maximum extent, in contrast to empirical evidence showing it reached the trough mouth (Sejrup et al., 1994; King et al., 1998; Nygård et al., 2005). Also, the maximum extent of confluence of the two ice sheets is "weak", in that an ice divide does not form in the North Sea, and ice extent is limited in the north of the basin, contrary to empirical evidence (King et al., 1998; Bradwell et al., 2008). However, ensemble members presented in Patton et al. (2016, 2017) are unable to simulate North Sea deglaciation if the maximum extent is consistent with empirical evidence of full glaciation. Therefore, up until now there have been no simulations of the North Sea deglaciation that are broadly consistent with empirical evidence. We hypothesise that this is because of the limitations of ice flow physics previously used, either shallow ice approximation (Boulton and Hagdorn, 2006), or a Blatter-Pattyn model (Pollard and DeConto, 2012; Patton et al., 2016, 2017).

Recent advances in ice sheet modelling permit new simulations of the North Sea deglaciation. In particular, the BISICLES ice sheet model's higher-order physics and adaptive mesh allow the accurate simulation of marine sectors of ice sheets (Cornford et al., 2013), such as the North Sea. A new basal sliding scheme coupled with a hydrology parameterisation also allows the simulation of spontaneous ice stream generation and evolution during ice advance and retreat, with good match to empirical evidence (Gandy et al., 2019). This means that two important controls on the North Sea deglaciation - marine dynamics and the influence of the NCIS - can now be accurately simulated for the first time.

Here, we present an ensemble of simulations of the deglaciation of the North Sea, using the state of the art BISICLES ice sheet model. We aim to simulate deglaciation in a manner that respects the majority of empirical evidence, and through this determine the likely mechanisms and style of deglaciation of the North Sea. Two research questions, motivated by the considerable uncertainty of deglaciation style in the North Sea, frame the analysis of the work;

1. What was the role of the Norwegian Channel Ice Stream in the deglaciation of the North Sea?

2. How do ice stream dynamics interact with other mechanisms driving deglaciation of the North Sea?

4.2   Methods

4.2.1   Ice Sheet Model

We use the BISICLES marine ice sheet model to simulate the North Sea sector of the Eurasian Ice Sheet. BISICLES is a higher-order ice sheet model with L1L2 physics simplified from the full Stokes flow equations (Schoof and Hindmarsh, 2010), using an adaptive mesh to allow the horizontal resolution to be increased at the grounding line, at the margin, and at regions of high velocity (Cornford et al., 2013). This means BISICLES can simulate grounding line migration without parameterisation, unlike models previously used to simulate the deglaciation of the North Sea (Patton et al., 2017). BISICLES has previously been successfully used to simulate the evolution of contemporary (Favier et al., 2014; Cornford et al., 2016; Gong et al., 2017) and palaeo (Gandy et al., 2018, 2019, Matero et al., in prep) ice sheets. We set-up BISICLES in a manner similar to Gandy et al. (2019), in that an idealised basal hydrology scheme is coupled to a Coulomb sliding law dependent on ice and basal water pressure, in order to simulate regions of ice streaming. This method has successfully simulated the majority of ice streams of the BIIS during advance and retreat of the ice sheet (Gandy et al., 2019). For the majority of experiments we set a 16 km × 16 km grid refined once in the North Sea sector to produce a horizontal resolution of 8 km × 8 km, except in the high resolution experiments subsequently described, which have a maximum horizontal resolution of 1 km × 1 km.

4.2.2 Spin-up

The spin-up is split into three stages; a build-up step, an advance step, and an ice dynamics perturbation step, all summarised in Table 4.1. The full domain extent is in Figure 4.1, and the build-up step starts with no ice cover. Two independent ice sheets covering the northern British Isles and Fennoscandia are grown using a SMB mask for 10,000 years, in a manner similar to Gandy et al. (2019). The basal hydrology and sliding law coupling is introduced at 5,000 years into the spin-up step to preserve computer time during the initial build-up of the ice dome.

The advance step is initiated from the end of the build-up step. The advance step grows the ice sheet to maximum extent, with confluence between the BIIS and Fennoscandian Ice Sheets in the North Sea. During the advance phase the SMB is defined as;

$$smb = \begin{cases} 0.3, & h>500 \\ 0.0, & h \leq 500 \\ -2.0, & h = 0.0 \end{cases} \qquad (4.1)$$

where smb is the annual SMB (m), and h is the surface elevation of the ice (m). This forcing eventually causes the ice sheet to be too extensive in the southern North Sea, where the bathymetry, meltwater routing, and river routing means it is possible a large proglacial lake formed (Sejrup et al., 2016). Smaller proglacial lakes of the southern North Sea have been mapped based on shallow seismic reflection data (Emery et al., 2019). A large proglacial lake of the southern North Sea has been suggested for several glacial cycles (Belt, 1874; Gibbard et al., 1988; Ehlers and Gibbard, 2004; Clark et al., 2012; Murton and Murton, 2012; Cohen et al., 2014; Sejrup et al., 2016; Roberts et al., 2018), but the exact size and location is not known. Currently, BISICLES cannot simulate the formation, evolution, or effects of proglacial lakes, so a region of negative SMB forcing is imposed in the southern North Sea to correct this margin (Figure A.5), allowing

a margin in the southern North Sea which is broadly consistent with empirical evidence (Dove et al., 2017; Roberts et al., 2018). The advance step runs for 9,000 model years, by which point there is confluence between the BIIS and the Fennoscandian Ice Sheet, forming an ice divide across the North Sea.

Reference	Start point	Length (yr)	SMB	Parameter Variation
BUILD-UP	N/A	10,000	Masked (Figure 4.3b)	N/A
ADVANCE	BUILD-UP end	9,000	0.3 m/y (>500 m a.s.l), or 0.0 m/y	N/A
ns_xxx_dynamics	ADVANCE end	1,000	0.3 m/y (>500 m a.s.l), or 0.0 m/y	70 ensemble member varying Coulomb friction angle, Weertman friction coefficient, and maximum till water depth
ns_xxx	ns_xxx_dynamics end	5,000	PyPDD	As above plus variation in PDD factors, sub-shelf melt, lapse rate, and precipitation

Table 4.1: Summary of the experiment set-up.

The final stage of the spin-up is a 1,000 year ice dynamics perturbation step. 70 ensemble members are initiated from the end of the advance step. Each ensemble member has 7 key parameters varied (Table 4.2), sampled using a maximin Latin Hypercube sampling technique, previously used to sample ice sheet model ensembles (e.g. Stone et al., 2010; Gregoire et al., 2016; Nias et al., 2016). Parameter values were sampled within uniform distributions of ranges shown in Table 4.2. This ensemble technique allows for the parameter space to be explored, and a variety of deglaciation behaviours to be simulated. In this ice dynamics perturbation step, however, only ice dynamics parameters are varied (f in the Coulomb sliding law, C in the Weertman sliding law, and the maximum till water depth). These parameters are varied before the deglaciation step to allow for the ice velocity to adjust to the change in sliding parameters. During this step the ice sheet extent continues to advance. At the end of this final spin-up step, all ensemble members have a confluence between the two ice sheets and an ice divide in the North Sea, and the majority (43/70) have the NCIS fully extended to the Norwegian Channel trough mouth as suggested by empirical data (Sejrup et al., 1994; King et al., 1998).

4.2.3 Deglaciation ensemble

The end of the spin-up step produces 70 ensemble members in good agreement with ice extent reconstructed for 23 ka BP (Roberts et al., 2018; Bradwell et al., 2019). Each ensemble member is then run for a 5,000 year deglaciation phase, where all 7 parameters are varied (Table 4.2). SMB is calculated every 25 years using the PyPDD model (Seguinot, 2013), forced using contemporary surface temperature and precipitation data (Fick and Hijmans, 2017) corrected with the anomaly from climate simulation snapshots of the deglaciation (Figure 4.2). The snapshot simulations are described by Morris et al. (2018), run with the HadCM3 coupled atmosphere-ocean-vegetation general circulation model (Gordon et al., 2000; Pope et al., 2000; Valdes et al., 2017), and are a refinement of those previously reported by Singarayer et al. (2011) with updated boundary conditions including ice mask, ice orography, bathymetry, and land–sea mask (Ivanovic et al., 2016). An east-west precipitation gradient is also imposed using the same pattern as used in Patton et al. (2016, 2017), to consider the influence of the Eurasian Ice Sheet on precipitation patterns. The modelled ice sheet surface is used to correct surface air temperatures every 25 years through the deglaciation. Sub-shelf melt rate is derived from Sea Surface Temperature (SST) values from the same simulations used to calculate SMB, using a linear relationship between SST (T) and sub-shelf melt rate (ssm) (Rignot and Jacobs, 2002).

$$ssm = -10T \tag{4.2}$$

To recreate isostatically adjusted bed topography, we adjust modern topography using reconstructions from a Glacio-Isostatic Adjustment (GIA) model (Bradley et al., in prep). GEBCO (Becker et al., 2009) provides modern offshore bathymetry, and SRTM (Farr et al., 2007) provides onshore topography. The Relative Sea Level (RSL) change is updated every 1,000 years, and topography is linearly interpolated between these points.
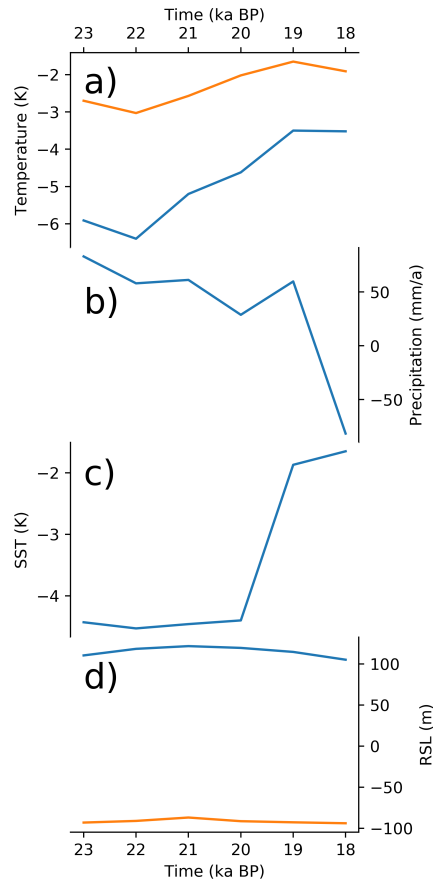
Figure 4.2: Forcing for the deglaciation simulations. a) June (orange) and December (blue) surface temperature anomaly for 23-18 ka BP, averaged across the domain (Figure 1), b) Precipitation anomaly, averaged across the domain, c) Sea Surface Temperature anomaly for 23-18 ka BP, d) Relative Sea Level for the Forth Valley (blue) and Hampshire (orange).

Not.	Parameter	Standard Value	Unit	Ensemble Minimum	Ensemble Maximum
C	Weertman Coefficient	1,000	Pa m^{-1} a^{-1}	500	2,000
f	Coulomb friction coefficient	0.5	-	0.4	0.6
W_0	Maximum till water depth	2.0	m	2.0	5.0
-	PDD factors	3.0 (snow) and 8.0 (ice)	mm K^{-1} d^{-1}	Standard - 2.0	Standard + 2.0
ssm	Sub-shelf melt	-	m/y/K	Melt rate -50.0	Melt rate + 150.0
-	Lapse rate	5.1	km^{-1}	4.5	8.0
-	Precipitation	From HadCM3 experiments	mm/y	25% f standard	175% f standard
ρ	Ice density	918	kg m^{-3}	-	-
g	Acceleration due to gravity	9.81	m s^{-2}	-	-
m	Weertman exponent	1	-	-	-
α	Till pressure factor	0.99	-	-	-
D	Till water drain factor	0.005	m/y	-	-

Table 4.2: Key parameter values and range of values used for the simulations. Only the first seven parameters (Weertman Coefficient-Precipitation) are varied in the deglaciation ensemble.

4.2.4 Model-data comparison

In order to determine which of the 70 ensemble members simulate behaviour consistent with the available empirical data, we use new quantitative model-data comparison tools (Ely et al., 2019b). Model-data comparison tools are used to identify a subset of Not Ruled Out Yet (NROY) ensemble members, which match the majority of empirical data. The Automated Proximity and Conformity Analysis (APCA) tool (Li et al., 2007; Napieralski et al., 2007) is used to compare modelled ice sheet margins and empirically mapped moraines. A subset of 132 moraines larger than 32 km long is used (Sejrup et al., 2016; Dove et al., 2017; Clark et al., 2018). A model-data match is defined when both the proximity is below a threshold of 10 km, and conformity is below a threshold of 4 km.

The Automated Timing Accordance Tool (ATAT) (Ely et al., 2019a) is used to identify matches between modelled deglaciation ages and geochronological data. Geochronological dates rated as Green or Amber by Small et al. (2017) were used, resulting in 110 geochronological dates for comparison with modelled deglaciation ages. ATAT calculates the spatially weighted Root Mean Square Error (wRMSE) between modelled deglaciation ages and geochronological data, accounting for the uneven spatial distribution of dates. ATAT also calculates the percentage of ice-free dates agreed within error, which is used to rank the ensemble members.

The Automated Flow Direction Analysis (AFDA) tool (Li et al., 2007) is used to identify matches between mapped flowsets and modelled flow direction. Flowsets larger than 256 km^2 (4 grid boxes at model resolution) are taken from Greenwood and Clark (2009b) and Hughes et al. (2014), resulting in 83 flowsets for comparison with the modelled flow directions. AFDA calculates the mean residual angle and variance of offset between modelled and empirically-derived flow directions. A model-data match is when both the mean residual vector within a flowset is below a threshold of 10°, and the mean variance is below a threshold of 0.03, as used in other studies (Napieralski et al., 2007; Ely et al.,

2019b). Simulations that matched more than 50% of the empirical data in all three comparison tools form the subset of NROY simulations.

4.3 Results

In this section, we first describe the general behaviour of the simulations in the deglaciation ensemble, then compare these results to the empirical data, and finally describe the results from high-resolution experiments of rapid NCIS retreat.

4.3.1 Ensemble results

The ice advance starts with separate ice sheets covering the BIIS and Fennoscandian Ice Sheet (Figure 4.3a,b). After 6,000 years of advance, there is confluence between the BIIS and the Fennoscandian Ice Sheet. The initial confluence occurs north of Dogger Bank, while the NCIS is already significantly advanced in the Norwegian Channel. The straight southern margin in the North Sea is caused by the SMB anomaly imposed to act as a proxy for the effects of a large proglacial lake.

In the deglaciation ensemble, the majority of ensemble members (59/70) simulate the separation of the BIIS and Fennoscandian Ice Sheets. In those simulations the final separation of the BIIS and the Fennoscandian Ice Sheet occurs in the southern North Sea, near the Jutland Bank (Figure 4.1). All 59 simulations that have ice sheet separation had a common deglaciation pattern. Beginning with full confluence of the BIIS and Fennoscandian Ice Sheet (Figure 4.4a-b), there is an initial retreat of the NCIS, with ice remaining to the east and west of the Norwegian Channel. As the grounding line of the NCIS continues to retreat in the Norwegian Channel, there is limited margin retreat to the west in the North Sea. In all simulations, ice cover remains on the Shetland Islands while the NCIS has considerably retreated (Figure 4.4e-h).
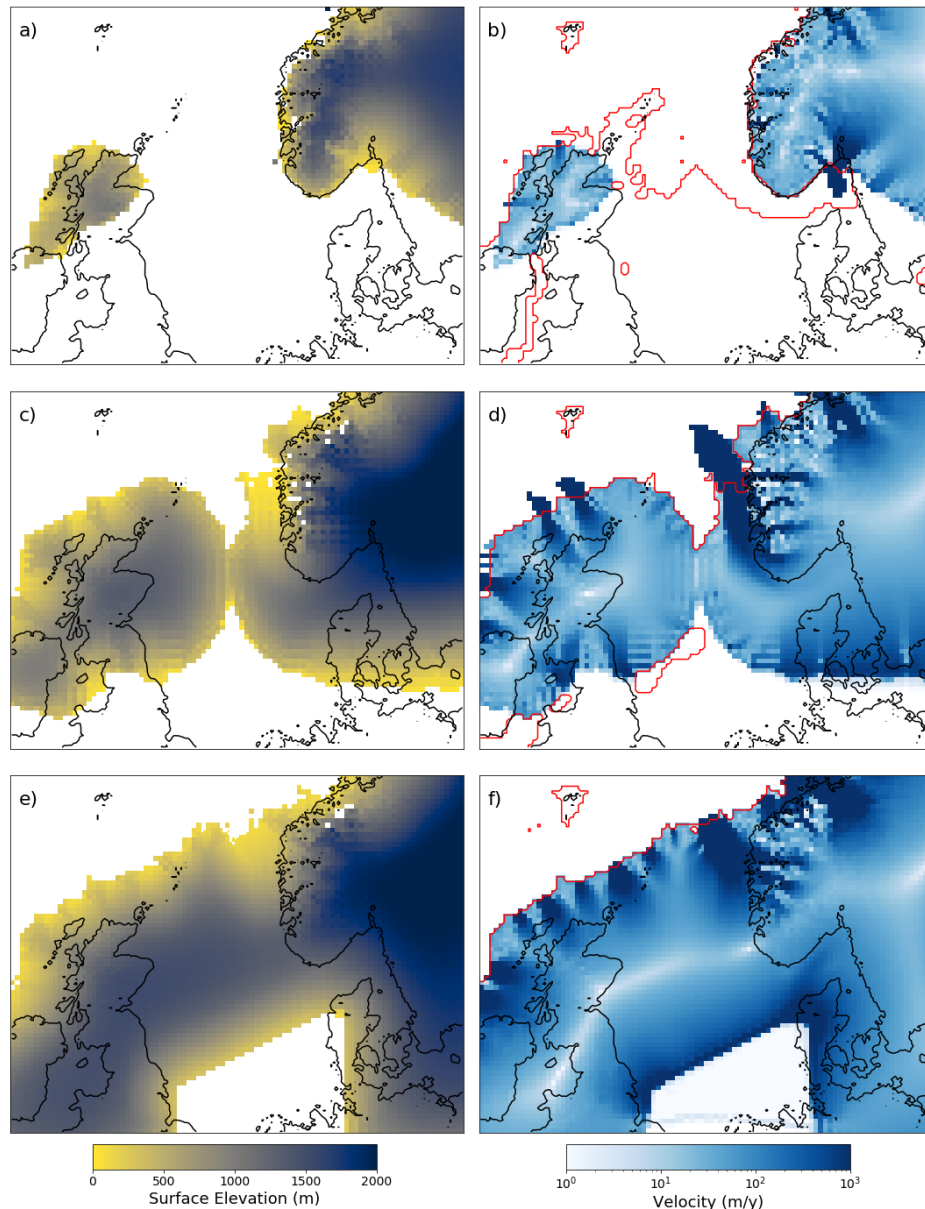
Figure 4.3: Snapshots at various stages during the spin-up stages of the experiments. a-b) Ice surface elevation and velocity (respectively) at the end of the build-up stage. c-d) Ice thickness and velocity during the advance stage, just after initial confluence between the BIIS and the Fennoscandian Ice Sheet, 6,000 years into the advance stage. e-f) Ice thickness and velocity at the end of the ice dynamics perturbation phase for *ns_034*.

In the majority of ensemble members, considerable NCIS retreat is concurrent with retreat of the western portion of the BIIS, resulting in limited ice cover in Ireland and a retreat of the Barra Fan Ice Stream (Figure 4.4g-j). Margin retreat in the southern North Sea and the Fennoscandian Ice Sheet is limited. This deglaciation pattern results in a narrow ice cap forming north of the Dogger
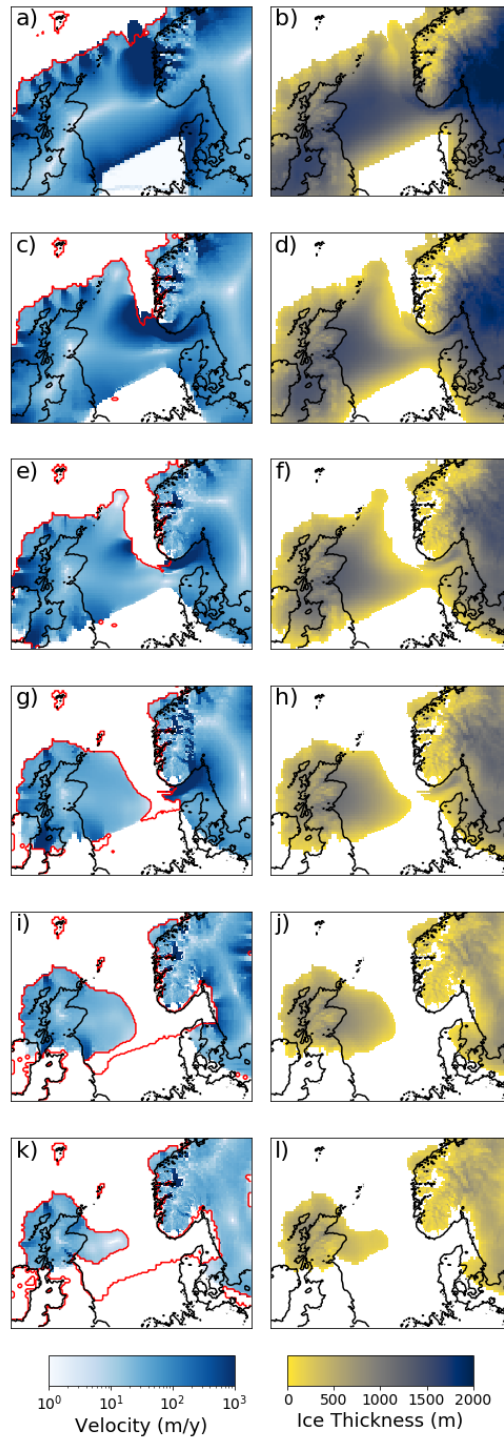
Figure 4.4: Pattern of North Sea deglaciation in one of the ensemble members ns_016 (from the identified NROY simulations). ns_016 is representative of the NROY simulations generally. The red contour shows the grounding line and palaeo coastline.

Bank (Figure 4.4k-l). This narrow cap is slow flowing and entirely recedes within 1,000 years of formation.

The point of separation between the BIIS and the Fennoscandian Ice Sheet is near the Jutland Bank and is consistent across the 59 ensemble members in which the separation occurs. The legacy of this separation style is that the modelled BIIS ice is often extensive in the North Sea, while significant deglaciation of the western margin of the BIIS has already occurred. This is consistent with the deglaciation pattern reconstructed along the Yorkshire and Lincolnshire coast (Clark et al., 2012; Bateman et al., 2015), and the required damming of proglacial lakes like Glacial Lake Pickering (Evans et al., 2017), explained through a North Sea Lobe feature (Bateman et al., 2015). The deglaciation style in the majority of ensemble members causes a Dogger Bank ice dome (Figure 4.4g-l). Ice streaming down the Yorkshire and Lincolnshire coast occurs in the majority (64/70) of simulations, and in 22 simulations this ice stream terminates with a lobate margin.

A simulated Dogger Bank ice dome still covers a large portion of the North Sea in the later stages of deglaciation (Figure 4.4g-l), and therefore ice often remained north of the Dogger Bank for 1-2 ka. By the end of the deglaciation simulation (at 18ka BP), the North Sea is fully deglaciated in 11.9% of the simulations, there is no British Isles ice cover in 7% of simulations, a small Scottish Ice Cap in 12.6% of simulations, and Fennoscandian ice cover in all simulations.

4.3.2 Model-data comparison

As expected, the qualitative model-data comparison tools show considerable variations in scores of model-data match, examples of model-data match are shown in Figure 4.5. The Automated Proximity and Conformity Analysis (APCA) tool calculates that for the 70 ensemble members on average 46.5% of moraines are matched, with the poorest matching ensemble member matching 24.6% of moraines, and a best matching ensemble member matching 67.7% of moraines. Of the entire ensemble, 36 simulations matched more than 50% of moraines.

The Automated Timing Accordance Tool (ATAT) provides a value of both the percentage of dates where model-data agreement occurs, and the wRMSE of
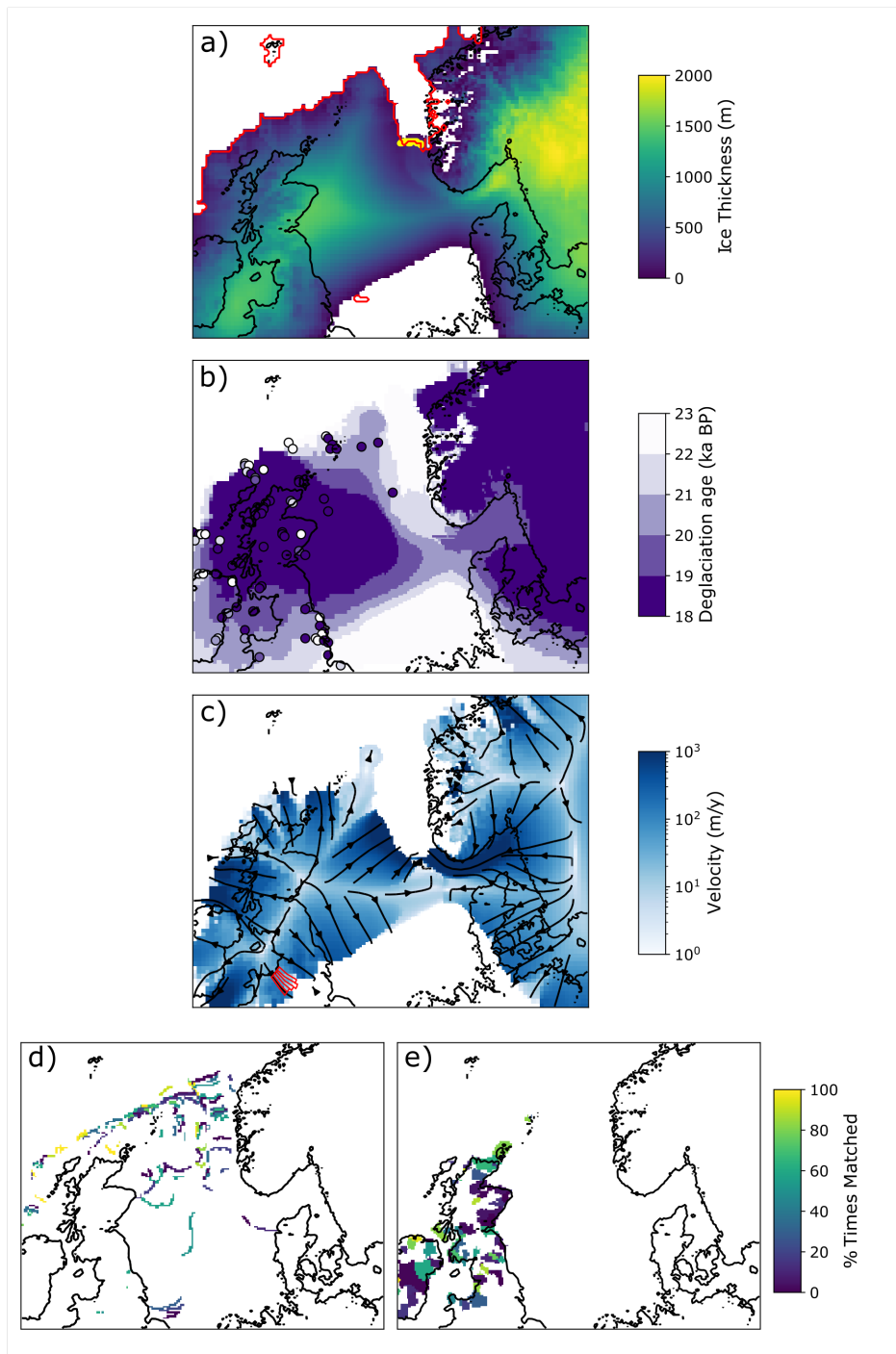
Figure 4.5: Qualitative comparison of selected model results and empirical data which are quantitatively compared using APCA, ATAT and AFDA. a) A snapshot of ice thickness during the deglaciation. A point of grounding line (red contour) and moraine (yellow) match is shown, for ensemble member ns_031, at 22500 ka BP. b) Modelled deglaciation age of ensemble member ns_016, with deglaciation ages shown in points of the same colour map. c) Ice flow velocity and direction of ensemble member ns_031 at 21750 ka BP, with an empirically mapped flowset shown in red. d) The percentage of ensemble members that match each moraine. e) The percentage of ensemble members that match each mapped flowset.
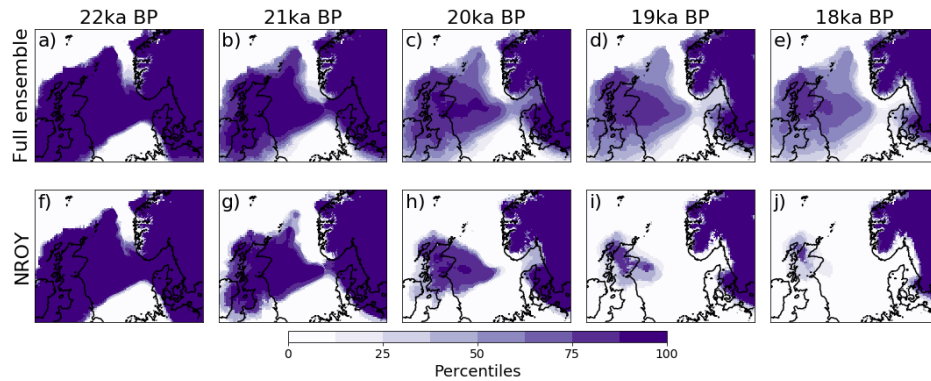
Figure 4.6: The percentage of ensemble members (top row) and NROY simulations (bottom row) with ice cover through the deglaciation experiment.

model-data difference for ice-covered dates where model-data agreement occurs. The wRMSE values are important because it is possible to "match" a high percentage of deglaciation ages, but have a high error on each age. The wRMSE values calculated here are low compared to uncertainties in the empirical data, with a mean wRMSE of 813 years (and a maximum of 1023 years). In comparison, the errors on a Terrestrial Cosmogenic Nuclide (TCN) date is in the order of 800 years (Small et al., 2017). On average, each ensemble member matches 52.7% of dates, with the poorest matching ensemble member matching 16.7% of dates, and the best matching ensemble member matching 74.5% of dates. The poorest matching ensemble members do not deglaciate sufficiently, resulting in the majority of geochronological dates remaining ice covered at the end of the simulation. Sporadic early deglaciation ages in central Scotland are never matched while also matching the majority of later (post-18 ka BP) deglaciation ages (Figure 4.5b). Of the entire ensemble, 44 simulations matched more than 50% of the deglaciation ages.

Finally, the Automated Flow Direction Analysis (AFDA) tool provides a percentage match between empirically mapped flowsets and modelled flow directions. This is the most stringent of the three quantitative tests because flow direction depends on a number of uncertain controls, such as the ice sheet thermal structure, the ice margins, evolution history, and the palaeo topography. The average match over the ensemble is 33.5% of mapped flowsets, with the poorest ensem-

ble member matching 10.8% of flowsets, and the best scoring ensemble member matching 59% of flowsets. Of the entire ensemble, 11 simulations matched more than 50% of flowsets. Each of these 11 simulations matched more than 50% of margins and deglaciation ages too, meaning that these 11 simulations form the NROY subset of simulations (Figure 4.6). The 50% threshold is chosen because a quantitative match to the empirical data is a stringent test, and are the result of trial and error changes to the threshold. For example, although the simulated margin behaviour in the Norwegian Channel is visually consistent with empirical reconstructions, moraines in the Norwegian Channel are matched <50% of the time. Simulated ice stream positions also are a good match for empirical ice stream reconstructions (Gandy et al., 2019), but individual smaller flowsets (Greenwood and Clark, 2009a; Hughes et al., 2014) are rarely matched. A minority of deglaciation ages in Scotland are also ~5 ka earlier than surrounding ages, requiring unusual margin positions it is unlikely models will represent (Clark et al., 2012).

4.3.3 High-resolution snapshot results

The 70 ensemble members run at 8 km resolution, and can provide evidence of periods of rapid retreat of the North Sea sector. However, for grounding line dynamics to be accurately simulated the horizontal resolution at the grounding line must be 1 km or finer (Gladstone et al., 2012). One ensemble member from the NROY simulations (*ns_016*) has two periods of rapid grounding line retreat of the NCIS, behaviour which is also represented in the other NROY simulations. We re-simulate these two periods of rapid retreat using 1 km horizontal resolution at the grounding line to better capture the dynamics of the rapid retreat. Other than the higher horizontal resolution, the experimental design is identical to the design of the coarser resolution ensemble members.

The simulations are re-run from 21900 and 20600 ka BP, for 320 years and 240 years respectively. The model mesh is refined down to 1 km at the grounding
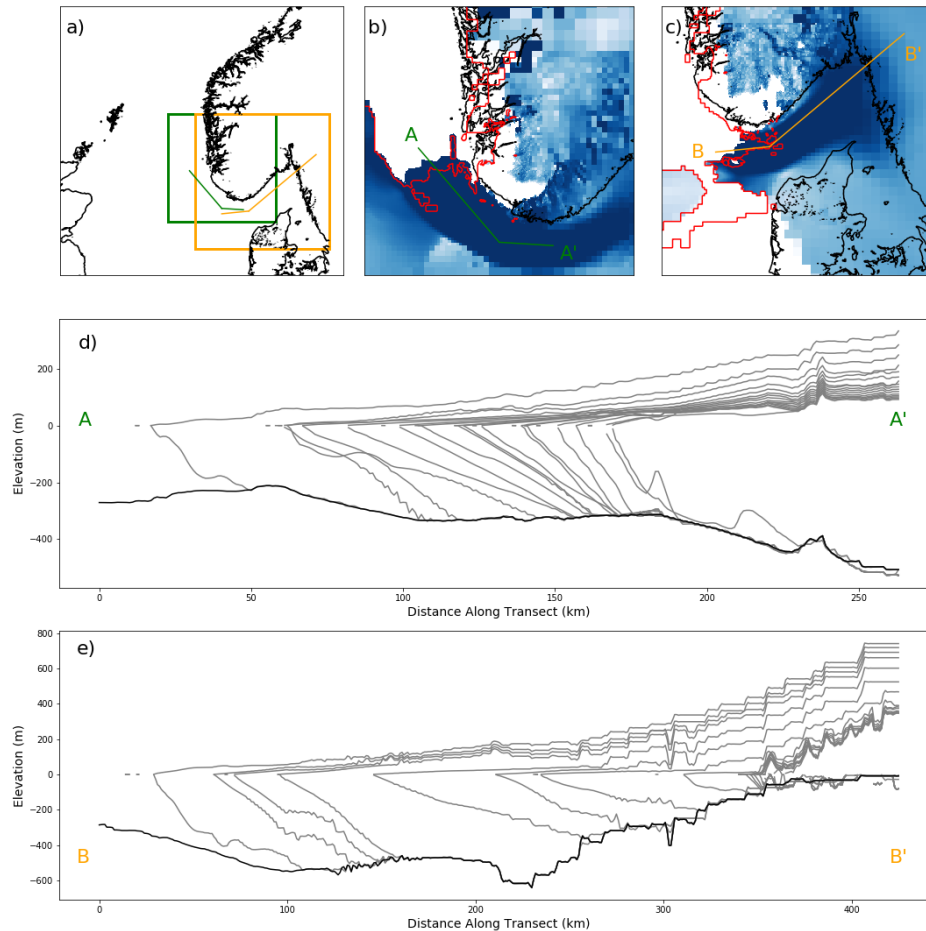
Figure 4.7: The high-resolution snapshot simulations. a) The locations of close up views in panel b (green box) and c (orange box) and the transects used in panel d and e. b) The NCIS just before a rapid grounding line retreat, with transect shown in panel d. c) The NCIS in the Skagerrak Straight just before a rapid retreat, with transect shown in panel e. Transects are shown every 20 years in panels d and e.

line at the regions shown in Figure 4.7b-c. The results show rapid grounding line retreat in regions of retrograde bed slope (Figure 4.7d-e), indicative of Marine Ice Sheet Instability. The simulated retreat is rapid; in both snapshot simulations the grounding line has a maximum retreat rate of >50 km in 20 years (Figure 4.7d-e). This grounding line retreat rate is comparable to simulations of future Thwaites Glacier grounding line retreat (Cornford et al., 2015). Both simulations, the later simulation in particular, show considerable thinning of the ice sheet upstream of the grounding line during the period of rapid retreat. In the later retreat period, there is upstream thinning of ∼2-3 m/y through the rapid retreat,

which is comparable to observed thinning rates of the contemporary Pine Island Glacier (Shepherd et al., 2001; Wingham et al., 2009).

The behaviour of the high-resolution simulations and the lower resolution ensemble member is broadly consistent, in that it demonstrates a period of rapid retreat, starting and concluding in the same regions of the Norwegian Channel. This provides confidence in the validity of the periods of rapid retreat simulated in the other ensemble members. However, using high-resolution simulations, more detailed behaviour of the grounding line is simulated.

4.4 Discussion

4.4.1 Combined instabilities

The simulations show the significant retreat of the NCIS is driven by the interacting factors of ice flow, surface lowering, and marine ice sheet instabilities. At the beginning of the deglaciation ensemble, with full ice extent over the North Sea, the NCIS has an effect on the surface profile of the ice sheet, causing a large (∼500 m) depression in the surface of the ice sheet (Figure 4.8a). This is similar to the surface expressions of similar contemporary ice streams, like Pine Island Glacier and Thwaites Glacier (Howat et al., 2019).

This large surface depression is important because it causes feedbacks between ice dynamics, further surface lowering, and marine ice sheet instabilities. The initial depression means that at the start of the deglaciation experiments the NCIS was vulnerable to surface melting (Figure 4.8b), allowing the surface of the NCIS to be lowered further. This has four effects. First, the lowering of the ice stream surface compared to neighbouring ice allows ice stream acceleration (Robel and Tziperman, 2016), driving further lowering. Second, the thinning exacerbates the lapse rate feedback that allows further surface melting as the surface lowers. Third, any thinning of the ice stream (which is located in a deep marine trough) means the ice stream becomes more vulnerable to rapid retreat
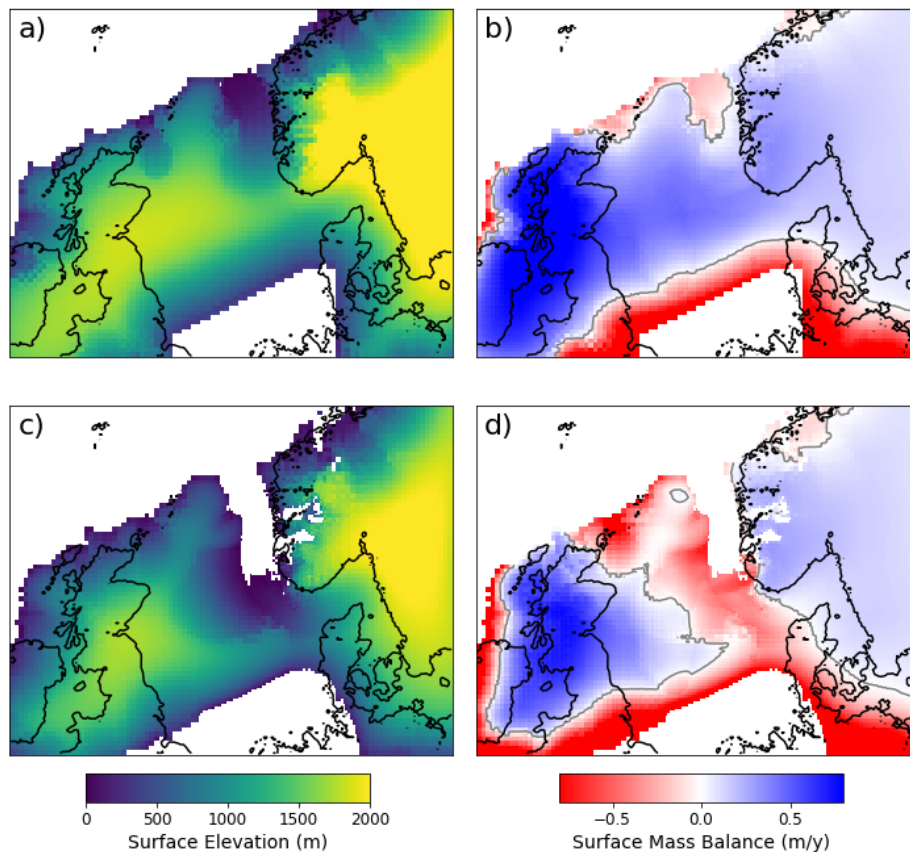
Figure 4.8: Ice sheet surface elevation and Surface Mass Balance at 23 ka BP (a-b) and 21.5 ka BP (c-d) in ensemble member *ns_002*.

as it approaches buoyancy. And finally, any grounding line retreat into a region of retrograde bed slope can cause marine ice sheet instability.

Notably, the NCIS remained grounded past the Skagerrak Straight by 18 ka BP in only 4 ensemble members. Those simulations show an advance of the BIIS and Fennoscandian Ice Sheets in other sectors. In the remaining ensemble members, the combined instabilities of ice flow, surface elevation feedbacks, and marine influence mean that once the NCIS begins to retreat it is likely to continue to retreat fully. It is important to note, however, that the NCIS does not experience an uninterrupted retreat for the entire length of the Norwegian Channel. There are periods of rapid grounding line retreat, and periods of grounding line stability. This is supported by the mapping of grounding zone wedges in the Norwegian Channel (Morén et al., 2018), which require a period of stability of the

grounding line to form. Including a more temporally variable climate based on ice core data, as used in previous simulations (e.g. Hubbard et al., 2009; Seguinot et al., 2016; Patton et al., 2017; Seguinot et al., 2018), would result in greater variability of retreat rate, and more periods of stability caused by climate forcing.

4.4.2 Styles of deglaciation

As discussed, empirical reconstructions of the separation of the BIIS and Fennoscandian Ice Sheet do not provide a consensus on the style of deglaciation. Bradwell et al. (2008) suggested that the separation began with the formation of a calving bay to the west of the Norwegian Channel, forming a large embayment in the northern North Sea. In contrast, Sejrup et al. (2016) suggested that deglaciation of the North Sea begun with the initial retreat of the NCIS, which debutressed the BIIS to the west, causing no initial significant margin retreat of the BIIS in the northwest whilst the NCIS retreated significantly, leading to an "unzipping" between the BIIS and the Fennoscandian Ice Sheet. The ensemble of simulations presented in this manuscript allows us to test the plausibility of each deglaciation scenario.

Here, none of the ensemble members began deglaciation of the North Sea through the formation of an embayment in the Witch Ground basin whilst the NCIS remained extended. Instead, there are key similarities between the "unzipping" scenario and the majority of simulations described here. In all simulations, the retreat of the NCIS precedes retreat into the Witch Ground basin. In the 11 NROY simulations, the NCIS retreats past the Skagerrak straight before BIIS North Sea Ice has entirely receded (Figure 4.6). Although the Witch Ground basin is a significant topographic depression in the context of the relatively flat North Sea, it is not a significant depression in comparison to the neighbouring Norwegian Channel, and no simulation in our ensemble demonstrates ice retreating in the Witch Ground basin but remaining stable in the Norwegian Channel. It has previously been suggested that because the NCIS was more vulnerable to ma-

rine and climate forced retreat, initial retreat into the Witch Ground basin while the NCIS remained fully extended is "enigmatic" (Clark et al., 2012; Hughes et al., 2016). Our findings also suggest that this deglaciation style is glaciologically implausible.

In contrast, there are similarities between the style of deglaciation in the NROY simulations, and the deglaciation reconstructed by Sejrup et al. (2016). Both the reconstruction and the simulations presented here suggest a key role of the NCIS, initially retreating before the rest of the North Sea. However, while simulations here place the final point of confluence before separation as in the Jutland Bank region, Sejrup et al. (2016) place it further North, to the west of the Norwegian Channel.

The simulations presented here were computationally costly, therefore only the deglaciation was included in the 70 member ensemble, rather than a full glacial cycle. Beginning these ensemble experiments from the end of a single advance and confluence simulation rather than a stable maximum extent in part helps represent the transient nature of the last glacial cycle, but it would still be preferable to run an ensemble of transient advance and retreat simulations, if computational cost permitted. With the current experiments it is not clear how sensitive the deglaciation style is to different styles of ice sheet build-up, so as computational costs reduce, an ensemble of a transient advance and retreat experiments would be advantageous. Alternatively, a computationally cheaper model can be used to simulate a full glacial cycle of the Eurasian Ice Sheet (Patton et al., 2016, 2017), if those models are able to simulate deglaciation of the North Sea.

4.4.3 Dogger Bank ice dome

A combination of margin, geomorphological, and dating evidence has resulted in the reconstruction of a North Sea Lobe, descending from the Firth of Forth and extending down to the north Norfolk coast (Evans and Thomson, 2010; Dove

et al., 2017). Specifically, the presence of a North Sea Lobe helps to explain dates showing ice free conditions across central England, while deglaciation is later along the Yorkshire and Lincolnshire coast (Bateman et al., 2015). Such an ice margin is also necessary to dam reconstructed proglacial lakes in northern and central England (Evans and Thomson, 2010; Bateman et al., 2015; Davies et al., 2019). The North Sea Lobe is an interesting feature because it is thought to have retreated rapidly (Bateman et al., 2015; Evans et al., 2017; Roberts et al., 2019), and the mechanisms controlling its extent and behaviour are poorly understood (Dove et al., 2017).

Although ice streaming down the Yorkshire and Lincolnshire coast is simulated in numerous ensemble members, a feature as prominent as the reconstructed North Sea Lobe is never simulated. In the majority of simulations, however, a Dogger Bank ice dome forms during deglaciation, where ice remains in the North Sea, retreating roughly radially from the point the BIIS and the Fennoscandian Ice Sheets disconnect. Essentially, we judge a North Sea lobe and a Dogger Bank ice dome to be differentiated by their easterly extent (Figure 4.9). This dome is the remnants of the ice divide that forms across the North Sea at maximum extent, and it is what remains when the majority of surrounding ice has retreated. This has similarities to the second scenario of North Sea deglaciation reconstructed by Clark et al. (2012), with a persistent ice dome in the southern North Sea. It has been suggested that a persistent North Sea ice dome would require a low equilibrium line and should be evident from relative sea level records around the North Sea (Hughes et al., 2016). Topographically or climatically, the southern North Sea is not an intuitive area to reconstruct an ice dome. Despite this, ice persisting in the North Sea concurrent with retreat of the western BIIS is a consistent feature of the ensemble members (Figure 4.6).

The simulation of a dome is consistent with much of the evidence that led to the hypothesis of the North Sea Lobe. For example. it allows ice cover in the North Sea with a margin down the Yorkshire and Lincolnshire coast, while ice is
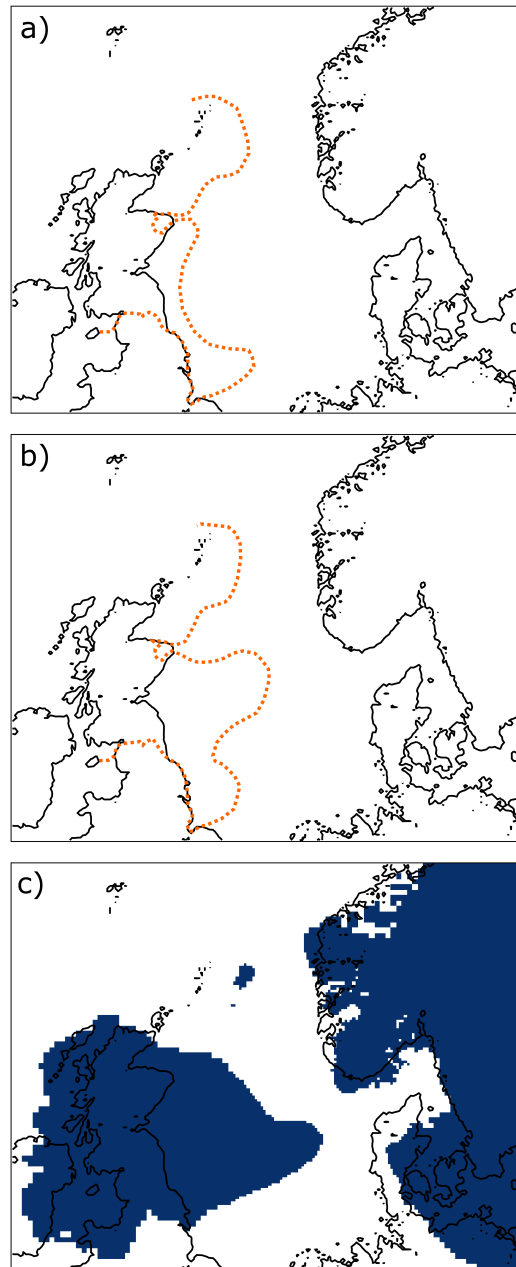
Figure 4.9: Prior reconstructions of North Sea Ice extent from Clark et al., (2012), split into Scenario 1 (a) and Scenario 2 (b) compared to the simulated Dogger Bank ice cap (c).

retreated in central England (Bateman et al., 2015; Davies et al., 2019). However, a Dogger Bank ice cap that descends down to the north Norfolk coast is never simulated in the ensemble. A lobate margin, albeit smaller than shown in Figure 4.9b, is still required to match empirical evidence in north Norfolk (Evans et al., 2019). Correctly simulating the timing and location of a surge is challenging, as it

is dependent on the correct evolution of the ice sheet thermal structure, which in turn is dependent on a number of uncertain parameters and boundary conditions.

4.4.4 Climate impacts

It is well established that the larger ice sheets of the last deglaciation have a considerable impact on the climate and ocean system, through large freshwater fluxes into the ocean (Clark et al., 2001; Golledge et al., 2014; Matero et al., 2017; Ivanovic et al., 2018, Margold et al., in prep), and changes to precipitation and atmospheric circulation (Hoskins and Karoly, 1981; Löfverström et al., 2016; Gregoire et al., 2018).
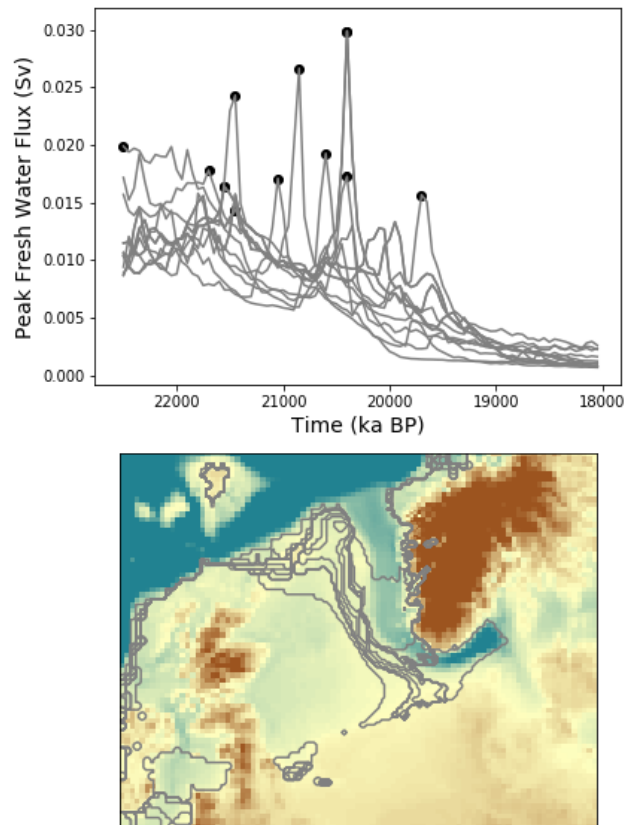
Figure 4.10: Top: the timing and amount of peak freshwater flux in the 11 NROY ensemble members. Grey curves show flux evolution of every NROY simulation. Bottom: the grounding line position at each of the 11 NROY points of freshwater flux.

The freshwater flux from the deglaciation of the North Sea sector is not constant through the deglaciation; there are periods of peak (∼5-10 times higher

than average) freshwater flux (Figure 4.10), always associated with rapid retreat of the NCIS grounding line. This further demonstrates the influence of the NCIS. The peak freshwater flux is ∼0.01-0.03 Sv in the 11 NROY ensemble members. This is a small peak freshwater flux, compared with ∼0.2 Sv simulated during collapse of the Laurentide-Cordilleran saddle (Gregoire et al., 2016, Margold et al., in prep). For further comparison, simulations of the onset of Heinrich Stadial 1 ∼18.5 ka BP often require an unrealistically high freshwater flux, with a peak flux above 0.15 Sv maintained for multiple millennia (Liu et al., 2009; Menviel et al., 2011). Ivanovic et al. (2018) simulated the onset of Heinrich Stadial 1 with a freshwater flux of ∼0.04 Sv at 18 ka BP, consistent with the ICE_6G_C reconstruction (Peltier et al., 2015). Melt from the contemporary Greenland ice sheet causes a freshwater flux of ∼0.01 Sv (McMillan et al., 2016).

It is uncertain how rapidly freshwater flux from the deglaciation of the North Sea would reach the North Atlantic, salinity and temperature gradients may cause it to "pool" in the North Sea rather than spread out of the basin. However, once the freshwater did leave the North Sea it would be in an influential location for deep water formation. Bigg et al. (2012) suggested from modelling and proxy evidence that the freshwater flux from the western Eurasian Ice Sheet likely did not have global consequence until 17-15 ka BP. On balance, we deem it is likely that this relatively small flux did not have significant climate or ocean effects, though this could be explored further with coupled ice sheet, climate, and ocean simulations.

4.5 Conclusions

We completed an ensemble of simulations of the deglaciation of the North Sea sector of the Eurasian Ice Sheet, using the BISICLES ice sheet model, simulating deglaciation in a manner that respects the majority of empirical evidence for the first time. We used a suite of quantitative model-data comparison tools to compare simulations to a large amount of empirical evidence. The simulations

show that the Norwegian Channel Ice Stream was influential in the separation of the British-Irish Ice Sheet and the Fennoscandian Ice Sheet, retreating through an interacting combination of Marine Ice Sheet Instability, elevation-lapse rate effects, and ice dynamics feedbacks. The retreat of the Norwegian Channel Ice Stream has effects on the surrounding ice masses, and facilitates further retreat of the BIIS. The simulations are consistent with a reconstructed style of deglaciation beginning with retreat of the NCIS, and suggest retreat to the west of the Norwegian Channel while the NCIS remains extended is implausible.

In the later stages of deglaciation, all NROY simulations produce a Dogger Bank ice dome, where ice remains extensive in the North Sea while the BIIS has significantly retreated in the west. We find this to be a plausible alternative to the North Sea lobe, and hypothesise a Dogger Bank ice dome forms as a consequence of deglaciating an ice divide in the North Sea. The significant progress made here in simulating deglaciation dynamics that respect the majority of empirical evidence is possible because of improved simulation of marine ice sheet dynamics and the evolution of ice streams. This demonstrates the importance of using an ice sheet model of sufficient skill when simulating the future evolution of marine based ice sheets.

Data Availability

We used a branch of the BISICLES ice sheet model, revision 3776 (https://anag-repo.lbl.gov/svn/BISICLES/public/branches/slc_dev_2018). Output files and required input files to reproduce the described experiments are accessible by contacting the corresponding author and will be deposited independently for final publication.

References

Bateman, M. et al. (2015). "Last glacial dynamics of the Vale of York and North Sea lobes of the British and Irish Ice Sheet". In: *Proceedings of the Geologists' Association* 126.6, pp. 712–730. DOI: 10.1016/J.PGEOLA.2015.09.005.

Becker, J. J. et al. (2009). "Global Bathymetry and Elevation Data at 30 Arc Seconds Resolution: SRTM30_PLUS". In: *Marine Geodesy* 32.4, pp. 355–371. DOI: 10.1080/01490410903297766.

Belt, T. (1874). *Glacial period.* DOI: 10.1038/010062c0.

Bigg, G. R., C. D. Clark, S. L. Greenwood, H. Haflidason, A. L. Hughes, R. C. Levine, A. Nygård, and H. P. Sejrup (2012). "Sensitivity of the North Atlantic circulation to break-up of the marine sectors of the NW European ice sheets during the last Glacial: A synthesis of modelling and palaeoceanography". In: *Global and Planetary Change* 98-99, pp. 153–165. DOI: 10.1016/j.gloplacha.2012.09.004.

Boulton, G. S., G. D. Smith, A. S. Jones, and J. Newsome (1985). "Glacial geology and glaciology of the last mid-latitude ice sheets." In: *Journal - Geological Society (London)* 142.3, pp. 447–474. DOI: 10.1144/gsjgs.142.3.0447.

Boulton, G. and M. Hagdorn (2006). "Glaciology of the British Isles Ice Sheet during the last glacial cycle: form, flow, streams and lobes". In: *Quaternary Science Reviews* 25.23-24, pp. 3359–3390. DOI: 10.1016/j.quascirev.2006.10.013.

Bradley, S. L., G. A. Milne, I. Shennan, and R. Edwards (2011). "An improved glacial isostatic adjustment model for the British Isles". In: *Journal of Quaternary Science* 26.5, pp. 541–552. DOI: 10.1002/jqs.1481.

Bradwell, T., D. Small, D. Fabel, C. D. Clark, R. C. Chiverrell, and M. H. Saher (2019). "Pattern , style and timing of British-Irish Ice Sheet retreat : Shetland and northern North Sea sector Pattern , style and timing of British – Irish Ice Sheet retreat : Shetland and northern North Sea sector". In: *Journal of Quaternary Science* November, jqs.3163. DOI: 10.1002/jqs.3163.

Bradwell, T. et al. (2008). "The northern sector of the last British Ice Sheet: Maximum extent and demise". In: *Earth-Science Reviews* 88.3-4, pp. 207–226. DOI: 10.1016/j.earscirev.2008.01.008.

Carr, S. J., R. Holmes, J. J. M. van der Meer, and J. Rose (2006). "The Last Glacial Maximum in the North Sea Basin: micromorphological evidence of extensive glaciation". In: *Journal of Quaternary Science* 21.2, pp. 131–153. DOI: 10.1002/jqs.950.

Clark, C. D., A. L. Hughes, S. L. Greenwood, C. Jordan, and H. P. Sejrup (2012). "Pattern and timing of retreat of the last British-Irish Ice Sheet". In: *Quaternary Science Reviews* 44, pp. 112–146. DOI: 10.1016/j.quascirev.2010.07.019.

Clark, C. D. et al. (2018). "BRITICE Glacial Map, version 2: a map and GIS database of glacial landforms of the last British-Irish Ice Sheet". In: *Boreas* 47.1, 11–e8. DOI: 10.1111/bor.12273.

Clark, P. U., S. J. Marshall, G. K. Clarke, S. W. Hostetler, J. M. Licciardi, and J. T. Teller (2001). "Freshwater forcing of abrupt climate change during the last glaciation". In: *Science* 293.5528, pp. 283–287. DOI: 10.1126/science.1062517.

Cohen, K. M., P. L. Gibbard, and H. J. Weerts (2014). "North Sea palaeogeographical reconstructions for the last 1 Ma". In: *Geologie en Mijnbouw/Netherlands Journal of Geosciences* 93.1-2, pp. 7–29. DOI: 10.1017/njg.2014.12.

Cornford, S. L. et al. (2015). "Century-scale simulations of the response of the West Antarctic Ice Sheet to a warming climate". In: *Cryosphere* 9.4, pp. 1579–1600. DOI: 10.5194/tc-9-1579-2015.

Cornford, S. L., D. F. Martin, V. Lee, A. J. Payne, and E. G. Ng (2016). "Adaptive mesh refinement versus subgrid friction interpolation in simulations of Antarctic ice dynamics". In: *Annals of Glaciology* 57.73, pp. 1–9. DOI: 10.1017/aog.2016.13.

Cornford, S. L., D. F. Martin, D. T. Graves, D. F. Ranken, A. M. Le Brocq, R. M. Gladstone, A. J. Payne, E. G. Ng, and W. H. Lipscomb (2013). "Adaptive mesh, finite volume modeling of marine ice sheets". In: *Journal of Computational Physics* 232.1, pp. 529–549. DOI: 10.1016/j.jcp.2012.08.037.

Cotterill, C. J., E. Phillips, L. James, C. F. Forsberg, T. I. Tjelta, G. Carter, and D. Dove (2017). "The evolution of the Dogger Bank, North Sea: A complex history of terrestrial, glacial and marine environmental change". In: *Quaternary Science Reviews* 171, pp. 136–153. DOI: 10.1016/j.quascirev.2017.07.006.

Davies, B. J., S. J. Livingstone, D. H. Roberts, D. J. Evans, D. M. Gheorghiu, and C. Ó Cofaigh (2019). "Dynamic ice stream retreat in the central sector of the last British-Irish Ice Sheet". In: *Quaternary Science Reviews* 225, p. 105989. DOI: 10.1016/j.quascirev.2019.105989.

Dove, D., D. J. Evans, J. R. Lee, D. H. Roberts, D. R. Tappin, C. L. Mellett, D. Long, and S. L. Callard (2017). "Phased occupation and retreat of the last British–Irish Ice Sheet in the southern North Sea; geomorphic and seismostratigraphic evidence of a dynamic ice lobe". In: *Quaternary Science Reviews* 163, pp. 114–134. DOI: 10.1016/j.quascirev.2017.03.006.

Ehlers, J. and P. Gibbard (2004). *Quaternary glaciations-extent and chronology: part I: Europe.* Elsevier.

Ely, J. C., C. D. Clark, D. Small, and R. C. A. Hindmarsh (2019a). "ATAT 1.1, the Automated Timing Accordance Tool for comparing ice-sheet model out-

put with geochronological data". In: *Geoscientific Model Development* 12.3, pp. 933–953. DOI: 10.5194/gmd-12-933-2019.

Ely, J. C. et al. (2019b). "Recent progress on combining geomorphological and geochronological data with ice sheet modelling, demonstrated using the last British–Irish Ice Sheet". In: *Journal of Quaternary Science*, pp. 1–15. DOI: 10.1002/jqs.3098.

Emery, A. R., D. M. Hodgson, N. L. Barlow, J. L. Carrivick, C. J. Cotterill, and E. Phillips (2019). "Left High and Dry: Deglaciation of Dogger Bank, North Sea, Recorded in Proglacial Lake Evolution". In: *Frontiers in Earth Science* 7, p. 234. DOI: 10.3389/feart.2019.00234.

Evans, D. J. A., M. D. Bateman, D. H. Roberts, A. Medialdea, L. Hayes, G. A. T. Duller, D. Fabel, and C. D. Clark (2017). "Glacial Lake Pickering: stratigraphy and chronology of a proglacial lake dammed by the North Sea Lobe of the British-Irish Ice Sheet". In: *Journal of Quaternary Science* 32.2, pp. 295–310. DOI: 10.1002/jqs.2833.

Evans, D. J., D. H. Roberts, M. D. Bateman, J. Ely, A. Medialdea, M. J. Burke, R. C. Chiverrell, C. D. Clark, and D. Fabel (2019). "A chronology for North Sea Lobe advance and recession on the Lincolnshire and Norfolk coasts during MIS 2 and 6". In: *Proceedings of the Geologists' Association* 130.5, pp. 523–540. DOI: 10.1016/j.pgeola.2018.10.004.

Evans, D. J. and S. A. Thomson (2010). "Glacial sediments and landforms of Holderness, eastern England: A glacial depositional model for the North Sea Lobe of the British-Irish Ice Sheet". In: *Earth-Science Reviews* 101.3-4, pp. 147–189. DOI: 10.1016/j.earscirev.2010.04.003.

Farr, T. G. et al. (2007). "The Shuttle Radar Topography Mission". In: *Reviews of Geophysics* 45.2, RG2004. DOI: 10.1029/2005RG000183.

Favier, L., G. Durand, S. L. Cornford, G. H. Gudmundsson, O. Gagliardini, F. Gillet-Chaulet, T. Zwinger, A. J. Payne, and A. M. Le Brocq (2014). "Retreat

of Pine Island Glacier controlled by marine ice-sheet instability". In: *Nature Climate Change* 4.2, pp. 117–121. DOI: 10.1038/nclimate2094.

Fick, S. E. and R. J. Hijmans (2017). "WorldClim 2: new 1-km spatial resolution climate surfaces for global land areas". In: *International Journal of Climatology* 37.12, pp. 4302–4315. DOI: 10.1002/joc.5086.

Gandy, N., L. J. Gregoire, J. C. Ely, C. D. Clark, D. M. Hodgson, V. Lee, T. Bradwell, and R. F. Ivanovic (2018). "Marine Ice Sheet Instability and Ice Shelf Buttressing Influenced Deglaciation of the Minch Ice Stream, Northwest Scotland". In: *The Cryosphere* 12.July, pp. 1–24. DOI: 10.5194/tc-2018-116.

Gandy, N., L. J. Gregoire, J. C. Ely, S. L. Cornford, C. D. Clark, and D. M. Hodgson (2019). "Exploring the ingredients required to successfully model the placement, generation, and evolution of ice streams in the British-Irish Ice Sheet". In: *Quaternary Science Reviews* 223, p. 105915. DOI: 10.1016/J.QUASCIREV.2019.105915.

Gibbard, P. L., J. Rose, and D. R. Bridgland (1988). "The History of the Great Northwest European Rivers During the Past Three Million Years [and Discussion]". In: *Philosophical Transactions of the Royal Society B: Biological Sciences* 318.1191, pp. 559–602. DOI: 10.1098/rstb.1988.0024.

Gladstone, R. M., A. J. Payne, and S. L. Cornford (2012). "Resolution requirements for grounding-line modelling: Sensitivity to basal drag and ice-shelf buttressing". In: *Annals of Glaciology* 53.60, pp. 97–105. DOI: 10.3189/2012AoG60A148.

Golledge, N. R., L. Menviel, L. Carter, C. J. Fogwill, M. H. England, G. Cortese, and R. H. Levy (2014). "Antarctic contribution to meltwater pulse 1A from reduced Southern Ocean overturning". In: *Nature Communications* 5. DOI: 10.1038/ncomms6107.

Gong, Y., T. Zwinger, S. Cornford, R. Gladstone, M. Schäfer, and J. C. Moore (2017). "Importance of basal boundary conditions in transient simulations:

Case study of a surging marine-terminating glacier on Austfonna, Svalbard". In: *Journal of Glaciology* 63.237, pp. 106–117. DOI: 10.1017/jog.2016.121.

Gordon, C., C. Cooper, C. A. Senior, H. Banks, J. M. Gregory, T. C. Johns, J. F. B. Mitchell, and R. A. Wood (2000). "The simulation of SST, sea ice extents and ocean heat transports in a version of the Hadley Centre coupled model without flux adjustments". In: *Climate Dynamics* 16.2-3, pp. 147–168. DOI: 10.1007/s003820050010.

Graham, A., L. Lonergan, and M. Stoker (2007). "Evidence for Late Pleistocene ice stream activity in the Witch Ground Basin, central North Sea, from 3D seismic reflection data". In: *Quaternary Science Reviews* 26.5-6, pp. 627–643. DOI: 10.1016/J.QUASCIREV.2006.11.004.

Greenwood, S. L. and C. D. Clark (2009a). "Reconstructing the last Irish Ice Sheet 1: changing flow geometries and ice flow dynamics deciphered from the glacial landform record". In: *Quaternary Science Reviews* 28.27-28, pp. 3085–3100. DOI: 10.1016/j.quascirev.2009.09.008.

— (2009b). "Reconstructing the last Irish Ice Sheet 2: a geomorphologically-driven model of ice sheet growth, retreat and dynamics". In: *Quaternary Science Reviews* 28.27-28, pp. 3101–3123. DOI: 10.1016/j.quascirev.2009.09.014.

Gregoire, L. J., R. F. Ivanovic, A. C. Maycock, P. J. Valdes, and S. Stevenson (2018). "Holocene lowering of the Laurentide ice sheet affects North Atlantic gyre circulation and climate". In: *Climate Dynamics* 51.9-10, pp. 3797–3813. DOI: 10.1007/s00382-018-4111-9.

Gregoire, L. J., B. Otto-Bliesner, P. J. Valdes, and R. Ivanovic (2016). "Abrupt Bølling warming and ice saddle collapse contributions to the Meltwater Pulse 1a rapid sea level rise". In: *Geophysical Research Letters* 43.17, pp. 9130–9137. DOI: 10.1002/2016GL070356.

Hindmarsh, R. C. (2009). "Consistent generation of ice-streams via thermo-viscous instabilities modulated by membrane stresses". In: *Geophysical Research Letters* 36.6, p. L06502. DOI: 10.1029/2008GL036877.

Hoskins, B. J. and D. J. Karoly (1981). "The steady linear response of a spherical atmosphere to thermal and orographic forcing." In: *Journal of the Atmospheric Sciences* 38.6, pp. 1179–1196. DOI: 10.1175/1520-0469(1981) 038<1179:TSLROA>2.0.CO;2.

Howat, I. M., C. Porter, B. E. Smith, M.-J. Noh, and P. Morin (2019). "The Reference Elevation Model of Antarctica". In: *The Cryosphere* 13.2, pp. 665–674. DOI: 10.5194/tc-13-665-2019.

Hubbard, A., T. Bradwell, N. Golledge, A. Hall, H. Patton, D. Sugden, R. Cooper, and M. Stoker (2009). "Dynamic cycles, ice streams and their impact on the extent, chronology and deglaciation of the British–Irish ice sheet". In: *Quaternary Science Reviews* 28.7-8, pp. 758–776. DOI: 10.1016/j.quascirev.2008.12.026.

Hughes, A. L., C. D. Clark, and C. J. Jordan (2014). "Flow-pattern evolution of the last British Ice Sheet". In: *Quaternary Science Reviews* 89, pp. 148–168. DOI: 10.1016/j.quascirev.2014.02.002.

Hughes, A. L., R. Gyllencreutz, Ø. S. Lohne, J. Mangerud, and J. I. Svendsen (2016). "The last Eurasian ice sheets - a chronological database and time-slice reconstruction, DATED-1". In: *Boreas* 45.1. DOI: 10.1111/bor.12142.

Ivanovic, R. F. et al. (2018). "Acceleration of Northern Ice Sheet Melt Induces AMOC Slowdown and Northern Cooling in Simulations of the Early Last Deglaciation". In: *Paleoceanography and Paleoclimatology* 33.7, pp. 807–824. DOI: 10.1029/2017PA003308.

Ivanovic, R. F., L. J. Gregoire, M. Kageyama, D. M. Roche, P. J. Valdes, A. Burke, R. Drummond, W. R. Peltier, and L. Tarasov (2016). "Transient climate simulations of the deglaciation 21–9 thousand years before present (version 1) –

PMIP4 Core experiment design and boundary conditions". In: *Geoscientific Model Development* 9.7, pp. 2563–2587. DOI: 10.5194/gmd-9-2563-2016.

Joughin, I., B. E. Smith, and B. Medley (2014). "Marine ice sheet collapse potentially under way for the thwaites glacier basin, West Antarctica". In: *Science* 344.6185, pp. 735–738. DOI: 10.1126/science.1249055.

King, E. L., H. Haflidason, H. P. Sejrup, and R. Løvlie (1998). "Glacigenic debris flows on the North Sea Trough Mouth Fan during ice stream maxima". In: *Marine Geology* 152.1-3, pp. 217–246. DOI: 10.1016/S0025-3227(98)00072-3.

Li, Y., J. Napieralski, J. Harbor, and A. Hubbard (2007). "Identifying patterns of correspondence between modeled flow directions and field evidence: An automated flow direction analysis". In: *Computers & Geosciences* 33.2, pp. 141–150. DOI: 10.1016/J.CAGEO.2006.06.016.

Liu, Z. et al. (2009). "Transient simulation of last deglaciation with a new mechanism for bolling-allerod warming". In: *Science* 325.5938, pp. 310–314. DOI: 10.1126/science.1171041.

Löfverström, M., R. Caballero, J. Nilsson, and G. Messori (2016). "Stationary Wave Reflection as a Mechanism for Zonalizing the Atlantic Winter Jet at the LGM". In: *Journal of the Atmospheric Sciences* 73.8, pp. 3329–3342. DOI: 10.1175/JAS-D-15-0295.1.

Matero, I. S., L. J. Gregoire, R. F. Ivanovic, J. C. Tindall, and A. M. Haywood (2017). "The 8.2 ka cooling event caused by Laurentide ice saddle collapse". In: *Earth and Planetary Science Letters* 473, pp. 205–214. DOI: 10.1016/j.epsl.2017.06.011.

McMillan, M. et al. (2016). "A high-resolution record of Greenland mass balance". In: *Geophysical Research Letters* 43.13, pp. 7002–7010. DOI: 10.1002/2016GL069666.

Menviel, L., A. Timmermann, O. E. Timm, and A. Mouchet (2011). "Deconstructing the Last Glacial termination: The role of millennial and orbital-

scale forcings". In: *Quaternary Science Reviews* 30.9-10, pp. 1155–1172. DOI: 10.1016/j.quascirev.2011.02.005.

Morén, B. M., H. P. Sejrup, B. O. Hjelstuen, M. V. Borge, and C. Schäuble (2018). "The last deglaciation of the Norwegian Channel - geomorphology, stratigraphy and radiocarbon dating". In: *Boreas* 47.1, pp. 347–366. DOI: 10.1111/bor.12272.

Morris, P. J., G. T. Swindles, P. J. Valdes, R. F. Ivanovic, L. J. Gregoire, M. W. Smith, L. Tarasov, A. M. Haywood, and K. L. Bacon (2018). "Global peatland initiation driven by regionally asynchronous warming." In: *Proceedings of the National Academy of Sciences of the United States of America* 115.19, pp. 4851–4856. DOI: 10.1073/pnas.1717838115.

Murton, D. K. and J. B. Murton (2012). "Middle and Late Pleistocene glacial lakes of lowland Britain and the southern North Sea Basin". In: *Quaternary International* 260, pp. 115–142. DOI: 10.1016/j.quaint.2011.07.034.

Napieralski, J., A. Hubbard, Y. Li, J. Harbor, A. P. Stroeven, J. Kleman, G. Alm, and K. N. Jansson (2007). "Towards a GIS assessment of numerical ice-sheet model performance using geomorphological data". In: *Journal of Glaciology* 53.180, pp. 71–83. DOI: 10.3189/172756507781833884.

Nias, I. J., S. L. Cornford, and A. J. Payne (2016). "Contrasting the Modelled sensitivity of the Amundsen Sea Embayment ice streams". In: *Journal of Glaciology* 62.233, pp. 552–562. DOI: 10.1017/jog.2016.40.

Nygård, A., H. P. Sejrup, H. Haflidason, and P. Bryn (2005). "The glacial North Sea Fan, southern Norwegian Margin: Architecture and evolution from the upper continental slope to the deep-sea basin". In: *Marine and Petroleum Geology* 22.1-2 SPEC. ISS. Pp. 71–84. DOI: 10.1016/j.marpetgeo.2004.12.001.

Patton, H., A. Hubbard, K. Andreassen, M. Winsborrow, and A. P. Stroeven (2016). "The build-up, configuration, and dynamical sensitivity of the Eurasian ice-sheet complex to Late Weichselian climatic and oceanic forcing". In: *Qua-*

ternary Science Reviews 153, pp. 97–121. DOI: 10.1016/j.quascirev.2016.10.009.

Patton, H. et al. (2017). "Deglaciation of the Eurasian ice sheet complex". In: *Quaternary Science Reviews* 169, pp. 148–172. DOI: 10.1016/j.quascirev.2017.05.019.

Peltier, W. R., D. F. Argus, and R. Drummond (2015). "Space geodesy constrains ice age terminal deglaciation: The global ICE-6G_C (VM5a) model". In: *Journal of Geophysical Research: Solid Earth* 120.1, pp. 450–487. DOI: 10.1002/2014JB011176.

Phillips, E., C. Cotterill, K. Johnson, K. Crombie, L. James, S. Carr, and A. Ruiter (2018). "Large-scale glacitectonic deformation in response to active ice sheet retreat across Dogger Bank (southern central North Sea) during the Last Glacial Maximum". In: *Quaternary Science Reviews* 179, pp. 24–47. DOI: 10.1016/j.quascirev.2017.11.001.

Phillips, E., D. M. Hodgson, and A. R. Emery (2017). "The Quaternary geology of the North Sea basin". In: *Journal of Quaternary Science.* Vol. 32. 2. John Wiley and Sons Ltd, pp. 117–126. DOI: 10.1002/jqs.2932.

Pollard, D. and R. M. DeConto (2012). "Description of a hybrid ice sheet-shelf model, and application to Antarctica". In: *Geoscientific Model Development* 5.5, pp. 1273–1295. DOI: 10.5194/gmd-5-1273-2012.

Pope, V. D., M. L. Gallani, P. R. Rowntree, and R. A. Stratton (2000). "The impact of new physical parametrizations in the Hadley Centre climate model: HadAM3". In: *Climate Dynamics* 16.2-3, pp. 123–146. DOI: 10.1007/s003820050009.

Rignot, E. and S. S. Jacobs (2002). "Rapid Bottom Melting Widespread near Antarctic Ice Sheet Grounding Lines". In: *Science* 296.5575, pp. 2020–2023. DOI: 10.1126/science.1070942.

Robel, A. A. and E. Tziperman (2016). "The role of ice stream dynamics in deglaciation". In: *Journal of Geophysical Research: Earth Surface* 121.8, pp. 1540–1554. DOI: 10.1002/2016JF003937.

Roberts, D. H. et al. (2018). "Ice marginal dynamics of the last British-Irish Ice Sheet in the southern North Sea: Ice limits, timing and the influence of the Dogger Bank". In: *Quaternary Science Reviews* 198, pp. 181–207. DOI: `10.1016/J.QUASCIREV.2018.08.010`.

Roberts, D. H. et al. (2019). "The mixed-bed glacial landform imprint of the North Sea Lobe in the western North Sea". In: *Earth Surface Processes and Landforms* 44.6, pp. 1233–1258. DOI: `10.1002/esp.4569`.

Schoof, C. (2007). "Ice sheet grounding line dynamics: Steady states, stability, and hysteresis". In: *Journal of Geophysical Research* 112.F3, F03S28. DOI: `10.1029/2006JF000664`.

Schoof, C. and R. C. Hindmarsh (2010). "Thin-film flows with wall slip: An asymptotic analysis of higher order glacier flow models". In: *Quarterly Journal of Mechanics and Applied Mathematics* 63.1, pp. 73–114. DOI: `10.1093/qjmam/hbp025`.

Seguinot, J. (2013). "Spatial and seasonal effects of temperature variability in a positive degree-day glacier surface mass-balance model". In: *Journal of Glaciology* 59.218, pp. 1202–1204. DOI: `10.3189/2013JoG13J081`.

Seguinot, J., G. Jouvet, M. Huss, M. Funk, S. Ivy-Ochs, and F. Preusser (2018). "Modelling last glacial cycle ice dynamics in the Alps". In: *The Cryosphere Discussions*, pp. 1–30. DOI: `10.5194/tc-2018-8`.

Seguinot, J., I. Rogozhina, A. P. Stroeven, M. Margold, and J. Kleman (2016). "Numerical simulations of the Cordilleran ice sheet through the last glacial cycle". In: *The Cryosphere* 10.2, pp. 639–664. DOI: `10.5194/tc-10-639-2016`.

Sejrup, H. P., C. D. Clark, and B. O. Hjelstuen (2016). "Rapid ice sheet retreat triggered by ice stream debuttressing: Evidence from the North Sea". In: *Geology* 44.5, pp. 355–358. DOI: `10.1130/G37652.1`.

Sejrup, H. P., H. Haflidason, I. Aarseth, E. King, C. F. Forsberg, D. Long, and K. Rokoengen (1994). "Late Weichselian glaciation history of the northern

North Sea". In: *Boreas* 23.1, pp. 1–13. DOI: 10.1111/j.1502-3885.1994.tb00581.x.

Shepherd, A., D. J. Wingham, J. A. Mansley, and H. F. Corr (2001). "Inland thinning of Pine Island Glacier, West Antarctica". In: *Science* 291.5505, pp. 862–864. DOI: 10.1126/science.291.5505.862.

Singarayer, J. S., P. J. Valdes, P. Friedlingstein, S. Nelson, and D. J. Beerling (2011). "Late Holocene methane rise caused by orbitally controlled increase in tropical sources". In: *Nature* 470.7332, pp. 82–86. DOI: 10.1038/nature09739.

Small, D., S. Benetti, D. Dove, C. K. Ballantyne, D. Fabel, C. D. Clark, D. M. Gheorghiu, J. Newall, and S. Xu (2017). "Cosmogenic exposure age constraints on deglaciation and flow behaviour of a marine-based ice stream in western Scotland, 21–16 ka". In: *Quaternary Science Reviews* 167, pp. 30–46. DOI: 10.1016/j.quascirev.2017.04.021.

Stone, E. J., D. J. Lunt, I. C. Rutt, and E. Hanna (2010). "Investigating the sensitivity of numerical model simulations of the modern state of the Greenland ice-sheet and its future response to climate change". In: *The Cryosphere* 4.3, pp. 397–417. DOI: 10.5194/tc-4-397-2010.

Svendsen, J. I., J. P. Briner, J. Mangerud, and N. E. Young (2015). "Early break-up of the Norwegian Channel Ice Stream during the Last Glacial Maximum". In: *Quaternary Science Reviews* 107, pp. 231–242. DOI: 10.1016/j.quascirev.2014.11.001.

Valdes, P. J. et al. (2017). "The BRIDGE HadCM3 family of climate models: HadCM3@Bristol v1.0". In: *Geoscientific Model Development* 10.10, pp. 3715–3743. DOI: 10.5194/gmd-10-3715-2017.

Wingham, D. J., D. W. Wallis, and A. Shepherd (2009). "Spatial and temporal evolution of Pine Island Glacier thinning, 1995–2006". In: *Geophysical Research Letters* 36.17, p. L17501. DOI: 10.1029/2009GL039126.

Chapter 5

Discussion and Conclusions

5.1 Research Aims and Questions

The aim of this thesis is to establish the role of ice dynamics in the evolution of the British-Irish Ice Sheet (BIIS). In Chapter 1, this overarching aim was sub-divided into three Research Questions (Table 5.1). Each research chapter in this thesis (Chapters 2-4) address these Research Questions. This was achieved through a series of ice sheet modelling experiments, and comparisons to empirical data. Using this, I am able to address the role of ice streams in the demise of the British-Irish Ice Sheet.

In this section, the research questions posed in the introduction of this thesis (Table 5.1) are addressed based on the results from the research chapters (Chapters 2-4).

Research Questions (RQ)	Chapters
RQ1: What was the role of marine processes in the deglaciation of the British-Irish Ice Sheet?	2+4
RQ2: How can the position, spacing, and evolution of ice streams of the British-Irish Ice Sheet be accurately simulated?	2+3
RQ3: How can ice stream dynamics interact with other mechanisms driving deglaciation?	2+3+4

Table 5.1: A summary of the research questions addressed in this thesis. Further detail is provided in the subsequent sections. Table reproduced from Chapter 1.

5.1.1 What was the role of marine processes in the deglaciation of the British-Irish Ice Sheet?

Empirical reconstructions of the deglaciation of the BIIS have suggested an influence from Marine Ice Sheet Instability (MISI) (Bradwell et al., 2019). The empirical evidence for this is threefold. First, the majority of the BIIS was grounded below sea level at maximum extent (Clark et al., 2012), meaning that the BIIS would have been vulnerable to marine processes. Second, there are regions of rapid retreat of the BIIS, reconstructed using geochronological dating. Third, these regions of reconstructed rapid retreat sometimes form on retrograde bed slopes (Bradwell et al., 2019), which is required to cause MISI. Despite this compelling circumstantial evidence, the rapid retreat could be the result of numerous other mechanisms, such as climate or ocean forcing, and numerical modelling was required to demonstrate the vulnerability of the BIIS to MISI. Numerical modelling is also required to simulate the interaction of MISI with other factors, like lateral topography, or the effect of ice shelf buttressing, which can allow a stable grounding line position on a retrograde bed slope (Gudmundsson, 2013).

The work in Chapter 2 tests the influence of MISI on the Minch Ice Stream using a series of idealised ice sheet model experiments. Whereas in reality rapid ice sheet change can be caused by a number of forcings and feedbacks, such as climate forcing, and ice sheet elevation lapse rate feedbacks, these experiments isolated the influence of MISI by removing other feedbacks. A constant climate forcing was used, and there was no surface mass balance lapse rate feedback. The Minch Ice Stream was forced with a constant climate and ocean forcing, causing a retreat from the continental shelf edge to the Scottish Highlands. At 800-year intervals during the simulated retreat, a separate experiment was started where the climate and ocean perturbations were reversed. This tested for hysteresis in the retreat of the Minch Ice Stream. Without a lapse rate feedback, assuming no influence of MISI, there should be no hysteresis in the retreat of the Minch Ice Stream.
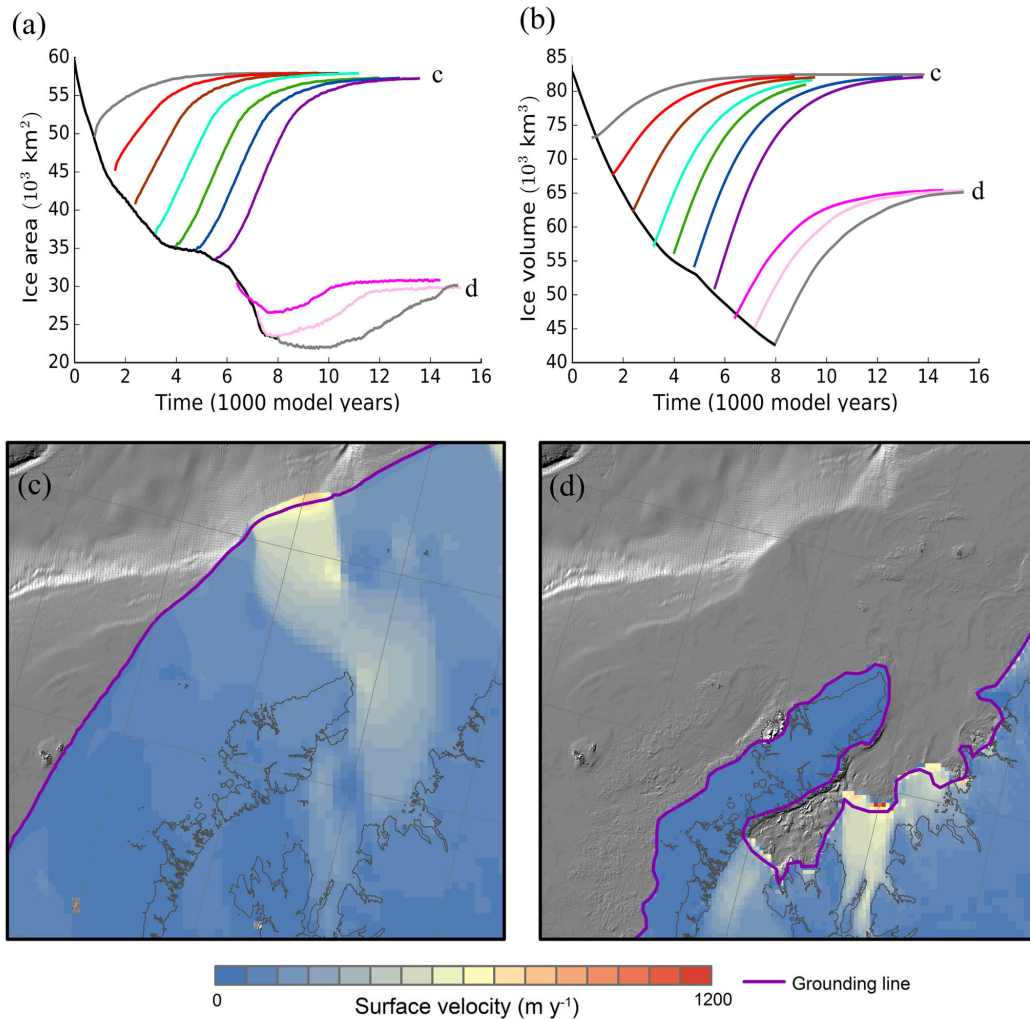
Figure 5.1: Results of the ensemble of READVANCE simulations testing instability in the Minch Ice Stream. (a, b) Evolution of the ice sheet area (a) and volume (b) over the Minch sector in the RETREAT (black) and READVANCE simulations (coloured lines). Line colours correspond to those of (Figure 2.6), such that the initialisation of the READVANCE simulations is 400 years later than the timing of the grounding line positions shown in Figure 2.6. Labels "c" and "d" indicate the "maximum" (c) and "collapsed" (d) stable states with corresponding panels showing the respective surface ice sheet velocity (m yr^{-1}) and grounding line locations (purple line). Figure reproduced from Chapter 2.

Instead, the simulations showed there was no hysteresis during the initial retreat of the ice stream, but if the grounding line retreated into the inner Minch, a region of retrograde bed slope, it instead recovered to a smaller ice volume and extent (Figure 5.1). This point of divergence is coincident with the start of a retrograde bed slope in the Minch, which can cause MISI. This is numerical

evidence that the Minch Ice Stream was vulnerable to MISI, in agreement with the empirical evidence (Bradwell et al., 2019).

Further work in Chapter 4 simulating the Norwegian Channel Ice Stream provided evidence of MISI at multiple points along the ice stream retreat. Two periods of rapid retreat were simulated at 1 km horizontal resolution, both experiencing grounding line retreat exceeding 2 km/y, as the grounding line enters a region of retrograde slope. Unlike the simulations in Chapter 2, here MISI occurs in tandem with rapid surface lowering and surface-elevation feedbacks, contributing to the rapid retreat of the grounding line. Periods of rapid grounding line retreat of the Norwegian Channel Ice Stream cause peaks in freshwater flux 5-10× the baseline level from the ice sheet. The results from Chapter 2 and Chapter 4 demonstrate that the BIIS experienced MISI during deglaciation.

In Chapter 2, the role of ice shelf buttressing was tested with idealised ice sheet model simulations. Ice shelves have a buttressing effect on the ice streams upstream of them, and the removal of large ice shelves in the Antarctic peninsula has been linked with the subsequent acceleration and thinning of upstream glaciers (Scambos et al., 2004). Empirical evidence for palaeo ice shelf evolution is sparse, being disconnected from the bed they do not have the geomorphic signatures of a grounded ice sheet. However, Bradwell et al. (2019) suggested that the Minch Ice Stream's demise was hastened by the collapse of its ice shelf.

The idealised retreat experiment used to test for hysteresis of retreat initially forms a small ice shelf, which becomes larger once in the Minch Straight, surrounded laterally by the Outer Hebrides and the Scottish Mainland. The retreat simulation was re-run with a higher sub-shelf melt rate, to force the collapse of the ice shelf. Once the ice shelf is removed, the higher sub-shelf melt rate has no effect because there is no sub shelf region for the flux to be applied to. By comparing the retreat with and without an ice shelf, it is possible to determine the role of ice shelf buttressing in the deglaciation of the Minch Ice Stream.
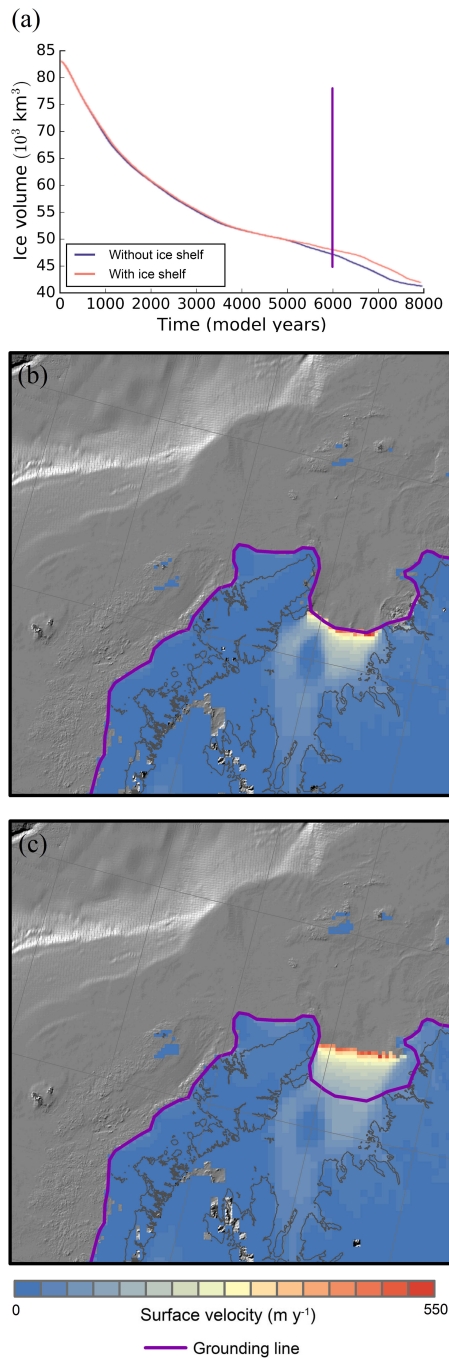
Figure 5.2: Effect of ice shelves. The contemporary coast is shown as a thin grey line. (a) Evolution of grounded ice sheet volume over the Minch sector in simulation RETREAT with ice shelves (red line) and RETREAT_NOSHELF in which ice shelves are forcibly removed (blue line). (b, c) Surface velocity and grounding line location (purple line) in RETREAT_NOSHELF (b) and RETREAT (c). Figure reproduced from Chapter 2.

The simulations find that for the first 5,000 years of retreat, while the ice shelf is laterally unconstrained, there is no difference between the retreat rate of the ice stream with and without an ice shelf. However, after 5,000 model years, once the ice shelf is laterally constrained by surrounding ice and land, there is a divergence in mass loss rates of the two experiments. The experiment with the ice shelf removed retreats faster, resulting in the ice volume being ~10% smaller by 7,000 model years. Empirical evidence of the last Eurasian ice sheet has the western ice margin constrained by the continental shelf edge across the majority of the Atlantic margin (Hughes et al., 2016). This suggests that ice shelves at maximum ice extent across the Atlantic margin would be similar to the Minch ice shelf in the early stages of deglaciation, limited in size by the continental shelf break, and unconstrained. It is likely, therefore, that ice shelves along this Atlantic margin were not influential in the retreat of the ice sheet until the grounding line retreated to areas laterally constrained by topography or surrounding ice. This work provides evidence that ice shelf buttressing may have been influential for portions of the retreat of the BIIS, but not for the majority of retreat.

Bradwell et al. (2019) suggest that the Minch Ice Stream collapse was initiated by the transition of the grounding line from a soft and deformable bed to a hard bed, causing dynamic thinning at the margin of the ice stream and subsequent collapse of the ice shelf. This would increase the vulnerability of the ice stream to Marine Ice Sheet Instability on the retrograde slope of the inner Minch. However, simulations of the Minch Ice Stream in Chapter 2 do not show this behaviour as the grounding line retreats over a region of higher basal friction, and show only a minor role of ice shelf buttressing (Figure 5.2). The simulations suggest that the process proposed by Bradwell et al. (2019) is not necessary to explain rapid retreat of the Minch Ice Stream out of step from wider climate forcing.

5.1.2 How can the position, spacing, and evolution of ice streams of the British-Irish Ice Sheet be accurately simulated?

In Chapter 2, ice streams of the BIIS were simulated by imposing lower basal friction coefficients in regions where ice streaming was reconstructed. This allowed for the Minch Ice Stream to be simulated (Figure 5.1c), as the ice stream location is well mapped. However, this method does not allow the simulation of ice streams that are not empirically reconstructed, or allow for the evolution of ice streams as they retreat, so it is not suitable to apply to the entire BIIS or Eurasian Ice Sheet.

Another set of experiments were designed to capture a wider variety of ice streams of the BIIS, in order to test the influence of ice streams on the demise of the entire BIIS. Simulating ice streams of the BIIS that were not well empirically reconstructed required a model that could simulate the initiation and evolution of ice streams without them being forced with a spatially varying basal friction coefficient. BISICLES was developed to include a sliding law which is sensitive to the presence of till water. For comparison, this version of the model is referred to as BISICLES_hydro, (https://anag-repo.lbl.gov/svn/BISICLES/public/branches/slc_dev_2018, revision 3776). BISICLES is a vertically integrated ice sheet model with L1L2 physics retained from the full Stokes flow equations (Schoof and Hindmarsh, 2010), including an approximation of membrane stress. These membrane stresses are necessary for producing ice streams of accurate width independent of resolution (Hindmarsh, 2009). A till-stored water layer at the base of the ice sheet evolves through a flux of basal meltwater and drainage from the till-stored water layer. The increasing saturation of the till layer reduces the basal shear stress according to a Coulomb sliding law.

BISICLES_hydro was initially tested using an idealised experiment. A square ice sheet was prescribed with calving margins on the low y-axis and high x-axis,
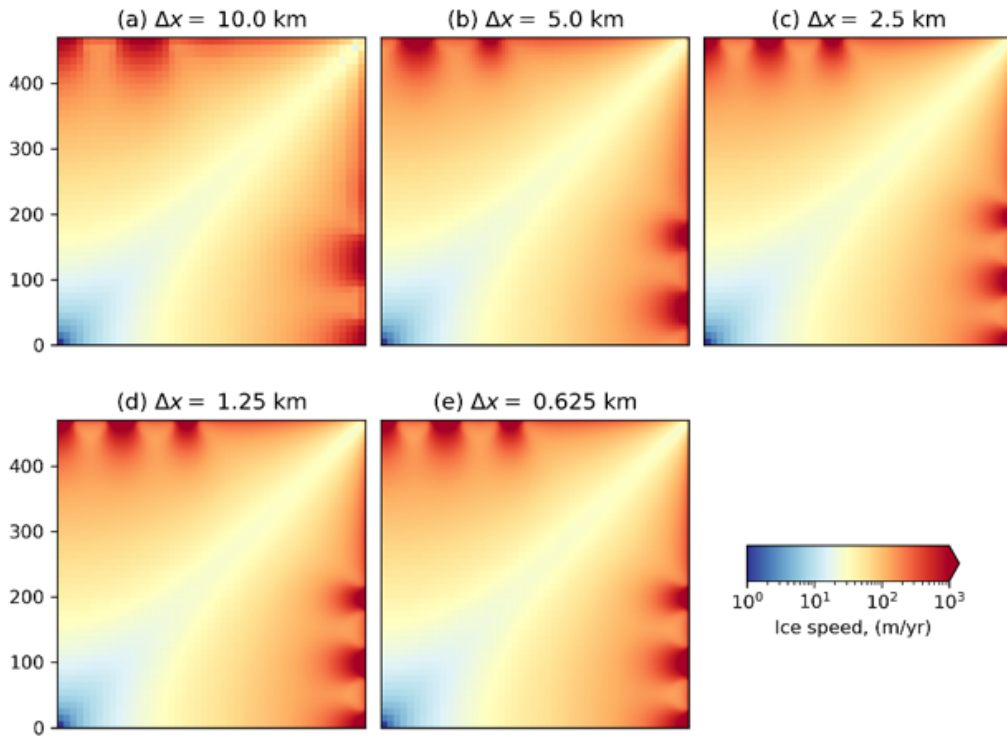
Figure 5.3: Simulated ice velocity with an idealised set-up using BISICLES_hydro. Increasing resolution increases the number of ice streams (a-e). Figure reproduced from the appendix.

exploiting symmetry to cut computational cost in the same manner as previously reported (Payne and Dongelmans, 1997; Hindmarsh, 2009). The simulations produce ice streams along the calving margin, spaced between areas of lower velocity. Two streams are produced along each front at the coarser resolutions (10 km and 5 km, Figures 5.31a,b), and there is a clearly visible difference in stream location between these cases. Refining to 2.5 km produces a third stream along both fronts (Figure 5.3c), once again straddling the symmetry axes to give five streams along each front in total, and this pattern is retained in both the 1.25 km and 0.625 km cases (Figure 5.3d,e). These idealised simulations demonstrate the ability of BISICLES_hydro to simulate the spontaneous generation of ice streams without forcing them with a spatially variable basal friction coefficient.

After testing BISICLES_hydro on an idealised symmetrical ice sheet, the empirical record of the BIIS was used to test the model. The BIIS offers a realistic bed geometry to test BISICLES_hydro, along with the extensive empirical record

of ice streaming to help test the skill of the model in simulating ice stream positions. These experiments idealise the climate forcing; the experiments are not intended to act as a reconstruction of the BIIS, rather the BIIS acts as a testbed for BISICLES_hydro to simulate reasonable ice stream width, spacing, and position over millennia.

The model domain is set up to cover the entire BIIS, and uses an idealised climate forcing to run a 10,000 year advance phase, followed by a 10,000 year retreat phase. By simulating an idealised glacial cycle, evolution in ice stream position can be observed, and compared to the empirical record. The simulated ice streams are compared to empirically mapped ice streams both with qualitative comparisons (Figure 5.4), and a quantitative tool that compares modelled and mapped flowsets.
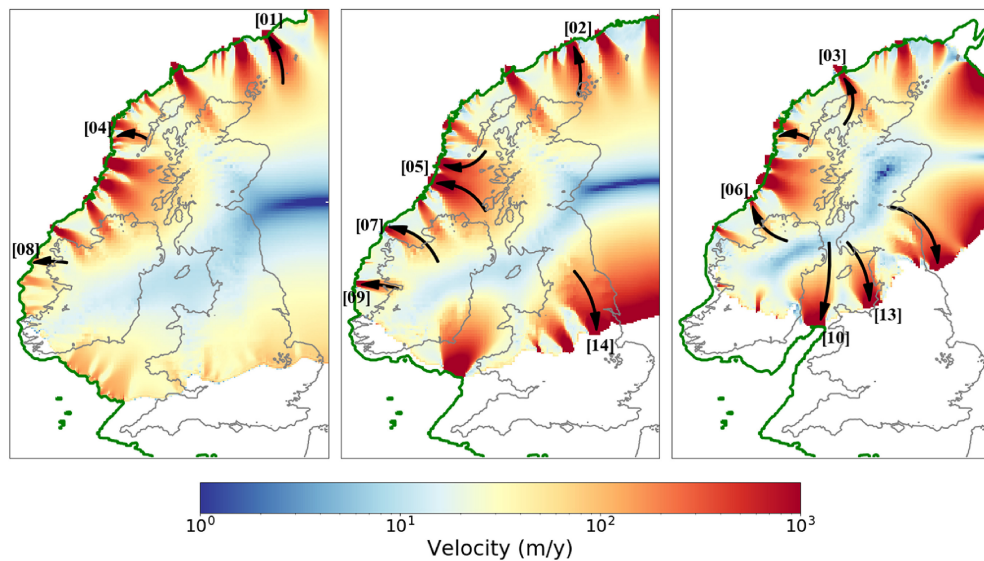
Figure 5.4: Ice velocity at 10,000, 12,500, and 15,000 model years. Locations of key ice streams empirically reconstructed in the literature are highlighted with black arrows, with ice streams numbered as in Figure 3.1 and Table 3.2. The wide ice streams in the North Sea are caused by a domain-edge effect. Figure reproduced from Chapter 3.

The simulated ice streams strongly match empirically reconstructed ice streams of the BIIS. The majority of ice streams (11/19) are both simulated and empirically mapped. The second largest group (5/19) are simulated, but there is limited empirical evidence for ice streaming. In one case, this prompted new empirical

mapping (Figure 3.11), providing evidence of ice streaming in a region where it was simulated. The smallest group (3/19) are not simulated despite empirical evidence. Overall, the model demonstrates significant skill in simulating the initiation and evolution of ice streams of the BIIS without being forced with a spatially varying basal friction coefficient, allowing future work modelling the deglaciation of palaeo ice sheets with an accurate representation of ice streaming.

5.1.3 How can ice stream dynamics interact with other mechanisms driving deglaciation?

Ice streams interact with other ice sheet processes to accelerate deglaciation. For example, it has been shown that surface melting can route to the ice sheet bed, and cause a subsequent seasonal acceleration of an ice sheet (Zwally et al., 2002). It has also been shown in idealised experiments that raising the Equillibrium Line Altitude (ELA) causes an acceleration of ice streams, increasing the rate of deglaciation (Robel and Tziperman, 2016). The surface profile of a streaming ice sheet causes depressions in the ice surface where ice velocity is higher, meaning that ice streams are more vulnerable to surface melting than inter-stream regions of the ice sheet. Millennial-scale climate variability, such as Heinrich events, suggest ice streams contribute to rapid ice sheet change (Calov et al., 2002; Alvarez-Solas et al., 2010; Ziemen et al., 2014). Further understanding interacting mechanisms of deglaciation is necessary to decrease the uncertainty of future ice sheet projections.

Simulations investigating marine processes of the Minch Ice Stream in Chapter 2 were designed to isolate the influence of marine processes on the ice stream. Although the entire marine margin of an ice sheet is vulnerable to marine instabilities, in the case of Marine Ice Sheet Instability, mass loss is proportional to depth at the grounding line and ice velocity. Therefore, as ice streams have velocities an order of magnitude faster than inter-ice stream regions, Marine Ice Sheet Instability can cause an order of magnitude more mass loss in ice streaming

regions. The simulations in Chapter 2 demonstrate how an ice stream interacting with marine processes can cause rapid ice sheet mass loss.

The simulations of an idealised advance and retreat cycle of the BIIS in Chapter 3 demonstrated an evolution of ice stream behaviour. As the area and volume of the ice sheet grew, the number of ice streams also grew (Figure 5.5), allowing more mass to be transported from the ice sheet interior to the margins. The most significant change in ice stream behaviour was during the retreat phase, where the SMB imposes melting at the southern margin of the ice sheet. This lowering steepens the ice surface at the ice stream onset zone, accelerating ice streaming, resulting in a shallower surface profile downstream of the onset zone. This means that during the advance phase there is only extensive streaming along the northern margin, whilst streaming also occurs along the southern margin during the retreat phase (Figure 5.5). The feedback between SMB and ice stream behaviour has been demonstrated in other model experiments (Robel and Tziperman, 2016), and this effect has been shown to promote rapid deglaciation.

Following the developments made in Chapter 3 in the ability to model palaeo ice streams, simulations of the deglaciation of the North Sea could now be undertaken. The North Sea sector of the Eurasian Ice Sheet was a shallow marine basin, topographically dominated by the Norwegian Channel, a deep ($\sim$200-600 m) trough on the western Norwegian coast. During the last glacial period, the channel was occupied by a large Norwegian Channel Ice Stream (Sejrup et al., 1994; King et al., 1998; Svendsen et al., 2015), with a width similar to the contemporary Thwaites glacier (Joughin et al., 2014). Uncertainties in the deglaciation style of the North Sea remain (Clark et al., 2012; Hughes et al., 2016), but the influence of the Norwegian Channel Ice Stream has been suggested from empirical evidence. Sejrup et al. (2016) suggested deglaciation of the North Sea triggered by retreat of the Norwegian Channel Ice Stream, leading to debuttressing of adjacent ice, and an "unzipping" of the BIIS and Fennoscandian Ice Sheet originating from the Norwegian Channel.
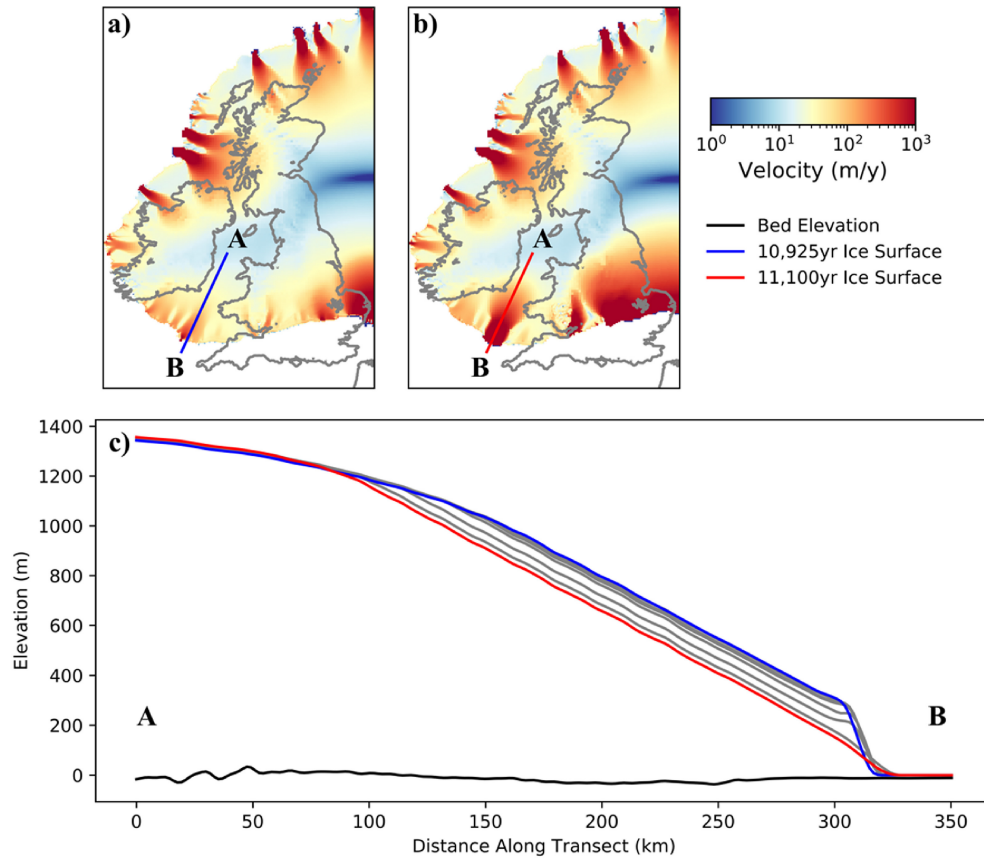
Figure 5.5: Transect of the ice surface at a period before and after the onset of significant ice streaming in the Celtic Sea (10,925 and 11,100 model years respectively). Grey curves show the ice surface at 25 year intervals between the two snapshots. Figure reproduced from Chapter 3.

Simulations of the North Sea demonstrate the considerable influence of the Norwegian Channel Ice Stream. Analysis of those simulations show that the Norwegian Channel Ice Stream deglaciated through combined instabilities of ice dynamics (causing a depression of the ice sheet surface around the Norwegian Channel Ice Stream), lapse rate feedbacks (causing higher surface melting as the ice stream lowers) (Figure 5.6), and Marine Ice Sheet Instability (causing periods of rapid retreat facilitated by thinning of the ice stream). The simulations demonstrate that ice streams contribute to the demise of the BIIS by interacting with other mechanisms of deglaciation, both from the ocean and atmosphere.
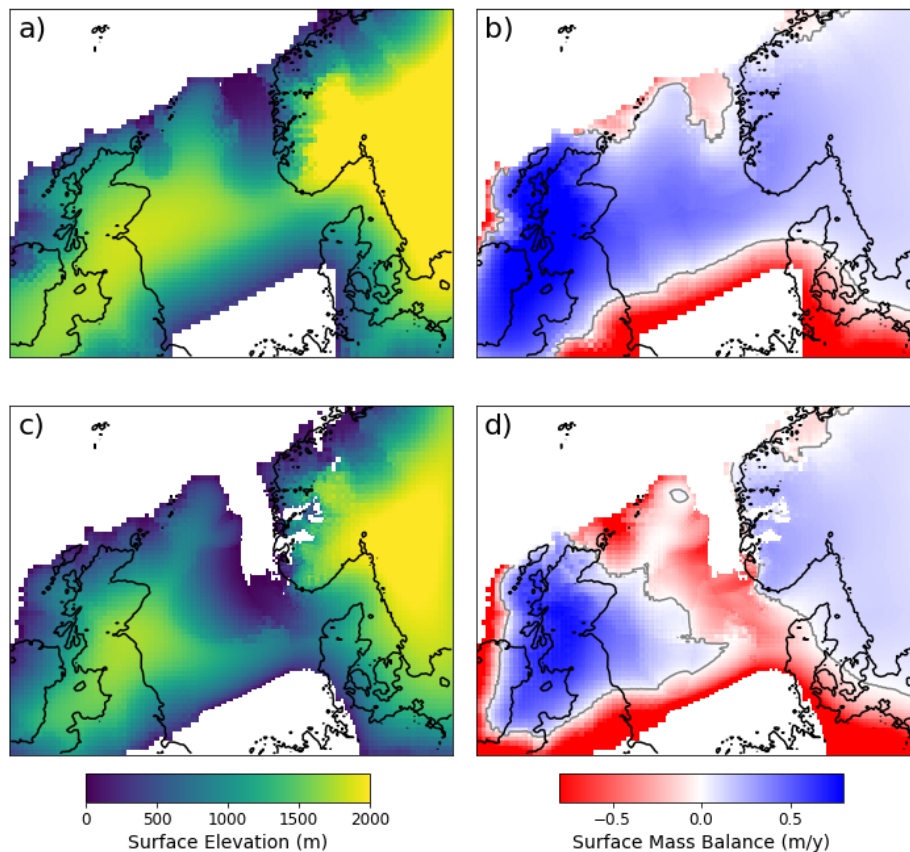
Figure 5.6: Ice sheet surface elevation and Surface Mass Balance at 23 ka BP (a-b) and 21.5 ka BP (c-d) in ensemble member *ns_002*. Figure reproduced from Chapter 4.

5.2 The role of ice streams in the demise of the British-Irish Ice Sheet

The experiments presented in the research chapters (Chapters 2-4) demonstrate that ice streams had a considerable role in the demise of the BIIS. The mechanisms of this role are numerous. First, ice streams of the BIIS were vulnerable to MISI, as demonstrated numerically in Chapter 2 and Chapter 4. Ice streams are vulnerable to MISI because they are likely to form in bathymetric troughs, and because ice streams cause a depression in the surface elevation of an ice sheet. It is also more influential when ice streams experience MISI compared to inter-stream regions, because the potential increase in ice flux across the grounding

line is proportional to ice velocity. Major contemporary ice streams are either experiencing, or are vulnerable to MISI (Favier et al., 2014; Joughin et al., 2014), and the work in Chapter 2 numerically demonstrated that the Minch Ice Stream was vulnerable to this same marine process. The simulations in Chapter 4 also demonstrate that the Norwegian Channel Ice Stream experienced MISI in the later stages of retreat.

Another process by which ice streams were influential in the demise of the BIIS was the feedback between surface melting and ice streaming. In the simulations presented in Chapter 3, increasing surface melting along the southern margin causes an increase in ice streaming, by steepening the ice surface at the ice stream onset zone, accelerating ice streaming. The feedback between SMB and ice stream behaviour has been demonstrated numerically (Robel and Tziperman, 2016), and has been shown to promote rapid deglaciation. This effect is also evident for the Norwegian Channel Ice Stream, simulated in Chapter 4. There, a combination of ice dynamics, surface lapse rate feedbacks, and marine ice sheet dynamics interact to allow rapid retreat of the Norwegian Channel Ice Stream. The work in Chapter 4 also demonstrates the large influence of a single ice stream on the retreat dynamics of an entire catchment. In essence, the deglaciation of the Norwegian Channel Ice Stream allows the deglaciation of the entire North Sea basin.

Overall, the demise of the BIIS was a function of a number of mechanisms. The most influential effect is changes in the climate and the surface mass balance of the ice sheet. However, the modelling results presented in this thesis suggests that ice streams helped facilitate the demise of the BIIS, and were influential drivers of retreat in some sectors. This work demonstrates the importance of correctly simulating ice stream dynamics when considering the future evolution of the Greenland and Antarctic Ice Sheets.

In the research chapters of this thesis new knowledge has been gained about the behaviour and evolution of the BIIS, and these are summarised in Figure 5.7.
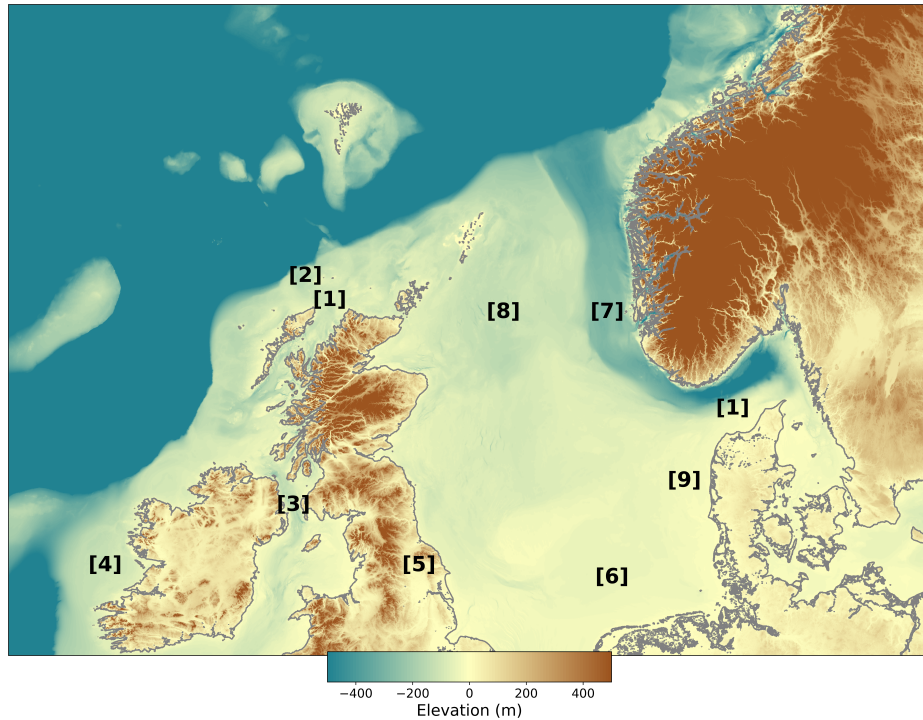
Figure 5.7: A summary of knowledge gained from the research described in this thesis. Numbered locations are detailed in the subsequent list.

1. The Minch Ice Stream and the Norwegian Channel Ice Stream experienced Marine Ice Sheet Instability in the later stages of retreat.

2. Ice shelf buttressing of the Minch Ice Stream was minimal until the ice stream margin became laterally constrained.

3. There is new model and data evidence of an ice stream in the North Channel.

4. Ice streams of western Ireland evolve significantly through a glacial cycle.

5. Surface mass balance forcing can increase ice streaming around the ice sheet margin.

6. A southern North Sea Lake correction is required to match the ice sheet margin in the North Sea.

7. Elevation-lapse rate feedbacks facilitate rapid retreat of the Norwegian Channel Ice Stream.

8. Initial North Sea ice retreat into the Witch Ground Basin appears to be glaciologically implausible.

9. Final separation of the BIIS and Fennoscandian Ice Sheets occurred near the Jutland Bank, away from the point of initial confluence.

5.3   Limitations and future work

5.3.1   Initial Ice Sheet States

The simulations completed as part of this thesis were comparatively computationally expensive. As an example, from the ensemble of simulations described in Chapter 4, one ensemble member took ∼10,000 core hours to complete. This was at the relatively coarse horizontal resolution of 8 km. This expense limited the model time the simulations could be run for, limiting the opportunity for full transient runs of the advance and retreat of the BIIS. Instead, in Chapter 2 the deglaciation simulations were started from a stable LGM maximum extent, avoiding the need to simulate the build-up of the ice sheet. An alternative method was used in Chapter 4, where a single idealised advance simulation was used as the starting point for the deglaciation ensemble. This avoided the assumption of a stable LGM maximum extent, but it is not clear how sensitive the resulting deglaciations are to the configuration at maximum extent. It is likely that part of the improved match between model and empirical evidence of the North Sea deglaciation in Chapter 4 is in part because of the initiation of the ice sheet extent to best match the empirical margins. As computational resources increase, it is preferential for future work to simulate a transient advance and retreat of an ice sheet. Future work should simulate the advance and retreat of the North Sea sector of the Eurasian Ice Sheet, and explore if this produces a more diverse range of deglaciation patterns.

5.3.2 Modelling Limitations

The research in this thesis is also subject to many limitations common to ice sheet modelling work. For example, the simulations of grounding line migration in Chapter 2 and 4 were at 0.5 and 1 km resolution respectively, which was deemed sufficient to simulate grounding line migration accurately (Gladstone et al., 2012). However, the computational cost of the simulations limits the ability to simulate the grounding line at higher resolution, and further test resolution dependence. Millennial-scale simulations of a large portions of an ice sheet, such as in Chapter 4, can also not yet be simulated at adequately fine grounding line resolution.

The representation of subglacial hydrology developed and used in this thesis is also a parameterisation, rather than a fully physically-based description of basal meltwater evolution. Horizontal transport of sub-glacial meltwater is ignored, despite efforts to map subglacial meltwater channels (Le Brocq et al., 2013; Livingstone et al., 2013), and it has been suggested that this process may be important to ice sheet dynamics (Chandler et al., 2013; Gong et al., 2017). Horizontal routing of subglacial meltwater is a planned future development of BISICLES.

Finally, the model-data comparison in this thesis was limited to indirect comparisons. For example, modelled flow direction was compared to flowset orientation, and modelled margins compared to moraines. Variable preservation of landforms, and remaining uncertainty in the formation of the landforms limits this indirect comparison. Progress has been made in GCMs to simulate climate proxies (Dentith et al., in prep), allowing for a more direct model-data comparison. An ice sheet model that also aimed to reproduce the palaeo record of landform assemblages would allow more direct model-data comparison.

5.3.3 Climate Forcing

Another limitation of the simulations presented in this thesis is that they are forced with GCM simulations which in turn are not forced with the simulated ice sheets. In some cases there are good reasons for this. In Chapter 2, the climate forcing was idealised so as to isolate the influence of MISI, the simulations were designed to test the processes of change rather than simulate a ice stream reconstruction. Similarly, in Chapter 3, an idealised climate was used because the focus of the experiments was to test the ice sheet model development. In Chapter 4, running the ice sheet simulations offline avoided the increased computation costs of fully coupled simulations, along with other significant technical challenges of running fully coupled simulations. This allowed for the deglaciation dynamics to be explored, but other research questions cannot be answered with offline simulations. For example, it is unclear what the climatic and oceanic effect of the peak freshwater flux from the deglaciation of the North Sea could have been.
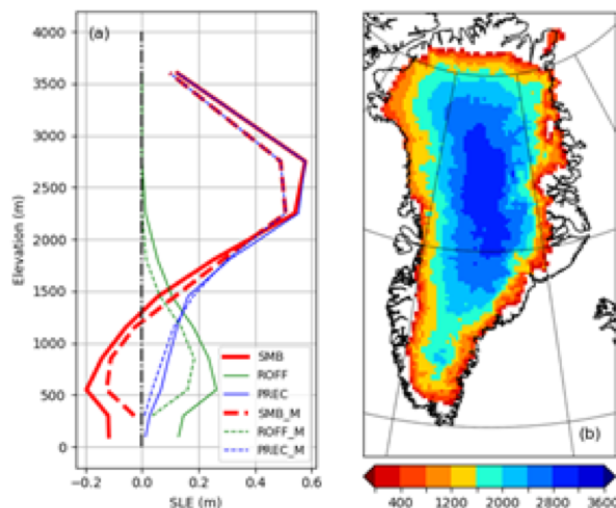
Figure 5.8: a) The vertical distribution of Greenland Ice Sheet SMB (red line) in FAMOUS-ice (solid) compares well to MAR, a specialised regional climate model (dashed). b) The spun-up contemporary Greenland Ice Sheet thickness resulting from the climate simulated with FAMOUS-ice. From Robin Smith and Steven George (personal communication), based on Smith et al., in prep.

Fully coupled simulations have been completed for intermediate complexity GCMs and ice sheet models (e.g. Marshall et al., 2003), but there are limita-

tions to these simulations. Recent progress has been made in efficiently coupling BISICLES to both HadCM3, a complex GCM, and FAMOUS (Figure 5.8), the fast-running version of HadCM3 (Smith, 2012). The coarser resolution of FA-MOUS allows for the simulation of millennia of coupled climate-ice experiments, and the present generation of FAMOUS has been used to successfully model past, present, and future climates (e.g. Smith and Gregory, 2012; Eby et al., 2013). This progress allows for new coupled simulations of the last deglaciation, although the low resolution of FAMOUS means that it would be more suitable for larger ice sheets such as the Laurentide Ice Sheet.

Smaller ice sheets, such as the BIIS, or the Patagonian Ice Sheet, could have improved simulation of surface mass balance by coupling to regional climate models with much higher resolution, such as RACMO (Van Meijgaard et al., 2008). RACMO is designed to calculate ice sheet surface mass balance, and has a sophisticated scheme considering the thermal properties of the snowpack, and ice sheet albedo. While full energy balance models remain too expensive to run for long palaeo-ice sheet simulations, statistical emulation techniques could provide comparable results with a reduced computational cost.

5.3.4 Beyond the British-Irish Ice Sheet

The BIIS was simulated here because it was a small marine based ice sheet, which is the best reconstructed ice sheet in the palaeo record (Clark et al., 2018). This meant that important ice sheet mechanisms could be simulated as part of a relatively small domain, and the performance of the model could be easily tested, as shown in the research chapters. However, the small size of the BIIS means it contributed only a tiny fraction of eustatic sea level rise during the last deglaciation, and it likely had very limited influence in altering the climate. Now that palaeo ice sheet model simulations have been successfully completed with BISICLES, it will be useful to undertake simulations in a more diverse range of contexts, including a large continental ice sheet like the Laurentide Ice Sheet,

more marine basins like the Barents Sea, and more topographically constrained glaciation like the Patagonian Ice Sheet.

5.4   Towards Improved Projections of Future Ice Sheet Change

The palaeo record has proved to be a useful tool to better understand contemporary ice sheets on a number of occasions. For example, there is evidence of ice stream shutdown on the Siple Coast of Antarctica (Jacobel et al., 2000), but it was research of palaeo ice stream beds that first provided evidence of the mechanisms which can cause ice stream shutdown (Stokes et al., 2006). Observations of palaeo-subglacial hydrological features have also been influential in building conceptual and numerical models of subglacial hydrology (Clark and Walder, 1994; Hewitt and Creyts, 2019). Recently, statistical analysis of simulations of mid-Pliocene Antarctica suggested that catastrophic collapse of marine ice cliffs was not a necessary mechanism to explain past sea level rise, and therefore revised estimates of sea level change in the 21st century (Edwards et al., 2019).

The work in this thesis was motivated by the requirement to improve future projections of ice sheet change, and it has provided results which can contribute towards that aim. The work in Chapter 2 simulating the Minch Ice Stream showed that the BIIS was vulnerable to the same marine processes as in West Antarctica, and therefore provides a useful analogue. Simulations of ice stream evolution, in Chapter 3, provides the necessary ice sheet model development and testing so that simulations of century-scale future ice sheet change (e.g. Cornford et al., 2015) can now simulate the evolving ice streaming. Finally, the research in Chapter 4 simulates behaviour of the Norwegian Channel Ice Stream, an ice stream with a similar width to the contemporary Thwaites Glacier. By demonstrating a good match to empirical data, the results suggests that BISICLES is capable of simulating ice stream and ice sheet change for long timescales. All

considered, the work in this thesis can contribute not just to improved simulations of palaeo ice sheet change, but also improved projections of future ice sheet change.

References

Alvarez-Solas, J., S. Charbit, C. Ritz, D. Paillard, G. Ramstein, and C. Dumas (2010). "Links between ocean temperature and iceberg discharge during Heinrich events". In: *Nature Geoscience* 3.2, pp. 122–126. DOI: 10.1038/ngeo752.

Bradwell, T. et al. (2019). "Ice-stream demise dynamically conditioned by trough shape and bed strength". In: *Science Advances* 5.4, eaau1380. DOI: 10.1126/sciadv.aau1380.

Calov, R., A. Ganopolski, V. Petoukhov, M. Claussen, and R. Greve (2002). "Large-scale instabilities of the Laurentide ice sheet simulated in a fully coupled climate-system model". In: *Geophysical Research Letters* 29.24, pp. 69–1–69–4. DOI: 10.1029/2002GL016078.

Chandler, D. M. et al. (2013). "Evolution of the subglacial drainage system beneath the Greenland Ice Sheet revealed by tracers". In: *Nature Geoscience* 6, p. 24. DOI: 10.1038/NGEO1737.

Clark, C. D., A. L. Hughes, S. L. Greenwood, C. Jordan, and H. P. Sejrup (2012). "Pattern and timing of retreat of the last British-Irish Ice Sheet". In: *Quaternary Science Reviews* 44, pp. 112–146. DOI: 10.1016/j.quascirev.2010.07.019.

Clark, C. D. et al. (2018). "BRITICE Glacial Map, version 2: a map and GIS database of glacial landforms of the last British-Irish Ice Sheet". In: *Boreas* 47.1, 11–e8. DOI: 10.1111/bor.12273.

Clark, P. U. and J. S. Walder (1994). "Subglacial drainage, eskers, and deforming beds beneath the Laurentide and Eurasian ice sheets". In: *Geological Society*

of America Bulletin 106.2, pp. 304–314. DOI: `10.1130/0016-7606(1994)106<0304:SDEADB>2.3.CO;2`.

Cornford, S. L. et al. (2015). "Century-scale simulations of the response of the West Antarctic Ice Sheet to a warming climate". In: *Cryosphere* 9.4, pp. 1579–1600. DOI: `10.5194/tc-9-1579-2015`.

Eby, M. et al. (2013). "Historical and idealized climate model experiments: An intercomparison of Earth system models of intermediate complexity". In: *Climate of the Past* 9.3, pp. 1111–1140. DOI: `10.5194/cp-9-1111-2013`.

Edwards, T. L. et al. (2019). "Revisiting Antarctic ice loss due to marine ice-cliff instability". In: *Nature* 566.7742, pp. 58–64. DOI: `10.1038/s41586-019-0901-4`.

Favier, L., G. Durand, S. L. Cornford, G. H. Gudmundsson, O. Gagliardini, F. Gillet-Chaulet, T. Zwinger, A. J. Payne, and A. M. Le Brocq (2014). "Retreat of Pine Island Glacier controlled by marine ice-sheet instability". In: *Nature Climate Change* 4.2, pp. 117–121. DOI: `10.1038/nclimate2094`.

Gladstone, R. M., A. J. Payne, and S. L. Cornford (2012). "Resolution requirements for grounding-line modelling: Sensitivity to basal drag and ice-shelf buttressing". In: *Annals of Glaciology* 53.60, pp. 97–105. DOI: `10.3189/2012AoG60A148`.

Gong, Y., T. Zwinger, S. Cornford, R. Gladstone, M. Schäfer, and J. C. Moore (2017). "Importance of basal boundary conditions in transient simulations: Case study of a surging marine-terminating glacier on Austfonna, Svalbard". In: *Journal of Glaciology* 63.237, pp. 106–117. DOI: `10.1017/jog.2016.121`.

Gudmundsson, G. H. (2013). "Ice-shelf buttressing and the stability of marine ice sheets". In: *The Cryosphere* 7, pp. 647–655. DOI: `10.5194/tc-7-647-2013`.

Hewitt, I. J. and T. T. Creyts (2019). "A Model for the Formation of Eskers". In: *Geophysical Research Letters* 46.12, pp. 6673–6680. DOI: `10.1029/2019GL082304`.

Hindmarsh, R. C. (2009). "Consistent generation of ice-streams via thermo-viscous instabilities modulated by membrane stresses". In: *Geophysical Research Letters* 36.6, p. L06502. DOI: 10.1029/2008GL036877.

Hughes, A. L., R. Gyllencreutz, Ø. S. Lohne, J. Mangerud, and J. I. Svendsen (2016). "The last Eurasian ice sheets - a chronological database and time-slice reconstruction, DATED-1". In: *Boreas* 45.1. DOI: 10.1111/bor.12142.

Jacobel, R. W., T. A. Scambos, N. A. Nereson, and C. F. Raymond (2000). "Changes in the margin of Ice Stream C, Antarctica". In: *Journal of Glaciology* 46.152, pp. 102–110. DOI: 10.3189/172756500781833485.

Joughin, I., B. E. Smith, and B. Medley (2014). "Marine ice sheet collapse potentially under way for the thwaites glacier basin, West Antarctica". In: *Science* 344.6185, pp. 735–738. DOI: 10.1126/science.1249055.

King, E. L., H. Haflidason, H. P. Sejrup, and R. Løvlie (1998). "Glacigenic debris flows on the North Sea Trough Mouth Fan during ice stream maxima". In: *Marine Geology* 152.1-3, pp. 217–246. DOI: 10.1016/S0025-3227(98)00072-3.

Le Brocq, A. M. et al. (2013). "Evidence from ice shelves for channelized meltwater flow beneath the Antarctic Ice Sheet". In: *Nature Geoscience* 6.11, pp. 945–948. DOI: 10.1038/ngeo1977.

Livingstone, S. J., C. D. Clark, J. Woodward, and J. Kingslake (2013). "Potential subglacial lake locations and meltwater drainage pathways beneath the Antarctic and Greenland ice sheets". In: *The Cryosphere* 7.6, pp. 1721–1740. DOI: 10.5194/tc-7-1721-2013.

Marshall, S. J., D. Pollard, S. Hostetler, and P. U. Clark (2003). "Coupling ice-sheet and climate models for simulation of former ice sheets". In: *Developments in Quaternary Science* 1.C, pp. 105–126. DOI: 10.1016/S1571-0866(03)01006-6.

Payne, A. J. and P. W. Dongelmans (1997). "Self-organization in the thermomechanical flow of ice sheets". In: *Journal of Geophysical Research: Solid Earth* 102.B6, pp. 12219–12233. DOI: 10.1029/97JB00513.

Robel, A. A. and E. Tziperman (2016). "The role of ice stream dynamics in deglaciation". In: *Journal of Geophysical Research: Earth Surface* 121.8, pp. 1540–1554. DOI: 10.1002/2016JF003937.

Scambos, T. A., J. A. Bohlander, C. A. Shuman, and P. Skvarca (2004). "Glacier acceleration and thinning after ice shelf collapse in the Larsen B embayment, Antarctica". In: *Geophysical Research Letters* 31.18, p. L18402. DOI: 10.1029/2004GL020670.

Schoof, C. and R. C. Hindmarsh (2010). "Thin-film flows with wall slip: An asymptotic analysis of higher order glacier flow models". In: *Quarterly Journal of Mechanics and Applied Mathematics* 63.1, pp. 73–114. DOI: 10.1093/qjmam/hbp025.

Sejrup, H. P., C. D. Clark, and B. O. Hjelstuen (2016). "Rapid ice sheet retreat triggered by ice stream debuttressing: Evidence from the North Sea". In: *Geology* 44.5, pp. 355–358. DOI: 10.1130/G37652.1.

Sejrup, H. P., H. Haflidason, I. Aarseth, E. King, C. F. Forsberg, D. Long, and K. Rokoengen (1994). "Late Weichselian glaciation history of the northern North Sea". In: *Boreas* 23.1, pp. 1–13. DOI: 10.1111/j.1502-3885.1994.tb00581.x.

Smith, R. S. (2012). "The FAMOUS climate model (versions XFXWB and XFHCC): description update to version XDBUA". In: *Geoscientific Model Development* 5.1, pp. 269–276. DOI: 10.5194/gmd-5-269-2012.

Smith, R. S. and J. Gregory (2012). "The last glacial cycle: Transient simulations with an AOGCM". In: *Climate Dynamics* 38.7-8, pp. 1545–1559. DOI: 10.1007/s00382-011-1283-y.

Stokes, C. R., C. D. Clark, O. B. Lian, and S. Tulaczyk (2006). "Geomorphological map of ribbed moraines on the Dubawnt Lake Palaeo-Ice Stream bed: A

signature of ice stream shut-down?" In: *Journal of Maps* 2.1, pp. 1–9. DOI: 10.4113/jom.2006.43.

Svendsen, J. I., J. P. Briner, J. Mangerud, and N. E. Young (2015). "Early break-up of the Norwegian Channel Ice Stream during the Last Glacial Maximum". In: *Quaternary Science Reviews* 107, pp. 231–242. DOI: 10.1016/j.quascirev.2014.11.001.

Van Meijgaard, E., L. H. Van Ulft, W. J. de Berg, F. C. Bosveld, B. den Hurk, G. Lenderink, and A. P. Siebesma (2008). "The KNMI regional atmospheric climate model RACMO version 2.1". In: *Koninklijk Nederlands Meteorologisch Instituut* 43.

Ziemen, F. A., C. B. Rodehacke, and U. Mikolajewicz (2014). "Coupled ice sheet–climate modeling under glacial and pre-industrial boundary conditions". In: *Climate of the Past* 10.5, pp. 1817–1836. DOI: 10.5194/cp-10-1817-2014.

Zwally, H. J., W. Abdalati, T. Herring, K. Larson, J. Saba, and K. Steffen (2002). "Surface melt-induced acceleration of Greenland ice-sheet flow". In: *Science* 297.5579, pp. 218–222. DOI: 10.1126/science.1072708.

Appendix A

A.1 Minch Retreat Video
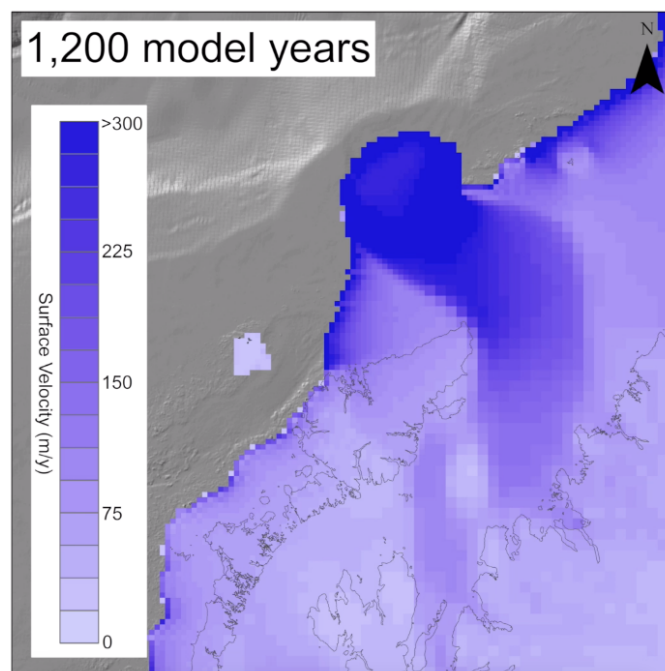
Figure A.1: A still from the video "Minch_retreat.mpg".

File "Minch_retreat.mpg" shows an animation of the RETREAT experiments.

The video is available online, in the Supplementary Information of the published manuscript in *The Cryosphere*.

A.2   Application to an Idealised Ice Sheet

We initially test BISICLES_hydro using an idealised experiment. We prescribe a square ice sheet with calving margins on the low y-axis and high x-axis, exploiting symmetry to cut computational cost in the same manner as previously reported (Payne and Dongelmans, 1997; Hindmarsh, 2009). Geothermal heat flux is uniform and set at 30 mW m^{-2}, surface heat flux is also uniform and set at 268 K. The ice sheet bed is flat and at 0 m elevation. A uniform surface mass balance of 0.3 m/y is set across the ice sheet to cause growth, and run to stability for 100,000 model years. Horizontal resolution (Δ_x) is varied to test for influence on ice stream width and spacing (Figure A.2), in a manner similar to the experiments of Hindmarsh (2009). These idealised experiments offer essentially a "worst case scenario" of resolution dependency, as the flat bed offers no troughs for preferential ice stream formation, which would tend to fix ice stream location between different horizontal resolutions.
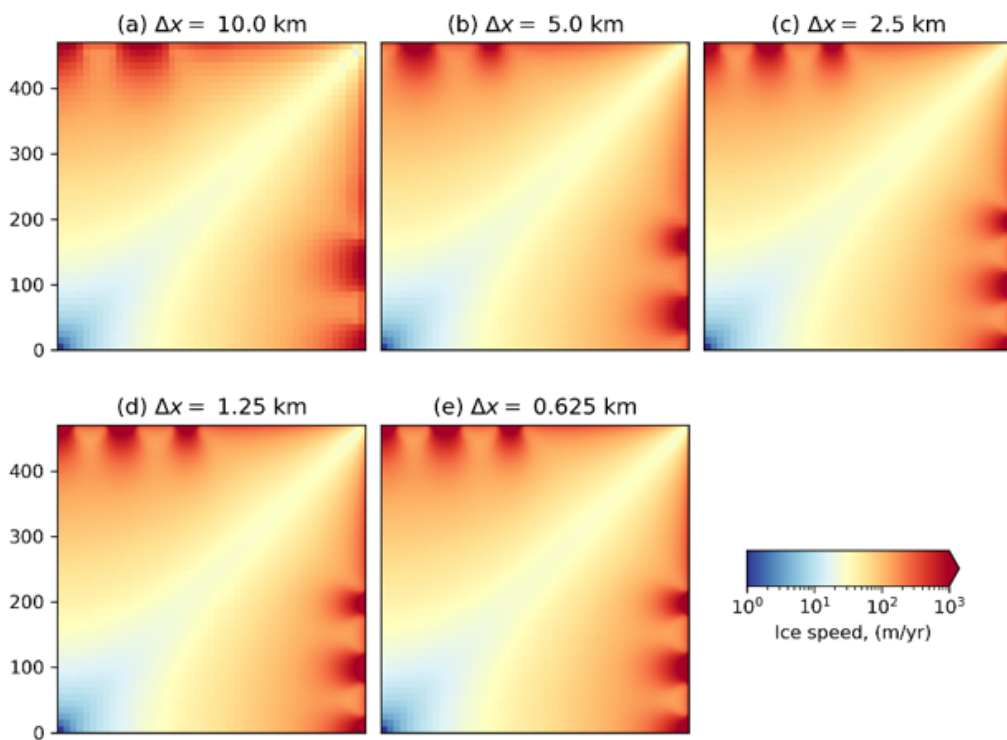
Figure A.2: Simulated ice velocity with an idealised set-up using BISICLES_hydro. Increasing resolution increases the number of ice streams (a-e).

The simulations produce ice streams along the calving margin, distinctly spaced between areas of lower velocity. Two streams are produced along each front at the coarser resolutions (10 km and 5 km, Figures A.2a,b), and there is a clearly visible difference in stream location between these cases. In fact, the 10 km simulations includes streams that straddles the symmetry axes so that the entire ice sheet would have three streams along each front, while the 5 km simulation has slow flow at the symmetry axes , so that the entire ice sheet would have four streams along each front. Refining to 2.5 km produces a third stream along both fronts (Figure A.2c), once again straddling the symmetry axes to give five streams along each front in total, and this pattern is retained in in both the 1.25 km and 0.625 km cases (Figure A.2d,e). In other words, the differences between simulations diminish progressively as the mesh is refined, but at typical ice sheet model resolution (5,10 km) those differences are still substantial, indicating a need for routine convergence tests in real-world applications.

A.3   Sensitivity tests

Sensitivity to various model parameters is tested by perturbing the model parameter for 1,000 model years, from ADVANCE 3,000-4,000 model years. The friction coefficient, the C in the $C(u_b)^{1/m}$ Weertman sliding law, is 3,000 as standard, and 1,500 and 6,000 at minimum and maximum respectively. The thickness of the till-stored water layer is 2 m as standard, and 1 m and 4 m at minimum and maximum respectively. The friction coefficient, the f in the $f(\sigma_0 - p)$ Coulomb sliding law, is 0.5 as standard and 0.25 and 0.75 at minimum and maximum respectively. The geothermal heat flux is 60 mW m^{-2} as standard, and 30 and 120 mW m^{-2} at minimum and maximum respectively. The till drain factor is 0.005 m/y as standard, and 0.0025 and 0.01 m/y at minimum and maximum respectively. RMSE values are calculated from the velocities simulated using "standard" parameters.

Varying till-stored water layer thickness, the till drain factor, and geothermal heat flux all have similar effects on the simulated ice streaming, in that they
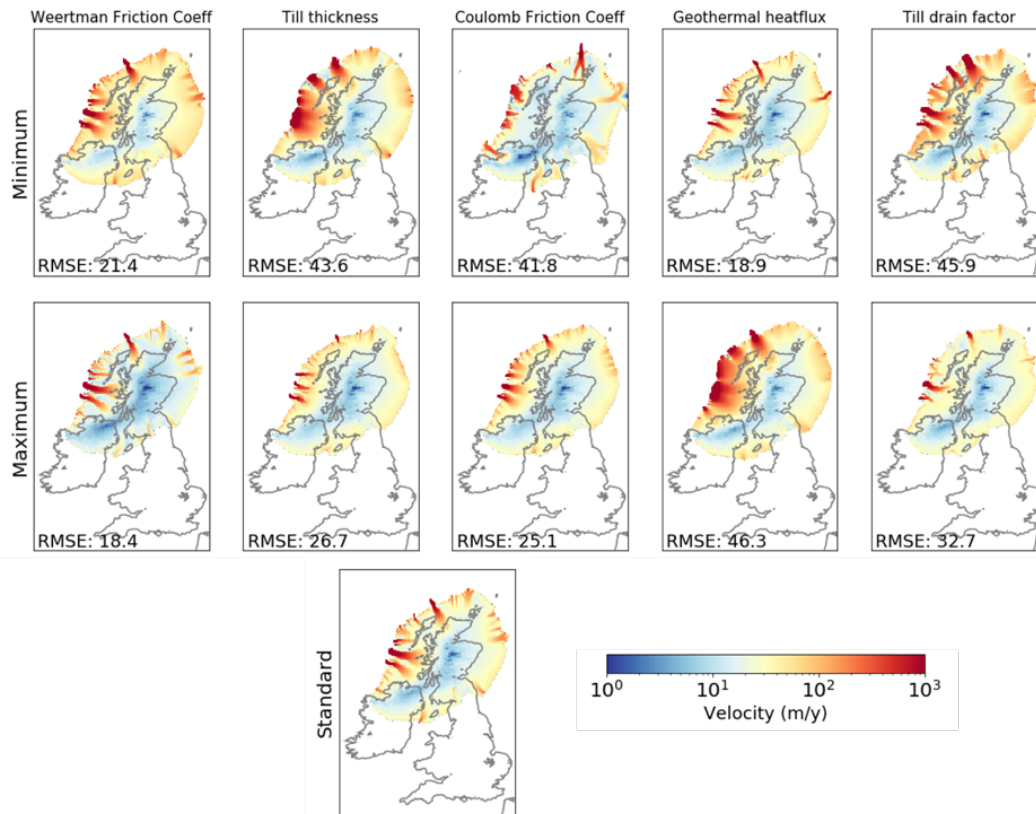
Figure A.3: Ice velocity a t=4,000 years, testing sensitivity to model parameters

control the width of the ice streams. Together, these parameters control the water pressure in the till layer, explaining why they have a similar effect. A low till-water thickness, low till drain factor, and high geothermal heat flux are all conducive to widespread saturation of the till layer, leading to wide ice streams. A high till-water thickness, high drain factor, and low geothermal heat flux all keep the areas of till saturation limited, and therefore ice streams remain narrow (Figure A.3).

The sliding coefficients in both the Weertman and Coulomb sliding laws change the simulated velocity patterns. The Weertman sliding law is primarily used for the interior of the ice sheet, and therefore changing the Weertman sliding friction coefficient primarily changes the velocities at the interior of the ice sheet, and has a limited impact on the pattern of ice streaming. The Coulomb sliding law operates at the ice sheet margins, and therefore has a more significant impact on the pattern of ice streaming. A low Coulomb sliding friction coeffi-

Chapter A

cient produces ice streams which are a poor match to empirical data, whilst a high Coulomb sliding friction coefficient maintains the spacing of ice streams, but each ice stream extends less far into the ice sheet interior.

A.4   ADVANCE + RETREAT video
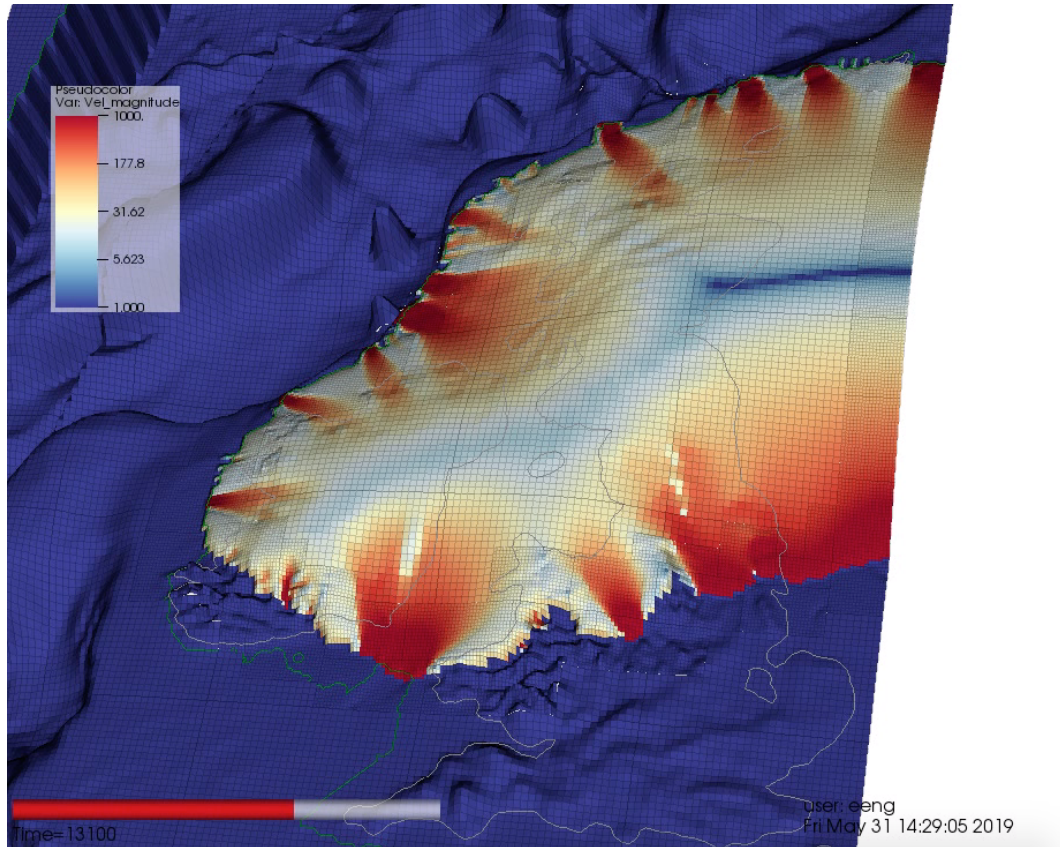
Figure A.4: A still from the video "ADVANCE_RETREAT.mpg".

File "ADVANCE_RETREAT.mpg" shows an animation of the ADVANCE and RETREAT experiments.

The video is available online, in the Supplementary Information of the published manuscript in *Quaternary Science Reviews*.

A.5   Resolution Dependency

We used AFDA to compare the skill of the model at simulating flow direction at different horizontal resolutions (Table A.2). A 4 km resolution and below the

scores remain similar, and a finer horizontal resolution does not result in a better rank against the empirical data. At 8 km resolution the scores are higher than the other experiments, showing that at 8 km resolution an extra level of mesh refinement improves the model-data match.

Simulation	Residual Variance	Residual Vector
BISICLES_HYDRO 8 km	0.032	14.1
BISICLES_HYDRO 4 km	0.024	12.6
BISICLES_HYDRO 2 km	0.025	12.2
BISICLES_HYDRO 1 km	0.025	12.2

Table A.1: Mean residual vector and variance scores for the Minch Ice Stream at t=4,000 model years. Each experiment is show in Figure 3.4.

A.6   Model Parameters Summary

Not.	Name	Value	Unit	MIN	MAX
ρ	Ice density	918	kg m^3	-	-
g	Acceleration due to gravity	9.81	m s^{-1}	-	-
m	Weertman exponent	3	-	-	-
C	Weertman constant	3,000	Pa m$^{-1/3}$a$^{1/3}$	1,500	6,000
f	Coulomb friction coefficient	0.5	-	0.25	0.75
α	Till pressure factor	0.99	-	-	-
W_0	Maximum till water depth	2	m	1	4
D	Till water drain factor	0.005	m/y	0.0025	0.01

Table A.2: Key model parameters used in all experiments in Chapter 4.

A.7   Table of ensemble parameters

Ref	PDD factor adjustment	Sub-shelf melt adjustment	Lapse rate	Precip % of standard	(f) Coulomb	(C) Weertman	(W_0) Maximum till water depth
ns_001	1.39	120.56	5.69	-61.13	0.0	1738.0	4.01
ns_002	-0.92	73.24	5.79	-30.26	1.0	1677.0	4.27
ns_003	-0.43	105.14	6.93	2.61	0.0	1142.0	4.35
ns_004	1.51	99.6	6.73	40.02	1.0	1913.0	4.76
ns_005	-1.28	49.44	6.16	16.3	0.0	1261.0	4.9

ns_006	-0.85	-46.34	6.24	30.63	0.0	1614.0	3.82
ns_007	1.63	-29.4	5.01	-63.99	0.0	731.0	3.56
ns_008	-1.11	89.88	6.02	-56.46	1.0	1039.0	3.51
ns_009	-0.6	24.32	7.71	-19.85	1.0	1796.0	4.17
ns_010	0.02	-4.3	4.5	49.96	1.0	880.0	3.21
ns_011	1.2	126.22	4.58	72.1	1.0	1405.0	2.96
ns_012	-1.32	-33.34	4.75	-44.15	0.0	1585.0	4.14
ns_013	-1.91	-37.72	5.94	42.24	1.0	1950.0	3.59
ns_014	1.86	135.76	7.22	47.57	1.0	1061.0	4.7
ns_015	-1.79	-25.04	6.5	29.76	1.0	1005.0	4.57
ns_016	-0.16	9.52	6.33	-50.81	0.0	500.0	2.13
ns_017	0.54	92.12	5.5	35.07	0.0	1754.0	2.41
ns_018	0.12	-12.44	4.91	19.41	1.0	1465.0	5.0
ns_019	0.77	80.72	6.99	66.67	1.0	1636.0	2.68
ns_020	-1.4	140.76	5.7	33.25	0.0	1343.0	3.66
ns_021	1.33	103.32	5.29	26.29	0.0	1634.0	3.77
ns_022	-1.66	97.9	6.4	-6.78	0.0	891.0	4.39
ns_023	1.08	143.84	7.56	-55.68	0.0	749.0	2.59
ns_024	-0.87	134.62	6.29	69.38	0.0	1383.0	2.37
ns_025	-1.17	115.96	8.0	60.72	1.0	1085.0	4.62
ns_026	1.31	128.54	7.26	21.47	1.0	1204.0	4.48
ns_027	1.44	150.0	7.42	51.7	1.0	837.0	4.21
ns_028	-1.61	-17.4	6.76	-26.97	1.0	1423.0	4.67
ns_029	0.64	122.6	7.34	-65.37	0.0	1495.0	4.55
ns_030	-1.55	4.48	5.62	-11.99	0.0	843.0	2.26
ns_031	1.9	145.28	6.69	-39.58	1.0	1560.0	2.82
ns_032	-0.29	64.6	6.14	7.7	0.0	1821.0	4.09
ns_033	-0.46	20.88	4.67	-49.26	0.0	1874.0	2.73
ns_034	1.55	24.14	5.9	0.99	1.0	592.0	2.45
ns_035	-1.0	84.5	6.07	-66.51	1.0	1837.0	3.74
ns_036	0.34	-38.7	6.85	-3.17	0.0	584.0	4.79
ns_037	-0.72	54.36	7.0	75.0	0.0	1378.0	3.33
ns_038	-1.72	10.86	7.38	45.67	0.0	1851.0	2.0
ns_039	1.12	67.36	4.87	18.8	1.0	1716.0	3.0
ns_040	-0.21	108.58	5.47	-75.0	0.0	958.0	4.93
ns_041	2.0	-19.16	5.33	43.97	1.0	1108.0	4.41
ns_042	-0.1	94.88	7.54	-51.48	1.0	2000.0	3.16
ns_043	0.84	-44.14	4.6	62.41	1.0	1291.0	3.87
ns_044	0.19	70.2	7.11	-23.54	0.0	1035.0	3.5
ns_045	0.49	-31.7	7.19	5.94	0.0	1241.0	2.48
ns_046	-0.26	30.84	6.88	-8.98	1.0	808.0	4.3
ns_047	1.8	-9.34	6.5	-34.03	0.0	1310.0	4.05
ns_048	-1.04	56.52	7.64	37.0	0.0	977.0	2.55
ns_049	-0.74	3.72	5.2	-36.39	0.0	1541.0	3.39

Chapter A

ns_050	0.25	115.52	7.79	-46.51	1.0	936.0	4.5
ns_051	1.76	34.02	5.41	55.23	0.0	707.0	2.06
ns_052	1.02	46.88	5.11	65.4	1.0	1919.0	3.1
ns_053	-1.22	42.34	4.84	-29.25	1.0	654.0	2.21
ns_054	0.11	62.78	5.08	-16.35	0.0	1227.0	3.94
ns_055	1.21	-50.0	7.9	-15.0	0.0	1316.0	3.26
ns_056	0.69	51.82	4.97	13.5	1.0	554.0	3.15
ns_057	-0.64	112.8	7.5	-37.19	0.0	1769.0	3.36
ns_058	0.43	-14.0	6.38	-40.77	0.0	908.0	2.17
ns_059	0.39	-23.26	6.57	10.39	0.0	1508.0	3.06
ns_060	-0.35	37.56	6.62	55.76	0.0	611.0	2.7
ns_061	-1.48	81.78	5.96	59.78	1.0	1697.0	2.88
ns_062	-0.01	41.12	7.07	-4.75	0.0	1449.0	2.63
ns_063	-2.0	60.0	5.22	12.39	1.0	649.0	3.42
ns_064	0.89	77.0	7.85	-18.3	0.0	684.0	3.91
ns_065	-0.54	14.54	5.59	-24.86	1.0	1152.0	2.93
ns_066	1.71	17.5	7.82	-1.49	1.0	1970.0	4.84
ns_067	0.92	27.34	5.39	-70.57	1.0	768.0	2.25
ns_068	-1.52	0.52	4.74	24.06	1.0	538.0	3.7
ns_069	-1.85	130.7	7.66	-59.47	1.0	785.0	2.81
ns_070	0.61	-2.24	5.83	-71.82	0.0	1172.0	2.3

Table A.3: Parameter values for each ensemble member. Adjustments are made from the standard values (Table 4.2).

A.8 Table of model-data comparison results

Ref	APCA (% Match)	ATAT (% Match)	ATAT wRMSE	AFDA (% Match)
ns_001	58.46	74.53	705.02	37.35
ns_002	59.23	49.06	890.15	33.73
ns_003	30.0	58.82	880.74	21.69
ns_004	39.23	47.73	950.93	26.51
ns_005	30.0	36.84	712.98	22.89
ns_006	29.23	44.44	693.27	16.87
ns_007	58.46	74.53	705.02	37.35
ns_008	67.69	60.0	778.68	44.58
ns_009	40.77	48.48	920.55	25.3
ns_010	33.08	51.22	1023.19	36.14
ns_011	40.77	52.17	941.37	37.35
ns_012	63.08	60.71	792.56	45.78
ns_013	24.62	30.77	344.37	15.66
ns_014	36.92	50.0	870.71	27.71
ns_015	26.92	31.25	735.65	15.66

ns_016	54.62	59.42	846.46	50.6
ns_017	43.08	53.85	896.07	28.92
ns_018	40.0	44.0	953.05	27.71
ns_019	35.38	53.57	897.54	21.69
ns_020	26.92	45.45	735.53	14.46
ns_021	64.62	57.69	830.29	49.4
ns_022	33.08	55.22	1023.19	36.14
ns_023	55.38	74.04	716.33	39.76
ns_024	29.23	16.66	737.27	10.84
ns_025	29.23	37.5	718.04	16.87
ns_026	42.31	54.54	856.15	33.73
ns_027	27.69	46.88	884.25	19.28
ns_028	30.77	48.65	885.55	24.1
ns_029	30.0	32.0	713.94	16.87
ns_030	27.69	46.88	884.25	24.1
ns_031	61.54	70.87	730.03	49.4
ns_032	32.31	48.78	963.25	19.28
ns_033	63.08	72.84	726.14	50.6
ns_034	62.31	63.74	763.91	50.6
ns_035	65.38	63.46	747.69	39.76
ns_036	56.15	52.83	948.26	33.73
ns_037	27.69	25.0	726.48	10.84
ns_038	29.23	16.66	737.27	10.84
ns_039	31.54	46.15	918.07	24.1
ns_040	57.69	71.03	719.91	43.37
ns_041	47.69	55.93	878.4	38.55
ns_042	63.85	62.38	758.98	50.6
ns_043	36.15	52.38	1006.78	27.71
ns_044	64.62	57.69	830.29	49.4
ns_045	55.38	55.17	892.47	32.53
ns_046	43.08	53.85	896.07	28.92
ns_047	60.77	71.7	723.27	39.76
ns_048	30.77	37.5	739.63	13.25
ns_049	63.08	56.32	789.6	55.42
ns_050	62.31	60.71	830.29	50.6
ns_051	55.38	55.17	892.47	32.53
ns_052	40.0	48.72	909.12	26.51
ns_053	63.08	60.71	792.56	45.78
ns_054	61.54	62.24	750.22	51.81
ns_055	62.31	55.95	810.51	49.4
ns_056	54.62	59.42	846.46	49.4
ns_057	61.54	56.76	866.14	48.19
ns_058	63.85	62.38	891.89	51.81
ns_059	53.85	59.68	884.73	31.33

ns_060	29.23	40.0	719.68	15.66
ns_061	28.46	31.25	726.19	12.05
ns_062	52.31	50.79	875.85	36.14
ns_063	28.46	38.46	726.9	19.28
ns_064	53.85	57.69	827.85	59.04
ns_065	61.54	62.24	750.22	51.81
ns_066	54.62	45.76	944.95	32.53
ns_067	56.15	74.04	711.63	39.76
ns_068	28.46	52.63	713.84	24.1
ns_069	60.77	49.18	891.89	39.76
ns_070	59.23	74.04	712.21	36.14

Table A.4: Scores from APCA, ATAT, and AFDA for each ensemble member. Scores highlighted in light green ranked scored more than 50% for a given comparison tool. Simulations highlighted in dark green scored more than 50% in all three comparison tools, and are therefore considered in the NROY subset.

A.9 Southern North Sea proglacial lake

Initial experiments considered no representation of a proglacial lake at the southern margin of the ice sheet in the North Sea. This results in an over-extended southern margin, whilst still simulating margins in the southwest and Norwegian Channel that did not yet meet maximum extent according to empirical data (Sejrup et al., 1994; King et al., 1998; Roberts et al., 2018). In the southern North Sea the bathymetry, meltwater routing, and river routing means it is possible a large proglacial lake formed. Smaller proglacial lakes of the southern North Sea have been reconstructed with shallow seismic reflection data (Emery et al., 2019), although reconstructing a larger lake would require more geographically extensive empirical and potentially modelling work.

The latest generation of ice sheet models, including BISICLES, do not yet have the ability to simulate the formation or effect of proglacial lakes. It would be expected that the presence of a large proglacial lake would arrest ice sheet advance at the margin with the lake. The presence of a lake in the southern North Sea is crucial to understanding deglaciation dynamics of the North Sea partly because of the proximity to the influential Norwegian Channel ice stream.
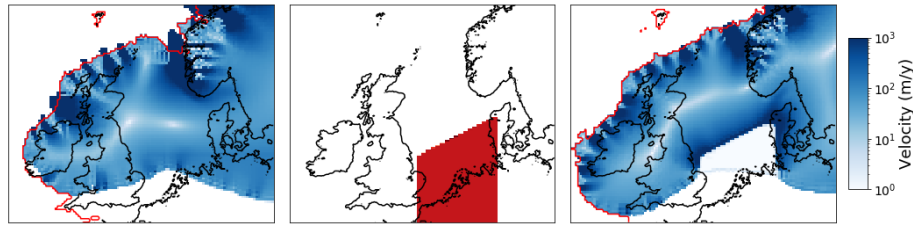
Figure A.5: The effect of imposing a SMB forcing to represent a proglacial lake in the southern North Sea. a) The ice sheet at the end of the advance stage without the representation of a proglacial lake. b) The area of SMB forcing, a forcing of -40 m/y is used in the marked region. c) The ice sheet at the end of the advance stage using the lake forcing shown in panel b.

We impose a SMB forcing in the southern North Sea (Figure A.5b) to act as a proxy for the effects of the presence of a lake. The effect of imposing this proxy lake forcing is to limit ice advance in the southern North Sea, while simultaneously allowing further ice advance in the southwest of the domain and the Norwegian Channel (Figure A.5c).

This is a better fit for the reconstructed ice sheet extent in the North Sea sector (Sejrup et al., 1994; King et al., 1998; Roberts et al., 2018) further motivating the representation of a lake in the simulations presented here. For future work it would be beneficial for ice sheet models to simulate the formation and effect of proglacial lakes, as they are assumed to be influential across terrestrial margins of other palaeo ice sheets (Krinner et al., 2004; Teller, 2015).

A.10   Parameter influence

Parameter variation in the ensemble was sampled using the Latin Hypercube technique. Unlike systematic sampling, this means all parameters are varied in tandem, and the results of each ensemble members are the result of all seven varied parameters.

The NROY simulations do not have significantly distinct parameter values from the rest of the ensemble (Figure A.6), NROY simulations have an almost full range of parameter values for all seven varied parameters. This is partly
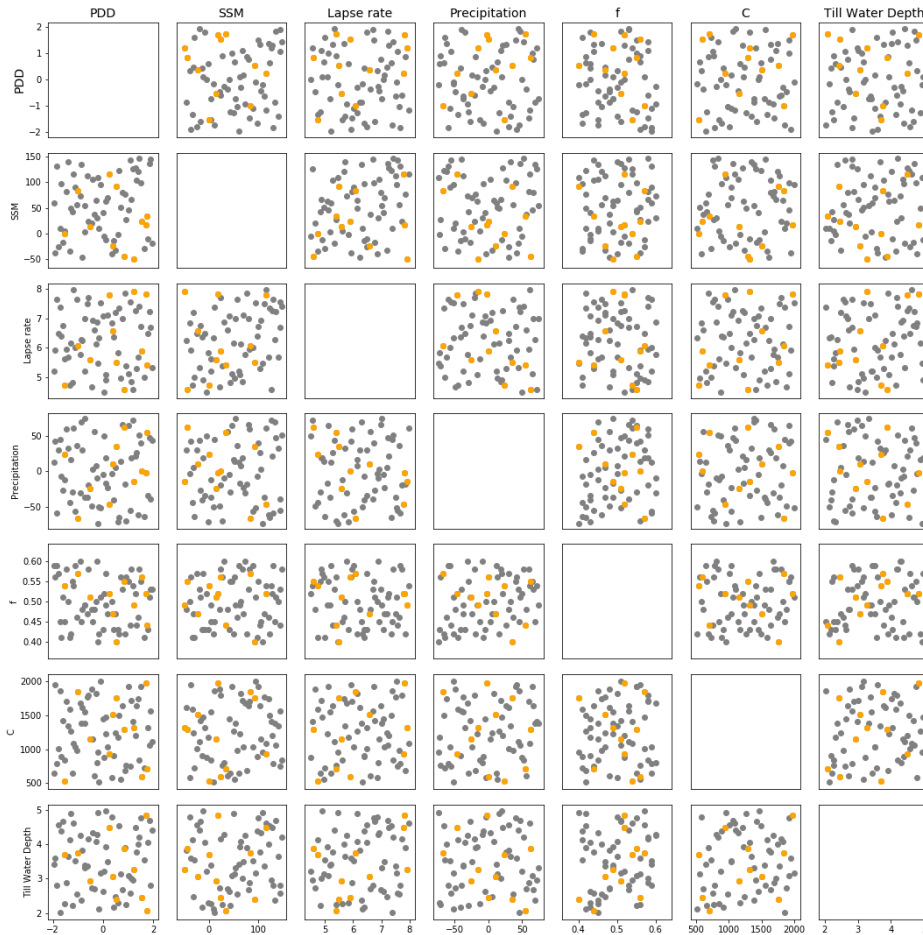
Figure A.6: Every combination of the seven parameters that are varied in the deglaciation ensemble. NROY simulations are highlighted in orange.

because all parameters are varied in tandem. As an example, a simulation with low precipitation (causing rapid retreat) may also have a high lapse rate (slowing retreat), meaning that NROY simulations appear to be unconstrained in the parameter space.

The retreat rate of the NCIS was also compared to parameter variation (Figure A.7), revealing some expected behaviour. Simulations with a low precipitation, and low Coulomb friction coefficient have a higher retreat rate, and simulations with a lower PDD factor, lower sub-shelf melt rate, and lower lapse rate have a slower retreat rate. The Weertman sliding coefficient and maximum till water depth show no relationship for NCIS retreat rate, and are therefore the least influential varied parameters. However, as previously show (Figure A.6), the
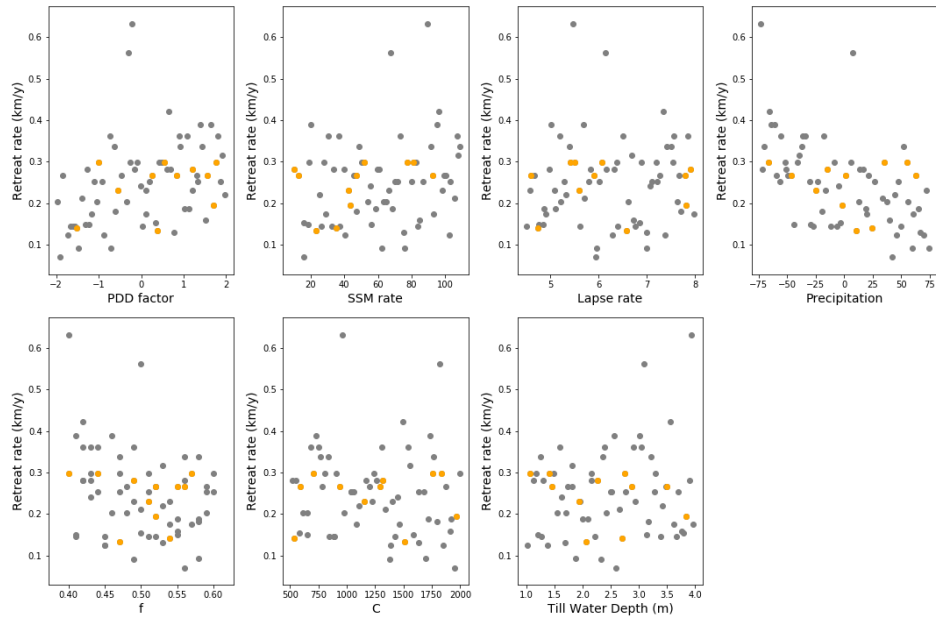
Figure A.7: Retreat rate of the Norwegian Channel Ice Stream (km/y) against the seven parameters varied in the ensemble. NROY simulations are highlighted in orange.

NROY simulations do not have distinct parameter values from the rest of the ensemble members.

Chapter A

References

Emery, A. R., D. M. Hodgson, N. L. Barlow, J. L. Carrivick, C. J. Cotterill, and E. Phillips (2019). "Left High and Dry: Deglaciation of Dogger Bank, North Sea, Recorded in Proglacial Lake Evolution". In: *Frontiers in Earth Science* 7, p. 234. DOI: 10.3389/feart.2019.00234.

Hindmarsh, R. C. (2009). "Consistent generation of ice-streams via thermo-viscous instabilities modulated by membrane stresses". In: *Geophysical Research Letters* 36.6, p. L06502. DOI: 10.1029/2008GL036877.

King, E. L., H. Haflidason, H. P. Sejrup, and R. Løvlie (1998). "Glacigenic debris flows on the North Sea Trough Mouth Fan during ice stream maxima". In: *Marine Geology* 152.1-3, pp. 217–246. DOI: 10.1016/S0025-3227(98)00072-3.

Krinner, G., J. Mangerud, M. Jakobsson, M. Crucifix, C. Ritz, and J. I. Svendsen (2004). "Enhanced ice sheet growth in Eurasia owing to adjacent ice-dammed lakes". In: *Nature* 427.6973, pp. 429–432. DOI: 10.1038/nature02233.

Payne, A. J. and P. W. Dongelmans (1997). "Self-organization in the thermomechanical flow of ice sheets". In: *Journal of Geophysical Research: Solid Earth* 102.B6, pp. 12219–12233. DOI: 10.1029/97JB00513.

Roberts, D. H. et al. (2018). "Ice marginal dynamics of the last British-Irish Ice Sheet in the southern North Sea: Ice limits, timing and the influence of the Dogger Bank". In: *Quaternary Science Reviews* 198, pp. 181–207. DOI: 10.1016/J.QUASCIREV.2018.08.010.

Sejrup, H. P., H. Haflidason, I. Aarseth, E. King, C. F. Forsberg, D. Long, and K. Rokoengen (1994). "Late Weichselian glaciation history of the northern North Sea". In: *Boreas* 23.1, pp. 1–13. DOI: 10.1111/j.1502-3885.1994.tb00581.x.

Teller, J. T. (2015). "Proglacial lakes and the southern margin of the Laurentide Ice Sheet". In: *North America and Adjacent Oceans During the Last Deglaciation.* Geological Society of America, pp. 39–69. DOI: 10.1130/dnag-gna-k3.39.